University of Nottingham
UK | CHINA | MALAYSIA

Investigating the interaction between *Neisseria meningitidis* and human FGFR1

Meshari Alsuwat

B.Sc., M.Sc.

Thesis submitted to the University of Nottingham for the degree of Doctor of Philosophy

April 2022

Molecular Bacteriology and Immunology Group
School of Life Sciences
University of Nottingham

Declaration

With exception of reference to other people's work, which has been duly acknowledge, I declare that the work presented in this thesis is the result of my own research and has not been submitted in any form for the award of a higher education degree elsewhere.

Meshari Alsuwat

April 2022

PhD Student
Molecular Bacteriology and Immunology Group
School of Life Sciences
University of Nottingham

Abstract

Neisseria meningitidis is one of the most common bacterial causes of meningitis. This organism colonises the nasopharyngeal epithelium of the upper respiratory tract, where it is considered to be a commensal species. It can subsequently traverse the nasopharyngeal epithelium and enter the bloodstream, which can lead to disease including sepsis and meningitis. To cause meningitis, *N. meningitidis* must further cross the blood–brain barrier (BBB) to reach the meninges. This requires it to first bind to endothelial cells in a process that is incompletely understood at present. However, previous reports have shown that epidermal growth factor receptor (EGFR) and fibroblast growth factor receptor 1 (FGFR1) might be involved.

Earlier research in our group has established that *N. meningitidis* interacts directly and specifically with the IIIc splice variant of FGFR1, a new cellular receptor for pathogenic meningococci. That study employed a PilQ-deficient meningococcal strain (Δ*pilQ*) with mutation of a key component of type IV pili (TFP), thereby revealing that these bacterial structures are important for FGFR1-mediated adhesion of *N. meningitidis* to host endothelial cells. However, other adhesins have been implicated in invasion of the host, and multiple virulence factors are evidently involved in the invasion of host tissues that occurs in meningococcal disease. Thus, as yet unidentified adhesins might play an important role in the pathogenesis of meningococcal disease through their interaction with host cell receptors. This study aimed to identify the specific bacterial ligands responsible for FGFR1-dependent attachment of *N. meningitidis* to human brain microvascular endothelial cells (HBMECs).

Discovery of several potentially important novel meningococcal ligands was enabled by searching for and comparing homologues in the closely-related commensal species *N. lactamica*. After analysing an initial set of 41 candidate meningococcal ligands, 18 proteins were identified without close homologues in *N. lactamica*, and this set was filtered down to a final set of four priority candidates as the focus of further study (MafA, Opc5, FadL and NMB0506). Knockout strains of *N. meningitidis* were produced for all four target genes. Interaction of the wild type and mutant meningococcal strains with HBMECs was compared in cellular adhesion and invasion assays. Of the genes targeted as potential FGFR1 ligands, only *fadL* showed a significant contribution towards attachment of *N. meningitidis* MC58 to the host cells, whereas all four genes of interest were found to play a significant role in meningococcal invasion of HBMECs.

A plasmid for production of recombinant Fc-FGFR1 IIIc was validated (pEF-Bos-ssFc-extFGFR1IIIc-ires-TPZ) and used to transfect HEK293T cells using the GeneJuice reagent. This permitted successful expression and purification of Fc-FGFR1 IIIc, along with a control (Fc-stop; i.e., Fc-tag only) as verified by SDS–PAGE and immunoblotting, and allowed for further investigation of the FGFR1-binding properties of the proposed bacterial ligands by whole-cell ELISA. Significantly lower binding to Fc-FGFR1 IIIc was seen for *N. lactamica* and MC58Δ*pilQ*/Δ*porA* mutant, compared to the wild type MC58 strain. However, no significant difference was evident for interaction of the mutants lacking *mafA*, *fadL*, *opc5* or *NMB0506*, relative to wild type.

For a more direct assessment of the interactions involved, the proteins encoded by the targeted bacterial genes were overexpressed in *E. coli* in order to evaluate their specific interactions with FGFR1 IIIc. Due to time constraints, expression and purification were only attempted for three of the original four proteins of interest (MafA, Opc5 and FadL). Whereas purified recombinant MafA was obtained successfully, purification of Opc5 and FadL under native conditions was not achieved since these proteins were not readily expressed in soluble form and were instead found in inclusion bodies. Nonetheless, far-western blotting with solubilised cell lysates from overexpression cultures showed no evidence of an interaction between either Opc5 or FadL and Fc-FGFR1 IIIc. However, an interaction was observed between MafA and the latter. This result was confirmed with a protein–protein interaction ELISA experiment conducted using purified recombinant proteins. Significant binding was observed between Fc-FGFR1 IIIc and MafA relative to control (1% BSA/PBS + MafA).

In summary, this study has demonstrated a novel role for FadL in attachment of *N. meningitidis* to human brain endothelial cells and established contributions of MafA, Opc5, FadL and NMB0506 to cellular invasion. This work has also provided evidence supporting a role for MafA as a meningococcal FGFR1 ligand. In the future, it is hoped that building on these findings will result in more effective therapeutic approaches against the disease.

Acknowledgements

I must express my deepest gratitude and thanks to ALLAH for giving me the strength and guidance to complete this degree. I would like to express my sincere gratitude to my supervisors, Dr. Karl Wooldridge, and Dr. Neil Oldfield, for their continuous support to carry out my PhD study in the Molecular Bacteriology and Immunology Group (MBIG) at the University of Nottingham and for their patience, motivation and immense knowledge. Their guidance and encouragement helped me in my research and in the writing of this thesis. Besides my supervisors, I would like to thank my internal examiner Dr. Christopher Penfold, and my external examiner Dr. Darryl Hill for their comments and suggestions to improve this study. I would also like to thank the group of Dr. Martinez-Pomares for their help with protein expression and purification.

I would like to acknowledge the scholarship that I have received from Taif University, College of Applied Medical Sciences and the financial support provided by the Saudi Cultural Bureau to pursue my PhD study at the University of Nottingham.

A very special thanks goes out to my colleagues in MBIG and friends for all the emotional support, good company and care. Last but not least, I would like to dedicate this thesis to my wife Taghreed, my daughter Rafa who was born when I was in my third year, my mother, and to my brothers and sisters for supporting me spiritually throughout writing this thesis. Without their precious support, it would not have been possible to conduct this research.

List of Presentations

Poster/oral presentation

Meshari Alsuwat, Karl G. Wooldridge and Neil J. Oldfield. Investigating the interaction between *Neisseria meningitides* and human fibroblast growth factor receptor 1 (FGFR1). Presented at School of Life Science PGR Symposium, 24-25th June **2019**, Nottingham, UK.

Meshari Alsuwat, Karl G. Wooldridge and Neil J. Oldfield. Investigating the interaction between *Neisseria meningitidis* and human FGFR1. Presented at School of Life Science PGR Symposium, 20-24th of July **2020**, Nottingham, UK.

Table of Contents

List of Abbreviations

ABC	ATP-binding cassette
ANOVA	Analysis of variance
App	Adhesion and penetration protein
AT	Autotransporter
Bam	β-barrel assembly machinery
BBB	Blood brain barrier
BCIP/NBT	5-Bromo-4-chloro-3-indolyl phosphate/nitro blue tetrazolium liquid substrate system
BCSFB	Blood–cerebrospinal fluid barrier
BglII	*Bacillus globigii* restriction endonuclease
BHI	Brain Heart Infusion
bp	Base pair
BSA	Bovine serum albumin
C4bp	C4b-binding protein
ca.	Approximately
$CaPO_4$	calcium phosphate

CDI	Contact-dependent inhibition
CEACAM	Carcinoembryonic antigen-related cell adhesion molecule
CFU	Colony-forming unit
CNS	Central nervous system
CO2	Carbon Dioxide
cps	Capsule polysaccharide synthesis
CSF	cerebrospinal fluid
DCs	Dendritic cells
dH2O	Distilled water
DMEM	Dulbecco's Modified Eagle's Medium
DMSO	Dimethyl sulfoxide
DNA	Deoxy ribonucleic acid
dNTPs	Deoxy nucleotide triphosphate
DTT	Dithiothreitol
DUS	DNA uptake sequence
E. coli	*Escherichia coli*

ECM	Endothelial cell medium
ECM-B	endothelial cell medium-basal
EcoRI	*Escherichia coli* strain R restriction endonuclease
EDTA	Ethylenediaminetetraacetic acid
EGFR	Epidermal growth factor receptor
ELISA	Enzyme-linked immunosorbent assay
et al	And others
FBS	Foetal bovine serum
FGFR1	Fibroblast growth factor receptor 1
fHbp	Factor H-binding protein
g/mg/µg/ ng	Gram/milligram/microgram/ nanogram
h/min/s	Hour/ minute/seconds
HBMECs	Human brain microvascular endothelial cells
HEK293T	Human embryonic kidney cells
His6	Hexahistidine
HSPGs	Heparan sulphate proteoglycans

HUVECs	Human umbilical vein endothelial cells
IgA1 protease	Immunoglobulin A1 protease
IMAC	Immobilized Metal Affinity Chromatography
IMD	Invasive meningococcal disease
INPCR	Inverse PCR
IPTG	Isopropyl-P-D-thiogalactopyranoside
K_2HPO_4	Dipotassium phosphate
Kan	kanamycin
Kb	Kilo base pair
kDa	Kilo Dalton
KH_2PO_4	Monopotassium phosphate
LAMP	Lysosome-associated membrane proteins
LB	Lysogeny Broth
LOS	Lipooligosaccharide
LPS	Lipopolysaccharides
M	Molar

MAPK	Mitogen activated protein kinases
MC58	A meningococcal serogroup B strain
MenACWY	Meningococci serogroup A, C, W, and Y
MHC	Histocompatibility complex
ml/ µl/ µg	Millilitre/ Microlitre/ Microgram
MLEE	Multi-locus enzyme electrophoresis
MLST	Multi-locus sequence typing
MOI	Multiplicity of infection
MspA	Meningococcal serine protease A
MVECs	Microvascular endothelial cells
MWCO	Molecular weight cut-off
Na2PO4	Sodium phosphate
NaCl	Sodium chloride
NadA	Neisseria adhesion A
NalP	*Neisserial* autotransporter lipoprotein
NANA	N-acetylneuraminic acid

NCBI	National Center for Biotechnology Information
NEB	New England Biolabs
NF-κB	Nuclear factor kappa-light-chain-enhancer of activated B cells
NHBA	Neisserial heparin-binding antigen
NhhA	Neisseria hia homologue
NTHI	non-typeable *H. influenzae*
OD	Optical density
OMPs	Outer membrane proteins
OMVs	Meningococcal outer membrane vesicles
Opa	Opacity protein A
Opc	Opacity protein C
ORF	Open reading frame
p	Probability value
PAMPs	Pathogen-associated molecular patterns
PBS	Phosphate buffer saline
PBST	PBS with 0.05% Tween 20

PCR	Polymerase chain reaction
PCV	Pneumococcal conjugate vaccine
pH	Unit of acidity/alkalinity
PLC	phospholipase C
PorA	Porin A
PorB	Porin B
PPV	Pneumococcal polysaccharide vaccine
pQE30	An N terminal his6 tag expression vector
RIPA	Radio immunoprecipitation assay
ROS	Reactive oxygen species
rpm	Revolutions per minute
RT	Room temperature
SBA	serum bactericidal antibodies
SDS	Sodium dodecyl sulphate
SDS-PAGE	Sodium dodecyl sulfate-polyacrylamide gel electrophoresis
SSM	Slipped strand mispairing

SWATH-MS	Sequential window acquisition of all theoretical mass spectra
T1SS	Type I secretion systems
T5SS	Type V secretion systems
TAAs	Trimeric autotransporter adhesins
Taq	*Thermus aquaticus* thermostable polymerase
Tat	Twin-arginine translocation
TB	Terrific Broth
TFP	Type IV Pili
TLR	Toll-like receptor
TNF-α	Tumour necrosis factor-α
TPSS	Two-partner secretion system
V	Volt
WT	Wild type
X-GAL	5-bromo-4-chloro-3-indolyl-b-D-galactopyranoside
β2AR	β2 adrenergic receptor
Δ	Delta (Deleted/missing)

× g	The centrifugal force applied as multiples of the earth's gravitation (g)
°C	Degrees Celsius

List Figures

List of Tables

Chapter 1: General Introduction

1.1 Background

Meningitis, also known as leptomeningitis or arachnoiditis, is characterised by inflammation of the protective membranes (meninges) surrounding the brain and spinal cord (Kim, 2010, Cain et al., 2019). Three major layers constitute the meninges: the dura mater, the pia mater and the arachnoid mater (Adeeb et al., 2012, Ghannam and Al Kharazi, 2019). The dura mater is the thickest, outermost layer, and offers effective protection for the brain and spinal cord. The arachnoid mater is located between the dura mater and the inner pia mater (Ghannam and Al Kharazi, 2019). The cerebrospinal fluid (CSF) circulates around the brain and spinal cord within the subarachnoid space: that is, between the arachnoid mater and the pia mater (Khasawneh et al., 2018, Telano and Baker, 2018).

In the case of meningitis, delayed diagnosis can cause serious damage to the central nervous system (CNS) (Harvey et al., 1999, Huang and Jong, 2009). Furthermore, infection of the CNS remains a key concern in terms of treatment delivery due to the possible morbidity and mortality that can occur during therapy (Dando et al., 2014, Dorsett and Liang, 2016). Meningitis is therefore classified as a medical emergency, as it can not only cause rapid fatality but can lead to life-changing outcomes due to the harmful effects of inflammation of the spinal cord and brain (Kim, 2010, Dorsett and Liang, 2016). In addition to inflammation, meningitis is defined by the presence of polymorphonuclear cells in the CSF following meningeal infiltration by pathogenic agents (Almeida et al., 2007).

1.2 Bacterial Meningitis

The aetiological agents of meningitis include bacteria, viruses, fungi and parasites (Chávez-Bueno and McCracken, 2005, Logan and MacMahon, 2008, Akkaya et al., 2017). The most frequent forms of the disease seen worldwide are viral meningitis and bacterial meningitis, but viral infection is usually less severe (Chávez-Bueno and McCracken, 2005, Thompson et al., 2006, Yadav and Rammohan, 2020). Historically, the most frequent bacterial agents responsible for the disease are

Haemophilus influenzae type B (Hib), *Neisseria meningitidis* and *Streptococcus pneumoniae* (Oordt-Speets et al., 2018, Cain et al., 2019); although *Listeria monocytogenes*, group B *Streptococci* and *Mycobacterium tuberculosis* (TB) are also important causes of bacterial meningitis (Doran et al., 2016, Griffiths et al., 2018). In addition, *Escherichia coli* K1 strains and *Streptococcus agalactiae* are the most common causes of meningitis in neonates (Robbins et al., 1974, Johnson et al., 2002, Wijetunge et al., 2015, Chambers et al., 2021).

Bacterial meningitis presents in a variety of ways and its incidence varies by geographic region (van de Beek et al., 2016, Mustapha and Harrison, 2018). Globally, the disease is associated with high mortality and morbidity rates, and the mortality rate has remained high despite the development of many new antibacterial agents (Zunt et al., 2018). Pathogens capable of causing meningitis possess a number of virulence determinants that allow them to invade the CNS by crossing the blood–brain barrier (BBB), which usually protects the CNS from pathogens (Chávez-Bueno and McCracken, 2005, Dando et al., 2014, Herold et al., 2019).

For example, *H. influenzae* strains are classified into two subcategories according to the presence or absence of a polysaccharide capsule (Potts et al., 2019). Encapsulated strains, types A–F, express one of six capsular polysaccharides, with type B (Hib) being the most virulent (Berndsen et al., 2012). Non-encapsulated strains are characterised by their inability to react with antisera against known *H. influenzae* polysaccharide capsules and are considered non-typeable *H. influenzae* (NTHI) (Satola et al., 2007, King, 2012). The Hib strains can cause severe invasive infections including sepsis, pneumonia, cellulitis, septic arthritis, paediatric meningitis and epiglottitis (Murphy, 2010). The incidence of meningitis induced by *H. influenzae* serogroup B has significantly decreased following introduction of the *H. influenzae* type B vaccine (Giufrè et al., 2011, Suga et al., 2018).

More than 90 serotypes of *S. pneumoniae* have been reported in the literature (Henriques-Normark and Tuomanen, 2013). Some of these are known to cause comparatively mild infections like sinusitis, otitis media and bronchitis, whereas

others are associated with more invasive and severe infections such as osteomyelitis, pneumonia, sepsis, meningitis and septic arthritis (Henriques-Normark and Tuomanen, 2013). The administration of the pneumococcal conjugate vaccine (PCV), protecting against 13 invasive serotypes, has lowered the prevalence of pneumococcal meningitis infections (Daniels et al., 2016). It is administered to children below two years, whereas the pneumococcal polysaccharide vaccine (PPV) is effective in the older adult population and patients at higher risk of infection (Andrews et al., 2012, Suzuki et al., 2017).

However, amongst the bacterial aetiological agents listed above, epidemic outbreaks of meningitis can only be caused by *N. meningitidis* (Agier et al., 2017), and this organism remains the most common causative agent of bacterial meningitis (Rouphael and Stephens, 2012, Mahmoud and Harhara, 2020). It is normally a harmless commensal bacterium residing in the nasopharynx, but can sometimes invade the bloodstream and cause disease, including sepsis and meningitis (Soriani, 2017).

1.3 The Genus *Neisseria*

Species of the bacterial genus *Neisseria* which belongs to the order *Neisseriales* and phylum Proteobacterium (class β-proteobacteria) are gram-negative cocci that arrange in paired diplococcal form (Garrity et al., 2005, Hung and Christodoulides, 2013). Members of the diplococcal *Neisseriaceae* family typically have flattened opposing sides with a coffee bean shape. Based on 16S rRNA sequencing, the genus *Neisseria* is further classified into 25 species (Bennett et al., 2012, Hung and Christodoulides, 2013).

Some species are commensal organisms that live in humans and other animals but have the ability to induce opportunistic infections under certain conditions (Hung and Christodoulides, 2013). Several species of *Neisseria* are commensal with humans, including: *N. elongata*, *N. sicca*, *N. cinerea*, *N. flavescens*, *N. mucosa*, *N. perflava*, *N. polysaccharea*, *N. lactamica* and *N. subflava* (Bennett et al., 2012, Hung and Christodoulides, 2013, Rotman and Seifert, 2014). The best-studied commensal *Neisseria* species is *N. lactamica*, which colonises the human

nasopharynx and shares extensive sequence homology with pathogenic *Neisseria* species, meaning it is closely related to *N. meningitidis* (Rotman and Seifert, 2014, Zhang, 2017).

Furthermore, although *N. meningitidis* (meningococci) and *Neisseria gonorrhoeae* (gonococci) have genetic and antigenic similarities, they differ in their habitat sites of colonisation, in the types of illnesses they cause, and in the expression of surface polysaccharide capsules (Stephens, 2009, Virji, 2009, Caugant and Brynildsrud, 2020). *N. meningitidis* colonises the human nasopharynx and is a major cause of bacterial meningitis and sepsis, whereas *N. gonorrhoeae* lives on the mucosal surfaces of the urogenital tract and can cause gonorrhoea, one of the most common sexually transmitted diseases (Virji, 2009, Hung and Christodoulides, 2013, Nadel and Ninis, 2018, Marrazzo and Apicella, 2019).

1.4 Characteristics of *N. meningitidis*

N. meningitidis, more generally known as the meningococcus, is a gram-negative, non-spore-forming bacterium that is further classified as a non-motile, a-flagellate diplococcus (Castillo et al., 2011a). Under the microscope, it has a predominantly coffee bean- or kidney-shaped morphology, with a width of approximately 0.8 µm (Castillo et al., 2011a). Biochemically, this bacterium is both catalase and oxidase-positive, and is characterised by an aerobic or facultative anaerobic lifestyle (Stephens, 2009, Rouphael and Stephens, 2012). It is also possible to classify a species based on the type of sugar it utilises: for example, *N. meningitidis* produces acid from both glucose and maltose, whereas *N. gonorrhoea* produces acid from only glucose.

1.5 Epidemiology of Invasive Meningococcal Disease (IMD)

Meningococcal disease continues to be associated with a high incidence of morbidity and mortality (Agrawal and Nadel, 2011). Worldwide, it is estimated that 135,000 deaths occur annually due to invasive meningococcal disease (IMD), out of more than 1.2 million cases diagnosed each year (Jafri et al., 2013, Martinón-Torres, 2016). As a matter of additional concern, 12–20% of patients who survive

the initial disease suffer from various long-term complications such as loss of vision, neurological disorders, deafness, kidney failure, lung problems, paralysis, amputation, epilepsy and memory loss (Pollard, 2004, Abio et al., 2013).

N. meningitidis may enter the bloodstream and be carried from the throat to ultimately penetrate the CNS and cause an infection that can overpower the body's defences. Approximately 1–10% of the population is thought to carry *N. meningitidis* in their throat at any given time (Caugant et al., 1994, Nguyen and Ashong, 2021), but carriage rates of adults who are asymptomatically harbouring the bacterium are higher in epidemic areas (10–25%) (Rude et al., 2019). The reasons for transition from asymptomatic carriage to invasive disease are incompletely understood; however, it is thought that various factors, including the genetic and capsular composition of pathogenic strains, play a role in the process (Gasparini et al., 2012). The bacterium can be transmitted through respiratory droplets to other individuals in close contact with a carrier, especially in overcrowded settings such as schools, universities, and military camps (Meyer and Kristiansen, 2016).

The annual prevalence of meningitis, as well as sepsis, varies considerably by region: from as low as 0.5–1 up to 1,000 cases per 100,000 population (Caugant and Maiden, 2009, Pizza and Rappuoli, 2015, Burman et al., 2019). The reasons for this epidemiological and geographical variation are not well understood, but environmental factors such as humidity have been suggested, and some social behaviours are thought to contribute particularly those that lead to close contact between individuals. Age is also a recognised risk factor. Infection rates are higher in young children than in adults, an observation ascribed to the waning of protective maternal antibodies combined with an absence of antibodies developed via carriage of commensal *Neisseria* or weakly pathogenic *N. meningitidis* (Erlich and Congeni, 2012, Bosis et al., 2015). However, older children and adolescents are also known to be particularly susceptible to meningitis due to a lack of protective antibodies, especially during epidemic outbreaks (Caugant and Maiden, 2009, Pelton, 2016, Burman et al., 2019).

The incidence of meningococcal disease in Europe, Australia and North America ranges from 0.3–3.0 cases per 100,000 individuals annually (Dwilow and Fanella, 2015, Pelton, 2016), whereas the rate can reach 10–1,000 cases per 100,000 population during epidemics in sub-Saharan Africa, which is known as the "meningitis belt" (Djingarey et al., 2012, Vuocolo et al., 2018). In the UK, Public Health England (PHE) reported 525 confirmed cases of IMD during 2018/2019 (Public Health England, 2019), with this count falling to 461 cases in 2019/2020 (Public Health England, 2021). During 2020/2021, 80 cases were confirmed, indicating a fall in incidence of the disease (UK Health Security Agency, 2022).

1.6 Historical Background of Invasive Meningococcal Disease (IMD)

In1661, the neurologist Thomas Willis provided the first accurate description of an epidemic of meningitis (Eadie, 2003, Tyler, 2009). In 1768, Robert Whytt recorded a type of meningitis caused by *M. tuberculosis*, which he referred to as "dropsy in the brain" (Whytt, 1768), and he is often credited with the first description of meningitis since this form appears to be more easily recognisable and accurate. In the early 19th century, the first clinical verification of meningitis was described by Vieusseux upon the occurrence of several deaths in the vicinity of Geneva, Switzerland (Vieusseux, 1805). Another breakthrough was achieved in 1884 by two Italian pathologists, Ettore Marchiafava and Angelo Celli, who discovered that gram-negative diplococci were present in the CSF of meningitis patients (Marchiafava and Celli, 1884). Shortly after this, in 1887, the Austrian pathologist Anton Weichselbaum managed to isolate *N. meningitidis* from a patient's CSF and characterise it as an aetiological agent (Stephens, 2009, Pace and Pollard, 2012). Weichselbaum succeeded in explaining, for the first time, the aetiological origin of meningococcal disease and its association with the bacterium then named 'diplococcus intracellular meningitidis', as well as describing "epidemic cerebrospinal meningitidis" outbreaks (Weichselbaum, 1887, de Souza and Seguro, 2008). Subsequently, Albert Neisser renamed the organism *N. meningitidis* following the characterisation of the related bacterium *N. gonorrhoeae* in 1879 (Neisser, 1879, Ala'Aldeen and Turner, 2006).

In the early 1900s, mortality rates from IMD during meningococcal outbreaks were approximately 75% (Flexner, 1913). One early treatment used was serum therapy, developed by Flexner and Joblin, which resulted in reduction of the mortality rate by about 30% (Flexner, 1913). Upon their release into medical practice, the sulphonamide antibiotics were embraced for the treatment of meningococcal infections (Schwentker et al., 1937), but resistance quickly developed, leading to the development of meningococcal vaccines in the 1960s (Artenstein et al., 1970).

1.7 Global Distribution of *N. meningitidis* Serogroups

Several serogroups of *N. meningitidis* have been used to classify different strains of the bacterium, characterised by variation in the molecular structure of the outer capsule (Borrow et al., 2017). The six meningococcal serogroups mainly responsible for IMD show considerable variation in their global distribution (Borrow et al., 2017) (Figure 1.1), and the reasons for these geographical differences are not well understood. Interestingly, some research has linked this variation to age group as well as geographical region (Nadel, 2012).

Serogroup A is strongly associated with outbreaks of meningococcal disease in the "meningitis belt" in sub-Saharan Africa, which extends from Senegal in the west to Ethiopia in the east (Mustapha and Harrison, 2018, Soeters et al., 2019). Outbreaks caused by *N. meningitidis* serogroup A occur mostly in dry seasons, every 8–10 years, with a 10% annual incidence of infection in the most serious epidemics (Stephens et al., 2007, Rouphael and Stephens, 2012). Despite the lack of specifically-identified causes, environmental factors such as high humidity and dust are thought to contribute (Rouphael and Stephens, 2012, Gabutti et al., 2015). There have also been reports of serogroup A infections in a number of Eurasian countries, including Russia, India and China (Stephens et al., 2007). In recent years, however, the introduction of the MenAfriVac vaccine in sub-Saharan African countries has greatly reduced the incidence of serogroup A IMD (Novak et al., 2012, Mustapha and Harrison, 2018).

Although serogroup B is reportedly less infectious than serogroup A, it remains the leading cause of meningitis in European countries and can lead to serious health

problems, morbidity and mortality (Tzeng and Stephens, 2000, Harrison et al., 2009). This serogroup is responsible for about 73% of IMD cases in European nations and 40% in the United States (Hedari et al., 2014), marking it out as the major aetiological agent of meningococcal disease in urbanised countries. For example, between 2014 and 2018, most clinical laboratories in England and Wales attributed meningococcal infections to serogroup B (Public Health England, 2021). Age is again a factor for serogroup B disease: in the United States, approximately 57% of cases are believed to affect infants (Judelsohn and Marshall, 2012).

Serogroup C meningococci are recognised as contributing to small-scale IMD outbreaks around the world, especially localised clusters of the disease in Europe and North America (Harrison, 2006). Fortunately, the MenC monovalent conjugate vaccine has helped to significantly reduce the incidence of serogroup C outbreaks in areas where it has been administered (Borrow et al., 2013, Cohn et al., 2013).

N. meningitidis serogroup Y has been identified as a common cause of IMD in the United States, where it accounts for about 30% of all cases; and it has also been recently reported more frequently in the Europe and the UK (Schoen et al., 2007, Bröker et al., 2015, Nadel and Ninis, 2018). Similarly, serogroup X is becoming more prevalent in parts of Africa, causing small- to medium-scale outbreaks (Gagneux et al., 2002, Boisier et al., 2007, Harrison et al., 2009).

Historically, serogroup W has accounted for only 1–2% of all IMD cases in Europe (Bröker et al., 2015). In 2000, serogroup W emerged in Saudi Arabia specifically among Hajj pilgrims leading it to become a more prominent cause of IMD worldwide due to the affected pilgrims returning to their home countries (Mustapha et al., 2016). This was held responsible for outbreaks of serotype W disease in Europe, the USA, Asia, Africa and the Middle East (Lingappa et al., 2003, Mustapha et al., 2015, Ladhani et al., 2015). Infections caused by serogroup W were also reported in 2002/2003 among children below the age of five in Burkina Faso (Traoré et al., 2006). Although global serogroup W cases have declined significantly, a surge in serogroup W IMD has been reported since 2009 in Europe, Australia, the UK, South America and Africa (Booy et al., 2019). For example, serogroup W caused

15% of all IMD cases in England and Wales in 2013, and 15% of patients died as a result of the fast endemic spread of a single clone belonging to the W sequence type 11 (W ST-11) complex (Mustapha et al., 2015, Ladhani et al., 2015). The MenACWY vaccine has therefore been introduced for adolescents in the UK, in response to the aforementioned recent epidemiological changes in carriage and invasive disease associated with *N. meningitidis* serotypes Y and W.

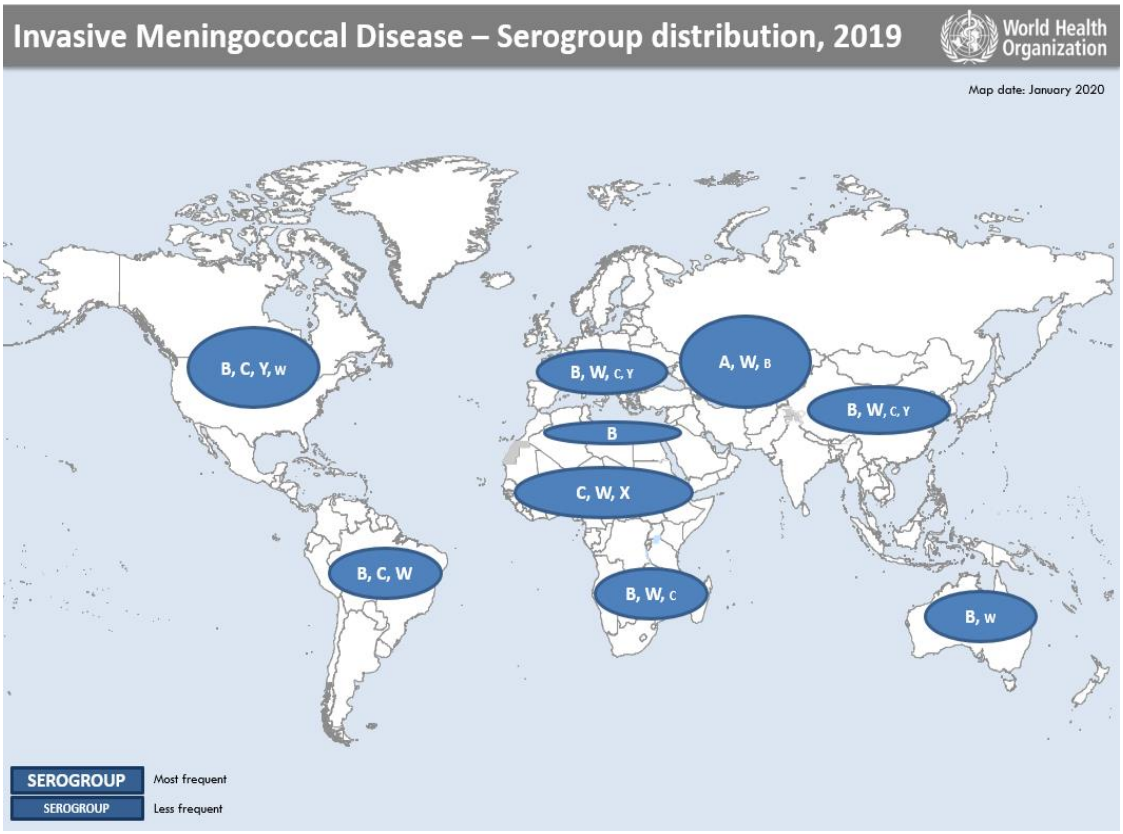

Figure 1.1: Global distribution of invasive meningococcal disease serogroups (WHO, 2019).

1.8 Molecular Classification of *N. meningitidis*

As described above, *N. meningitidis* isolates were traditionally classified into serological groups based on variation in the antigenic properties of their capsule polysaccharides. Twelve serogroups (A, B, C, E, H, I, K, L, M, W, X, Y and Z) have been identified on this basis, six of which (A, B, C, W, X, and Y) account for about 90% of all deadly meningococcal infections worldwide (Pollard and Levin, 2000, Stephens et al., 2007, Stephens, 2009).

In addition to variations in capsule polysaccharides, other antigenic meningococcal surface components have been used for molecular classification of *N. meningitidis* subtypes. Specifically, these are lipopolysaccharides (LPS) also known as lipooligosaccharides (LOS) and two outer membrane proteins (OMPs): major outer membrane protein P.IB (PorB) and major outer membrane protein P.IA (PorA), which are used to define serotypes and serosubtypes, respectively (Frasch et al., 1985, Stephens et al., 2007). These molecular typing techniques were perhaps more prevalent before the advent of modern genotyping approaches, but are nonetheless important in identifying and characterising meningococcal strains.

Based on variations in expression of LOS, *N. meningitidis* strains can be grouped into 12 different immunotypes (Mandrell and Zollinger, 1977, Jennings et al., 1999, Stephens, 2009). These reflect differences in the composition of the three variable oligosaccharide chains of meningococcal LOS (Mubaiwa et al., 2017), and can be determined, for example, by whole-cell ELISA (Scholten et al., 1994). Three of these immunotypes (L1, L8, and L10) are usually associated with carriage, whilst three others (L3, L7 and L9) account for two-thirds of invasive isolates recovered from blood and CSF (Jones et al., 1992, Hill et al., 2010). Relatedly, 20 serotypes have been distinguished on the basis of variation in PorB (class 2/3 antigen), and 10 serosubtypes on the basis of PorA (class 1 antigen) variation (Ala'Aldeen and Turner, 2006).

Other serotyping techniques have been developed based on immunoglobulin A1 (IgA1) proteases and pili (Stephens et al., 1985, Manchanda et al., 2006). However, due to the high frequency of antigenic and phase variation in the outer membrane structures of meningococci, alternative genetic approaches have been developed for the characterisation of *N. meningitidis* strains.

This has led to major progress in understanding the genetic basis of meningococcal disease. Such approaches have made it possible to identify the unique genes associated with *N. meningitidis* and recognise the involvement of other *Neisseria* species. Other methods are available to assist in classification, such as multi-locus enzyme electrophoresis (MLEE), an electrotyping technique developed based on the

presence of cytosolic enzyme isoforms with varying molecular weight and electrophoretic mobility (Maiden et al., 1998, Yazdankhah and Caugant, 2004, Ala'Aldeen and Turner, 2006). The MLEE technique is used to stratify genetically highly diverse, connected strains of serogroup A into different subgroups; and for serogroups B and C, to align lineage and clonal groups or complexes. However, only a few clonal complexes have been reported as being responsible for the majority of meningococcal disease cases.

An advanced bioinformatics tool, multilocus sequence typing (MLST), has been used in *N. meningitidis* molecular typing for cluster analysis, and to predict epidemiological trends (Maiden et al, 1998, Birtles et al., 2005, Brehony et al., 2007). In the original form of this methodology, small fragments (433–501 bp) were amplified and sequenced from seven housekeeping genes (*abcZ*, *adk*, *aroE*, *gdh*, *fumC*, *pdhC* and *pgm*), with a specific allele number then assigned for each sequence, allowing for classification by sequence type (ST). With the widespread availability of whole-genome sequencing, an expanded number of genes can now be considered, allowing for more in-depth analysis of meningococcal strains (Maiden et al., 1998, Feavers et al., 1999, Stephens et al., 2007, Stephens, 2009). Thus, other genes such as porins (*porA*, *porB*) and *fetA* are now sometimes also included for 'fine tuning' of meningococcal sequence typing (Mustapha et al., 2015), given the increasing availability of sequence data.

As well as being classified into sequence types (STs) according to the nucleotide sequences of the seven MLST housekeeping gene fragments (Maiden et al., 1998), meningococcal clones with at least four identical loci are further grouped into clonal complexes (CCs), with most of these being associated with a single core ST. In total, over 10,000 STs are known, and these have been grouped into more than 40 CCs (Waśko et al., 2015). Importantly, the majority of IMD is caused by a small subset of CCs, known as hyperinvasive lineages (Potts et al., 2018), which are characterised by high disease to carriage ratios. For example, the ST-5 and ST-8 complexes have ratios of 19.5 and 24.5, respectively (Siena et al., 2018). Relatedly, the ST-11 CC is currently of worldwide concern due to rapid expansion of these strains along with evidence for increasing carriage rates (Oldfield et al., 2017).

1.9 Clinical Manifestation of Invasive Meningococcal Disease (IMD)

The immune system is the body's most effective method of defence against bacterial colonisation. As part of the innate immune response, protection against *N. meningitidis* is conferred by epithelial and phagocytic cells, as well as complement proteins (Gasparini et al., 2015, Pizza and Rappuoli, 2015, Hodeib et al., 2020). However, *N. meningitidis* can use several different strategies to evade the immune system and adapt to the host environment, enabling it to form colonies, survive in the bloodstream, and replicate in the CSF (Gasparini et al., 2015, Hodeib et al., 2020). Uncontrolled *N. meningitidis* multiplication can occur within the CSF due to the lack of complement proteins and immunoglobulins in this environment; however, polymorphonuclear leukocytes are infused into the area by means of the local inflammatory response (Stephens et al., 2007, Coureuil et al., 2013).

Early clinical signs of meningococcal disease include fever, headache, photophobia, stiff neck and rash; then purpura fulminans, also known as non-haemorrhagic rash. In cases of bloodstream infection, purpura fulminans precedes the occurrence of significant inflammation in the CSF (Coureuil et al., 2013, de Castro and Ramos-e-Silva, 2020). Other complications of meningitis can be observed, for instance, seizures and/or convulsions can act as independent symptoms of infection; and in some cases, arthritis and pericarditis may be observed (Brandtzaeg and van Deuren, 2012, Vázquez et al., 2016). Meningococcal infections are additionally characterised by rapid bacterial multiplication and consequent septic shock, which can lead to extensive thrombosis, vascular leakage and cardiovascular system failure (Coureuil et al., 2013).

Overall, IMD has three major clinical manifestations: meningitis without sepsis; meningitis with sepsis; and sepsis without meningitis. The first of these, meningitis without sepsis, is the most common presentation and constitutes up to 45% of all IMD cases, with a relatively low mortality rate (approximately 5%) compared to the other two (Brandtzaeg and van Deuren, 2012). Moreover, meningitis without sepsis is commonly experienced in more developed countries, whereas meningitis with sepsis occurs more frequently in developing nations (Brandtzaeg and van Deuren,

2012). Accumulation of meningococci in the bloodstream, together with their components (particularly LOS), produces inflammation. This can result in an excessive innate immune response, characterised by elevated levels of inflammatory cytokines such as IL-6, IL-8 and IL-10 (Hill et al., 2010), potentially contributing to circulatory collapse due to the resultant intravascular clotting and thrombotic lesions (Stephens et al., 2007).

1.10 Diagnosis and Treatment

In order to make a laboratory diagnosis of *N. meningitidis*, blood and CSF samples must be cultured (Castillo et al., 2011b). The bacterium is cultured using specialised environmental conditions together with enriched media containing lysed blood cells: for example, blood agar, chocolate agar or Mueller–Hinton agar. Plates are incubated under controlled conditions, at a pH from 7.0 to 7.4, at a temperature from 35–37°C, and with 5% CO_2 (Garrity et al., 2005, Ala'Aldeen and Turner, 2006, Castillo et al., 2011b).

Laboratory culture is thus the most widely used method for diagnosing *N. meningitidis* infection. Colonies on blood agar are generally spherical, greyish, clear, smooth, non-haemolytic and lustrous. For more immediate detection and identification of *N. meningitidis*, other approaches have been applied on a wider scale in the medical microbiology laboratory; for example, to identify the soluble *N. meningitidis* antigen in CSF taken from patients. The polymerase chain reaction (PCR) can also be applied to the detection of pathogens related to bacterial meningitis. This approach was first developed in the 1980s, as an indispensable tool among other molecular biology approaches, to amplify target DNA sequences from patient samples (UK Health Security Agency, 2021). Various PCR-based assays are now routinely used in the diagnosis of clinical *N. meningitidis* infections, as a complement to conventional culture-based techniques (Castillo et al., 2011b).

In general, patients suspected of having invasive meningococcal disease (IMD) are administered intravenous antibiotics, thus minimising the risk of morbidity and mortality. This risk is increased if clinical diagnosis and treatment are delayed (Sudarsanam et al., 2013, Sarfatti and Nadel, 2015), so, although clinical symptoms

and microbiological testing are both deemed critical for accurate diagnosis of IMD, antibiotic treatment of patients must be started early, before laboratory results are obtained. Meningitis is currently treated using penicillin or ceftriaxone, a third-generation cephalosporin antibiotic (John, 1994, Faella et al., 2006, Sudarsanam et al., 2013, Sarfatti and Nadel, 2015). A moderate dosage of corticosteroid may also be used alongside the antibiotic treatment, to reduce inflammation and attempt to mitigate neurological complications (Brouwer et al., 2010, Sarfatti and Nadel, 2015, McGill et al., 2016). However, bacterial meningitis is becoming a more serious problem due to the increasing emergence of multidrug-resistant infections, demonstrating the need to search for effective new medicines (Hoffman and Weber, 2009).

1.11 Pathogenesis of Meningococcal Infection

The mechanisms responsible for nasopharyngeal colonisation by *N. meningitidis* remain incompletely understood, as do the factors that influence the progression from commensal colonisation to IMD, including its entry into the bloodstream by crossing the nasopharyngeal mucosa. However, it is thought that meningococcal virulence factors, susceptibility of the host and environmental conditions all play respective roles in disease transition (Pace and Pollard, 2012, Schoen et al., 2014). The pathogenesis of *N. meningitidis* is evidently a complex process, and illustrates how under certain conditions bacteria can invade the oropharyngeal and digestive mucosal membranes, remain and survive in the blood, and eventually cross the BBB (Coureuil et al., 2012).

N. meningitidis is categorised as an epicellular, rather than an extracellular, bacterium because it is able to attach tightly to cell membranes, induce extensions on the host cell membrane and proliferate within host cells (Dumenil, 2011). Several steps are therefore known to be involved in the interaction between meningococci and their human host.

Initially, *N. meningitidis* adheres to cells of the host respiratory epithelium after colonising the ciliated exterior surface of the nasopharyngeal epithelium. Invasion of the respiratory tract can then occur (Doran et al., 2016, Weyand, 2017). From

there, meningococci favour invasion of the intravascular region, through which they can gain entry into the bloodstream and proceed to multiply therein, potentially leading to sepsis (Pathan et al., 2003, Doran et al., 2016). As shown in Figure 1.2, meningitis occurs if the bacteria subsequently traverse the BBB and enter the subarachnoid space.

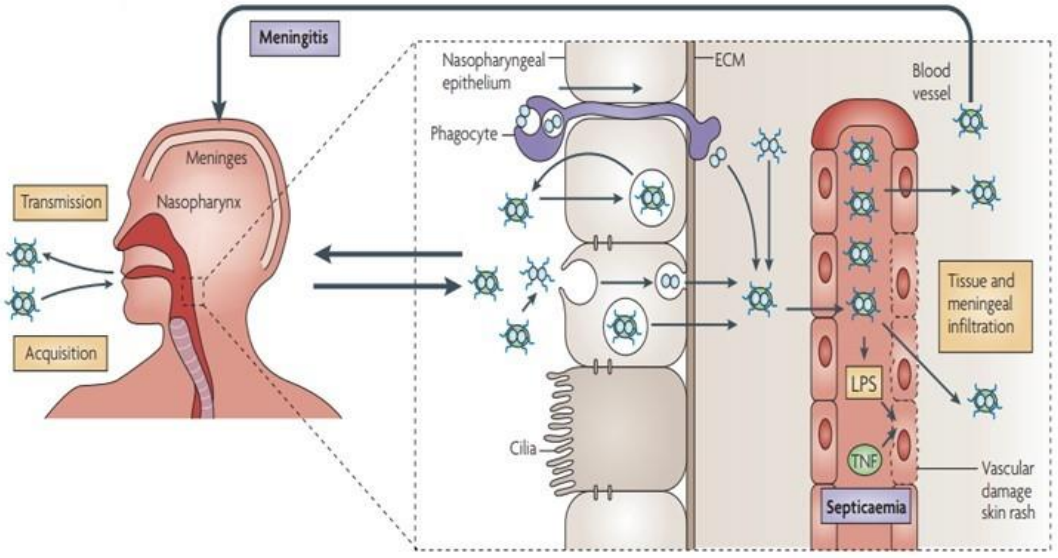

Figure 1.2: Stages of pathogenic *N. meningitidis* infection. The meningococcus, generally transmitted through respiratory droplets or direct oral contact, can invade cells of the human oropharynx and adhere to nasopharyngeal tissue, which occurs via meningococcal adhesins including the type IV pili (TFP). Meningococci can subsequently invade nasopharyngeal cells and enter the circulation, penetrating into deeper tissues and causing meningococcaemia in the bloodstream. Usually, bacteria entering the bloodstream would be killed by the complement system, but encapsulated bacteria have the potential to proliferate uncontrollably in this environment and be disseminated to other areas of the body, resulting in inflammation and sepsis. In some cases, *N. meningitidis* crosses the BBB, reaches the CSF and enters the meninges, where it can cause meningitis (Virji, 2009).

1.11.1 Adhesion to and Invasion of the Respiratory Mucosa

N. meningitidis normally resides in the nasopharynx (Figure 1.2) and is usually transmitted from one individual to another via infected respiratory droplets (Stephens, 2009, Chang et al., 2012). The human nasopharyngeal epithelial barrier thus forms the key source for meningococcal transmission (Virji, 2009, Barrile et al., 2015). Invasion of the mucosal membranes of the host's respiratory tract by *N. meningitidis* is the initial phase associated with the carriage state, as well as with the development of IMD (Rouphael and Stephens, 2012, Schoen et al., 2014). The reasons why some individuals develop infectious disease and others remain healthy

are as yet unexplained, although human genetic polymorphism has been identified as a potential mechanism, at least in relation to purpura fulminans development (Brouwer et al., 2009, Wright et al., 2009). In addition, oropharyngeal invasion by meningococci can lead, within several weeks of acquisition, to an antibody reaction comprising three major groups of immunoglobulins, which may serve as an immunisation activity (Yazdankhah and Caugant, 2004).

Several specific biomolecules are required by *N. meningitidis* for effective colonisation and infection of host organisms, and these are the major factors responsible for invasion of the host's mucosal sites (Stephens, 2009, Hill et al., 2010). *N. meningitidis* is unique among *Neisseria* species in its capacity to produce a number of such virulence factors. Furthermore, encapsulated meningococci, which are surrounded by a protective polysaccharide capsule, can survive in the bloodstream or elsewhere within the host, and the capsule might additionally confer resistance to dehydration (Tzeng et al., 2016).

Colonisation by *N. meningitidis* starts with its adhesion to epithelial cells of the nasopharynx, and meningococcal type IV pili (TFP) are known to play a significant role in enhancing this bacterial attachment. Bacterial TFP have similarly been implicated in a variety of infective processes, including attachment to endothelial cells, bacterial aggregation, twitching motility, bacterial movement and natural transformation (Carbonnelle et al., 2006, Pizza and Rappuoli, 2015).

Initial meningococcal colonisation involves adhesion to non-ciliated epithelial cells within the nasopharynx: a process initiated by TFP, which extend beyond the bacterial capsule (Kirchner et al., 2005, Sutherland et al., 2010). The minor pilin subunit PilC is located at the top of the pilus strand, and binds to the CD46 receptor on the surface of the host's epithelial cells (Källström et al., 1997). Once attached to the epithelial surface, meningococci are then able to aggregate, or adhere to each other, and proliferate to form microcolonies at the original attachment site (Mikaty et al., 2009, Schwerk et al., 2012). Contact-dependent downregulation of bacterial capsular biosynthesis also occurs, and is crucial to promote meningococcal binding,

permit microcolony formation and establish the carriage state on human mucosal surfaces (Deghmane et al., 2002, Yasukawa et al., 2006, Tzeng et al., 2016).

During this stage, multiple bacterial surface adhesins mediate attachment to host cells, including: autotransporter adhesin NhhA (NhhA), *Neisseria* adhesin A (NadA), opacity outer membrane proteins (Opa, Opc), the autotransporter meningococcal serine protease A (MspA/AusI), and adhesion and penetration protein (App). It is known that NhhA binds heparan sulphate proteoglycans (HSPGs), laminin and vitronectin, but the specific cellular receptors targeted by NadA, MspA and App are currently under investigation (Scarselli et al., 2006, Hill et al., 2010, Hung and Christodoulides, 2013). However, adhesins are able in a general sense to jointly interact with extracellular matrix proteins such as fibronectin, vitronectin and integrins (Virji et al., 1996, Sa E Cunha et al., 2010). Therefore, once attachment and colonisation are established, meningococci can penetrate the mucosal epithelium.

1.11.2 Spread and Survival in the Bloodstream

Once the mucosal barrier has been breached, *N. meningitidis* can access the bloodstream and potentially go on to establish a variety of infections. Invading meningococci might induce inflammatory responses, complement activation or coagulation cascades (Hill et al., 2010, Coureuil et al., 2012). In particular, the lipid A component of meningococcal LOS contributes to activation of comparatively intense inflammatory reactions, including the induction of chemokines and cytokines linked to meningococcal sepsis (Brandtzaeg et al., 2001, Braun et al., 2002, Hill et al., 2010, Lewis and Ram, 2014). Apart from this, meningococcal outer membrane vesicles (OMVs) play a vital role in triggering bacterial survival within the host. These OMVs consist of lipids, outer membrane proteins, LOS and some periplasmic proteins (Lappann et al., 2013). Shedding occurs via a controlled process that allows for budding and release without significant damage to cellular membrane integrity (Schwechheimer et al., 2013), and release of OMVs is enhanced as part of bacterial stress responses (Lappann et al., 2013). Upon exposure to meningococcal LOS, pro-inflammatory cytokines, including tumour necrosis

factor-α (TNF-α), are released in host cells, and the production of reactive oxygen species (ROS) is elevated in association with meningococcal LOS (Schubert-Unkmeir et al., 2010). In most cases, this induction is associated with a toll-like receptor 4 (TLR-4) interaction (Chow et al., 1999).

In addition to the above, endothelial cell adhesion mediated by meningococcal TFP induces signalling pathways that ultimately result in widespread destruction of intercellular junctions, thereby facilitating meningococcal passage through the BBB (Coureuil et al., 2009, Doran et al., 2016). A two-stage process occurs at the site of initial bacterial cell attachment. Firstly, TFP-mediated interaction with one or more host receptors promotes formation of a cortical plaque consisting of the membrane receptor and bacterial structural proteins. Secondly, receptor activation induces intracellular signalling to remodel the host cell's cytoskeleton and recruit additional transmembrane components (Merz et al., 1999, Coureuil et al., 2010, Coureuil et al., 2012). It has also clearly been shown that *N. meningitidis* has a strong capability for recruitment of the Par3/Par6/PKCζ polarity complex, which is normally involved in the creation of tight linkages between endothelial cells. Meningococci essentially hijack this signalling complex to induce the cellular remodelling that allows them to invade the endothelial layer (Coureuil et al., 2009).

Meningococci within the bloodstream also use specific strategies to overcome host defences, which in this context include active serum bactericidal antibodies (SBA), opsonophagocytosis and complement-mediated lysis (Kahler et al., 1998, Geoffroy et al., 2003, Hellerud et al., 2010, Hill et al., 2010). Meningococcal factor H-binding protein (fHbp) and PorA can bind the human proteins complement factor H and C4b-binding protein alpha chain (C4bp), respectively, resulting in bacterial resistance to complement-mediated killing within the blood (Jarva et al., 2005, Madico et al., 2006). Binding of meningococcal Opc to vitronectin additionally promotes tolerance of the bacterium to serum-mediated killing (Sa E Cunha et al., 2009, Sa E Cunha et al., 2010). The host immune response can also be modulated by the bacterial capsule and LOS, as well as many adhesin proteins (Franzoso et al., 2008, Hill et al., 2010). With respect to the former, immune evasion can result from changes in the meningococcal capsule composition or structure (for example, hypo-

or hyper-encapsulation, antigenic "switching", or acetylation) (Deghmane et al., 2002, Tzeng et al., 2016).

1.11.3 Crossing the Blood–Brain Barrier and Penetration of the Meninges

The BBB is considered to be both a functional and structural barrier, and offers effective protection to the CNS against various pathogens, including microbes, and toxins (Abbott et al., 2010, Al-Obaidi and Desa, 2018). Its main function is to regulate the movement of substances such as nutrients between the brain and circulatory system (Kim, 2008, Abbott et al., 2010), and it represents the first line of defence for the CNS against noxious agents (Abbott, 2002, Zhang et al., 2021). The BBB is composed of a range of cell types, including microvascular endothelial cells (MVECs), which are located at the interface between the blood and the brain. Acting together, these cells are able to form an effective barrier since they have tight junctions between them. Endothelial cells in the human brain are characterised by low rates of pinocytosis as well as the closeness of their junctions, as shown in Figure 1.3 (Dando et al., 2014).

Adhesion of *N. meningitidis* to these endothelial cells of the BBB is an important first stage in meningeal penetration. Initial attachment is greatly influenced by two related factors shear stress and blood flow rate (Mairey et al., 2006, Bernard et al., 2014, Borkowski et al., 2020), but once such attachment has taken place, meningococci can use several mechanisms to cross the barrier and enter the CNS. In some cases, adhesin–receptor interactions activate cellular signalling processes that facilitate meningococcal penetration by inducing pericellular (between cells) transcytosis; i.e., bacterial passage through the endothelial layer by transcellular transport, which occurs passively (Hill et al., 2010). Alternatively, bacteria can utilise the paracellular pathway to cross the BBB by opening tight junctions, or directly inducing cytotoxicity, to cause disruptions in the endothelial barrier and allow them to cross into the CNS as shown in Figure 1.3 (Coureuil et al., 2009). Thus, paracellular access of *N. meningitidis* to the CNS involves damage to host cells that induces BBB permeability (Doran et al., 2016). Finally, *N. meningitidis*

can infect phagocytes (Trojan-horse mechanism) and be transported intracellularly (Kim, 2008).

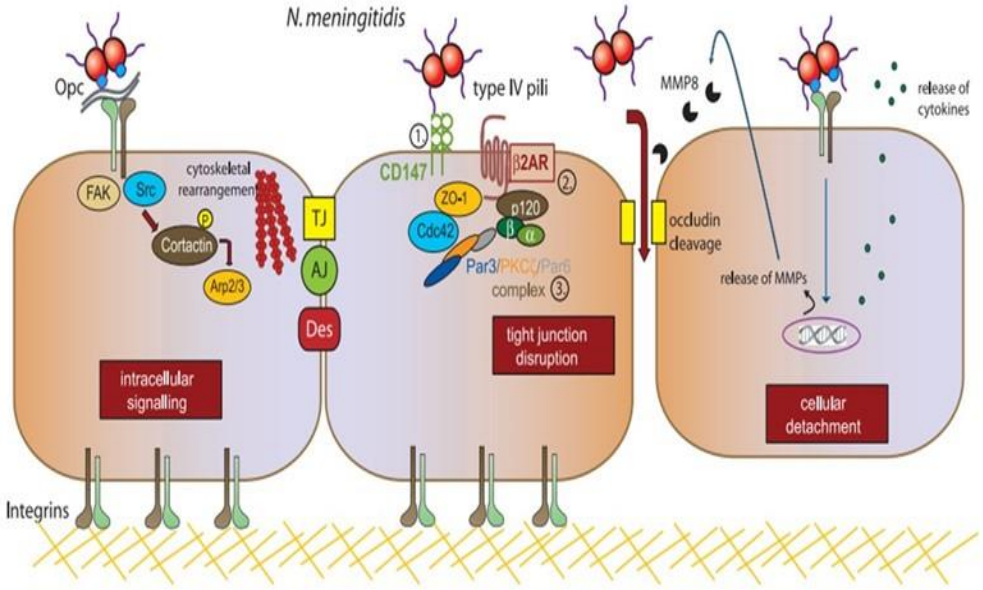

Figure 1.3: Diagram illustrating the interaction of *N. meningitidis* with brain endothelial cells and activation of signalling pathways. Meningococci initially bind to the surface of host cells, then proliferate and create small aggregates known as microcolonies at the site of attachment. These aggregates lead to the formation of cortical plaques that manifest together with the appearance of CD147, which triggers spreading of the microcolonies. Multiple host signalling pathways are activated in the brain endothelial cells by *N. meningitidis*: (1) Recruitment of the CD147 receptor to the cell surface; (2) Stimulation of the β2-adrenoceptor (AR)/β-arrestin pathway; (3) Parallel activation of c-Src, leading to ectoptic activation of the polarity complex Par3/Par6/PKCζ. The recruitment of tyrosine kinases (c-Src and FAK) also causes activation and phosphorylation of the cortactin/Arp2/3 complex resulting in rearrangement of the cytoskeleton. Moreover, meningococcal infection also targets the tight junction protein blocking, which can be cleaved. Diagram adapted from Schubert-Unkmeir (2017).

Other cells of the BBB, astrocytes and microglia, work together to regulate the effectiveness of the barrier formed by MVECs, and their activity greatly influences the ability of microorganisms to traverse the BBB (Kim, 2008, Dando et al., 2014). Astrocytes show antimicrobial activity, such as indoleamine 2,3-dioxygenase activity, which is thought to be responsible for protection against movement of microorganisms across the barrier. Pericytes modulate brain signal transduction pathways, and these too affect the ability of bacteria and other microorganisms to traverse the BBB, as shown in Figure 1.4 (Kim, 2008). If bacteria do reach the brain, they are recognised by immune cells, which then become activated. Circulating granulocytes and monocytes/macrophages also infiltrate the infected brain (Doran et al., 2016).

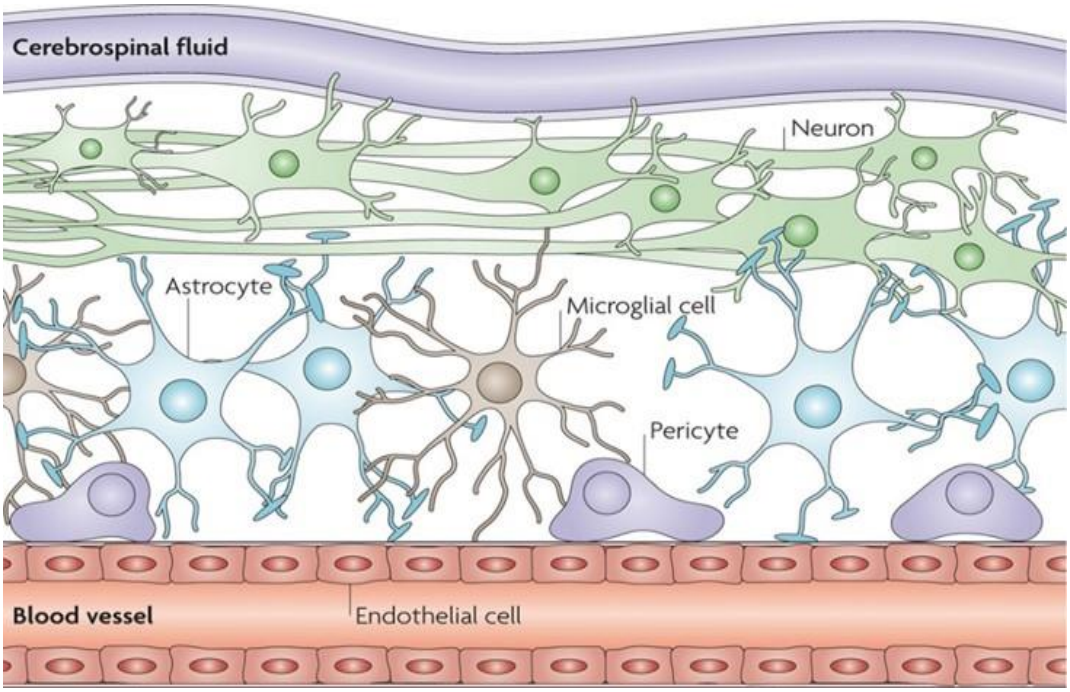

Figure 1.4: Structure of the blood–brain barrier. The blood–brain barrier (BBB) consists of microvascular endothelial cells, astrocytes, microglia and pericytes. It creates an environment that regulates the flow of molecules in and out of the brain, and defends the CNS from small particles and contaminants that propagate through the bloodstream, and from penetration by microorganisms (Kim, 2008).

1.11.4 *N. meningitidis* in the Subarachnoid Space

Various host receptor factors regulate *N. meningitidis* entry into the subarachnoid space, where the bacterium can survive and induce an inflammatory response, leading to pathophysiology including further disruption of the BBB and pleocytosis (Van Amersfoort et al., 2003, Kim, 2008). According to Engelhardt (2008), bacteria can multiply rapidly upon reaching the CSF due to the weakened host defences within this environment. Multiple factors contribute to this compromised host defence, including low levels of complement proteins and immunoglobulins within the CSF, as well as reduced opsonic capacity. Together, these factors lead to a reduction in host immunity and a diminished capacity to destroy bacteria through phagocytosis.

Thus, meningococci entering the subarachnoid zone cannot easily be controlled, as this space is an immunologically privileged site. Here, invading bacteria release large amounts of endotoxin (Brandtzaeg et al., 1989, Bjerre et al., 2003, Stephens et al., 2007), which in most cases remains and accumulates within the subarachnoid space. Furthermore, the associated disruption of the microvascular endothelium can cause microvascular thrombosis, hypotension, severe tissue damage, systemic shock, multiple organ failure and death (Van Deuren et al., 2000, Stephens et al., 2007).

1.12 Prevention of Invasive Meningococcal Disease (IMD)

Vaccines have historically been one of the most cost-effective ways of preventing disease and reducing IMD cases and deaths. As a result of the development and use of meningococcal vaccines, significant progress has been made in preventing and controlling the disease. The emergence of new technologies and the strengthening of vaccine delivery systems could save millions of lives and improve the health of populations in developing countries (Dretler et al., 2018, Vuocolo et al., 2018).

1.12.1 Capsule Polysaccharide Vaccines

Historically, Historically, vaccines based on capsular polysaccharides were designed and employed against specific *N. meningitidis* serogroups including A, C,

Y and W. Capsule based vaccines generate effective responses in terms of protective antibodies against disease-associated strains, and remained effective during the 1960s and 1970s (Gotschlich et al., 1969, Gold et al., 1977). However, these vaccines have three important limitations. Firstly, because polysaccharide antigens cannot stimulate T cells, they cannot enhance mutation or antibody class switching in the induction of immunological memory, particularly in children under two years of age (Gold et al., 1975, Vinuesa et al., 2001). Secondly, and relatedly, they cannot induce long-term immunological memory (Gotschlich et al., 1969) and have poor immunogenic capability; which again especially applies in children under two years of age (Bilukha and Rosenstein, 2005). Thirdly, since they only have short-term protective capability, repeat doses are required every four years. This raises the possibility of hyporesponsiveness; that is, attenuation of the SBA response against *N. meningitidis* (MacDonald et al., 1998, Pollard et al., 2009, Pace and Pollard, 2012). So, although the serogroup-specific protection provided by these vaccines is effective in adults, they are ineffective in young children beyond the short term (Durando et al., 2015).

1.12.2 Conjugate vaccines

As a result of the short-lived memory problem with capsule-based vaccines, it was required to consider alternative approaches for producing long-term meningococcal disease protection (Pollard et al., 2009, Trotter and Maiden, 2009). It is now well established that conjugate vaccines are most effective in children under two years, where they are able to reduce nasopharyngeal carriage to a significant level and are consequently able to create herd immunity (Jódar et al., 2002, Snape and Pollard, 2005). As a result, these vaccines produce immunity from birth, induce a memory of immunity, provide longer-lasting protection and provide a booster response with subsequent dosages (Borrow et al., 2017).

The introduction of the meningococcal conjugate vaccine against serogroup C, MenC, in 1999 has led to a significant reduction in morbidity and mortality for IMD caused by *N. meningitidis* strains of that group. Following the introduction of the vaccine in the UK, researchers observed a 66% reduction in meningococcal

infections by serogroup C (Balmer et al., 2002, Maiden et al., 2002, Findlow et al., 2019). Consequently, the MenC vaccine will protect against IMD caused by *N. meningitidis* serogroup C, whilst indirectly protecting unvaccinated children and adults via the decrease in carriage of these meningococci. Therefore, herd immunity has been provided (Chang et al., 2012).

The vaccine was initially made available as part of normal infant immunisation programmes at two, three and four months of age, and as a single-dose "catch-up" for children aged between one and 18 years. Many other countries subsequently adopted MenC conjugate vaccines in their national immunisation programmes, and reduced incidence of serogroup C IMD has been achieved as a result (Borrow et al., 2013).

The related MenAfriVac vaccine was developed to purposely address serogroup A strains of *N. meningitidis*, since these are the dominant strains in the sub-Saharan African region. This was also a conjugate vaccine, consisting of group A polysaccharide linked to tetanus toxoid as the carrier (Hedari et al., 2014, Meyer and Kristiansen, 2016). Utilisation of this vaccine in sub-Saharan Africa has been identified as an effective measure in minimising serogroup A meningococcal carriage, as well as inducing herd protection (Mustapha and Harrison, 2018).

The effectiveness of the original conjugated vaccine in the UK contributed greatly towards the generation of tetravalent (or quadrivalent) conjugated vaccines against serogroups A, C, Y and W (Harrison et al., 2010). These meningococcal vaccines (MenACWY) can now be applied globally in the health care sector, to offer effective prevention and control of IMD in several countries (Presa et al., 2019); for example, a tetravalent vaccine has been used to immunise adolescents who are at risk of IMD (Vetter et al., 2016). Similarly, a tetravalent MenACWY vaccine is used to immunise UK travellers who are planning to visit *N. meningitidis* endemic areas (Crum-Cianflone and Sullivan, 2016).

However, the same approach may not be sufficient to effectively realise a vaccine against *N. meningitidis* serogroup B (Gasparin and Panatto, 2011), the strains most commonly associated with IMD in developed nations. Significantly, the

meningococcal serogroup B capsule does not function well as the basis for a vaccine because its immunogenicity is quite low, particularly in children (Tan et al., 2010, Durando et al., 2015). Alternative vaccines have therefore been developed against serogroup B, based on outer membrane proteins instead (Borrow et al., 2017).

1.12.3 Vaccines against Serogroup B Meningococci

Apart from being the leading cause of IMD in developed nations, serogroup B meningococci contribute to an estimated more than half of all cases worldwide. For example, when IMD was a significant burden in England and Wales from 2006 to 2011 especially among infants, young children and adolescents 87% of these cases were caused by serogroup B (Ladhani et al., 2012). Moreover, it was estimated that more than 80% of IMD cases in England from 2011–2021 were caused by serogroup B (Public Health England, 2021), but as noted above, the generation of polysaccharide vaccines against this serogroup has proven problematic (Chang et al., 2012, Rivero-Calle et al., 2019). The serogroup B capsule consists of polysialic acid, a structure that is also present on human neurons (Wyle et al., 1972, Finne et al., 1987, Griffiss et al., 1991, Serruto et al., 2012). As a result of this, substitution of the *N*-acetyl groups of the sialic acid residues with *N*-propionyl groups was investigated. However, the induced antibodies did not function appropriately or as expected (Bruge et al., 2004, Sadarangani and Pollard, 2010). Therefore, vaccine development for serogroup B has focused mainly on cell-surface protein antigens.

To design vaccines that can effectively prevent *N. meningitidis* serogroup B (MenB), non-capsular surface structures have been investigated as antigens (Rivero-Calle et al., 2019). Considerable attempts have been made in this regard, with research mainly focusing on cell surface structures, primarily OMPs or OMVs, which as stated earlier include intact outer membranes, lipids, lipopolysaccharides and periplasmic components (Holst et al., 2009).

Meningococcal porins PorA and PorB were the most abundant proteins in the first-generation OMV vaccine against MenB (Sierra et al., 1991, Boslego et al., 1995). Regardless of the wider effectiveness of vaccines produced on this basis, they have the ability to boost immunity against PorA (Tappero et al., 1999), an

immunodominant antigen within OMVs. Since PorA variations are considerable among MenB strains, it is often difficult to determine the strain specificity against MenB (Tappero et al., 1999, Sanders et al., 2015), and OMV vaccines might only be effective against a single epidemic strain expressing a specific PorA variant (Devoy et al., 2005, Serruto et al., 2012). Thus, it has been suggested that multiple strains should be used to make OMV vaccines, in order to widen their application (Sandbu et al., 2007, Balhuizen et al., 2021). Another approach is the utilisation of meningococcal mutants to prepare OMV vaccines, which involves inactivation of the PorA gene alongside overexpression of other, minor OMPs (Martin et al., 2000, Weynants et al., 2007).

The vaccine commonly known as 4CMenB, or Bexsero in certain countries, is a multivalent meningococcal vaccine designed and licensed by GlaxoSmithKline (Gorringe and Pajón, 2012, Feavers and Maiden, 2017). It contains the recombinant antigenic protein components NadA, fHbp and Neisserial heparin-binding antigen (NHBA) together with OMVs from a New Zealand epidemic strain (Gorringe and Pajón, 2012, Serruto et al., 2012). Evidence suggests it produces significant immunological responses in infants (Gorringe and Pajón, 2012), and the UK now includes Bexsero on its schedule of infant immunisations. Another serogroup B vaccine, Trumbena, has been approved by the European Commission as a preventative medicine for IMD associated with MenB in adults and adolescents aged 10 or older (Beeslaar et al., 2018). The vaccine is predicted to protect against only 78% of the invasive MenB strains in Europe and so requires further development, perhaps through the inclusion of additional components (Vogel et al., 2013).

Some serogroup B vaccines, including Trumenba, are based on two variants of the fHbp protein, and these have obtained approval in certain countries (McNeil et al., 2013, Seib et al., 2015). This type of vaccine may be beneficial to individuals between the ages of 10 and 25, and since teenagers and adolescents play an important role in the epidemiology of IMD, targeting them for vaccination could significantly reduce the spread of the disease (Vetter et al., 2016).

1.13 Iron Acquisition in *N. meningitidis*

Iron is essential for normal cellular function in humans, and iron-binding proteins play a critical role in regulating its entry to cells, use, and transport throughout the body. The most important of these are lactoferrin, transferrin, ferritin and haemoglobin (Wandersman and Delepelaire, 2004). In fact, most living organisms require iron as a micronutrient, with the exception of lactic acid bacteria that use manganese and cobalt instead (Krewulak and Vogel, 2008). Therefore, iron is essential for the survival and virulence of *Neisseria* species; however, unlike most gram-negative bacteria, they do not produce siderophores but rely instead on serum transferrin derived from their human host (West and Sparling, 1985, Cornelissen and Hollander, 2011, Cornelissen, 2018). *N. meningitidis* has consequently developed efficient mechanisms for acquiring iron during colonisation and invasive disease, through expression of certain surface proteins (Rokbi et al., 1997).

Specifically, two large surface proteins constitute the neisserial iron transport system: transferrin-binding protein A (TbpA), a carrier protein of 100 kDa that belongs to the TonB family; and transferrin-binding protein B (TbpB), an 80 kDa co-receptor that is attached to the bacterial outer membrane through lipid anchors (Noinaj et al., 2012). Neither of these proteins is present in any clinical isolate of pathogenic *Neisseria*. TbpA binds transferrin, with or without iron bound, with high affinity, but TbpB is specific for iron-containing transferrin only (Boulton et al., 1998, Krell et al., 2003). TbpA has the ability to extract and import iron without TbpB, although the reaction is more efficient in the presence of TbpB; hence its designation as a co-receptor (Irwin et al., 1993, Anderson et al., 1994). The *tbpA* and *tbpB* genes have the ability to induce bactericidal antibodies against *N. gonorrhoeae* and *N. meningitidis* in mice, making them potential candidates for vaccine development (Price et al., 2007, Weynants et al., 2007).

1.14 Virulence Factors of *N. meningitidis*

The major recognised virulence factors of *N. meningitidis* are summarised in Figure 1.5. They include the polysaccharide capsule, type IV pili (TFP), LOS and various outer membrane proteins such as porins (PorA and PorB) and adhesion molecules

(Opa and Opc) (Virji, 2009, Rouphael and Stephens, 2012). Pathogenic *N. meningitidis* avoids the secretion of various molecules and relies on expression of particular virulence factors, including components of the polysaccharide capsule, whose surface features can be used to invade the host by exploiting the appropriate cellular mechanisms. In this regard, the host's defences are often avoided via the expression of appropriate bacterial surface components; and in addition through the shedding of OMVs, which may deflect or modulate the immune response (Wall, 2001). Aside from the capsule, other important meningococcal virulence factors are located in the bacterial cell envelope comprising the cytoplasmic membrane, peptidoglycan cell wall and outer membrane (including its associated proteins and non-protein surface antigens such as LPS).

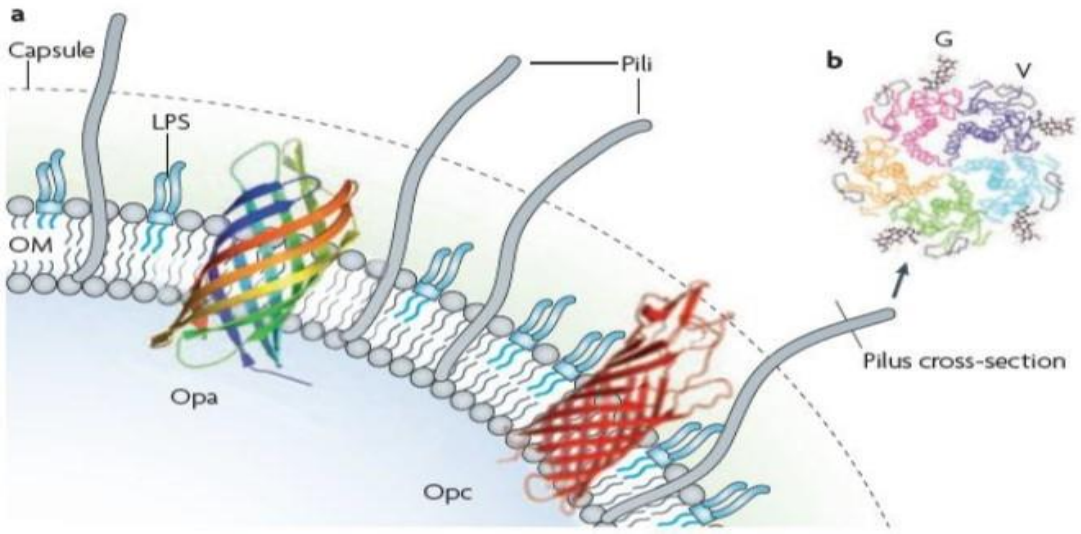

Figure 1.5: Cross-section of the outer membrane of *N. meningitidis*, showing the major virulence factors. (A) Pili are the most common adhesins for *N. meningitidis*, and protrude through the capsule. Opa and Opc are significant outer membrane adhesins that enhance interactions with host cell receptors. As shown here, LPS interact with membrane adhesins and can also form interactions with different host cell surface receptors. (B) Cross-sectional view of the pilus fibre, containing the variable domains (V) and glycans (G) that are positioned externally. The stable domains are effectively protected from the host by their placement internally, within the fibres (Virji, 2009).

1.14.1 Capsule

Virulent strains of *N. meningitidis* are usually encapsulated: they are known to generate a polysaccharide capsule that surrounds the cell surface and constitutes a major virulence factor, playing an essential role when the bacterium enters the bloodstream (Nassif, 1999, Bradley et al., 2005, Tzeng et al., 2016, Herold et al., 2019). As mentioned above, capsular polysaccharides are thought to partially mask the OMPs of *N. meningitidis* and thus to greatly enhance protection of the pathogen against the host's defence mechanisms, including antibody and complement-mediated killing, and phagocytosis (Bradley et al., 2005, Schneider et al., 2007, Stephens, 2009, Coureuil et al., 2012, Tzeng et al., 2016). Moreover, the capsule provides the bacterium with effective protection against the impacts associated with harsh environmental conditions, and prevents dehydration whilst outside the host (Stephens, 2009).

As mentioned above, twelve serogroups have been identified on this basis, six of which account for about 90% of all deadly meningococcal infections worldwide. The pathogenicity of different meningococcal serogroups can vary in terms of their antigenic features and the molecular structure (Stephens et al., 2007, Stephens, 2009). The exact chemical nature of the capsule varies between serogroups, and meningococci with both serogroup B and C type capsules have been associated with outbreaks of IMD. These strains are the most common cause of sporadic meningococcal disease all around the world, but particularly in developed countries (Rosenstein et al., 1999, Chang et al., 2012). The capsular polysaccharides of these serogroups are similar in their structure, consisting of homopolymers of sialic acid in this case, *N*-acetylneuraminic acid (NANA) but differing in the way the monomeric units are linked: α2→8 for serogroup B, and α2→9 for serogroup C, as shown in Table 1.1 (Rosenstein et al., 1999, Tzeng and Stephens, 2021). In contrast, the capsules of meningococcal serogroups W and Y are made up of partially *O*-acetylated NANA in combination with other sugars (Tzeng et al., 2016). The capsule of serogroup A is not based on NANA at all, but is instead composed of *N*-acetylated, (α1→6)-linked D-mannosamine-1-phosphate units as also shown in Table 1.1 (Ala'Aldeen and Turner, 2006, Virji, 2009).

According to Hill et al. (2010), the presence of sialic acid reduces the ability of the host's immune system to identify the encapsulated bacteria, because sialic acids are often expressed on host cell surfaces. Several clinical and epidemiological investigations have verified that the capsule plays a significant role in meningococcal pathogenesis, and have further demonstrated that all pathogenic isolates from individuals with IMD are encapsulated (Morley and Pollard, 2001, Stephens et al., 2007).

Table 1.1: Chemical structures of the capsular polysaccharides in meningococci (Virji, 2009).

Serogroup	Capsule structure		
A	Homopolymers of *N*-acetylated-D-mannosamine-1-phosphate	*N*-acetylated, (α1→6)-linked D-mannosamine-1-phosphate	Non-sialic acid capsule
X		(α1→4)-*N*-acetyl-D-glucosamine-1-phosphate	
B	Homopolymers of sialic acids	(α2→8)-*N*-acetylneuraminic acid	Sialic acid capsule
C		(α2→9)-*N*-acetylneuraminic acid	
W	Heteropolymers of sialic acids containing disaccharides	6-D-glucose(α1→4)-*N*-acetylneuraminic acid	
Y			

The meningococcal capsule is encoded by a gene cluster located within the capsule polysaccharide synthesis (*cps*) locus (Frosch et al., 1989, Harrison et al., 2013, Tzeng et al., 2016, Bartley et al., 2017). Some strains have lost the *cps* genes and are referred to as capsule null (*cnl*). These strains are common in carriers but are generally regarded as non-pathogenic, and are much less likely to cause disease (Johswich et al., 2012).

The *cps* locus usually consists of three regions located within the 24 kb virulence island of the *N. meningitidis* genome (Frosch et al., 1989, Rouphael and Stephens, 2012, Bartley et al., 2017). One region is responsible for polysaccharide biosynthesis, whereas the others encode proteins required for extracellular transport of capsule components from the cytoplasm to the bacterial cell surface (Frosch et al., 1989, Rouphael and Stephens, 2012). The regions of the operon responsible for capsular biosynthesis have a similar genomic organisation across serogroups B, C, W and Y, but not serogroup A. Furthermore, capsular switching can occur: a mechanism leading to structural variations that can enable meningococci to avoid capsule-specific host immunity induced either by serotype-specific vaccines, meningococcal carriage, or other encapsulated bacteria (Rouphael and Stephens, 2012). Capsule type switching occurs through natural transformation and recombination, via horizontal genetic exchange between strains of different serogroups (Swartley et al., 1997, Harrison et al., 2013, Tzeng et al., 2016).

The capsule offers meningococci a range of protective properties. It confers resistance to desiccation while the organism is outside the human host, assists in transmission and colonisation, and provides effective protection from phagocytosis and complement fixation (Read et al., 1996, Virji, 1996, Schneider et al., 2007), allowing meningococci to survive in the bloodstream and CSF (Nassif et al., 1999). The capsule is therefore required as an anti-phagocytosis virulence factor when in the bloodstream, and its synthesis must be maintained as a prerequisite for dissemination within the host (Panatto et al., 2011, Strelow and Vidal, 2013). However, although the capsule offers protection against the host immune response, it effectively prevents interaction of the bacterium with the epithelial cells of the

nasopharynx, so capsule synthesis must be interrupted for cellular attachment and invasion to occur (Yazdankhah and Caugant, 2004).

1.14.2 Lipooligosaccharide

The LOS of *N. meningitidis*, and other gram-negative bacteria, are the primary endotoxins present in the outer membrane of this class of pathogens (Brandtzaeg et al., 2001, Idosa et al., 2019). In *N. meningitidis*, LOS play an important role in various biological processes related to pathogenesis. These include adherence to and colonisation of host surfaces, complement evasion, triggering of inflammation and activation of the host innate immune response (Plant et al., 2006, Rouphael and Stephens, 2012, Johswich, 2017, Idosa et al., 2019). As a result of their immunomodulatory activities, LOS significantly contribute to multiple organ failure and septic shock in meningococcal disease, which can result in fatality (Brandtzaeg et al., 1989, Kahler and Stephens, 1998, Brusletto et al., 2020). Moreover, meningococcal LOS are subject to phase variation, allowing the organism to switch between different immunotypes (Brandtzaeg et al., 2001, Berrington et al., 2002, Hill et al., 2010).

Unlike the LOS of many gram-negative bacilli such as the *Enterobacteriaceae*, the LOS of *N. meningitidis* lack the repeating polysaccharide O-antigens that protrude into the extracellular space (Kahler and Stephens, 1998, Kurzai et al., 2005). Neisserial LOS comprise three oligosaccharide chains, named as α, β and γ (Arking et al., 2001, Rouphael and Stephens, 2012). Meningococcal LOS contain a highly conserved oligosaccharide inner core region composed of diheptose sugars (HepI and HepII) that is attached, via 3-deoxy-D-manno-2-octulosonic acid (KDO), to a lipid A moiety rooted to the outer membrane (Kahler and Stephens, 1998, Jennings et al., 1999, Tzeng et al., 2002, Kahler et al., 2018). The lipid A moiety is composed of two residues of glucosamine associated with fatty acids. The outer core consists of a more complex series of sugar residues, and is made up of galactose, glucose, *N*-acetylglucosamine and NANA (Kahler et al., 1996, Kahler et al., 2006, Stephens, 2009). In meningococci and gonococci, this is linked to the inner core heptoses (Rahman et al., 1998).

Meningococcal LOS contribute to the pathogenesis of IMD by binding to Toll-like receptors (TLRs) present on the surface of host immune cells, including monocytes and dendritic cells (Brightbill and Modlin, 2000, Johswich, 2017, Hodeib et al., 2020). Stimulation of TLRs results in endothelial damage and capillary leakage (Brightbill and Modlin, 2000, Zughaier et al., 2004, Bergounioux et al., 2016). Also, the lipid A moiety of meningococcal LOS has been shown to induce the inflammatory response characteristic of sepsis (Brandtzaeg et al., 2001, Bergounioux et al., 2016), and the presence of type IV pili (TFP) has additionally been demonstrated to act synergistically with LOS to amplify the toxicity of the latter (Dunn et al., 1995). Furthermore, LOS exhibit strong in vitro toxicity towards endothelial cells (Doran et al., 2016).

1.14.3 Type IV Pili (TFP)

TFP are complex, protein-based organelles produced by *N. meningitidis* that usually extend beyond the bacterial capsule (Strom and Lory, 1993, dos Santos Souza et al., 2020). They are relatively thin, flexible fibres ranging from 6–8 nm in width, are several micrometres long, and are laterally aggregate, meaning they are capable of forming bundles (Mattick, 2002, Biais et al., 2010, dos Santos Souza et al., 2020). Furthermore, TFP are highly dynamic structures that undergo fast expansion and retraction processes (Mattick, 2002, Carbonnelle et al., 2009, dos Santos Souza et al., 2020). They play crucial roles in a number of bacterial processes including biofilm formation, host cell adhesion, DNA transformation and twitching motility, as well as phage transduction (Mattick, 2002, dos Santos Souza et al., 2020). Meningococcal pili belong to the type IV pilus family. They direct the motility of bacteria and expedite DNA uptake, which might become a source of genetic variation, facilitate DNA repair, or provide the organism with a source of carbon, nitrogen and phosphorus (Chen and Dubnau, 2004, Barnier et al., 2021).

They are also of importance in meningococcal pathogenesis, since TFP are major mediators of host cell adhesion: a process considered to be the first step in interaction with both epithelial and endothelial cells of the host (Virji et al., 1992, Tzeng and Stephens, 2000, Coureuil et al., 2012). Interaction of *N. meningitidis* TFP

with a host cell can lead to an increase in intracellular calcium concentration, in turn activating signal transduction pathways within the cell (Källström et al., 1998, Asmat et al., 2014). Pili also enhance the interaction of meningococci with endothelial cells via the β2 adrenergic receptor (β2AR), which induces intracellular signalling pathways; and CD147, which is known to be involved in adhesion (Coureuil et al., 2010, Maïssa et al., 2017, dos Santos Souza et al., 2020). In particular, stimulation of host signalling pathways is responsible for disruption of the BBB during CNS infiltration (Kirchner et al., 2005, Kolappan et al., 2016, dos Santos Souza et al., 2020). Through their role in DNA uptake, TFP also facilitate genetic transformation and adaptation of meningococci to their host environment (Mattick, 2002).

Twitching motility is another important virulence-associated activity mediated by TFP. In this case, pili are retracted back into the bacterium to their origin (Coureuil et al., 2012, Gault et al., 2015). Successive cycles of extension and retraction can result in movement of about 1 mm per second on cell surfaces. It also reduces the gap between bacteria and the eukaryotic membranes to which they have attached, facilitating closer cellular interaction and tighter adhesion of meningococci onto the surface of host cells (Winther-Larsen et al., 2005, Virji, 2009).

Our understanding of the structure of meningococcal pili is based on the crystal structure of gonococcal pilus filaments determined by electron microscopy (Craig et al., 2006, Li et al., 2012), and the analysis undertaken by Hélaine et al. (2005) that clearly identified fifteen proteins as actively involved in the biosynthesis of *N. meningitidis* TFP. This process is achieved via four major steps: functional maturation, assembly, counter-notification and emergence on the cell surface. The fifteen proteins, commonly referred to as Pil proteins, are ComP and other subunits named PilC to PilX; however, the most significant roles are played by PilC, PilE and PilQ, as shown in Figure 1.6 (Kirchner et al., 2005, Virji, 2009).

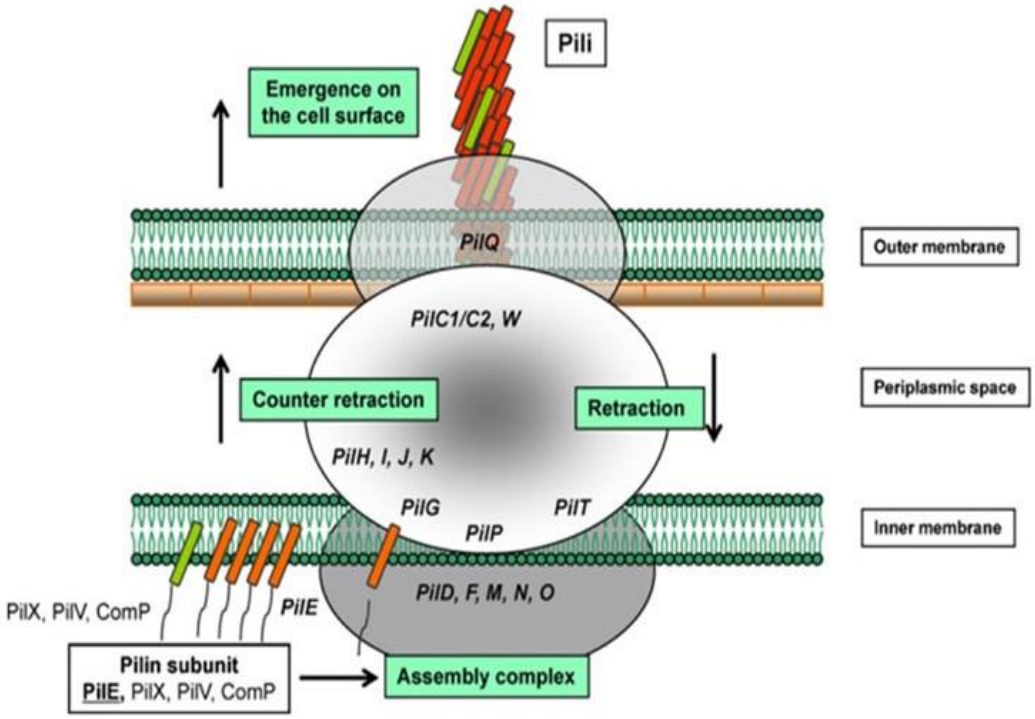

Figure 1.6: Schematic of the *N. meningitidis* type IV pilus showing the cellular location of Pil proteins, which are involved in the assembly and maturation of function of the fibre. During pilus generation, individual pilin subunits (PilE) are assembled by a multi-protein platform complex (PilD, PilF, PilM, PilN, PilO, PilP) located at the interior membrane, at the edge of the intracellular space. The PilQ secretin enables translocation of the growing fibre to the cell surface. Other components of the pilus work to counteract retraction (PilC1/C2, PilG, PilH, PilI, PilJ, PilK, PilW). Of these, PilC1/C2 and PilW are found on the exterior membrane, whereas PilG is associated with the interior membrane. A number of components (PilC1, PilW, PilI, PilJ, PilK, PilX, PilV, ComP) play key roles in the function of the pilus. Diagram reproduced from (Carbonnelle et al., 2009).

1.14.3.1 PilC

Two PilC proteins are found in *N. meningitidis*, PilC1 and PilC2 (Rudel et al., 1995). They are large proteins (110 kDa) that are normally located at the tip of the pilus, where they can readily mediate bacterial adhesion to host cells (Rudel et al., 1995, Kirchner et al., 2005, Barnier et al., 2021). The PilC proteins play important roles in pilus-mediated transformation, strengthening of the bacterial surface and increased adherence to human cells (Nassif et al., 1994, Kirchner and Meyer, 2005).

Interestingly, PilC1 and PilC2 perform same roles but bind to human cells with different specificities (Barnier et al., 2021). Although some research identified PilC1, but not PilC2, as a mediator of meningococcal adhesion to human cells, later work revealed that PilC2 also plays an important role, albeit in a highly cell type-specific manner (Morand et al., 2009). Furthermore, both variants exert considerably different influences upon host cells: for example, PilC1 is capable of regulating the epidermal growth factor receptor (EGFR) signalling pathway, as well as human cell motility, whereas PilC2 is not (Morand et al., 2009). However, both homologues are known to integrate bacterial piliation with transforming ability (Nassif et al., 1994).

1.14.3.2 PilE

In *Neisseria* species, PilE is the major structural component of TFP, and contains two primary domains: a hydrophobic, N-terminal α-helical region, and a predominantly β-sheet head with a C-terminal disulphide bond (Fernández and Berenguer, 2000, Imhaus and Duménil, 2014). The PilE protein is initially localised to the inner membrane, to which it is fixed by its hydrophobic N-terminal sequence (Fernández and Berenguer, 2000, Kolappan et al., 2016). The protein is then assembled into helical fibres, with the α-helical region buried inside the middle of the structure (Parge et al., 1995, Hélaine et al., 2005), creating a helical cylindrical structure that makes up the long shaft of the bacterial pilus (Kolappan et al., 2016). Thus, PilE is essential for meningococcal pilus biogenesis, and is indirectly required for host adhesion by promoting functional display of the PilC adhesin in the context of the pilus fibre (Winther-Larsen et al., 2001, Morand et al., 2004).

Furthermore, PilE can also carry a number of posttranslational modifications. It can be glycosylated, phosphorylated, or modified with *O*-linked phosphorylcholine and *O*-linked phosphoethanolamine (Virji, 1997, Hill et al., 2010). The physiological role of pilin modification is not well understood, but it is possibly involved in escape from host immune responses. Several glycoproteins are associated with pathogenicity in gram-negative bacteria, meaning that glycan substitution of surface structures plays important roles in both pathogenesis and the host immunological

response (Schmidt et al., 2003). In the case of *N. meningitidis*, glycosylation of the pilus may be blocked through alternative activation of the complement pathway (Kahler et al., 2001). Additionally, phosphorylcholine modifications allow C-reactive protein to interact with the bacteria, enhancing opsonisation and ultimately phagocytosis by immune cells such as macrophages and neutrophils (Casey et al., 2008, Söderholm et al., 2011).

1.14.3.3 PilQ

The PilQ protein belongs to the secretin protein family. Secretin homologues are found in a number of bacterial secretion systems, including type II secretion systems (Collins et al., 2001, Collins et al., 2003). PilQ is able to form a homomultimeric channel in the bacterial outer membrane, consisting of 12 identical subunits and creating a symmetrical secretin pore of approximately 900 kDa combined molecular weight (Yen et al., 2002). The structure forms a large, centralised cavity enclosed by a 'cap' and 'plug', with four 'arm' features on each side (Collins et al., 2001, Collins et al., 2005). Thus, the PilQ complex is the channel through which the assembled pilus fibre is extruded from the bacterial surface (Collins et al., 2005). In addition to its role in TFP biogenesis, PilQ has been reported as an adhesin mediating binding to the laminin receptor present on host cells (Orihuela et al., 2009). It is also required for extrusion of a filamentous phage that is encoded in the genome of many meningococcal strains, especially those belonging to hypervirulent lineages (Bille et al., 2005, Coureuil et al., 2012).

1.14.4 Major Outer Membrane Proteins

1.14.4.1 Opacity proteins

Opacity protein A (Opa) and opacity protein C (Opc), also known as class 5 outer membrane protein, are major outer membrane proteins of *N. meningitidis* (Sarkari et al., 1994, Cunha et al., 2009). The proteins are of similar size, with a molecular weight of about 27–31 kDa, and also share a degree of sequence homology (Cunha et al., 2009, Hill et al., 2010). Nonetheless, they show significant structural and functional differences despite belonging to the same family.

Opa proteins are expressed in both *N. gonorrhoeae* and *N. meningitidis*, whereas Opc proteins are only found in the latter. Opa proteins contain an eight β-strand transmembrane barrel structure, with four extracellular surface-exposed loops that are displayed on the bacterial surface. Three of these four loops are highly variable, both within and among different *N. meningitidis* strains (Malorny et al., 1998, Hung and Christodoulides, 2013). Most meningococci have three or four *Opa* loci, which are subject to genetic variation through several mechanisms, including slipped strand mispairing (SSM), point mutations, insertions and deletions (Aho et al., 1991, Hill et al., 2010). In contrast to Opa, Opc has ten β-strands and five extracellular loops. It is encoded by the *opcA* gene, which is transcriptionally regulated by SSM variation of a polycytidine tract in the promoter region (Zhu et al., 1999, Prince et al., 2002).

Both proteins play a vital role in meningococcal virulence and pathogenicity through their recognised roles in bacterial adhesion to, and penetration of, host epithelial and endothelial cells (Sarkari et al., 1994, Hill et al., 2010). However, it is uncertain whether Opa and Opc can mediate adhesion in vivo in the presence of the polysaccharide capsule. Some reports have indicated that their adhesive properties can only be demonstrated in vitro if the capsule is absent, although Opa/Opc overexpression can overcome the masking impact of the capsule if present (Unkmeir et al., 2002, Hill et al., 2010).

Both proteins mediate bacterial adhesion through binding to heparan sulphate proteoglycans (HSPGs) (De Vries et al., 1998, Virji et al., 1999). As described by Rabenstein (2002), heparin and heparan sulphate are closely-related biomolecules consisting of strongly sulphated glycans (polysaccharides), with heparin found predominantly in mast cell granules and heparan sulphate present in plasma, in the extracellular matrix and on the surface of most mammalian cells, where it can form HSPGs through covalent attachment to various proteins. By interacting with HSPGs, Opc can support, but cannot maintain, meningococcal adhesion and invasion of host endothelial cells (Virji et al., 1994). Given this, as well as the low affinity of the interactions, it is possible that HSPGs are not the sole class of ligand for Opc. Consistent with this idea, it has been found to interact with extracellular

matrix glycoproteins such as vitronectin and fibronectin, as have some Opa variants (Sa E Cunha et al., 2010). Furthermore, vitronectin and fibronectin are both capable of mediating Opc-dependent meningococcal adhesion to human endothelial cells via interaction with either $\alpha_V\beta_3$ or $\alpha_5\beta_1$ integrins, respectively, promoting attachment to and invasion of these host cells in a process termed 'sandwich' adherence (Virji et al., 1994, Unkmeir et al., 2002). Thus, bacterial Opc promotes association of meningococci with endothelial cell integrin receptors by binding to two known ligands of these receptors: the serum factors fibronectin and vitronectin.

Opc has been shown to mediate invasion of human umbilical vein endothelial cells (HUVECs) (Virji et al., 1995, Sa E Cunha et al., 2009) as well as epithelial cells such as Hep-2, Chang and A549, albeit to a lesser extent than for endothelial cells (Virji et al., 1993, Sa E Cunha et al., 2009). Some meningococcal lineages which lack the *Opc* gene, including the A4 cluster and the ET-37 complex, are capable of causing meningococcal sepsis but are not commonly associated with cases of meningitis (Sarkari et al., 1994, Seiler et al., 1996, Sa E Cunha et al., 2009). This may be explained by the fact that Opc is known to play a significant role in penetration of the BBB.

The Opa proteins can mediate adherence to, and invasion of, epithelial cells in the absence of serum proteins via attachment to HSPGs (Cunha et al., 2010, Doran et al., 2016), and can also bind the major members of the human carcinoembryonic antigen-related cell adhesion molecule family (CEACAMs) (Virji et al., 1996, Kuespert et al., 2011), as discussed further below.

1.14.4.2 PorA and PorB

Porins are among the most common proteins found in the outer membranes of meningococci, which express two major classes of such pore-forming proteins: PorA and PorB. The first of these, PorA, is a class 1 outer membrane protein expressed by most strains, with a molecular weight of around 45 kDa. PorB proteins are found in all meningococci, and can be further subdivided into class 2 and 3 outer membrane proteins; namely, PorB2 and PorB3, of approximate molecular weight 41 kDa and 38 kDa, respectively (Frasch et al., 1985, Hitchcock, 1989,

Minetti et al., 1997). PorA and PorB variants form the basis for division of meningococci into various sub-serotypes and serotypes, respectively (Frasch et al., 1985, Ala'Aldeen and Turner, 2006). In most cases, they constitute β-barrel proteins that can combine in trimers and are capable of forming pores in the bacterial outer membrane (Frasch et al., 1985, Minetti et al., 1997). The major role played by these pores is to regulate the exchange of ions between the bacterial periplasm and the surrounding environment. In this respect, PorA is cation-selective, whereas PorB is more anion-selective but can also facilitate cation translocation (Peak et al., 2016). The porins of *Neisseria* pathogens may also activate B cells and other antigen-presenting cells, via a pathway dependent upon both Toll-like receptor 2 (TLR2) and myeloid differentiation primary response protein MyD88 (MyD88) (Massari et al., 2002).

PorA contains eight surface-exposed loops and sixteen transmembrane regions (Van Der Ley et al., 1991, van den Elsen et al., 1999). It has two major variable domains, VR1 and VR2, which are located within loops I and IV, respectively (McGuinness et al., 1993). Meningococcal PorA can act as a complement regulator by associating with human C4b-binding protein (C4bp), leading to suppression of complement activity and thus contributing to serum resistance of *N. meningitidis* (Jarva et al., 2005). According to Orihuela, Mahdavi, Thornton et al. (2009), PorA is also a ligand for the laminin receptor, implying one mechanism by which the bacterium can make contact with the vascular endothelium of the BBB. The capacity to make this interaction was subsequently localised to loop IV of PorA (Abouseada et al., 2012).

PorB family members can function as pore-forming proteins inside eukaryotic cells, and were initially reported to localise to mitochondria and prevent apoptosis through modification of the mitochondrial membrane potential (Massari et al., 2000). However, other researchers have since found the opposite effect, demonstrating pro-apoptotic properties of PorB (Deghmane et al., 2009). Peak, Jennings, Jen et al. (2014) later concluded that porins only have a minor function in apoptotic suppression, since other bacterial components are involved. As well as influencing apoptosis, PorB has been reported to promote the production of the co-stimulatory molecule CD86, and of MHC class II, in a TLR2/MyD88-dependent pathway linked

to its immunopotentiating capacity (Massari et al., 2000, Massari et al., 2005). Meningococcal PorB also appears to mediate antimicrobial susceptibility, since a knockout strain showed increased resistance to cefsulodin (a cephalosporin antibiotic) and tetracycline in vitro (Peak et al., 2014).

1.14.5 Factor H-binding Protein (fHbp)

Factor H-binding protein (fHbp) is a 28 kDa lipoprotein found on the surface of *N. meningitidis* that enhances its survival in human blood by binding to complement factor H, which normally plays an essential role in modulating activation of the complement alternative pathway (Schneider et al., 2009, Biagini et al., 2016, Da Silva et al., 2019). Thus, in common with other pathogens, meningococci can resist complement-dependent killing in serum by isolating a host regulatory factor (Welsch et al., 2008, Coureuil et al., 2012, McNeil et al., 2013), providing insight into how critical this pathway is in the innate immune response against bacterial infection (Welsch et al., 2008), as discussed further below. Mechanistically, it was shown that *N. meningitidis* fHbp sequesters complement factor H through protein mimicry of host carbohydrates (Masignani et al., 2003, Schneider et al., 2009, McNeil et al., 2013). Its level of meningococcal surface expression is strain-dependent, and it has been shown to have high immunogenicity in both humans and mice (Seib et al., 2011, McNeil et a, l., 2013).

Most *N. meningitidis* strains contain the *fHbp* gene (also known as *gna1870*), although considerable sequence diversity is known, and the level of protein expression varies significantly between strains as noted above (Biagini et al., 2016). Some pathogenic strains do not express fHbp, and among these, some have an associated frameshift mutation in *fHbp* whereas others have lost the gene completely (Harris et al., 2011, Lucidarme et al., 2011). Although it was suggested that variations in the *cps* locus and the associated changes in capsule synthesis might render *fHbp* dispensable in some cases (Lucidarme et al., 2011), it was subsequently shown using antibody-based methods that the level of capsular polysaccharide expression had no effect on surface display of an *fHbp* variant (McNeil et al., 2009, Lucidarme et al., 2011).

For serogroup C meningococci, sequence variants of *fHbp* can be divided into two subfamilies, A and B, based on phylogenetic analysis (Harris et al., 2011). Members of one subfamily do not cross-protect against strains expressing fHbp from the other (Poolman and Richmond, 2015, Da Silva et al., 2019). Furthermore, reflecting its functional significance as an important surface-exposed antigen, fHbp is an antigenic component of both the Trumenba and Bexsero (4CMenB) vaccines against serogroup B meningococci (McNeil et al., 2013, Da Silva et al., 2019). Given that variations in *fHbp* have been better characterised in serogroup B meningococci, the strain coverage of vaccines targeting serogroup B remains to be fully clarified (Su and Snape, 2011, McNeil et al., 2013, Gandhi et al., 2016, Feavers and Maiden, 2017, Da Silva et al., 2019).

1.14.6 Neisserial Autotransporter Lipoprotein (NalP)

Neisserial autotransporter lipoprotein (NalP) is a surface-exposed autotransporter (AT) protein with serine protease activity, similar to that of the subtilisins. By the same mechanism detailed for Opc above, *nalP* demonstrates phase-variable expression due to SSM of a polycytidine tract in the promoter region (Van Ulsen et al., 2003, Oldfield et al., 2013, Dufailu et al., 2018). The NalP protein regulates the secretion of its internal autocatalytically-generated passenger fragment, and of other surface proteins, into the extracellular environment (Turner et al., 2002, Van Ulsen et al., 2003). Its N-terminal signal sequence has a lipobox motif at its C-terminal end, containing a cysteine residue that is lipidated in vivo; a feature that was originally thought to allow for retention on the outer membrane, but later shown to be important for enzymatic function (Van Ulsen et al., 2003, Leyton et al., 2012). At the bacterial cell surface, NalP facilitates the cleavage of various other ATs, including IgA protease (resulting in proteolytic release of the α-peptide), App, and other surface-exposed lipoproteins, as well as neisserial heparin-binding antigen (NHBA) (Van Ulsen et al., 2003, Serruto et al., 2010, Roussel-Jazédé et al., 2013). Additionally, NalP has been linked with cleavage of human complement C3, which protects *N. meningitidis* against complement activation (Del Tordello et al., 2014). NalP is also involved in biofilm formation of *N. meningitidis* where it contributes to

bacterial lattice formation via a mechanism that depends upon its protease activity (Arenas et al., 2013, Dufailu et al., 2018).

1.14.7 Immunoglobulin A1 Protease (IgA1)

The IgA1 protease is among the major virulence factors secreted by gram-negative bacteria such as *N. meningitidis*, and is one of the most promising protective neisserial antigens (Roussel-Jazede et al., 2014). Several autoproteolytic cleavage steps are involved in the maturation of this AT protein, leading to extracellular release of the approximately 100 kDa IgA1 protease domain (Klauser et al., 1993, Roussel-Jazede et al., 2014). Of the two subtypes of IgA in human serum, namely IgA1 and IgA2, the former is by far the more prevalent, amounting to 90% of total IgA content (Engström et al., 1990, Vidarsson et al., 2005, Spoerry et al., 2021). The meningococcal IgA1 protease is therefore important for bacterial survival and colonisation within the host, and cleaves IgA1 species in the hinge region between the Fab and Fc domains. The cleaved Fab fragment is still capable of binding its antigen, but activation of the immune response by binding to complement is decreased (Vidarsson et al., 2005, Spoerry et al., 2021). In addition, survival of *N. meningitidis* in epithelial cells is enhanced through IgA1 protease cleavage of the late endosomal component, lysosome-associated membrane protein 1 (LAMP1) (Lin et al., 1997).

1.14.8 Minor Outer Membrane Virulence Factors

Other less significant adhesins of *N. meningitidis* include Adhesion and Penetration Protein (APP) (Hadi et al., 2001), meningococcal serine protease A (MspA) (Turner et al., 2006), autotransporter adhesin NhhA (Peak et al., 2000), and neisserial adhesin A (nadA) (Capecchi et al., 2005).

1.14.8.1 Adhesion and Penetration Protein (App)

App is a serine protease AT homologous to *Haemophilus* adhesion and penetration protein (Hap) in *H. influenzae* (Hadi et al., 2001, Serruto et al., 2003, Pizza and Rappuoli, 2015). It has been established as a conserved antigen among meningococci, being expressed during carriage and infection to induce B cell, T cell

and bactericidal antibody responses (Hadi et al., 2001, van Ulsen et al., 2001, Serruto et al., 2003). Initial reports referred to App in *N. meningitidis* as an adhesin, identifying its capacity to bind to epithelial (but not endothelial) cells, and it was suggested that auto-cleavage might enhance bacterial colony formation or invasion (Serruto et al., 2003). App is homologous with other immunogenic AT proteins present on surface of *N. meningitidis* (Hadi et al., 2001), and also shares significant sequence identity with the meningococcal IgA1 protease (Turner et al., 2006, Van Ulsen and Tommassen, 2006).

1.14.8.2 Meningococcal Serine Protease A (MspA)

MspA, sometimes referred to as autotransporter serine protease (Asp), shares homology with both App and IgA1 protease, showing approximately 36% and 33% sequence identity, respectively, with these proteins (Turner et al., 2006, Khairalla et al., 2015). In common with App, the passenger domain of MspA contains the catalytic triad characteristic of serine proteases (Carbonnelle et al., 2009), and autocatalytic proteolysis results in extracellular release of this domain (Oldfield et al., 2013). Both proteins show demonstrable immunogenicity in humans, producing a bactericidal reaction during invasive infection (Turner et al., 2006). In common with some other meningococcal virulence factors, MspA displays phase-variable expression, and is upregulated in blood (Turner et al., 2006, van Ulsen et al., 2006, Khairalla et al., 2015). It was also found that *E. coli* expressing recombinant MspA adhered significantly more strongly to both human brain microvascular endothelial cells (HBMECs) and bronchial epithelial (BEAS-2B) cells than control strains, confirming its adhesion properties (Turner et al., 2006).

1.14.8.3 Neisseria hia homologue (NhhA)

Autotransporter adhesin NhhA, also known as *Neisseria* hia homologue, is a 591-amino acid AT protein found in the outer membrane of *N. meningitidis* (Scarselli et al., 2006). It is a homologue of the AIDA-I adhesin found in *E. coli* (Benz and Schmidt, 1992, Peak et al., 2000), but was originally named Neisseria hia homologue due to its high similarity with the Hia and Hsf adhesins of *H. influenzae* (67% and 74%, respectively) (van Ulsen et al., 2001, Sjölinder et al., 2008,

Tommassen and Arenas, 2017). Most meningococcal strains express NhhA on their surface. It is able to bind to human epithelial cells as well as components of the extracellular matrix, such as laminin and heparin sulphate, and is involved in bacterial adhesion, nasopharyngeal colonisation and disease progression (Peak et al., 2000, Sjölinder et al., 2008, Scarselli et al., 2006). Published data confirm the pathological role of NhhA in meningococci, particularly demonstrating a significant contribution to evasion of complement-mediated killing and phagocytosis (Sjölinder et al., 2008). It was later shown to decrease the phagocytic activity of macrophages by promoting caspase-dependent apoptosis, leading to the conclusion that it possibly contributes to meningococcal disease severity (Sjölinder et al., 2012).

1.14.8.4 Neisseria Adhesin A (nadA)

NadA is a trimeric autotransporter protein, found mainly in pathogenic meningococcal strains, which plays an important role in bacterial adhesion and invasion of host tissues (Capecchi et al., 2005, Liguori et al., 2018). It is characterised as a homologue of both YadA from *Yersinia enterocolitica* and UspA2 from *Moraxella catarrhalis* (Van Ulsen and Tommassen, 2006, Liguori et al., 2018, Thibau et al., 2020). It is known to bind to human epithelial cells, and is assumed to play a crucial role in meningococcal disease given its more frequent association with virulent *N. meningitidis* strains: it is present in almost half of disease isolates (Comanducci et al., 2002, Nägele et al., 2011, de Filippis et al., 2012, Thibau et al., 2020). Consistent with this, NadA can produce strongly bactericidal antibodies (Serruto et al., 2012) and is consequently an important antigenic protein used as one component of the tetravalent MenB vaccine (4CMenB) that targets *N. meningitidis* serogroup B (Seib et al., 2012, Masignani et al., 2019).

1.15 Pathways of Protein Secretion in *N. meningitidis*

Bacteria require secretion mechanisms to effect protein transmission to recipient cells, or to translocate proteins from the cytoplasm into other adjacent cellular compartments, particularly into or across membrane surfaces of the cytoplasm (Backert and Meyer, 2006, Green and Mecsas, 2016). Gram-negative bacteria use a number of different pathways to secrete virulence factors and other proteins into the

extracellular space (Dautin and Bernstein, 2007). These pathways are also associated with the secretion of surface-modifying components that can enhance bacterial invasion of host cells and tissues. Therefore, secreted proteins play important roles in the bacterial life cycle because they can have toxin-like impacts, or modulate the ability to interact with host cells (Dautin and Bernstein, 2007, Desvaux et al., 2009).

Gram-negative bacteria, including meningococci, have interior and exterior cell membranes: two major hydrophobic barriers distinctly separated by a periplasmic gap containing a peptidoglycan layer (Morley and Pollard, 2001, Lee et al., 2010). In contrast, gram-positive bacteria usually possess a relatively thick outer peptidoglycan layer with a single cell membrane separating it from the cytoplasm (Silhavy et al., 2010). Gram-negative bacteria therefore face particular challenges in transmitting proteins to be secreted across the double membrane (Schwechheimer and Kuehn, 2015).

Various secretion systems have been characterised in gram-negative bacteria that allow them to achieve this, and they have been classified using six well-defined categories: Type-I, Type-II, Type-III, Type-IV, Type-V (including AT systems) and Type-VI secretion systems, together with the two-partner secretion system (TPSS); as shown in Figure 1.7 (Tseng et al., 2009). Most extracellular proteins of *N. meningitidis* are secreted via two well-known subclasses of the Type-V system: the AT mechanism (including App, MspA and IgA protease), also known as Type-Va; or TPSS, also known as Type-Vb (Van Ulsen and Tommassen, 2006, van Ulsen et al., 2014).

General secretion pathways, namely the Sec pathway and the Tat (two-arginine translocation, or twin-arginine translocation) pathway, are initially employed by some of the above secretion pathways for translocation across the inner (cytoplasmic) membrane into the periplasmic gap (Natale et al., 2008, Kudva et al., 2013, van Ulsen et al., 2014). These general secretion pathways are conserved across all domains of life, and are considered to be the most important for bacterial proteins (Papanikou et al., 2007). In gram-negative bacteria, proteins initially

exported into the periplasm via the Sec/Tat pathways are subsequently transmitted through the adjacent membrane(s) by other transport systems. Several proteins can be processed via these secondary channels to invade bacterial membranes, and subsequently be released independently (Robinson and Bolhuis, 2004, Tseng et al., 2009, Papanikou et al., 2007). In most cases, this mechanism is known as Tat-dependent or Sec-dependent protein secretion (Natale et al., 2008, Green and Mecsas, 2016).

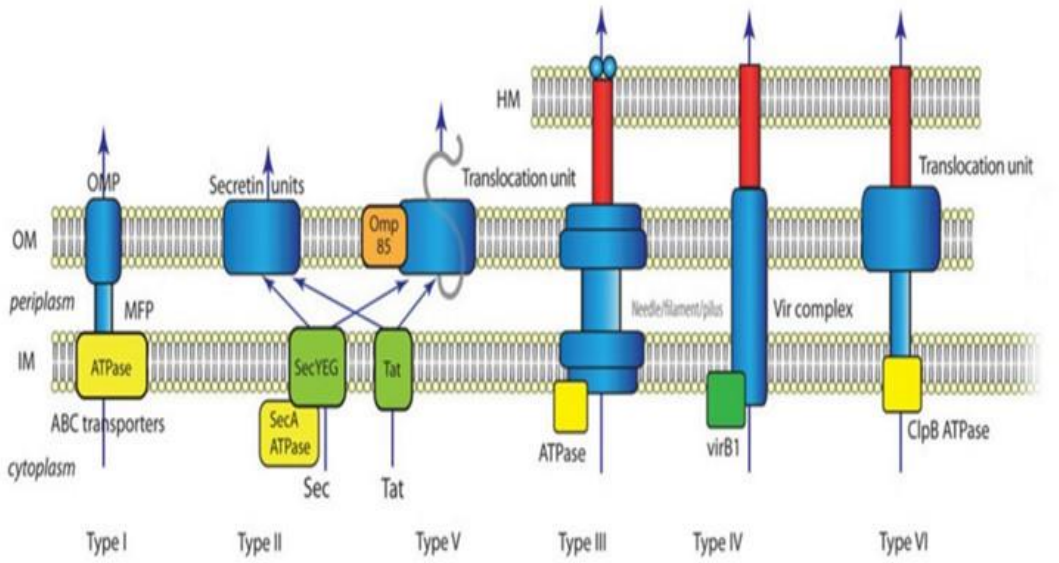

Figure 1.7: The six protein secretion pathways of gram-negative bacteria, designated types I–VI. Gram-negative bacteria have six distinct secretion pathways that are essential for protein export. Normally**,** both bacterial membranes are involved in this process**.** The Type-II and Type-V pathways are Sec-dependent, relying on initial protein transmission into the periplasm via the Sec system followed by secondary transport through the outer membrane(s). The other four major pathways; i.e., Type-I, Type-III, Type-IV and Type-VI, are Sec-independent. They are involved in exporting proteins directly from within the bacterial cytoplasm (Tseng et al., 2009).

1.15.1 Type-I Secretion Systems

Type-I secretion systems (T1SS) were initially discovered in different gram-negative bacteria in which their respective substrates are transported, in a single-step process, through both the internal and external membranes (Desvaux et al.,

2004). Normally, T1SS have three fundamental structural elements, and their distinguishing feature is the use of a large family of transport proteins, ATP-binding cassette (ABC) transporters, to export small molecules such as cellular toxins and antibiotics out of the cell, in addition to proteinaceous substrates (Green and Mecsas, 2016). The ABC transporter is located in the inner membrane, controls the substrate specificity of the system, and drives translocation of substrates across the membrane using energy derived from ATP hydrolysis (Smith et al., 2002, Kanonenberg et al., 2013, Morgan et al., 2017). Bacteria possess numerous T1SS with different specificities, which can thus be utilised to independently transport various substrates. Interestingly, protein substrates for T1SS are often functionally associated with host interactions; for example, adhesins or digestive enzymes such as lipases and proteases (Delepelaire, 2004, Green and Mecsas, 2016).

Another structural element of T1SS is the membrane fusion protein (MFP), situated in the periplasmic gap, which forms a specific channel that bridges the cell envelope (Delepelaire, 2004). This enables the substrate to cross to the final component of the system, a pore-forming outer membrane factor (OMF) in the external membrane through which it can access the extracellular space (Thomas et al., 2014).

The structure described above is exemplified by the well-studied T1SS for haemolysin A found in *E. coli* (Mackman and Holland, 1984, Andersen, 2003, Linhartová et al., 2010). The three major components of this system are HlyB (the ABC transporter), HlyD (the MFP) and TolC (the OMF). The genes which encode T1SS proteins are often histrionically clustered, together with their substrate-encoding genes, and this is known for *hlyB*, *hlyD* and *hlyA* (which encodes haemolysin A) in *E. coli* (Binet et al., 1997, Hadi et al., 2001, Wooldridge et al., 2005). Genes that encode elements of T1SS for secretion of repeat-in-toxin (RTX) family proteins are often organised this way, although interestingly, a different structure was identified for RTX secretion components in *N. meningitidis* (Wooldridge et al., 2005).

1.15.2 Type-V Secretion Systems

Autotransporter (AT) systems are an important subclass of Type-V secretion systems (T5SS) (Jose et al., 1995, Henderson et al., 2004, Leo et al., 2012). The AT pathway (Type-Va) is one of three major subclasses of T5SS (Figure 1.8), with the others being the two-partner secretion pathway (TPSS or Type-Vb) and the trimeric secretion pathway (Type-Vc). As defined by Van Ulsen et al. (2014), the two other T5SS subclasses are the patatin-like autotransporters (Type-Vd) and the intimin/invasin reversed-domain autotransporters (Type-Ve).

Initial transport of T5SS substrate proteins across the inner membrane into the periplasm is mediated by the Sec complex, whilst transport across the outer membrane to the cell surface is mediated by the Bam complex, with periplasmic chaperones (SurA, Skp, DegP) also involved in some species (Dalbey and Kuhn, 2012, Hussain et al., 2020). The latter step relies on a C-terminal transport domain (sometimes known as the translocator domain, helper domain or β-domain) which is a common feature of AT proteins. The domain which is translocated and ultimately secreted is known as the passenger domain or extracellular domain. In most cases, ATs have a wide-ranging ability to move different domains to the cell surface, where additional processing steps can occur, resulting in multiple possibilities (Henderson et al., 2004, Dautin and Bernstein, 2007).

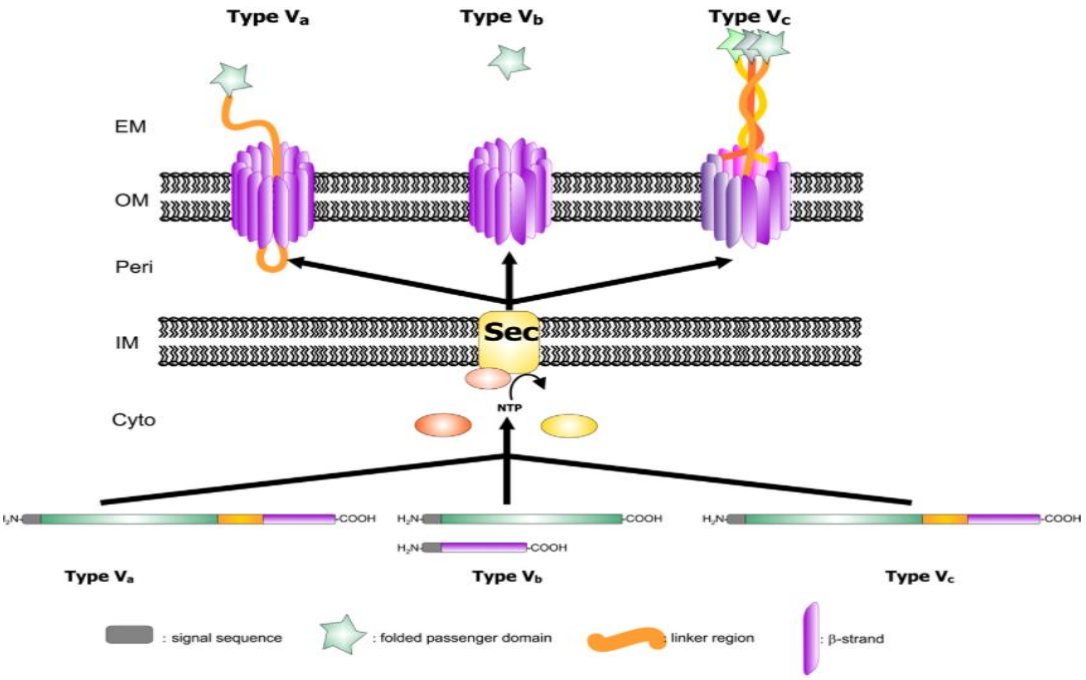

Figure 1.8: Schematic representation of type V secretion systems (T5SS). The three major T5SS subclasses are illustrated as follows, from left to right: Type-Va systems (AT proteins); Type-Vb (two-partner secretion system, or TPSS); and Type-Vc (trimeric secretion pathway). The four major functional protein domains involved are the signal sequence, passenger domain, linker region and β-domain (transport domain). Effector proteins containing an unusual, but characteristic, extended N-terminal signal sequence are present in most T5SS. Synthesised AT proteins are first transmitted from the cytoplasm into the periplasm using the Sec machinery. At this stage, cleavage of the signal sequence can occur. Meanwhile, the β-domain is inserted into the exterior membrane, forming a pore within the membrane. Upon generation of the β-barrel structure, the passenger domain is inserted into the pore and translocated to the bacterial cell surface. At the cell surface, further processing can take place depending on the bacterial species (Henderson et al., 2004).

1.15.2.1 Type-Va Secretion: Classical AT Systems

The AT proteins are a large family of secreted or surface-exposed proteins found in gram-negative organisms (Henderson et al., 1998, Dautin and Bernstein, 2007). Monomeric ATs are classical Type-Va secretion systems that have been comprehensively studied (Leo et al., 2012), and several important virulence factors

fall under this category; for example, meningococcal IgA protease, NalP, MspA and App (Turner et al., 2009). Furthermore, it has long been known that adhesins are important substrates for this pathway, including AIDA-I in *E. coli* (Benz and Schmidt, 1989, Dautin and Bernstein, 2007) and pertactin in *Bordetella pertussis* (Leininger et al., 1991).

Three distinct domains characterise AT proteins structurally. The first of these is the signal sequence (also called the leader sequence or signal peptide), located at the N-terminal end of the protein, which is necessary to direct the protein to the inner membrane where it may then be exported into the periplasm via the Sec/Tat pathways (Leininger et al., 1991, van Ulsen et al., 2014). The passenger domain, or exoprotein, is typically located in the middle of the sequence, and is responsible for effecting the various functional roles of different ATs. The last of the major domains usually comprises the C-terminal part of the protein, and is variously referred to as the autotransporter domain, translocator domain or β-domain. It normally consists of a short-chain linker region, made up of both β-sheet and α-helical structures, and a core region that adopts a β-barrel tertiary structure that can embed into the exterior cell membrane (Henderson et al., 2004), forming a pore-like structure that facilitates transport of the rest of the protein through the membrane.

Initially, it was assumed that ATs had the ability to insert themselves into the external bacterial cell membrane without involvement from other factors. However, an essential protein complex known as the β-barrel assembly machinery (Bam) was later identified, which folds AT β-domains and inserts them into the membrane, and is now recognised as an essential factor for both the biogenesis of ATs and the correct localisation of OMPs (Voulhoux et al., 2003, Knowles et al., 2009). The first member of this complex to be characterised was the outer membrane protein assembly factor BamA, initially identified as Omp85 in *N. meningitidis* and YaeT in *E. coli*, and now known to be an essential gene that is conserved in gram-negative bacteria (Genevrois et al., 2003, Knowles et al., 2009). In addition to BamA, the β-barrel assembly complex contains four other subsidiary proteins, and contributes to the correct processing of OMPs as well as facilitating the secretion of ATs. The β-barrel assembly machinery therefore assists in translocation processes involving

movement of the β-domain into and/or across the exterior bacterial membrane (Knowles et al., 2009), followed by translocation of the passenger domain into the extracellular space once the folded β-domain is inserted within the outer membrane (Saurí et al., 2012).

1.15.2.2 Two-Partner Secretion Pathway (Type-Vb Systems)

In the two-partner secretion pathways (Type-Vb secretion system), the passenger domain and autotransporter domain are found in two separate proteins known respectively as the TpsA and TpsB partners (Jacob-Dubuisson et al., 2001), with both generally containing the N-terminal signal sequence that defines initial Sec/Tat-mediated translocation across the internal membrane (Henderson et al., 2000, Leyton et al., 2012). Upon reaching the periplasm, the TpsB autotransporter domain is inserted into the external membrane as in the case of AT proteins, allowing passage of TpsA to the cell surface, where the passenger domain might undergo additional proteolytic processes enabling it to achieve its physiological roles (Jacob-Dubuisson et al., 2001). The Type-Vb pathway is exemplified by filamentous hemagglutinin (FHA), a major virulence factor of *Bordetella pertussis* (Willems et al., 1994, Jacob-Dubuisson et al., 2013); and the genome of *N. meningitidis* contains up to five TpsA- and two TpsB-encoding genes (Van Ulsen and Tommassen, 2006, Van Ulsen et al., 2008).

1.15.2.3 Type-Vc: Trimeric Autotransporter Secretion Systems

Secretion systems of Type-Vc form highly interwoven trimeric structures that are similar to those of Type-Va. Historically, these proteins were referred to as trimeric autotransporter adhesins (TAAs) because they were shown to bind to human cells and extracellular matrix proteins (Heise and Dersch, 2006). The typical domain structure of TAAs comprises a trimeric N-terminal head domain and a C-terminal anchor region, bridged by intermediate ‘neck’ and coiled ‘stalk’ sections. The anchor region embeds into the bacterial outer membrane to form a pore through which the N-terminal domain can be translocated into the extracellular space (Mil-Homens and Fialho , 2011).

The most well-known example of a TAA is YadA, a virulence factor of *Yersinia pestis* and a member of the oligomeric coiled-coil adhesin (Oca) family; a known subfamily of the surface-attached oligomeric ATs (Henderson et al., 2004, Heise and Dersch, 2006, Mühlenkamp et al., 2015). However, it was earlier research by St. Geme, III and Cutter (2000) that characterised the first Type-Vc TAA, identifying the *H. influenzae* Hia adhesin as a trimeric protein with analogous features to known ATs, except that it does not undergo cleavage between the surface-exposed and β-barrel domains at the cell surface. At the time, this kind of trimeric conformation and secretion mode constituted a novel secretion system for ATs that is now classified as a Type-Vc system. Meningococci possess one AT protein belonging to the Oca family: NadA (Capecchi et al., 2005, Desvaux et al., 2004).

1.16 Immune Reponses against *N. meningitidis*

The innate immune system is the first line of defence against *N. meningitidis* infection, which is especially a risk to infants and toddlers whose immune systems are immature and still developing, and who are more susceptible to disease after loss of maternal antibodies. A common habitat for *N. meningitidis* is the nasopharynx, where it is often found as a commensal species as discussed earlier. Despite its potential for virulence, disease progression is rare and appears to mostly be limited to only a few *N. meningitidis* sequence types (Racloz and Luiz, 2010).

Meningococci can, however, cause two types of potentially fatal disease: meningitis and sepsis. Sepsis is defined as a condition that occurs as a result of the presence of bacteria in the blood, and is characterised by systemic over-induction of the immune system produced by an infection; hence its historical name, systemic inflammatory response syndrome (SIRS) (Remick, 2007, Szatanik et al., 2011). Meningococcal gene expression levels at various stages of colonisation, as well as the host's genetic background, are important factors in maintaining a normal balance in interactions between bacteria and host. For example, certain risk factors have been associated with elevated susceptibility to meningococcal disease: a lack of bactericidal antibodies; CD16, CD36 or TLR4; mannose binding deficiency; or polymorphisms

in the macrophage migration inhibitory factor (*MIF*) gene associated with higher likelihood of contracting meningococcal disease that affect expression levels of its protein product (Wright et al., 2009, Renner et al., 2012).

The nasopharyngeal epithelium in humans contains a variety of innate immune cells, including dendritic cells (DCs), neutrophils and macrophages. Meningococci that cross the mucosal barrier can interact directly with these innate immune cells. In particular, DCs are able to recognise signs of infection through pattern recognition receptors (PRRs). They serve as a link between the innate and adaptive immune systems, and play a significant role in promoting induction and maturation of the immune system (Le Bon and Tough, 2002, Schmitt et al., 2009, Wang et al., 2020). A variety of pathogens can be taken up by macrophages and presented by major histocompatibility complex (MHC) molecules for recognition by activated CD4 and T lymphocytes via their T cell receptors; and these play an important role as effector cells during inflammation (Wang et al., 2020). As meningitis infection progresses, neutrophils become activated, and are often found in the CSF of patients who are suffering from meningococcal disease since they constitute the majority of the immune cells found there. Neutrophils migrate towards the site of infection in response to chemotactic triggers (Doran et al., 2016, Krüger et al., 2018).

1.17 The Complement System

Components of the complement system are major constituents of the immune system and form an integral part of innate immunity. Importantly, the complement system plays a critical role in defence against gram-negative bacteria, and in particular, meningococcal infections (Figueroa and Densen, 1991, Hellerud et al., 2010, Krüger et al., 2018). The complement system comprises 30 plasma proteins, as well as additional membrane-bound receptors for regulation. They are mostly produced in the liver, but also by other tissues such as the epithelial cells of the nasopharyngeal mucosa, and are found in the bloodstream as either soluble or membrane-associated proteins (Lo et al., 2009). Complement activation is mediated by three main pathways: the classical pathway (CP), which involves the binding of the C1 complex to antigen–antibody complexes; the lectin pathway, which is based

on pattern recognition of microbial surface-exposed carbohydrates and related molecules; and the alternative pathway (AP), which involves the binding of complement C3 to a target antigen (Lo et al., 2009, Lewis and Ram, 2014). All three pathways converge with the cleavage of complement component C3, initiating a cascade that leads to formation of the membrane attack complex (MAC) and a pore in the cell membrane, resulting in cell death (Lewis and Ram, 2014). Complement activation can also recruit macrophages, leading to killing of the pathogen by phagocytosis (Ricklin et al., 2010). Besides the main activation pathways, complement activation products can also be produced by proteases that are released by neutrophils and macrophages, including plasminogen, kallikrein and factor XII (Sarma and Ward, 2011, Renné and Stavrou, 2019).

Pathogenic strains of *N. meningitidis* can evade complement-mediated killing in various ways; for example, through fHbp, which is a component of serogroup B meningococcal vaccines, as discussed above. This bacterial protein binds human complement factor H, a key regulator of the alternative pathway that is important for directing complement activation against pathogens rather than host tissues. Specifically, factor H binds to host cells through their polyanionic surface structures (e.g., heparan and sialic acids) and protects against complement attack of self by inactivating bound C3b (complement component 3b). Pathogens generally do not possess the same polyanionic surface structures that can bind factor H, making them prone to C3b amplification and complement-mediated killing (Ferreira et al., 2010). Thus, using fHbp to sequester host factor H provides meningococci with protection against complement attack.

Similarly, C4bp is a potent inhibitor of the classical and lectin pathways of the complement system. It acts as a negative regulator of the C3-convertase of both pathways (C4b2a), blocking formation of C3b (Krukonis and Thomson, 2020). Therefore, recruitment of C4bp by meningococci (through binding to PorA) will also protect them against complement-mediated killing by inhibiting downstream activation. Finally, vitronectin inhibits assembly of the MAC of the complement system. Mechanistically, this process is not fully understood, but vitronectin is thought to inhibit both C5b-7 complex formation and polymerisation of complement

C9 (Singh et al., 2010, Prasada et al., 2017). Normally, this negative regulation is important to protect host tissues from attack (Menny et al., 2021), but it can also be exploited by pathogenic bacteria such as *N. meningitidis* which bind it through NhhA and Opc, as mentioned above as a means of immune evasion.

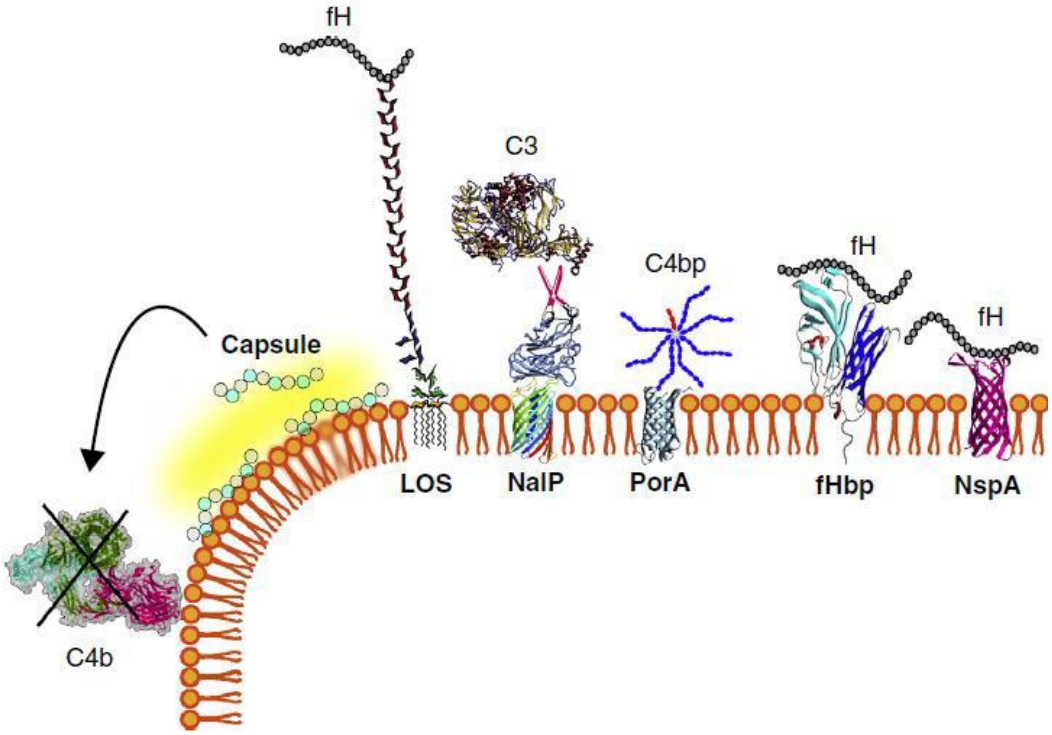

Figure 1.9: Interaction between some outer membrane structures of *N. meningitidis* and components of the complement system. The structures shown are the capsular polysaccharide, lipopolysaccharide (LPS/LOS), and various OMPs: NalP, PorA, fHbp and NspA. Image adapted from Pizza and Rappuoli (2015).

1.18 Interactions between *N. meningitidis* and Host Receptors

The immune system is capable of detecting foreign bodies such as bacteria and viruses through a variety of complementary mechanisms (Mariani et al., 2019). Activation of the innate immune system, the first line of defence against microbes, begins when PRRs detect evolutionarily-conserved pathogen-associated molecular patterns (PAMPs) that are present on pathogens (Medzhitov and Janeway, 2000, Mogensen, 2009, Vance et al., 2009, Carrillo et al., 2017). As noted above, the lectin pathway of complement activation is an example of this recognition mechanism.

PAMPs are specific molecules that are unique to pathogens, such as LPS, lipoteichoic acid and bacterial DNA; these molecules therefore comprise lipids, proteins and nucleic acids (Saïd-Sadier and Ojcius, 2012). A PAMP is characterised by being invariant across entire classes of pathogens, being essential for the pathogen's survival, and being distinguishable in terms of being 'self' or 'non-self' (Janeway, 1989, Mogensen, 2009). It is important to note that PRRs are capable of recognising danger signals if they are situated in abnormal locations or contain abnormal molecular components due to infection, inflammation or other forms of cellular stress (Beg, 2002, Matzinger, 2002). Thus, by detecting PAMPs through PRRs, innate immune cells are capable of identifying and responding to pathogens and their products.

As already discussed, certain virulence factors play an important role in interactions between *N. meningitidis* and host cells, and in combination with their host receptors, several bacterial adhesins mediate invasion of endothelial cells and the induction of inflammation. The polysaccharide capsule, which masks the outer membrane proteins, is also important for bacterial replication and survival within host epithelial cells (Virji, 2009). The capsule allows the bacterium to evade immune recognition whilst internalised, and is essential for meningococcal traversal of the epithelial layer by the transcellular route, which has also been shown to depend on the host microtubule network (Nikulin et al., 2006, Sutherland et al., 2010).

The meningococcal membrane opacity proteins, Opa and Opc, mediate direct adhesion to host cells by binding to extracellular matrix components and the CEACAM receptors (Virji, 2000, Griffiths et al., 2007, Sa E Cunha et al., 2009), as was explained above. More specifically, Opa binds to CEACAM1, and this interaction can initiate meningococcal cellular invasion (Virji et al., 1999, De Jonge et al., 2003, Carbonnelle et al., 2009). CEACAM1 is expressed by many cell types (e.g., epithelial cells) or in a regulated manner (e.g., endothelial cells and lymphocytes) (Gray-Owen and Blumberg, 2006, Kim et al., 2019). Interestingly, Carbonnelle, Hill, Morand et al. (2009) suggested that the interaction between meningococci and CEACAMs is at the crossroads of colonisation and pathogenesis, as the interaction promotes adhesion without significant invasion, thereby favouring

colonisation. During inflammation, however, the same receptors may also become portals of entry into host tissues (Carbonnelle et al., 2009).

The human Toll-like receptor (TLR) family consists of 10 members, and these receptors recognise a wide variety of bacteria and their products (Kawasaki and Kawai, 2014). The TLRs play an essential role in the recognition of PAMPs and activation of immune responses, as well as having apparent neurodevelopmental involvement (Too et al., 2016). Three members of the TLR family are known to be involved in meningococcal recognition: TLR2, TLR4 and TLR9 (Schmitt et al., 2009). Receptor activation initiates TLR-mediated signalling pathways, wherein transcription factors such as nuclear factor kappa B (NF-κB) and interferon regulatory factors (IRFs) are translocated to the nucleus to activate responses resulting ultimately in pathogen elimination (Kawai and Akira, 2010). For example, induction of NF-κB-responsive genes leads to the synthesis and release of various proinflammatory cytokines, including IL-1, IL-8, IL-6 and TNF-α (Kany et al., 2019). Furthermore, severe sepsis is associated with high concentrations of TNF-α and IL-6, as well as IL-10 (Sabelnikovs et al., 2012). More specifically, TLR4 plays a central role in sensing bacterial LPS, whose detection depends upon two accessory factors LPS-binding protein (LBP) and CD14 and produces an intense inflammatory response (Janeway, Jr. and Medzhitov, 2002, Ciesielska et al., 2021). It has been demonstrated experimentally that *N. meningitidis* causes elevated cytokine production in human meningioma (Humphries et al., 2005).

There may be a difference between the signalling mechanisms responsible for bacteria entering brain endothelial cells and those responsible for the release of chemokines and cytokines. For example, during challenge of HBMECs with *N. meningitidis*, phosphorylation of the c-Jun N-terminal kinases 1 and 2 (JNK1 and JNK2) was found to be necessary for uptake of the bacteria, but not for cytokine release (Sokolova et al., 2004). Inhibition of JNK1 and JNK2 reduced *N. meningitidis* internalisation without affecting adhesion (Sokolova et al., 2004, Kim, 2006). Binding of meningococci to epithelial cells also activates p38 mitogen-activated protein kinase (p38 MAPK) signalling, which is the pathway responsible for cytokine release (IL-6 and IL-8) via activation of NF-κB (Sokolova et al., 2004).

Sokolova et al. (2004) showed that eukaryotic cellular responses to *N. meningitidis* are mediated both through receptor tyrosine kinases (RTKs) and non-RTKs. Analysis of human genomic sequences showed that RTKs account for 58 of the 90 known human tyrosine kinases, with the remaining 32 classified as non-RTKs (Robinson et al., 2000, Brunet et al., 2016). RTKs transfer the γ-phosphate of ATP to the hydroxyl group of tyrosine residues in target proteins (Hunter, 1998, Schlessinger, 2000), and the most abundant RTKs are the epidermal growth factor-related RTK (ErbB) family. The ligands of this class of proteins are important for cell proliferation, motility and differentiation, and they are found in a range of tissues with various distributions and intensities. There are four homologous receptors in the ErbB family: EGFR/ErbB1, ErbB2, ErbB3 and ErbB4 (Wieduwilt and Moasser, 2008, Slanina et al., 2014).

In general, phosphorylation within the kinase domain is used to regulate the catalytic activity of protein kinases, usually activating the enzyme via phosphoryl transfer to a highly conserved tyrosine residue found within the activation loop (Kornev et al., 2006). Transactivation of ErbB receptors, which leads to the release of growth factor receptor ligands, may occur as a consequence of this activation mechanism via phosphorylation in the cytoplasmatic domains of these receptors (Slanina et al., 2010, Slanina et al., 2014). Interestingly, phosphorylation at the typical activation loop site in EGFR, Tyr845, does not significantly impact catalytic activity , but it does result in conformational stabilisation of the kinase domain, and has been suggested to be part of a signal propagation and amplification mechanism (Shan et al., 2012, Slanina et al., 2014). Furthermore, EGFR phosphorylation at Tyr845 is regulated by integrin interactions and involves c-Src, the kinase which phosphorylates EGFR at this site (Biscardi et al., 1999, Slanina et al., 2014).

EGFR is an important receptor for bacterial interactions with host cells, and plays a vital role in establishing contact between *N. meningitidis* and human cells (Slanina et al., 2014). Initial binding of *N. meningitidis* to host cells is followed by proliferation to give microcolonies, which EGFR is known to form clusters below in A431, Chang and HEC-1B cells, in a process that relies on bacterial TFP expression (Slanina et al., 2014, Fu et al., 2019). Thus, microcolonies form

complexes with EGFR and other substances, leading to cortical plaque formation (Simonis and Schubert-Unkmeir, 2016). In response to meningococcal attachment, phosphorylation of EGFR occurs at Tyr845 independently of extracellular ligand binding, and is demonstrably involved in uptake of the bacteria by host cells, establishing a role for EGFR in invasion of HBMECs (Slanina et al., 2014). The available evidence therefore suggests that EGFR plays a number of roles in the invasion of HBMECs by *N. meningitidis*. Entry of meningococci into these cells seems clearly to be mediated by EGFR, which accumulates around the attachment site in the case of colonisation but remains evenly distributed on the surface of uninfected cells (Slanina et al., 2014).

A related RTK, fibroblast growth factor receptor 1 (FGFR1), might also be involved in meningococcal pathogenesis. It is part of the FGFR receptor family, encoded by four genes (*FGFR1–4*) but comprising more than 48 major isoforms due to alternate splicing (Duchesne et al., 2006). Similarly, more than 30 FGF ligands for these receptors are known, encoded by 22 genes. The FGF/FGFR axis has an important role in development (Brooks et al., 2012), but its dysregulation has been associated with cancer as well as developmental disorders. Interestingly, co-operativity between FGFR1 and EGFR has recently been described in lung cancer (Quintanal-Villalonga et al., 2019), and there is also evidence for involvement of both receptors in meningococcal disease. Previous work from our group (Azimi et al., 2020) has established that *N. meningitidis* interacts with FGFR1 on HBMECs, and that this interaction involves bacterial TFP. Furthermore, knockdown of FGFR1 resulted in decreased meningococcal attachment and invasion. The FGF/FGFR system might therefore play an important, but relatively understudied, role in the pathogenesis of IMD.

1.19 Aims

Building on existing work from our laboratory, the overall aim of this study was to further investigate the role of FGFR1 in the interaction of *N. meningitidis* with HBMECs, and in particular, to identify novel meningococcal ligands for this host receptor. This focus was also chosen due to the known role of FGFR1 in

differentiation and development of the endothelial cells of the BBB, making it of potential relevance to the pathogenesis of IMD.

As a starting point for this work, we will take a published meningococcal interactome with HBMECs, comprising 41 bacterial proteins (Kánová et al., 2018). Through bioinformatic analysis, candidate FGFR1 ligands will be identified from among these proteins and narrowed down to a focused set of the four top priority protein/gene candidates.

Knockout strains for these genes will then be generated from *N. meningitidis* MC58, to assess the impact of the priority target genes on HBMEC attachment and invasion, using established assays. The effect of FGFR1 inhibition on these processes will also be investigated. In addition, ELISA assays will be employed to directly measure the binding of wild type and knockout bacterial strains to recombinant FGFR1. The bacterial proteins of interest will also be overexpressed in *E. coli* and purified, to establish whether interaction with recombinant FGFR1 can be detected by ELISA and far-western blotting.

Through this strategy, it is hoped that specific meningococcal ligands for FGFR1 will be identified, and that this will lead to the development of new therapeutic options in the future.

Chapter 2: Materials and Methods

2.1 Bacterial strains, growth conditions and media

2.1.1 *E. coli* growth media

E. coli were grown in Lysogeny Broth (LB; Sigma), on Lysogeny Agar (LA; Sigma), or in Terrific Broth (TB), supplemented as appropriate with ampicillin (100 μg ml^{-1}), kanamycin (50 or 100 μg ml^{-1}), spectinomycin (50 μg ml^{-1}) or streptomycin (50 μg ml^{-1}). Antibiotics were purchased from Sigma-Aldrich. TB was prepared in the lab and included yeast extract (24 g), tryptone (12 g), 4 ml of Glycerol, KH_2PO_4 (2.31 g) and K_2HPO_4 (12.54 g) per 1 L, made up in dH_2O. The bacterial strains, competent cells, and plasmids used in this study are listed in Table 2.1 and Table 2.2. All bacteria were stored in 2 ml cryovials containing 25 porous beads and cryopreservative, or 500 μl of culture broth mixed with 500 μl of glycerol, shaken and kept at -80°C.

2.1.2 *N. meningitidis* growth media

The American Type Culture Collection (ATCC) provided serogroup B meningococcal strain MC58 and *N. lactamica* (ATCC 23970), which were cultured on chocolate horse blood agar (Oxoid) at 37°C for 16–18 h in the presence of 5% carbon dioxide (CO_2). For either Brain Heart Infusion (BHI) agar or liquid growth, *Neisseria* strains were supplemented with kanamycin (100 μg ml^{-1}), spectinomycin (50 μg ml^{-1}), or streptomycin (50 μg ml^{-1}), together with 1% Vitox (Oxoid).

2.2 Bacterial growth curves

Neisseria strains were streaked onto chocolate blood agar plates and incubated overnight at 37°C in the presence of 5% CO_2. A single colony was inoculated into 10 ml of BHI broth containing 1% Vitox and cultures were incubated overnight at 37°C with shaking at 200 rpm. The next day, the cultures were diluted with 15 ml fresh BHI broth and adjusted to an OD_{600} value of 0.05. Following this, incubation was resumed at 37°C with shaking at 200 rpm. The OD_{600} measurements were taken every hour for eight hours. Each experiment included three replicates per strain.

Table 2.1. Plasmids used in this study

Plasmids	Relevant characteristics	Antibiotic resistance	Source/Reference
pEF-Bos-ss-Fc-extFGFR1 IIIc-ires-TPZ	FGFR1 IIIc cloned into the mammalian expression vector pEF-BOS	Ampicillin	Sheyda Azimi 2014
pEF-Bos-ss-Fc-stop-LRP-ires-TPZ	Fc- stop cloned into the mammalian expression vector pEF-BOS	Ampicillin	Shaun. Morroll.
pMT1	*NMB1053* plus 0.60 kb upstream and 0.73 kb downstream flanking sequence from MC58 cloned into pGEM®-T Easy	Ampicillin	This study
pMA1	*NMB0375* plus 0.86 kb upstream and 1.182 kb downstream flanking sequence from MC58 cloned into pGEM®-T	Ampicillin	This study
pMR1	*NMB0088* gene plus 0.862 kb upstream and 0.917 kb downstream flanking sequence from MC58 cloned into pGEM®-T Easy	Ampicillin	This study
pMK1	*NMB0506* gene plus 1.435 kb upstream and 0.873 kb downstream flanking sequence from MC58 cloned into pGEM®-T Easy	Ampicillin	This study
pMT2	Re-ligated pMT1 after removing *NMB1053* by inverse PCR	Ampicillin	This study
pMA2	Re-ligated pMA1 after removing *NMB0375* by inverse PCR	Ampicillin	This study
pMR2	Re-ligated pMR1 after removing *NMB0088* by inverse PCR	Ampicillin	This study

pMK2	Re-ligated pMK1 after removing *NMB0506* by inverse PCR	Ampicillin	This study
pMA3	pMA2 cloned with kanamycin resistance cassette of 1.5 kb	Ampicillin Kanamycin	This study
pMT3	pMT2 cloned with kanamycin resistance cassette of 1.5 kb	Ampicillin Kanamycin	This study
pMK3	pMK2 cloned with kanamycin resistance cassette of 1.5 kb	Ampicillin Kanamycin	This study
pMA4	pMA2 cloned with Omega resistance cassette of 2.0 kb	Ampicillin Spectinomycin Streptomycin	This study
pMT4	pMT2 cloned with Omega resistance cassette of 2.0 kb	Ampicillin Spectinomycin Streptomycin	This study
pMR4	pMR2 cloned with Omega resistance cassette of 2.0 kb	Ampicillin Spectinomycin Streptomycin	This study
pMK4	pMK2 cloned with Omega resistance cassette of 2.0 kb	Ampicillin Spectinomycin Streptomycin	This study
pMT5	*NMB1053* from MC58 cloned into pQE30	Ampicillin	This study
pMA5	*NMB0375* from MC58 cloned into pQE30	Ampicillin	This study
pMR5	*NMB00088* from MC58 cloned into pQE30	Ampicillin	This study
pJMK30	Source of a kanamycin resistance cassette	Ampicillin Kanamycin	(Van Vliet *et al.*, 1998)
pHP45Ω	Source of Omega cassette	Ampicillin Spectinomycin Streptomycin	(Prentki and Krisch, 1984)

pGEM® -T Easy	Linearized cloning vector with a single 3´-terminal thymidine at both ends	Ampicillin	Promega
pGEM® -T	Linearized cloning vector with a single 3´-terminal thymidine at both ends	Ampicillin	Promega
pQE30	Cloning vector enabling a His-tag sequence to be incorporated at the N terminus of any protein expressed from a cloned gene	Ampicillin	Qiagen

Table 2.2. Bacterial strains used in this study

Strains	Relevant characteristics	Antibiotic resistance	Source/ Reference
N. meningitidis MC58Δ*pilQ/*Δ*porA*	*NMB1812* (*pilQ*) replaced by kanamycin cassette and *NMB1429* (*porA*) replaced by Omega	Kanamycin Spectinomycin	(Orihuela *et al.* 2009)
N. meningitidis MC58Δ*NMB1053-kan*	MC58 with *NMB1053* replaced by a kan cassette	Kanamycin	This study
N. meningitidis MC58Δ*NMB0506-kan*	MC58 with *NMB0506* replaced by a kan cassette	Kanamycin	This study
N. meningitidis MC58Δ*NMB0375-Omega*	MC58 with *NMB0375* replaced by an Omega cassette	Spectinomycin Streptomycin	This study
N. meningitidis MC58Δ*NMB0088-Omega*	MC58 with *NMB0088* replaced by an Omega cassette	Spectinomycin Streptomycin	This study
N. meningitidis (MC58)	Wild type serogroup B isolate		ATCC
N. lactamica	ATCC 23970		ATCC
E. coli JM109	Cloning and expression strain		Promega

2.3 Protein and nucleic acid sequence analysis

The genomic database of *N. meningitidis* MC58 was accessed at https://www.ncbi.nlm.nih.gov/nuccore/NC_003112.2. BLAST searches were performed using the server at http://blast.ncbi.nlm.nih.gov/Blast.cgi. Signal peptides were predicted using the SignalP 3.0 server at http://www.cbs.dtu.dk/services/SignalP/. Promoter predictions were performed using the server at http://www.bioinformatics.org/sms2/ and other genome analysis tools were accessed at https://www.genome.jp/. Additional DNA and protein analyses were performed using the DNAMAN software (Lynnon BioSoft) and SnapGene.

2.4 DNA manipulation

2.4.1 Extraction of chromosomal DNA

N. meningitidis strains were grown overnight on chocolate agar plates at 37°C with 5% CO_2. The cultured plates were then scraped with a sterile loop and the collected bacteria were resuspended in 180 µl of ATL buffer and 20 µl of proteinase K (20 mg ml^{-1}). Following this, the sample was vortex and then heated at 56°C for 30 min until complete lysis of cells had occurred. 200 µl of Lysis solution C was added, vortex, incubated at 56°C for 10 min. 200 µl of ethanol was added to lysis solutions and vortex, transferred mixture to a spin column and centrifuged at 6500 × *g* for 1 min. The bound DNA was then washed twice with wash solution. Finally, 200 µl elution buffer (EB) was used to collect the DNA in a centrifuge tube after centrifugation at 6500 × *g* for 1 min.

2.4.2 Extraction of plasmid DNA

The Sigma GenElute™ Plasmid Miniprep Kit was employed for the extraction of plasmid DNA, which was performed according to the manufacturer's instructions. Briefly, *E. coli* cells containing the targeted plasmid were cultured overnight at 37°C with shaking at 200 rpm. The next day, bacterial cells were harvested via centrifugation at 14,000 × *g* for 1 min. The resultant pellets were then resuspended

in 200 µl of resuspension solution. Then, 200 µl of lysis buffer was added and the sample thoroughly mixed, and 400 µl of neutralisation solution was subsequently added. After centrifugation at 12,000 × *g* for 10 min, the supernatant was added to a GenElute™ column which was then centrifuged at 12,000 × *g* for 1 min. The column was washed with wash buffer (70% ethanol), before finally the plasmid DNA was eluted in 100 µl of water. The extracted plasmid DNA was stored at - 20°C.

2.4.3 DNA quantification

DNA was quantified using a NanoDrop 1000 spectrophotometer (Agilent Technologies).

2.4.4 Restriction enzyme digestion

For restriction digestion, 100–200 ng of plasmid DNA was used for screening purposes, while for plasmid vector digestion, 500–1000 ng of DNA was used. Either way, the plasmid DNA was digested with appropriate enzymes at 37°C for approximately 3 h, or overnight. The digestion enzymes and buffer were purchased from New England Biolabs (NEB), and were used according to the manufacturer's instructions.

2.4.5 Dephosphorylation of DNA fragments

Antarctic phosphatase was used according to the protocol provided by the supplier, NEB. Plasmid DNA (1 µg) was incubated with 5 units of Antarctic phosphatase with 10 × reaction buffer in a final volume of 50 µl. The incubation was performed at 37°C for 60 min in a water bath. The reaction was stopped by heat inactivation at a temperature of 65°C for 5 min.

2.4.6 A-tailing

A-tailing of PCR products was performed according to the protocol provided by the manufacturer (pGEM®-T Vector System, Promega). Following these instructions, PCR product (7 µl), *Taq* DNA polymerase (1 µl), and 10 × Polymerase Reaction Buffer with $MgCl_2$ (1 µl) were mixed thoroughly, with dATP added to a final

concentration of 0.2 mM. The next step was addition of deionised water up to a final reaction volume of 10 µl, followed by incubation for 15–30 min at 70°C.

2.4.7 Ligation

The final volume of ligation reactions was 10 µl. The insert DNA and plasmid vector were used at a molar ratio of 1:1 or 1:3. A typical ligation reaction consisted of: 50 ng vector; insert DNA; T4 DNA ligase (Promega) (1 µl); and 10 × ligation buffer (Promega) (1 µl), with the final volume made up to 10 µl with dH_2O. The ligation reaction was kept at 16°C for 1 h, or overnight at 4°C.

2.4.8 Purification of PCR and gel-extracted DNA products

DNA fragments, restriction digestion products and PCR products were purified according to the manufacturer's instructions using a PCR purification kit (Sigma–Aldrich). After agarose gel electrophoresis, the desired band was excised from the gel using Gene Catcher pipette tips.

2.5 Primer design and DNA sequence analysis

Nucleotide primers designed using DNAMAN version 4.13 (Lynnon BioSoft) were used for the amplification of specific bacterial genes, as illustrated in Table 2.3 below. For mutagenesis, primers were designed to ensure the presence of at least one DNA uptake sequence (DUS; GCCGTCTGAA). Sanger sequencing of plasmids was performed by Source Bioscience, with sequencing data subsequently analysed using DNAMAN and SnapGene.

Table 2.3. Primers used in this study

Used	Primer name	DNA Sequence (5'->3')	Restriction site
NMB1053 Amplification (1)	NMB1053-F1	TAACCGAAACCGGACGAACC	
NMB1053 Amplification (1)	NMB1053-R1	CCCATCACCAAGCCCAGATT	
NMB0506 Amplification (1)	NMB0506-F1	ACAACTACCGGACATTTTGGAG	
NMB0506 Amplification (1)	NMB0506-R1	CGTTATACCTTGGGATTCCATG	
NMB0375 Amplification (1)	NMB0375-F1	CGGAACGGACGCGGATTTTT	
NMB0375 Amplification (1)	NMB0375-R1	AAAGCATCATTCGTAACAGCGT	
NMB0088 Amplification (1)	NMB0088-F1	AAGTCAGCGATGTGGCAAACGC	
NMB0088 Amplification (1)	NMB0088-R1	CGTGCCGATACCGTTACCGTA	
InvPCR NMB-1053 Amplification (2)	NMB1053-invF2	GCGCGC**AGATCT**GCTCTTGTGCAGCGGCGGCAGTA	*BglII*
InvPCR NMB-1053 Amplification (2)	NMB1053-invR2	GCGCGC**AGATCT**GTGGCGACGTATCGCTCACCATCC	*BglII*
InvPCR NMB-0506 Amplification (2)	NMB0506-invF2	GCGCGC**AGATCT**CCAATGTTCCAAGTACACCTACTACG	*BglII*
InvPCR NMB-0506 Amplification (2)	NMB0506-invR2	GCGCGC**AGATCT**GCTGCTACTCCAGTTCCGGCTGCCG	*BglII*
InvPCR NMB-0375 Amplification (2)	NMB0375-invF2	GCGCGC**AGATCT**CGGCGACACAACCGCCCAAAACCG	*BglII*
InvPCR NMB-0375 Amplification (2)	NMB0375-invR2	GCGCGC**AGATCT**CGGTCAGTGTGCCGCAGGCTGT	*BglII*

InvPCR NMB-0088 Amplification (2)	NMB-0088 invF2	GCGCGC**AGATCT**ACATCCACATCAACGACACCAGC	*BglII*
InvPCR NMB-0088 Amplification (2)	NMB-0088 invR2	GCGCGC**AGATCT**CGTTGACCGACTGTGTGCCG	*BglII*
NMB1053F Amplification (3)	NMB1054-seqF	AGTCCCGTCATTCCCGCGCAG	
NMB1053R Amplification (3)	NMB1051-seqR	TCGAGCAAGGCAACGTGGC	
NMB0506F Amplification (3)	NMB0502-seqF	GGAAGAATTACAAACATTCACCC	
NMB0506R Amplification (3)	NMB0508-seqR	GCATGGGCAATCTTGTGGGTGGTATATCGC	
NMB0375F Amplification (3)	NMB0377-seqF	CGTACTGATACGGATGGACGGCG	
NMB0375R Amplification (3)	NMB0374-seqR	GCTTCGATGGTTGCTTTAATTTGC	
NMB0088F Amplification (3)	NMB0089-seqF	GCATCAACAAACGCGGTGGC	
NMB0088R Amplification (3)	NMB0086-seqR	CGACAACACGGTCGGTATGG	
Kanamycin cassette Amplification	30-KAN-CTERM	GGTATGACATTGCCTTCTGCG	
Kanamycin cassette Amplification	30-KAN-NTERM	CATCCTCTTCGTCTTGGTAGC	
Omega cassette Amplification	Omega-F	CGATCACGGCACGATCATCG	
Omega cassette Amplification	Omega-R	CGCAATAGTTGGCGAAGTAATCG	
NMB0375 Amplification (4)	MafApQE30-F	GCG**GGATCC**GGCACACTGACCGGCATACC	*BamHI*
NMB0375 Amplification (4)	MafApQE30-R	GCG**GGATCC**TTATCCTCCTTTGCGGCGGCG	*BamHI*
NMB0088 Amplification (4)	FadLpQE30-F	GCG**GGATCC**TCCGGCTACCACTTCGGCAC	*BamHI*
NMB0088 Amplification (4)	FadLpQE30-R	GCG**GGATCC**TTATTTGAATTTGTAGGTGTATTCG	*BamHI*

NMB1053 Amplification (4)	Opc5pQE30-F	GCG**GGATCC**GAGCTTCAAACCGCT AATGAG	*BamHI*
NMB1053 Amplification (4)	Opc5pQE30-R	GCG**GGATCC**TCAGAATTTTATGCCG ACGCG	*BamHI*

2.6 Agarose gel electrophoresis

Agarose gels (1%) were pre-stained with 1× SYBR® Safe DNA Gel Stain (Invitrogen; 0.1 µl ml^{-1}). DNA fragments were separated by electrophoresis using a 1% w/v agarose gel in 1 × TAE (Tris–acetate–EDTA (Ethylenediamine tetraacetic acid)) buffer (Sigma) for 50 min at a voltage of 110 V. A 1 kb DNA ladder (New England Biolabs) was used on each gel, and an ultraviolet scanner was used to visualise DNA fragments.

2.7 Polymerase chain reaction (PCR)

All polymerase chain reaction (PCR) analyses were performed using a C1000 Thermal Cycler (Bio-Rad) as described in Sections 2.7.1 and 2.7.2.

2.7.1 PCR protocol using *Taq* polymerase

10 µl reaction mixtures typically contained 1 µl of 2 µM (2 pmol $µl^{-1}$) of each primer, 1 µl of 2 mM dNTPs, 0.1 µl of *Taq* polymerase (New England Biolabs), 1 µl of template plasmid (*ca.* 1 ng), and 1 µl of 10 × reaction buffer (New England Biolabs), and were made up to 10 µl using dH_2O. The reaction conditions consisted of an initial denaturation step conducted for 5 min at 95°C, followed by 30 cycles of: 30 s at 95°C; 30 s at 54-62°C (annealing temperature determined by the melting temperature of the primer pair); and 1 min per 1 kb of product at 68°C. This was followed by a final incubation step for 5 min at 68°C. Reaction tubes were maintained in the thermocycler at 4°C until removal, and samples either used immediately or stored at -20°C.

2.7.2 Phusion High-Fidelity DNA Polymerase

50 µl reaction mixtures typically contained 5 µl of 2 µM (2 pmol $µl^{-1}$) of each primer, 5 µl of 2 mM dNTPs, 1 µl of template plasmid (*ca.* 1 ng), 5 µl of 10 ×

reaction buffer, and 0.5 µl Phusion High-Fidelity DNA Polymerase (New England Biolabs), made up to 50 µl by addition of dH_2O. High-fidelity PCR was completed through a designed amplification protocol which included the following steps. Initial denaturation for 3 min at 95°C was followed by 30 cycles consisting of: 30 s of denaturation at 95°C; 30 s at 54-66°C of annealing (temperature determined by the melting temperature of the primer pair); and 1 min of extension at 72°C per kb of the expected product. Following this, a final extension step was performed at 72°C for 10 min. Once completed, the PCR product was kept at 4°C.

2.8 Bacterial transformation

2.8.1 Transformation of *E. coli* JM109

E. coli JM109 competent cells were purchased from Promega and stored at -80°C until use. 50 µl aliquot of competent cells was thawed on ice before adding about 5 µl (100 ng) of ligation reaction mixture, which was gently mixed with the competent cells before incubating the mixture on ice for 20 min. Subsequently, the cells were heat-shocked at 42°C in a water bath for about 50–60 s, without shaking. The mixture was then immediately removed from the water bath and kept on ice for 2–3 min. Then, 950 µl of SOC medium (Invitrogen) was added and the mixture incubated for about 1.5 h at 37°C with shaking at 200 rpm. Finally, aliquots of the transformation mixture were plated out onto LB agar plates containing appropriate antibiotics, followed by incubation at 37°C overnight.

2.8.2 Natural transformation of *N. meningitidis*

N. meningitidis was streaked onto a chocolate blood agar plate and grown overnight at 37°C in an atmosphere of 5% CO_2. Next, a single colony was selected and inoculated into 10 ml of BHI broth containing 1% Vitox. The tube was shaken in a 37°C incubator at 200 rpm for about 2 h, until the OD_{600} reached 0.5. Then, approximately 200 µl of the culture was aliquoted onto BHI agar with 1% Vitox. After drying, plates were incubated for 100 min at 37°C with 5% CO_2. Mutagenic DNA (20 µl; *ca.* 2 µg) was then added to the culture spots and left to absorb at 37°C for 4 h or overnight in an incubator with 5% CO_2. Control plates contained no DNA.

A sterile loop was used to remove the bacterial growth, which was then resuspended in 1 ml of BHI broth and aliquots plated onto BHI agar plates supplemented with 1% Vitox and appropriate antibiotics. The plates were then incubated at 37°C with 5% CO_2 for up to 48 h. Colonies appearing on the plates were screened by PCR.

2.9 Culture of human embryonic kidney cells (HEK293T)

Human embryonic kidney cells (HEK293T) were obtained from ATCC and were grown in 5% CO_2 at 37°C in different size tissue culture flasks (Corning): 25 cm^2, 75 cm^2 or 225 cm^2 for small, medium, or large-scale cultures, respectively. Cells were grown in Dulbecco's Modified Eagle's Medium (DMEM; Gibco) supplemented with 0.5% L-Glutamine, 10% (v/v) foetal bovine serum (FBS; Sigma) and 5% (v/v) penicillin–streptomycin (Sigma). Replacement of growth medium was carried out every 48 h during the culture of cells.

2.9.1 Propagation of HEK293T cells

Once HEK293T monolayers had reached 80% confluency, the growth medium was removed, and the cells washed once in phosphate buffered saline (PBS; Sigma). Trypsin–EDTA (5 ml; Sigma) was then added and the flask incubated for 5 min at 37°C. Once the cells were detached from the flask, 5 ml of fresh DMEM (with supplements as above) was added and the resulting suspension centrifuged at 1,500 × *g* for 10 min. Cells were resuspended in new growth medium (to a final volume of 10 ml and seeded into three new 75 cm^2 culture flasks).

2.9.2 Cryopreservation and thawing of HEK293T cell cultures

Cell pellets prepared by trypsinisation as above were transferred into cryogenic vials after resuspension in 1 ml of 10% DMSO in PBS. Vials were placed at -20°C for 18–24 h, then transferred to storage at -80°C, or for long-term storage -150°C. When required, cryopreserved cell cultures were thawed in a water bath at 37°C for 5 min and mixed with 10 ml of fresh growth medium, then centrifuged for 10 min at 1,500 × *g*, after which they were resuspended once more in fresh growth medium and used to seed a 75 cm^2 culture flask.

2.9.3 Determination of cell number and cell viability

Cell suspensions (10 µl aliquots) were mixed thoroughly with 90 µl of Trypan blue (Invitrogen), and then loaded onto a haemocytometer for counting using a light microscope. Cells were counted and the ratio of live to dead cells determined.

2.10 Expression and purification of Fc-tagged proteins in mammalian cells

2.10.1 Transfection of HEK293T cells using calcium phosphate precipitation

Cells were grown in 75 cm^2 culture flasks until 30% confluent, then transfection mixes were prepared by mixing plasmid DNA (1–3 µg ml^{-1}) with 2 M $CaCl_2$ (155 µl) and dH_2O up to a final volume of 1.5 ml. After thorough mixing, 1.5 ml of 2 × Hepes Buffered Saline: (HBS: Sigma) was then added to the DNA/$CaPO_4$ precipitate and the mixture was incubated at room temperature for 10–15 min until it appeared slightly milky. The mix was added dropwise to the medium in 75 cm^2 flasks and then the cells were incubated at 37°C in a 5% CO_2 incubator for 18 h. The growth medium was replaced with UltraCHO Cell Medium (Invitrogen) and incubation continued for a further 48 h. A fluorescence microscope (Nikon) was used to observe the expression of GFP-topaz protein and record images, in order to compare the number of GFP-expressing cells (successfully transfected) with cells that were not transfected (no GFP).

2.10.2 Transfection of HEK293T cells using Lipofectamine 3000

For small-scale transfections, cells were allowed to grow in a 25 cm^2 flask to 90% confluence. Transfection utilised two tubes. In the first tube, 11 µl of the Lipofectamine 3000 reagent (Invitrogen) was mixed with Opti-MEM medium (500 µl). In the second tube, Opti-MEM (500 µl) and plasmid DNA (6 µg) were thoroughly mixed with Lipofectamine 3000 (8 µl), and the mixture incubated at room temperature for 5 min. This was then combined with the contents of the first tube and the mixture incubated for 45 min at room temperature. The transfection

mixture was then added dropwise to the prepared cells in flask, which were incubated at 37°C in humidified conditions with 5% CO_2 for 18 h. The growth medium was then replaced with DMEM supplemented with 5% v/v penicillin–streptomycin but without FBS, and the cells were incubated for a further 48 h. The cells were then observed using a fluorescence microscope (Nikon) as in Section 2.10.1 to determine transfection efficiency. For larger-scale transfections, 75 cm^2 flasks were used and the volumes of reagents increased proportionately.

2.10.2.1 Preparation of cell lysates

Approximately 72 h following transfection, the growth medium from a 25 cm^2 culture flask was discarded and the cells washed with cold PBS then added 5 ml of radio immunoprecipitation assay (RIPA: Sigma-Aldrich) buffer supplemented with phosphatase inhibitors (Thermo Scientific) and cOmplete™ Mini EDTA-free Protease Inhibitor Cocktail (Merck Millipore). The plates were then placed on ice for 30 min. The cells were scraped, and lysates were collected in microfuge tubes and then centrifuged at 17,000 × *g* for 20 min at 4°C, in order to remove cell debris, and the resultant clarified cell lysate was transferred to a clean tube and stored at - 80°C.

2.10.2.2 Purification of Fc-tagged recombinant proteins from cell lysate

Protein A/G-Sepharose (GE Healthcare Bioscience) was utilised to purify Fc-tagged recombinant proteins. The clarified cell lysate (3 ml) was diluted 1:1 (v/v) with binding buffer (0.05 M sodium borate, 0.15 M sodium chloride pH 8). Then, 10 µl of Sepharose beads per millilitre of sample was added to the diluted lysate in an Eppendorf tube and the contents incubated with shaking at 4°C overnight. An empty column (Source BioScience Life Sciences) was prepared and washed 5 × with binding buffer, using 3 ml per wash. The cell lysate with the beads was then added to the column, which was incubated for 10 min. The flow-through was collected and the column washed with 0.5 M sodium chloride binding buffer (3 × 3 ml). Fc-tagged proteins were eluted with 300 µl per fraction of 0.1 M glycine pH 2.5 and neutralised with 50 µl per fraction of 1 M Tris–HCl pH 9 immediately after elution.

2.10.3 Transfection of HEK293T cells with GeneJuice reagent

For large-scale transfection experiments, cells were grown in a 225 cm^2 flask until a confluency of about 60% was reached. The following day, the medium was substituted with 18 ml DMEM supplemented with 0.5% L-Glutamine, 10% (v/v) FBS and 5% (v/v) penicillin–streptomycin. After 4 h incubation, transfection mixtures were prepared comprising 1.8 ml of serum-free Opti-MEM (Gibco) containing 0.5% L-Glutamine, 5% (v/v) penicillin–streptomycin and GeneJuice reagent (54 µl; Merck Millipore). These components were mixed and incubated together for 10 min. Then, 23 µg plasmid DNA was added to the transfection mixture followed by further incubation at room temperature for 15 min. The transfection mixture was added dropwise to the flask and mixed gently by rocking. Flasks were then incubated at 37°C in humidified conditions with 5% CO_2 for 18 h. The growth medium was then substituted with Opti-MEM (Gibco) with 5% (v/v) penicillin–streptomycin, and the cells incubated for a further 6–8 days. Supernatants were collected in a 250 ml Corning bottle and centrifuged at 3,000 × *g* for 15 min at 4°C. The process was repeated in a clean container, and the supernatant was filtered through a 0.22 µm filter into a clean flask. Cells were observed using a ZOE microscope (Nikon).

2.10.3.1 Purification of Fc-tagged recombinant proteins from culture supernatant

PBS (500 ml) was added to Econo-Column® chromatography columns (Bio-Rad) and the meniscus position was marked. The PBS was then removed and Protein A/G-Sepharose (GE Healthcare Bioscience) was added up to the 500 ml mark. The column was thoroughly washed with PBS (25 ml) then the filtered culture supernatant was applied. Weakly-interacting proteins were removed through a further wash with 50 mL of PBS. Fc-tagged proteins were then eluted by adding 10-drop quantities of 0.1 M glycine pH 2.8 to the column and collecting the eluate as individual fractions, which were neutralised promptly with 1 M Tris–HCl pH 8 (50 µl). The column was stored in 20% ethanol at 4°C. The resulting fractions were

resuspended in 4 × SDS–PAGE sample buffer and heated to 100°C for 5 min prior to SDS-PAGE and immunoblotting analysis.

2.11 Expression of recombinant proteins in *E. coli*

Fresh LB broth (19 ml or 475 ml for small- and large-scale preparations, respectively) containing 100 µg ml $^{-1}$ ampicillin was inoculated with 1 ml or 25 ml, respectively, of an overnight culture of *E. coli* JM109 harbouring the appropriate expression plasmid. Cultures were grown to an OD_{600} of *ca.* 0.5, at which point 1 ml of pre-induced culture was taken for SDS–PAGE analysis. The remaining culture was immediately induced with 1 mM isopropyl β-D-1-thiogalactopyranoside (IPTG) and incubated at 37°C for 4 h with agitation at 200 rpm. Samples were taken at hourly intervals for SDS–PAGE analysis, which was carried out after harvesting cells by centrifugation at 13,000 × *g*. The resulting pellets were resuspended in 1 × SDS–PAGE sample buffer and heated to 100°C for 5 min prior to SDS-PAGE and immunoblotting analysis. For large-scale preparations, 50 ml aliquots of the culture were centrifuged at 4,500 × *g* for 15 min at 4°C. Cell pellets were collected and stored at -80°C until needed.

2.12 Protein purification using immobilised metal affinity chromatography (IMAC)

IMAC was employed to purify His-tagged proteins under native conditions, using an AKTA Prime Plus system (GE Healthcare) in accordance with the manufacturer's guidelines. Harvested cells were resuspended in 30 ml lysis buffer (50 mM sodium phosphate, [pH 7.4]; 300 mM NaCl, 10 mM Imidazole, [pH 7.4]). Sonication was performed on ice in brief bursts (15 s on and 15 s off) for 10 min with a Model 705 Sonic Dismembrator (Fisher Scientific) at an amplitude of 15 microns. The lysate was centrifuged for 30 min at 10,000 × *g* at 4°C. A peristaltic pump was used to load the supernatant (clarified lysate) onto a 5 ml HisTrap FF Crude column installed on the AKTA PrimePlus system at a flow rate of 1 ml min $^{-1}$. The column was washed with wash buffer (50 mM sodium phosphate [pH 7.4], 300 mM NaCl, and 50 mM imidazole, [pH 7.4]). Elution of the bound His-tagged

protein was then performed with elution buffer (50 mM sodium phosphate, 300 mM NaCl, and 500 mM imidazole, [pH 7.4]). Fractions were collected using a gradient elution method and monitored using a chromatogram. The eluates were kept at 4°C for further analysis. Aliquots were collected during the purification process and processed for SDS–PAGE and immunoblot analysis.

2.13 Desalting and concentration of purified proteins

Purified protein fractions were pooled and transferred into a Spectra/Por dialysis membrane (Spectrum Labs) and dialysed at 4°C against 1 L of 20% glycerol in PBS for 48 h. The dialysis buffer was refreshed by exchanging it for new buffer every 24 h. The desalted recombinant protein was then concentrated by centrifugation at 4,500 × g at 4°C using 5 ml 10 kDa molecular weight cut-off (MWCO) Vivaspin tubes (Sartorius).

2.14 Protein quantification

For protein quantification, the protein concentration was measured using a Nanodrop spectrophotometer (ND-1000; Agilent Technologies).

2.15 Antibodies and reagents

Antibodies were purchased from Sigma unless otherwise stated. An anti-human IgG (Fc-specific) alkaline phosphatase conjugate was used for enzyme-linked immunosorbent assay (ELISA), far-western blotting and immunoblotting procedures. It was used for ELISA and immunoblotting at 1:5,000 dilution. Anti-goat IgG (whole molecule) alkaline phosphatase was used as a secondary antibody at 1:30,000 dilution. The rabbit anti-FGFR1 primary antibody (Ab-154) was used at 1:1,000 dilution. Anti-rabbit IgG–alkaline phosphatase was used as a secondary antibody at 1:30,000 dilution. A mouse anti-penta-histidine monoclonal primary antibody (Qiagen; 1:2000 diluted) was used to detect histidine-tagged proteins, and an anti-mouse IgG alkaline phosphate conjugate (1:10,000 dilution) was used as secondary antibody. The chemical inhibitor of FGFR1, SU5402, was purchased from Calbiochem.

2.16 Sodium dodecyl sulphate polyacrylamide gel electrophoresis (SDS–PAGE) and immunoblot analysis

2.16.1 SDS–PAGE analysis

SDS–PAGE was used to separate proteins using the Bolt™ Mini Gel Tank device (Novex®, Life Technologies, Thermo Fisher Scientific). Each sample was mixed with 5 × SDS sample buffer (1 g SDS, 5 ml glycerol, 25 mg bromophenol blue, 62.5 mM Tris [adjusted pH 6.8], 1 ml 2-mercaptoethanol; made up to 10 ml with dH_2O) or 4 × SDS sample buffer (1.6g of SDS, 8ml (100%) autoclaved glycerol, 5ml 1M Tris-HCl pH6.8, a small amount of Bromophenol Blue and HPLC quality dH_2O to make up volume to 20ml) and heated at 95–100°C for 5 min. Next, 12–20 µl of each sample was loaded onto a 10% polyacrylamide gel and run at 125 V for 60–90 min alongside ColorPlus™ pre-stained protein ladder (New England Biolabs). After running, gels were stained with SimplyBlue Safe Stain (Thermo Fisher Scientific) for 1 h at room temperature, with gentle agitation. Gels were then de-stained with deionised water by incubation overnight at room temperature, also with gentle agitation.

2.16.2 Immunoblotting analysis

After proteins were resolved, gels were soaked for 10 min in semi-dry blotting buffer (480 mM Tris-Base, 390 mM Glycine, 0.375% w/v SDS and 200 ml methanol made up to 1,000 ml with dH_2O) before being transferred to nitrocellulose membrane (Sigma) using a Trans-Blot® semi-dry transfer machine (Bio-Rad) for 30 min at 10 V. Membranes were blocked with 5% skimmed milk powder in PBS for 2 h at room temperature, or overnight at 4°C, with gentle agitation. After blocking, membranes were incubated at room temperature for 2 h with primary antibody diluted into fresh blocking buffer. Membranes were then washed three times using PBS containing 0.1% Tween-20 (PBST), for 5 min each time. To detect bound primary antibody, the membrane was probed for 1 h on an orbital shaker with secondary antibody diluted in blocking buffer. The secondary antibody solution was removed, and the membrane washed as before. Bound secondary antibodies were

visualised using a 5-bromo-4-chloro-3-indolyl phosphate/nitro blue tetrazolium (BCIP/NBT) liquid substrate system (Sigma).

2.17 Far-western blotting

Whole-cell lysates (20 µg ml^{-1}) were run on 10% polyacrylamide gels. After this was complete, gels were soaked for 10 min in semi-dry blotting buffer and proteins transferred to nitrocellulose membrane via Trans-Blot® (Bio-Rad) semi-dry transfer for 20 min at 30 V. Proteins were denatured by incubation of the membrane in denaturing and renaturing buffer (Appendix) containing 6 M guanidine–HCl at room temperature for 30 min. Then, the guanidine (denaturant) concentration was gradually reduced, in a stepwise manner, to promote refolding (renaturation) of the bound proteins. The membrane was washed with denaturing and renaturing buffer (Appendix) containing 3 M guanidine–HCl for 30 min at room temperature. Then, washing was conducted using denaturing and renaturing buffer (Appendix) with a concentration of 1 M and then 0.1 M guanidine–HCl at 4°C for 30 min, and finally denaturing and renaturing buffer (Appendix) with no guanidine–HCl at 4°C overnight. The next day, membrane blocking was performed using 5% skimmed milk in PBST buffer overnight at 4°C with gentle agitation. After that, the membrane was incubated with purified bait protein (2 µg ml^{-1}) in protein-binding buffer (Appendix) overnight at 4°C with gentle agitation. Unbound bait protein was removed using three washes with PBST buffer, for 10 min each time. The detection of bound bait was then carried out using appropriate primary and secondary antibodies as outlined in Section 2.16.2.

2.18 Preparation and fixation of whole Neisserial cells

Neisserial strains were grown in 10 ml BHI broth overnight at 37°C with shaking. The OD_{600} was then measured, and the culture was diluted 1:20 with fresh BHI broth and incubated again until the OD_{600} reached $\geq$ 0.5. Cells were harvested by centrifugation at 2,000 × *g* for 10 min at 4°C. The bacterial pellets were resuspended in 10 ml of filtered PBS and re-centrifuged, and this washing step was repeated twice. Next, the pellets were resuspended in 10 ml of 0.5% v/v formaldehyde (EMS;

15710-S) in PBS and incubated at 4°C for 30 min with gentle agitation. After fixing the bacteria, the sample was centrifuged at 2,000 × *g* for 10 min at 4 C, and the pellets washed in PBS and resuspended in 10 ml of sodium carbonate buffer (10 mM sodium carbonate Na_2CO_3, 90 mM sodium bicarbonate $NaHCO_3$, pH 7.4). The OD_{600} of each strain was checked and adjusted to 0.17 to ensure uniformity between strains.

2.19 Whole-cell ELISA

Microplate wells (Thermo Fisher Scientific, Nunc Immobilizer Amino 12X8 Strips) were homogenously coated with 100 µl of formaldehyde-fixed whole cell suspension, prepared as above, and incubated overnight at 4°C with gentle agitation. Control wells were coated with 1% (w/v) BSA in PBS. Wells were then washed three times with 0.05% v/v Tween-20 in PBS, then 100 µl per well of 1% BSA/PBS was added to each well to reduce nonspecific binding, followed by incubation for 2 h at room temperature with gentle agitation. The wash steps were repeated, then 100 µl per well of Fc-FGFR1 IIIc (2 µg ml^{-1}) or Fc-stop (1 µg ml^{-1}) was added in 1% BSA/PBS, followed by overnight incubation at 4°C with gentle agitation. The next day, the wash steps were repeated again. Then, 100 µl of the appropriate antibody diluted in 1% BSA/PBS was added and the mixture incubated overnight at 4°C. After washing the plate three times once more, colour was developed by the addition of 200 µl phosphatase substrate (Sigma; each tablet dissolved in 5 ml of glycine buffer [100 mM glycine, 1 mM zinc-chloride($ZnCl_2$), 1 mM magnesium-chloride ($MgCl_2$), pH 10.4]). A GloMax® microplate reader (Promega) was used to read the plates at an absorbance of 405 nm.

2.20 ELISA (protein–protein interaction)

This experiment was carried out as per the previous section, with the following differences: wells were coated with 100 µl aliquots of Fc-stop (0.3 µg ml^{-1} in PBS) or Fc-FGFR1 IIIc (1 µg ml^{-1} in PBS); and coated plates were probed with purified MafA (NMB0375; 1 µg ml^{-1} in 1% BSA/PBS), or pyocin S3 (2 µg ml^{-1} in 1% BSA/PBS) as a negative control.

2.21 Adhesion and invasion assays

2.21.1 Culture of human brain microvascular endothelial cells

Human brain microvascular endothelial cells (HBMECs; ScienCell Research Labs) were routinely grown in T-75 flasks (Biocoat, BD Biosciences). Before seeding the cells, the flask was coated with 10 ml of bovine fibronectin solution (1 µg ml^{-1} bovine fibronectin [Sigma] in PBS, sterilised by filtration [0.22 µm filter]), and incubated at 37°C with 5% CO_2. Cells were grown in endothelial cell medium (ECM; ScienCell Research Labs) supplemented with 1% (v/v) Endothelial Cell Growth Supplement, 10% (v/v) FBS, 1% (v/v) endothelial cell glial supplement (ECGS), and 1% (v/v) antibiotic (streptomycin and ampicillin)–antimycotic supplement (Sigma). When the cells reached about 90% confluence, the medium was removed, and the cells were washed with 5 ml of PBS. Trypsin–EDTA (5 ml; Sigma) was then added and the cells incubated for 5 min at 37°C in 5% CO_2, or until cells detached from the flask. Then, an equal volume of growth medium was added for neutralisation. A quarter of this solution was then returned to the flask and the volume made up to 10 ml using complete growth medium. This study used HBMECs that had been grown to various passage numbers, ranging from passage 17–29. For the cell association and invasion assays, HBMEC monolayers were allowed to grow to confluence in 24-well tissue culture plates (coated with fibronectin) at 37°C and 5%CO_2 overnight. When the monolayer reached 100% confluence, the medium was replaced with 2 ml endothelial cell medium-basal (ECM-B) per well, with no FBS or antibiotics.

2.21.2 Culture of *N. meningitidis* and *N. lactamica*

Neisserial strains were grown on chocolate agar plates overnight at 37°C in 5% CO_2. The bacteria were then inoculated into 20 ml of BHI broth and cultured for 2 h at 37°C with shaking at 200 rpm. Cultures were centrifuged at 4,000 × *g* for 5 min at 37°C, and the pellets resuspended in ECM-B (with no FBS or antibiotics). All bacterial suspensions were then adjusted to an OD_{600} of 0.4, with a minimal variation of 0.005.

2.21.3 Association assays

HBMECs were grown in a 24-well plate and infected as described above, in Section 2.21.1 and 2.21.2. To measure the number of input bacteria, bacterial cell suspensions were serially diluted from 10^{-1} to 10^{-7} in warmed ECM-B in 96-well plates and aliquots applied to chocolate agar plates. Plates were incubated at 37°C for 18–24 h in the presence of 5% CO_2. HBMECs were infected with *N. meningitidis* (MC58) or *N. lactamica* with (MOI: 10) = 1×10^7 / well and incubated for 4 h at 37°C in 5%CO_2. After this, bacterial suspensions were removed, and the monolayers washed three times with PBS (1 ml) before being disrupted by vigorous pipetting in 0.1% Saponin in PBS. Serial 10-fold dilutions were prepared from 10^{-1} to 10^{-4} in PBS in a 96-well plate, with aliquots plated onto dry chocolate agar plates and incubated for 18 h at 37°C in 5% CO_2, prior to enumerating the bacteria by colony counting.

2.21.4 Invasion assay

HBMEC monolayers were infected as described in Section 2.21.1 and 2.21.2. After the bacteria were allowed to interact with the monolayers for 4 h at 37°C in 5% CO_2, the bacterial suspensions were removed, and the wells washed with PBS as above. Then, 2 ml ECM-B with gentamicin (100 µg ml^{-1}) was applied to each well and the plates incubated for a further 60 min to kill extracellular bacteria. The monolayers were washed three times with 1 ml per well of PBS, then disrupted and homogenised in 1 ml PBS with 0.1% Saponin as described in Section 2.21.3. Viable meningococci were counted by serial dilution of homogenised suspensions followed by plating, overnight culture, and enumeration, as described in Section 2.21.3.

2.22 FGFR1 Inhibition by SU5402 in HBMECs

The chemical inhibitor 3-[(3-(2-carboxyethyl)-4-methylpyrrol-2-yl)methylene]-2-indolinone (SU5402) was used to investigate the possible effects of inhibiting the activation of FGFR1 during meningococcal infections. HBMECs were grown in 24-well tissue culture plates, as described above in Section 2.21.1. After overnight incubation, the growth medium was exchanged for ECM-B without supplements

(FBS and antibiotics). Meanwhile, bacterial colonies were inoculated into 20 ml BHI broth for *N. meningitidis* and *N. lactamica*, following the method in Section 2.21.2. The serum starved HBMECs were treated with SU5402 (0.5 µM, 2 µM, 10 µM or 20 µM), then incubation was continued for 1 h at 37°C in an atmosphere of 5% CO_2. At this point the medium was removed before adding bacterial suspensions, but there was no need to wash the cells. The bacterial cultures were centrifuged at 4,000 × *g* in a microcentrifuge for 5 min and the pellets resuspended thoroughly in ECM-B (without FBS and antibiotics) and the OD_{600} re-measured, equilibrated, and the volume of bacterial suspension required per well was calculated. The appropriate amounts of bacteria were added to the samples in 24-well plates in fresh ECM-B medium. The plates were then incubated for 4 h at 37°C with 5% CO_2 for the cell adhesion assay, as described in Section 2.21.3. After the 4 h incubation for bacterial adhesion, a cellular invasion assay was then performed as described in Section 2.21.4.

2.23 Statistical Analysis

GraphPad Prism 9.2.0 was employed for statistical analysis. Samples were analysed in triplicate, and each experiment was repeated at least three times. Statistical significance was measured using a two-tailed Student's t-test or one-way ANOVA. A *p*-value of >0.05 was considered non-significant (ns), while values ≤0.05, ≤0.01, ≤0.001 or ≤0.0001 were considered significant (*), very significant (**), highly significant (***) and very highly significant (****), respectively.

Chapter 3: Bioinformatics identification and initial characterisation of potential meningococcal FGFR1 ligands

3.1 Introduction

Although significant advances have been made in the investigation of *N. meningitidis* pathogenesis, the genome of this gram-negative bacterium has yet to be explored completely. Even though the complete sequence of the meningococcal genome is known, relatively few of the identified genes have been studied in detail. As a result, the pathogenicity of the organism is not yet fully understood, suggesting that a substantial number of possible targets for novel anti-infective agents and vaccines have yet to be identified.

N. meningitidis has been found to colonise the nasopharynx in 3–20% of healthy individuals, however, in some the bacterium is able to enter the bloodstream, resulting in direct contact with neurovascular cells and thereby enabling it to reach the brain via passage through the (BBB) (Sjölinder and Jonsson, 2010, Tzeng and Stephens, 2021). The human BBB contains four key structural components: microglia, astrocytes, pericytes and the basal lamina, together with two types of junctions; namely, adherents junctions and tight junctions, which are both located within the inter endothelial cleft (Abbott et al., 2010, Banks, 2015, Hurtado-Alvarado et al., 2017). Due to the presence of these junction structures, the BBB is protective in the sense that only certain types of molecules can be transported through the barrier, thereby limiting the permeability of the paracellular space (Abbott et al., 2010). The BBB therefore functions to protect the CNS from bacteria and toxins, as well as maintaining brain homeostasis and allowing communication between the CNS and the blood (Dando et al., 2014, Banks, 2015). However, some pathogens such as *N. meningitidis* can cross the barrier, despite its highly sophisticated and unique structure, and infiltrate the CNS (Ballabh et al., 2004, Doran et al., 2016).

It has been suggested that cerebral microvascular endothelial cells, which form the BBB, may act as an entry point for *N. meningitidis* to access the brain (Quagliarello

et al., 1986, Eugène et al., 2002, Orihuela et al., 2009). As infection progresses, increased permeability of the BBB is caused by an increase in pinocytosis. In this process, bacteria attached to the cell surface are internalised via invagination (inward folding) of the cell membrane and 'pinching off' of part of the remodelled membrane to form intracellular vesicles. In turn, this leads to disruption of the intercellular junctions of the cerebral capillaries (Tunkel and Scheld, 1993, Schubert-Unkmeir et al., 2010, Join-Lambert et al., 2010). Despite this, extracellular bacteria that cause meningitis do not cause encephalitis which is normally associated with intracellular pathogens such as *Listeria monocytogenes* and consistent with this, there is no evidence to suggest that they can multiply within the parenchyma of the brain (Join-Lambert et al., 2010). Furthermore, *N. meningitidis* can enter the CSF by crossing the blood–cerebrospinal fluid (B-CSF) barrier (Borkowski et al., 2014). It has been proposed that this passage might occur via the choroid plexus, since histological examinations of brain tissue have confirmed the presence of the bacterium in the endothelium of the choroid plexus and meninges (Pron et al., 1997). However, if the choroid plexus was the relevant bacterial portal, it would suggest that meningitis should be linked to ventriculitis, but this implication is inconsistent with observations in post-mortem samples (Join-Lambert et al., 2010).

Nonetheless, if *N. meningitidis* does enter the CSF, the host defence system is inadequate to control the bacterial infection and its associated pathology. The host response mostly relies on innate immune cells such as non-parenchymal (macrophages) and parenchymal (microglia) cells, as well as perivascular blood-derived monocytes (Prinz and Priller, 2017); but due to a local deficiency of complement proteins and immunoglobulins, invading *N. meningitidis* is able to multiply uncontrollably in this environment despite the presence of polymorphonuclear leukocytes resulting from local inflammation (Stephens et al., 2007, Coureuil et al., 2012).

The fact that *N. meningitidis* is among the few bacterial species capable of invading the meninges suggests that specific virulence factors are required for it to enter the subarachnoid space (Join-Lambert et al., 2010, Coureuil et al., 2012). However,

there is still a lack of knowledge regarding the specific receptor ligand interactions involved in the transport of *N. meningitidis* because meningococci are unique human pathogens (Stephens, 2009). This makes it difficult to develop animal models that faithfully reflect the disease in humans to aid investigation of how they traverse host protective barriers such as the B-CSF barrier (Mairey et al., 2006, Schubert-Unkmeir, 2017). The majority of our knowledge of the *N. meningitidis* infection pathway has consequently been obtained from studies using organ or primary cell cultures, or immortalised cell lines. As an example of the latter, the interaction between *N. meningitidis* and brain capillaries has been investigated using various cell lines; for example, HBMEC (Stins et al., 1997, Sokolova et al., 2004, Simonis et al., 2014).

Specifically, some studies have established that pathogenic *N. meningitidis* circulating in the blood might present ligands that bind to receptors on host cells, thereby initiating cellular signalling that encourages bacterial growth and immune escape from host effectors, including the complement system; thereby allowing the pathogen to cross the BBB (Virji, 2009, Coureuil et al., 2017). A number of virulence factors are known to be responsible for direct interactions between *N. meningitidis* and human endothelial cells. These include TFP, along with the surface proteins Opa and Opc, which alter endothelial monolayers and open the intracellular space. However, since pathogenic forms of the bacterium are usually encapsulated, Opa and Opc are likely to remain at least partly concealed by the polysaccharide capsule, and may therefore not interact with their host receptors whilst the bacterium is in the bloodstream (Unkmeir et al., 2002, Virji, 2009, Miller et al., 2013). Adhesion to host cells can be facilitated by the combination of Opa and lipopolysaccharide (Bonnah et al., 2005, Virji, 2009); however, an unencapsulated meningococcal strain can only penetrate HBMECs if it expresses the surface adhesin Opc, which binds to the human serum factor and fibronectin. This acts as a bridging interaction that anchors the bacterium to the integrin receptor of the host cells (Unkmeir et al., 2002).

As mentioned above, attachment of *N. meningitidis* to HBMECs is mediated primarily by TFP, which control both adhesion and signalling between encapsulated meningococci and endothelial cells (Virji, 2009, Coureuil et al., 2017). Although high levels of cerebral microcirculatory shear stress might possibly inhibit initial attachment, *N. meningitidis* proliferates once attached and is therefore able to resist the effects of high blood flow by forming microcolonies, which are characterised by strong intercellular bacterial interactions in addition to strong interactions with the host (Mairey et al., 2006, Mikaty et al., 2009). Invasion of HBMECs by *N. meningitidis* occurs primarily through paracellular mechanisms, signalling events and intracellular junction disruption, although in vitro studies have also shown that a very small number of meningococci (both encapsulated and unencapsulated) can become internalised by both Human umbilical vein endothelial cells (HUVECs) and HBMECs (Virji et al., 1991, Nikulin et al., 2006).

The bacterial TFP are long filamentous structures consisting of pilin subunits, which are assembled into helical fibres by complex molecular machinery and secreted via a pore in the outer membrane (Craig and Li, 2008). In employing TFP to adhere to endothelial cells, *N. meningitidis* uses the cell surface receptor CD147 (Basigin/EMMPRIN) (Bernard et al., 2014), a member of the immunoglobulin (Ig) superfamily that is highly expressed on the surface of brain capillaries, and has four known isoforms in humans (Liao et al., 2011). Ex vivo incubation of human brain tissue with meningococci revealed direct association of bacteria with CD147 positive brain endothelial cells, notably leptomeningeal cells in Virchow-Robin spaces an association that was shown to be dependent upon CD147 (Bernard et al., 2014). Meningococcal cells were found near cortical brain vessels, but did not, however, seem to be associated with either glia or neurons, neither of which express CD147 (Le Guennec et al., 2020). It therefore appears that the ability of *N. meningitidis* to colonise the meninges and capillaries of the human brain depends on the expression of CD147 (Le Guennec et al., 2020). The type IV pilus protein PilQ and the outer membrane protein PorA were also shown to both bind to the 37/67-kDa laminin receptor on HBMECs (Orihuela et al., 2009, Abouseada et al., 2012).

Following initial attachment to host cells, *N. meningitidis* -induced β2-adrenoceptor/β-arrestin signalling causes the development of membrane protrusions and cortical plaques in brain endothelial cells (Coureuil et al., 2010). At the same time, TFP-mediated translocation of β-arrestin to the cortical plaque also acts as a molecular scaffold for subsequent *N. meningitidis* -induced signalling events that open up the paracellular pathway (Coureuil et al., 2010). A number of factors are involved in this process, including recruitment of the Par3/Par6/PKCζ polarity complex to cortical plaque in a Cdc42-dependent manner and the accumulation of adherens and tight junctional proteins underneath the site of bacterial adhesion (Coureuil et al., 2009). Polarity complexes normally play an important role in the formation of intercellular junctions between HBMECs (Doran et al., 2016). However, under the influence of meningococci, their recruitment results in re-routing of proteins involved in the formation of endothelial adherens and tight junctions (Join-Lambert et al., 2010, Kánová et al., 2019). These junctional proteins localise to the site of bacterial adhesion, resulting in the opening of intercellular spaces that allows *N. meningitidis* to pass through the endothelial layer (Coureuil et al., 2009). Interestingly, *N. meningitidis* recruits junctional components only in endothelial cells (Lécuyer et al., 2012). Although it is recognised that TFP have only weak affinity for both the CD147 and the β2AR receptors (Bernard et al., 2014; Le Guennec et al., 2020), the ability of meningococci to assemble into highly-ordered clusters at sites of bacterial adhesion significantly improves their resilience in overcoming shear stress when adhering to endothelial cells (Maïssa et al., 2017).

Besides TFP components, other candidate adhesins have been identified that have been reported to play an important role in meningococcal adhesion to host cells. One such protein, belonging to the group of porins, is the major outer membrane protein PorB (P.IB; NMB2039), which is abundant on the outer membrane of pathogenic *Neisseria* (Wetzler, 2010); however, there is currently no detailed knowledge of meningococcal PorB protein interactions with HBMECs or their downstream effects on cell signalling. In contrast, the PorB homologue of *N. gonorrhoeae* associated with disseminated disease ($PorB_{IA}$) was found to bind to human endoplasmin (Gp96/GRP-94) on the surface of both endothelial and epithelial cells, resulting in

subsequent bacterial uptake mediated by a second host factor, scavenger receptor expression endothelia cells class F member 1 (SREC-I) (Rechner et al., 2007). Thus, it is possible that *N. meningitidis* PorB similarly binds to endoplasmin and/or SREC-I of HBMECs.

Opa and Opc are the two most abundant proteins in the meningococcal outer membrane and a role for the former in adhesion has been characterised (Carbonnelle et al., 2009). The human protein CEACAM1 is widely expressed by endothelial cells, and has been identified as a host receptor for Opa binding. Accordingly, CEACAM1 expression on endothelial cells is significantly upregulated as a result of meningococcal activation of TNF-α during intravascular dissemination (Muenzner et al., 2000, Muenzner et al., 2001, Doran et al., 2016).

Several other adhesins are involved in endothelial cell interactions, but with unknown recognition receptors. It was shown that MspA mediates adhesion to bronchial epithelial cells and HBMECs, but this study was done with *E. coli* expressing recombinant *N. meningitidis* MspA rather than with meningococci directly (Turner et al., 2006). A comparison of adhesion to human cells using MC58*ΔmspA* and wild type bacteria (MC58) would help confirm whether MspA is important for host cell attachment (Hung and Christodoulides, 2013). Meningococcal association with HBMECs is also reportedly mediated by FBA and GapA-1, in a capsule-independent manner (Tunio et al., 2010a, Tunio et al., 2010b). Moreover, the meningococcal adhesion complex protein (ACP) was found to promote adhesion to HUVECs, also independently of encapsulation (Hung et al., 2013). NadA is another of the adhesins on the surface of *N. meningitidis*, which is known to interact with several cell types (including HBMECs) and contribute to the development of infection (Franzoso et al., 2008, Kánová et al., 2018, Mertinková et al., 2020).

A range of cell signalling events can assist pathogenic *N. meningitidis* in crossing the BBB, and these are initiated downstream of interactions between pathogen ligands and surface receptors on the cells of the neurovasculature (Coureuil et al., 2017). For example, interaction with TFP of the meningococcus activates the host

β_2-adrenoreceptor as described above, resulting in cortical plaque formation and facilitating a range of signalling functions that contribute to bacterial infection (Coureuil et al., 2012, Coureuil et al., 2017). In analysing the interactome of *N. meningitidis* to explore these mechanisms further, Kánová et al. (2018) utilised a data-independent acquisition (DIA) approach, namely, sequential window acquisition of all theoretical mass spectra (SWATH-MS), to complement traditional mass spectrometry-based proteomics techniques (e.g., shotgun proteomics and SRM methods). When SWATH-MS, bioinformatics analysis and proteome labelling were used together, the combined approach successfully facilitated identification of previously uncharacterised meningococcal ligands that can interact with HBMECs: a finding that was verified experimentally for five bacterial surface proteins (Kánová et al., 2018).

The same study initially detected a larger group of 84 *N. meningitidis* proteins that could bind to HBMECs, and after excluding predicted cytoplasmic proteins, a final set of 41 surface-exposed *N. meningitidis* proteins was identified as potentially interacting directly with the endothelial cells (Kánová et al., 2018). Previous work in our group has validated interactions between HBMECs and specific bacterial ligands that might perform a critical function in pathogen adhesion. For example, activated FGFR1 is trafficked and recruited within HBMECs to internalised *N. meningitidis*, and ELISA experiments verified a direct interaction of the extracellular IIIc domain of FGFR1 with meningococcal strain MC58, but not with the commensal *N. lactamica* strain ATCC 23970 (Azimi et al., 2020). Following on from this data, it seems reasonable to assume that the meningococcal TFP plays an important functional role in the binding of the bacterium to FGFR1, since binding of a *pilQ* mutant meningococcus to FGFR1 was substantially reduced relative to wild type (Azimi et al., 2020). The *pilQ* mutant showed disrupted subunit secretion, compromising formation of the filament such that the observed effect can be explained by an absence of other TFP components (e.g., PilE, PilX and PilV) on the meningococcal surface (Brown et al., 2010). However, interaction of meningococci with host cells is known to reply upon multiple bacterial surface components in addition to TFP, and this remains unexplored for FGFR1. It is also worth noting, as

illustrated by the examples above, that high-affinity interaction of *N. meningitidis* with individual host receptors tends to rely on specific surface-exposed bacterial proteins (i.e., outer membrane proteins). Thus, one or more of these factors might reasonably be assumed to play a role in meningococcal engagement of FGFR1.

As mentioned above, the search by Kánová et al. (2018) for proteins of *N. meningitidis* that bind to HBMECs initially identified 84 candidate proteins via SWATH-MS analysis of the affinity-purified experimental interactome (Kánová et al., 2018). Of the initial 84 candidates showing potential binding to HBMECs, 41 bacterial proteins were predicted to be surface-exposed, and these were further classified into three subgroups based on their likelihood of contact with receptors. Specifically, the first group consisted of 21 outer membrane (OM) proteins (high priority candidates); the second group consisted of 14 inner membrane proteins (medium priority candidates); and the third group consisted of 6 secretory proteins (low priority candidates). Gene ontology analysis revealed that seven of the 41 surface-exposed proteins are related to transport, five of which (NMB1497, NMB0280, NMB1126, NMB0461 and NMB1429) are solely annotated as transport proteins, with the other two having multiple annotations including transport, ion binding, cell adhesion, response to stress and signal transduction. A systematic bioinformatics pipeline was then utilised to establish a shortlist of potential bacterial ligands by filtering to select predicted surface-exposed proteins, including secretory and outer membrane proteins, as these were deemed more likely to bind to host cells. Excluding cytoplasmic proteins at this stage would have filtered out "moonlighting" proteins (such as FBA and GapA-1) that work in our group has already shown can be present on the meningococcal surface and interact with host cells (Tunio et al., 2010a, Tunio et al., 2010b). However, the filtering process was justifiable (predicted cytoplasmic or periplasmic locations) in terms of reducing the candidate set to a more manageable number of proteins might interact with FGFR1, and of likely prioritising the potential ligands of most interest.

Several investigations have, in fact, been undertaken to identify precisely which proteins are used by bacteria for host cell adhesion: for example, MafA1 of

N. gonorrhoeae (a homologue of *N. meningitidis* NMB0375) was reported to be involved in bacterial adhesion (Kánová et al., 2018). The function of MafA has recently been studied in *N. meningitidis*, with current evidence suggesting that it plays a role in bacterial protein secretion and induction of host cell signalling; more specifically, a TLR-dependent, pro-inflammatory cytokine response (Kánová et al., 2019, Arenas et al., 2020). Relatedly, the function of the major outer membrane protein PorB has presently only been characterised in *N. gonorrhoeae*, where it interacts with human endoplasmin and SREC-I as mentioned earlier (Rechner et al., 2007). In addition, the invasion/adhesion protein NadA (NMB1994) and the putative lipoprotein NMB1126 are also known to have affinity for epithelial cells (Kánová et al., 2018).

Considering the above, bioinformatics analysis of the 41 HBMEC-interacting proteins identified by Kánová et al. (2018) was first carried out in this study, to identify putative novel meningococcal adhesins/invasins that might be ligands for FGFR1, but that do not have a close homologue in the commensal *N. lactamica*. Based on this analysis (as described in the next section), the next aim was to create mutants of the four priority candidate genes *mafA*, *opc5*, *fadL* and *NMB0506* in *N. meningitidis* strain MC58, and compare the growth characteristics between the wild type and mutant strains. Adhesion and invasion assays were then carried out to determine whether the loss of any one of these candidate HBMEC-interacting proteins reduced meningococcal adhesion and/or invasion.

3.2 Results

3.2.1 Bioinformatics approach to identify potential *N. meningitidis* ligands interacting with HBMECs

The main aim of this project was to identify novel surface-exposed proteins of *N. meningitidis* that act as ligands for host epithelial cells, and more specifically, the extracellular ligand-binding domain (IIIc) of the FGFR1 receptor. The set of proteins reported by Kánová et al. (2018) was adopted as a starting point for this analysis, since it was the first high-throughput study that attempted to identify a comprehensive interactome of meningococci with HBMECs. However, only a handful (5/41) of the filtered set of candidates interacting proteins were followed up in the published study, and the host cell receptor(s) involved were not identified. In searching for potential meningococcal ligands for FGFR1 IIIc, this experimentally-determined interactome (Kánová et al., 2018), therefore appeared to be a valid starting point, especially since the functional roles of the identified proteins in meningococcal adhesion are currently underexplored.

Given that *N. meningitidis* interacts with HBMECs via FGFR1, but the closely-related commensal species *N. lactamica* does not (Azimi et al., 2020), the full set of 41 meningococcal interacting proteins from Kánová et al. (2018) was analysed to distinguish candidate interacting proteins in *N. meningitidis* (strain MC58) that do not have a close homologue in *N. lactamica* (ATCC 23970) with the expectation that some of the proteins unique to meningococci might represent FGFR1 IIIc ligands. For the purposes of this bioinformatics analysis, the NCBI repository was used to compare the relevant loci in *N. meningitidis* with the reference genome of the *N. lactamica* strain. Since these are related species that share many close protein homologues, we thought it reasonable to propose the following filtering criteria to select candidates for the bacterial ligand for FGFR1 IIIc: firstly, that it is expressed by *N. meningitidis* but is not found in (or expressed by) the commensal species *N. lactamica*; or secondly, that if it is also expressed by commensals, the structural features must differ significantly between the pathogenic and commensal species (taken as meaning a sequence identity of below 95%, for the purposes of this study).

Complete meningococcal sequences for each candidate protein were obtained from NCBI (http://www.ncbi.nlm.nih.gov/genome/blast/). Subcellular localisation as predicted by PSORTb were obtained from v3.0.3 (https://www.psort.org/psortb/) and subcellular localisation as predicted and obtained by CELLO v2.5 (http://cello.life.nctu.edu.tw/). Table 3.1 lists the proteins of interest for which a close homologue in *N. lactamica* (>95% sequence identity) was not found. Among these, the priority candidates for further investigation are those predicted as outer membrane proteins, expected to be found on the surface of the bacteria where they can easily interact with HBMECs. Some such candidates including PorA, TbpA and TbpB have already been mutated in previous work, to study their functional roles. Others, however, remain to be analysed by mutagenesis, including *mafA*, *opc5*, *fadL* and *NMB0506*, which were all selected for a detailed follow-up investigation in the present study. For one of these proteins (*NMB0506*), no identifiable homologue was found in *N. lactamica*. But for Opc5, MafA, FadL the low sequence identity (36.8%, 95% and 93%) respectively, suggested important functional differences between species. Although MafA has a relatively high sequence identity with *N. lactamica* the highest among the chosen candidates it was selected based on the evidence that it appears to be an important virulence factor, considering some recent research on this topic. As mentioned above, MafA has been studied in both *N. meningitidis* and *N. gonorrhoeae*, and it was one of the potential adhesins followed up by Kánová et al. (2018), who found it to be strongly associated with attachment to HBMECs. However, the host cell receptor is as yet unknown. Thus, in the context of recent literature, MafA is a particularly interesting lead in the current search for meningococcal FGFR1 ligands.

Table 3.1. Proteins from the meningococcal interactome with HBMECs characterised by SWATH-MS that do not have a close homologue in *N. lactamica.* strain ATCC 23970. Ordered locus number in the genome of *N. meningitidis* strain MC58. The Description column indicates the annotated function for the encoded protein in the UniProt database, and the Function column contains more detailed information on the expected function of the protein, according to NCBI and UniProt. Sequence identity with the homologue in *N. lactamica* strain ATCC 23970. The Expect value (E-value) from BLAST is a metric that shows the significance of an alignment. Prediction of most likely subcellular localisation, used for subsequent prioritisation of candidates for further study in this project. These consensus assignments were based on the combined results from PSORTb and CELLO, two online tools for prediction of subcellular localisation. Of these, PSORTb was developed specifically for bacterial and archaeal sequences (Yu et al., 2010), whereas CELLO can make predictions for either bacterial or eukaryotic proteins (Yu et al., 2004, Yu et al., 2006).

N	Locus number	Description	PSORTb	CELLO	Function	BLAST E-value	% Identity	Consensus
1	NMB1053	class 5 outer membrane protein	inner membrane	outer membrane	Plays an important role in meningococcal adhesion and invasion of both epithelial and endothelial cells.	0.014	36.84%	outer membrane
2	NMB1994	putative adhesin/ invasin	outer membrane	extracellular	YadA-like autotransporter adhesin. Binds collagen and other components of the extracellular matrix.	1.00E−29	64.10%	outer membrane
3	NMB1126	putative lipoprotein NMB1126/ NMB1164	unknown	extracellular	CsgG/HfaB family protein. Curli biogenesis system outer membrane secretion channel CsgG forms a secretion channel in the outer membrane.	2.00E−128	86.55%	outer membrane

4	NMB1429	major outer membrane protein P.IA	outer membrane	outer membrane	Outer membrane porin. Forms aqueous channels for the diffusion of small hydrophilic molecules across the outer membrane. Slightly cation selective.	2.00E−90	43%	outer membrane
5	NMB2039	major outer membrane protein P.IB	outer membrane	outer membrane	Slightly cation selective porin, similarly to NMB1429.	2.00E−177	74.56%	outer membrane
6	NMB1533	outer membrane protein H.8	outer membrane	periplasmic	Azurin-like protein of the cupredoxin superfamily, involved in energy production and conversion. Binds one copper ion per subunit.	6.00E−100	85.64%	outer membrane
7	NMB0992	auto-transporter adhesin NhhA	unknown	extracellular	YadA family autotransporter adhesin. Involved in adhesion of capsulated meningococci to host epithelial cells. Interacts with laminin and heparan sulfate, promoting the adherence to the extracellular matrix (ECM) components.	3.00E−131	95.79%	outer membrane
8	NMB0375	adhesin MafA	unknown	outer membrane	MafA proteins have a role in virulence with reported activities in adhesion and transcytosis of pathogenic *Neisseria*, a priori unrelated to MafB activities.	0.0	95%	outer membrane
9	NMB1497	probable TonB-dependent receptor NMB1497	outer membrane	outer membrane	Outer membrane haeme/haemo-globin receptor/trans-porter. May act as a channel to allow import of extracellular nutrients, such as iron-siderophore complexes or non-Fe compounds.	6.00E−45	25.60%	outer membrane

10	NMB1483	putative lipoprotein NlpD	unknown	periplasmic	LysM domain-containing protein involved in cell wall / membrane / envelope biogenesis. Also contains a 1,4-β-*N*-acetylmuramoyl hydrolase domain (peptidoglycan hydrolase superfamily).	5.00E−145	92.15%	outer membrane
11	NMB0088	putative outer membrane protein NMB0088	outer membrane	outer membrane	OmpP1/FadL family transporter. Long-chain fatty acid transport protein responsible for transport of hydrophobic compounds across the bacterial outer membrane.	0.0	93%	outer membrane
12	NMB0313	surface lipoprotein assembly modifier 1	unknown	outer membrane	Required for correct export to the cell surface of some cell outer membrane lipoproteins in *Neisseria* (and heterologously in *E. coli*).	2.00E−63	29.69%	outer membrane
13	NMB1898	lipoprotein	unknown	periplasmic	Outer membrane protein assembly factor BamE, lipoprotein component of the BamABCDE complex (β-barrel assembly machinery) that inserts proteins with β-barrel topology into the outer membrane.	3.00E−125	97%	inner membrane
14	NMB0506	toxin CdiA	unknown	outer membrane / periplasmic	DUF637 (possible haemagglutinin) and FhaB domain-containing protein. FhaB is involved in haeme utilisation or adhesion (intracellular trafficking, secretion and vesicular transport).	**No significant similarity found**	**No significant similarity found**	inner membrane
15	NMB1415	iron-regulated protein FrpC	extracellular	extracellular	RTX family cytotoxin FrpC. Contains the RTX toxin-related COG2931 domain (Ca^{2+}-binding protein).	**No significant similarity found**	**No significant similarity found**	secretory protein

16	NMB1409	FrpA/C-related protein	unknown	outer membrane	Unknown function	**No significant similarity found**	**No significant similarity found**	secretory protein
17	NMB0585	iron-regulated protein FrpA	extracellular	extracellular	FrpC-like protein. Paralog of NMB1415 (with three internal deletions) that contains COG2931 and enterohaemolysin EhxA domains. Related to a class of RTX proteins that are capable of calcium-dependent autoproteolytic cleavage and cross-linking.	**No significant similarity found**	**No significant similarity found**	secretory protein
18	NMB1779	toxin CdiA	outer membrane	extracellular	Multidomain protein containing a haemagglutinin activity domain, DUF637 (possible haemagglutinin) domain, FhaB domain (involved in haeme utilisation or adhesion), and autotransporter adhesin AIDA-I domain. Reported to be part of a TPSS involved in adhesion to epithelial cells.	7.00E−59	40.17%	secretory protein

3.2.2 Bioinformatics analysis of NMB0375, NMB1053, NMB0088 and NMB0506 locus

For the four candidate genes selected for detailed investigation in the bioinformatics analysis above, namely, NMB0375 (*mafA*), NMB1053 (*opc5)*, NMB0088 (*fadL)* and *NMB0506,* further evaluation was performed to predict the possible functions and subcellular localisation of the encoded proteins, since they form the focus of the next part of this study as outlined above. In *N. meningitidis* serogroup B (MC58), the 942 bp *mafA* (*NMB0375*) gene is predicted to encode a 313-amino acid protein with a molecular weight of approximately 34 kDa. The downstream of *mafA* is polymorphic toxin MafB class 1 (*NMB0374*) and the upstream is anhydro-N-acetylmuramic acid kinase (*NMB0377*) of *mafA* in the same orientation. A similar genomic arrangement is found in strain Z2491 of (serogroup A) meningococci 98%. The sequence similarity of *mafA* in strain FAM18 with MC58 exceeds 98%. In addition, the *mafA* sequences of gonococcal strain FA1090 and *N. lactamica* strain 020-06 are over 98% identical to that of MC58.

In *N. meningitidis* serogroup B, the NMB1053 (*opc5)* locus contains a reading frame of 819 bp, which encodes a 29.9-kDa 221-amino acid protein. In the same orientation of *opc5* is the downstream gene *NMB1052* (encoding a DedA family protein, and the upstream gene *NMB1054,* which encodes a hypothetical protein There is a similar genomic arrangement in strain Z2491 meningococci (serogroup A), but not in strain FAM18 meningococci of (serogroup C). The sequence identity of *opc5* between gonococcal strain FA1090 and MC58 is 67%. There was no significant similarity observed between MC58 *opc5* and that of strain FAM18, or *N. lactamica* strains 020-06.

The *fadL* (NMB0088) gene in strain MC58 of *N. meningitidis* contains a 1401 bp as a reading frame that encodes a 50.5 kDa 466-amino acid protein. The *fadL* gene is located after *NMB0086* (lysozyme inhibitor LprI family protein) and *NMB0087* (encoding a hypothetical protein), both being downstream and in the opposite orientation; however, *NMB0089* (pyruvate kinase) is upstream of *fadL*, and in the same orientation. There is a similar arrangement in strain Z2491 (serogroup A)

meningococci, and similarity was also found in strain FAM18 (serogroup C) meningococci. The sequence identities of *fadL* in strains Z2491 and FAM18 with MC58 are 98% and 94%, respectively. In addition, the *fadL* sequences of gonococcal strain FA1090 and *N. lactamica* strain 020-06 are over 92% identical to that of MC58.

In *N. meningitidis* MC58, the 1521 bp *NMB0506* locus encodes a 52.6 kDa hypothetical protein. This gene is in the same orientation as the upstream gene *NMB0505* and the downstream locus *NMB0507*, both of which encode hypothetical proteins. A similar genomic arrangement is found in strain Z2491 (serogroup A) and strain FAM18 (serogroup C) meningococci. Compared to strain MC58, the sequence similarity of the hypothetical protein encoded by *NMB0506* in strains FAM18 and Z2491 is above 98%. No significant sequence similarity with this protein could be identified in gonococcal strain FA1090.

3.2.3 Generation of *mafA, opc5, fadL* and *NMB0506* mutants

3.2.3.1 Cloning of *mafA, opc5, fadL* and *NMB0506,* and their flanking DNA, into pGEM-T Easy or pGEM-T vectors

The aim of these cloning experiments was to create *mafA, opc5, fadL* and *NMB0506* knock-out mutants of *N. meningitidis* strain MC58. The gene sequences for *mafA, opc5, fadL* and *NMB0506,* including their flanking upstream and downstream regions, were amplified by PCR using primer pairs NMB0375-F1/NMB0375-R1, NMB1053-F1/NMB1053-R1, NMB0088-F1/NMB0088-R1 and NMB0506-F1 /NMB0506-R1, respectively (Table 2.3). The target regions were amplified from *N. meningitidis* MC58 genomic DNA using appropriate thermocycling parameters. After analysing the PCR products by agarose gel electrophoresis, bands corresponding to the expected sizes were observed for all target genes: 3.2 kb, 2.1 kb, 3.0 kb and 3.9 kb for *fadL, opc5, mafA* and *NMB0506*, respectively; and as shown in Figure 3.1, Figure 3.2, Figure 3.3, and Figure 3.4, respectively. To enable construction of recombinant plasmids, the amplified DNA was first purified using a DNA purification kit, to remove any contamination of the amplicons with other PCR

products, and to avoid any detrimental effect of remaining reagents on the subsequent A-tail synthesis and ligation reactions.

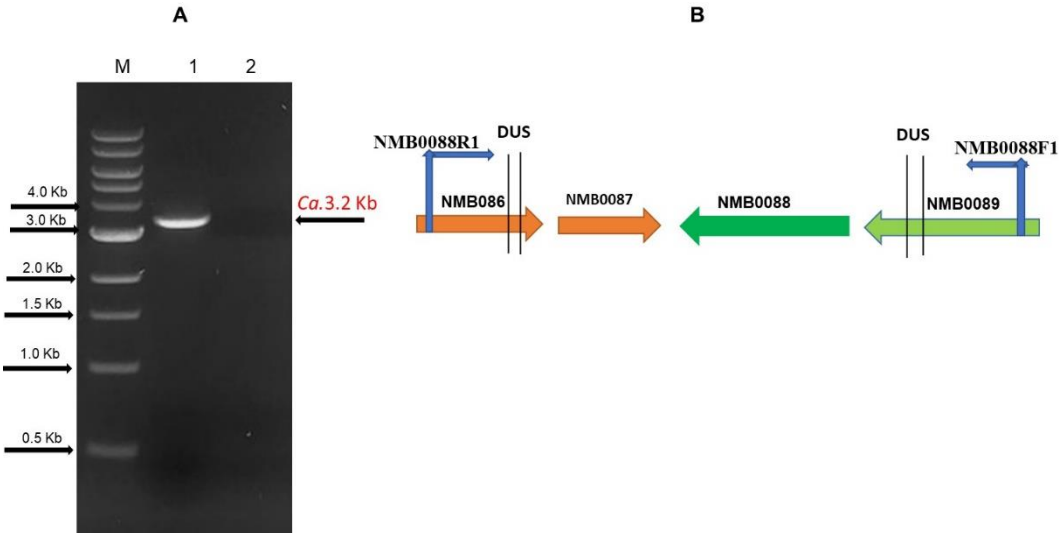

Figure 3.1: Analysis by 1% agarose gel electrophoresis, showing successful PCR amplification of NMB0088. Chromosomal DNA of *N. meningitidis* MC58 was used as template for the PCR amplification of NMB0088 (*fadL*) with upstream and downstream flanking regions. (A) Lane M: 1 kb marker; Lane 1: a predicted 3.2 kb band corresponding to NMB0088 (*fadL*) and upstream and downstream sequence; Lane 2: negative control without template DNA. (B) Map of the amplified fragment which includes the *fadL* coding sequence (1,401 bp) and also additional upstream and downstream sequences of 862 bp and 917 bp, respectively. There are four copies of the neisserial DNA uptake sequence (5′-GCCGTTGTAA-3′), which is required for efficient uptake of DNA in natural transformation of *N. meningitidis* within the amplified fragment, with two upstream and two downstream of *fadL*.

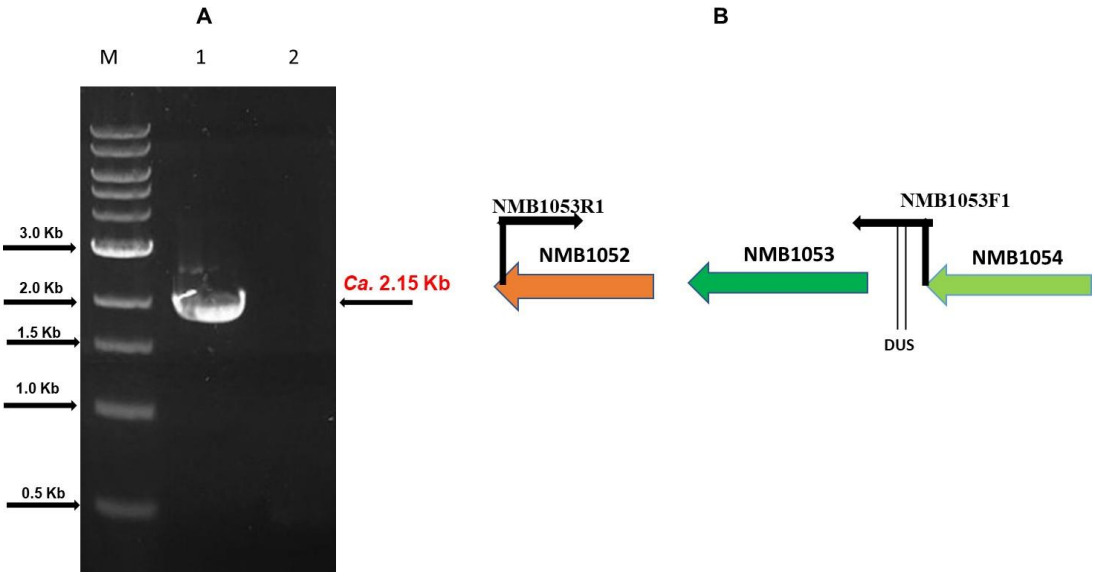

Figure 3.2: Analysis by 1% agarose gel electrophoresis, showing successful PCR amplification of NMB1053. Chromosomal DNA of *N. meningitidis* MC58 was used as template for the PCR amplification of NMB1053 (*opc5*), with upstream and downstream flanking regions. (A) Lane M: 1 kb marker; Lane 1: a predicted 2.15 kb band corresponding to NMB1053 (*opc5*) and upstream and downstream sequence; Lane 2: negative control without template DNA. (B) Map of the amplified fragment which includes the *opc5* coding sequence (819 bp), and also additional upstream and downstream sequences of 600 bp and 731 bp, respectively. There are two of the neisserial DNA uptake sequence (5′-GCCGTTGTAA-3′), which is required for efficient uptake of DNA in natural transformation of *N. meningitidis* within the amplified fragment, with two upstream of *opc5*.

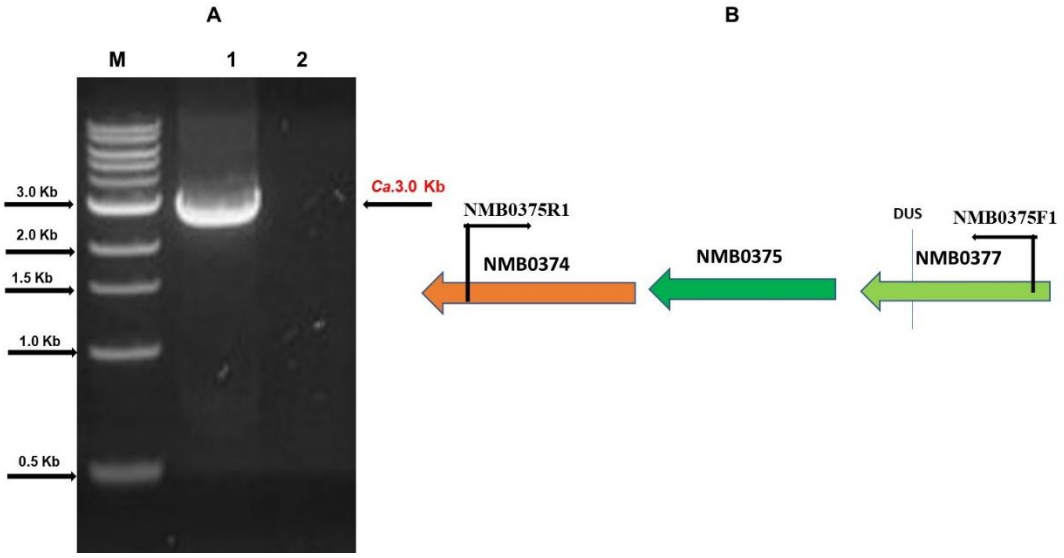

Figure 3.3: Analysis by 1% agarose gel electrophoresis, showing successful PCR amplification of NMB0375. Chromosomal DNA of *N. meningitidis* MC58 was used as template for the PCR amplification of NMB0375 (*mafA*), with upstream and downstream flanking regions. (A) Lane M: 1 kb marker; Lane 1: a predicted *ca.* 3.0 kb band corresponding to NMB0375 (*mafA*) and upstream and downstream sequence; Lane 2: negative control without template DNA. (B) Map of the amplified fragment which includes the *mafA* coding sequence (942 bp), as described above, with additional 1,182 bp downstream and 859 bp upstream sequences. Within the upstream fragment of *mafA* there is one copy of the neisserial DNA uptake sequence (5′-GCCGTTGTAA-3′), which is required for efficient uptake of DNA in natural transformation of *N. meningitidis* within the amplified fragment, with one upstream of *mafA*.

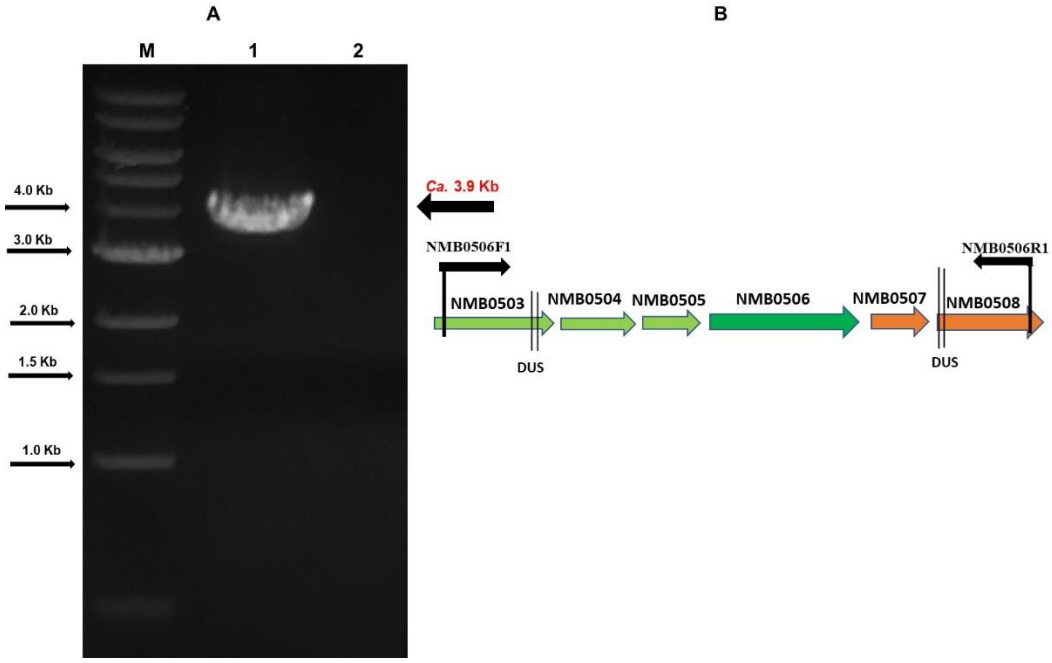

Figure 3.4: Analysis by 1% agarose gel electrophoresis, showing successful PCR amplification of NMB0506. Chromosomal DNA of *N. meningitidis* MC58 was used as template for the PCR amplification of *NMB0506*, with upstream and downstream flanking regions. (A) Lane M: 1 kb marker; Lane 1: a predicted *ca*.3.9 kb band corresponding to NMB0506 (*hypothetical protein*) and upstream and downstream sequence; Lane 2: negative control without template DNA. (B) Map of the amplified fragment which includes the *NMB0506* coding sequence (1,521 bp), and also contains an upstream sequence of 1,435 bp and a downstream sequence of 873 bp. There are four copies of the neisserial DNA uptake sequence (5′- GCCGTTGTAA-3′), which is required for efficient uptake of DNA in natural transformation of *N. meningitidis* within the amplified fragment, with two upstream and two downstream of *NMB0506*.

A-tailed PCR products were then generated by a separate A-tail synthesis step. To simplify the introduction of cloned inserts, single 3′-terminal thymidine overhangs are present on both strands of the linearised pGEM-T Easy and pGEM-T vectors. The purpose of these T-overhangs at the insert site is to increase the ligation efficiency of PCR products with A-tails (which are generated by some thermostable DNA polymerases, including *Taq* polymerase as mentioned in section 2.4.6, whilst preventing re-circularisation of the vector).

Next, three of the inserts (*opc5*, *fadL* and *NMB0506*) were ligated into the pGEM-T Easy vector, and *mafA* was ligated into the pGEM-T vector; then all ligation products were used to transform *E. coli* JM109 competent cells. After incubation overnight, transformants containing inserts were identified by blue/white screening. Potential clones were screened using restriction digestion.

Screening of clones in Figure 3.5. showed successful cloning of *fadL* into pGEM-T Easy, to give construct pMR1, as confirmed by restriction digestion with *EcoRI*, which was expected to yield two bands of 3.0 kb and 3.2 kb and *SalI*, which yielded one linearised fragment of the expected size (6.2 kb).

Screening of clones in Figure 3.6 showed successful cloning of *opc5* into pGEM-T Easy, to give construct pMT1, as confirmed by restriction digestion with *EcoRI*, which yielded two bands of the expected sizes (3.0 kb and 2.15 kb) and *SalI*, which yielded one linearised fragment of the expected size (5.15 kb).

Screening of clones in Figure 3.7. showed successful cloning of *mafA* into pGEM- T, to give construct pMA1, as confirmed by restriction digestion with *SalI*, which was expected to yield two bands of 4.5 kb and 1.5 kb, and *SphI*, which was expected to yield a single linearised band of 6.0 kb.

Confirmation of successful cloning of *NMB0506* into pGEM-T Easy is shown Figure 3.8, to give construct pMK1, as confirmed by restriction digestion using *EcoRI*, which gave two bands of the expected sizes (3.0 kb and 3.9 kb).

DNA sequencing of all plasmids was conducted which confirmed insert orientation and the absence of PCR-generated errors.

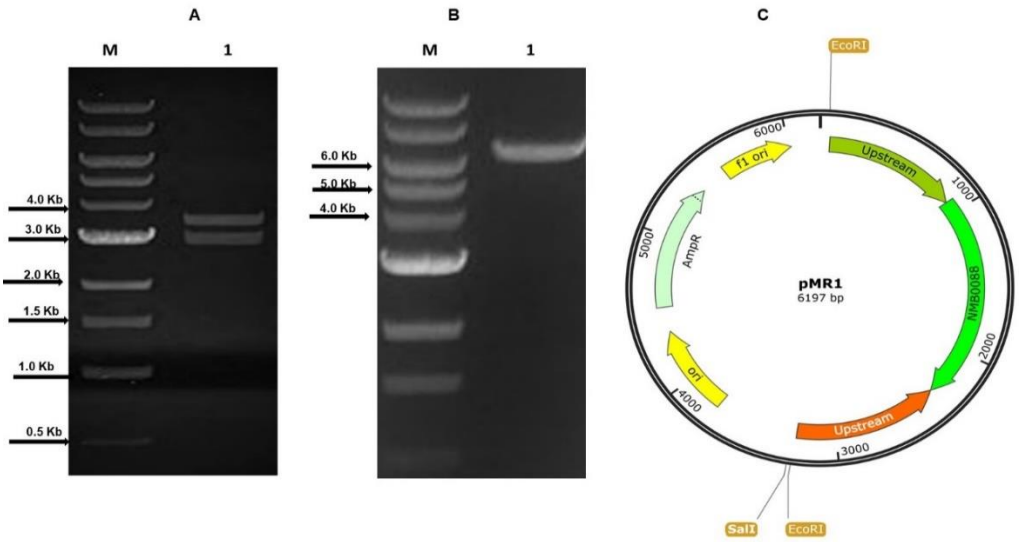

Figure 3.5: Analysis by 1% agarose gel electrophoresis of restriction digests of pMR1 by *EcoRI* and *SalI* for verification of cloning of the NMB0088 (*fadL*) containing PCR product. (A) Lane M: 1 kb marker; Lane 1: *EcoRI* digestion of pMR1 yielded two bands of the expected sizes of *ca*. 3.2 kb (upstream + NMB0088 + downstream) and 3.0 kb (vector backbone) as shown in panel C. (B) Lane M: 1 kb marker; Lane 1: *SalI* digestion of pMR1 yielded one band of the expected size of *ca.* 6.2 kb. (C) Map of pMR1 showing the cloning of *NMB0088* with their stream in pGEM-T Easy vector.

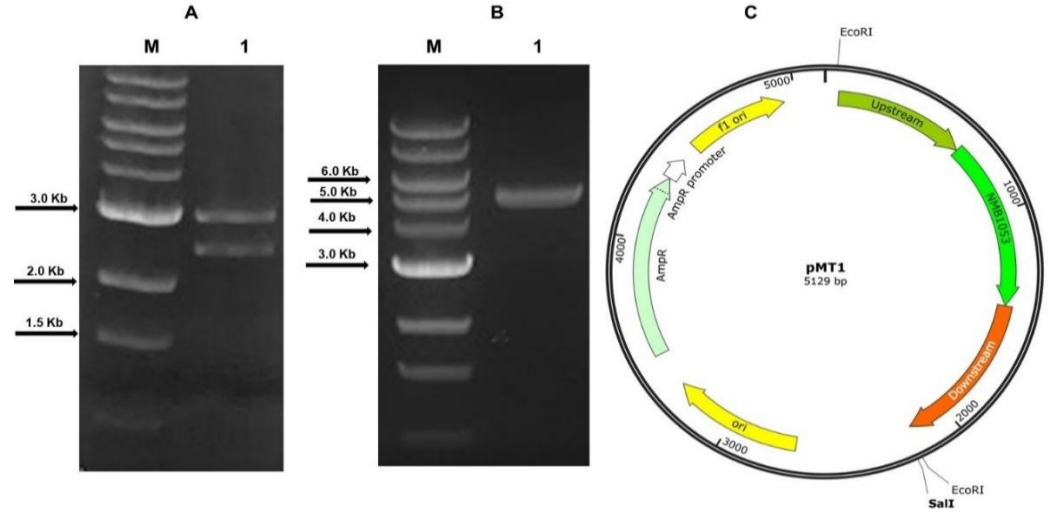

Figure 3.6: Analysis by 1% agarose gel electrophoresis of restriction digests of pMT1 by *EcoRI* and *SalI* for verification of cloning of NMB1053 (*opc5)*. (A) Lane M: 1 kb marker; Lane 1: *EcoRI* digestion of pMT1 yielded two bands of the expected sizes of *ca*. 2.15 kb (upstream + NMB1053 + downstream) and *ca*. 3.0 kb (vector backbone) as shown in panel C. (B) Lane M: 1 kb marker; Lane 1: *SalI* digestion of pMT1 yielded a single band of the expected size, *ca*.5.15 kb. (C) Map of pMT1 showing the cloning of *NMB1053* with their stream in pGEM-T Easy vector.

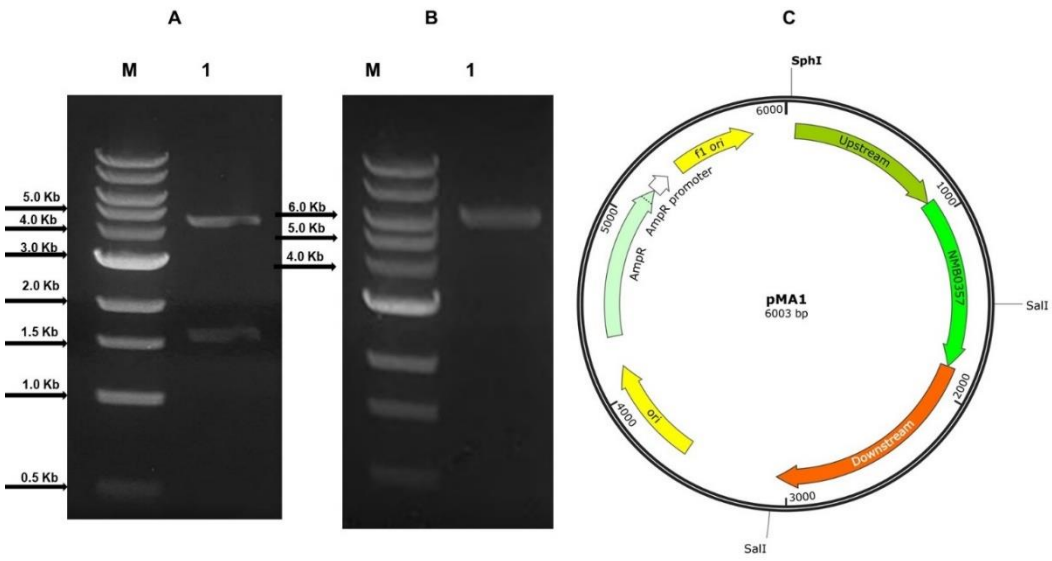

Figure 3.7: Analysis by 1% agarose gel electrophoresis of restriction digests of pMA1 by *SalI* and *SphI* for verification of cloning of NMB0375 (*mafA*). (A) Lane M: 1 kb marker; Lane 1: *SalI* digestion of pMA1 yielded two bands of about *ca.* 4.5 kb (part of NMB0375 + upstream and vector) and *ca.* 1.5 kb (small part of vector, downstream and small part of NMB0375) as shown in Map 3.7.C. (B) Lane M: 1 kb marker; Lane 1: *SphI* digestion of pMA1 yielded one band at the expected size of *ca.* 6.0 kb as shown in the panel C. (C) Map of pMA1 showing the cloning of *NMB0375* with their stream in pGEM-T vector.

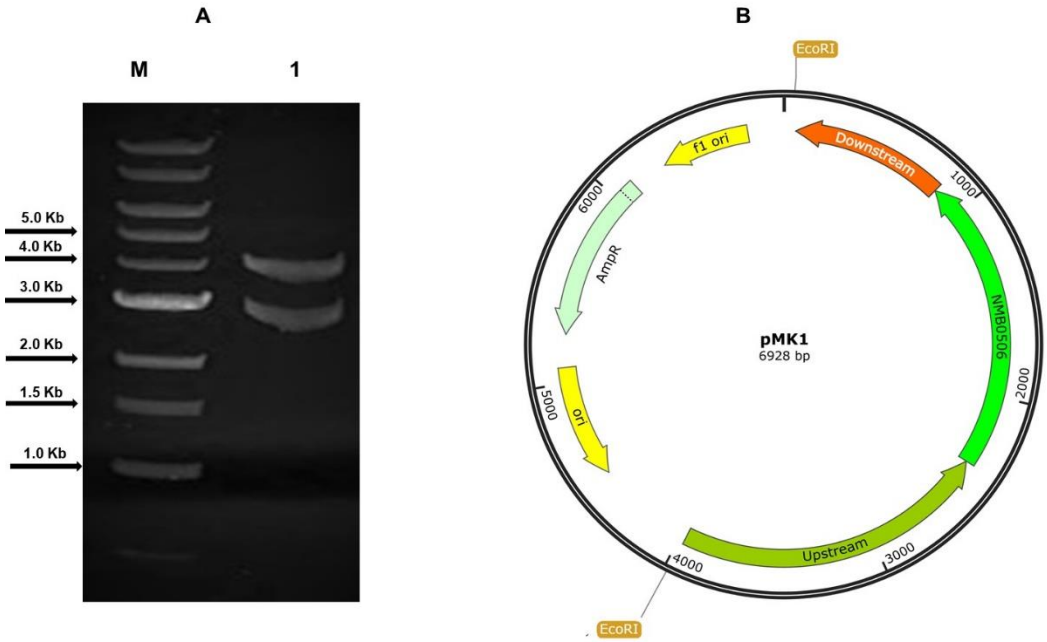

Figure 3.8: Analysis by 1% agarose gel electrophoresis of restriction digests of pMK1 by *EcoRI* for verification of cloning of *NMB0506*. (A) Lane M: 1 kb marker; Lane 1: *EcoRI* digestion of pMK1 produced two bands of approximately *ca*. 3.9 kb (upstream + NMB0506 + downstream) and *ca.* 3.0 kb (vector backbone) as shown in panel B. (B) Map of pMK1 showing the cloning of *NMB0506* with their stream in pGEM-T Easy vector.

3.2.4 Inverse PCR (INPCR) mutagenesis of *mafA, opc5, fadL* and *NMB0506*.

The inverse PCR technique was used to delete the coding sequences for *fadL*, *opc5*, *mafA* and *NMB0506* from the appropriate plasmid template (pMR1, pMT1, pMA1 or pMK1) using the primer pairs NMB0375-invF2/NMB0375-invR2, NMB1053- invF2/NMB1053-invR2, NMB-0088-invF2/NMB-0088-invR2 and NMB0506-invF2/NMB0506-invR2, respectively (Table 2.3). After the reactions were complete, the size of each PCR product was analysed by running on a 1% agarose gel to confirm the deletion of the targeted *fadL*, *opc5*, *mafA* and *NMB0506* sequences as shown in Figure 3.9, Figure 3.10, Figure 3.11, and Figure 3.12, respectively. This inverse PCR approach resulted in the expected bands corresponding to the vector with *fadL*, *opc5*, *mafA* or *NMB0506* flanking regions, after deletion of the target sequences. The inverse PCR primers were used to

introduce a *BglII* site at either end of the amplicon allowing for circularisation of the amplified product.

The PCR products all analysed by agarose gel electrophoresis to confirm that bands of the expected sizes were present. Then, all four PCR products were purified, digested with *BglII*, and again purified using a DNA purification kit. The pMR2, pMT2, pMA2 and pMK2 plasmids were also *BglII* digested, followed by dephosphorylation in order to prevent self-ligation (re-circularisation). Following treatment with T4 ligase, the DNA samples were then used to transform *E. coli* JM109 for subsequent extraction and confirmation.

DNA sequencing was conducted by Source Bioscience and was used to confirm introduction of a unique *BglII* site, as well as to check for PCR-generated errors. One correct clone was chosen for each construct, with the coding sequence of the gene deleted but retaining the upstream and downstream flanking gene regions in the vector. A sample of each plasmid was then digested with *BglII* and cleaned up using a DNA purification kit, and followed by dephosphorylated before ligation reactions with the inserts to prepare for ligation of an antibiotic resistance cassette.

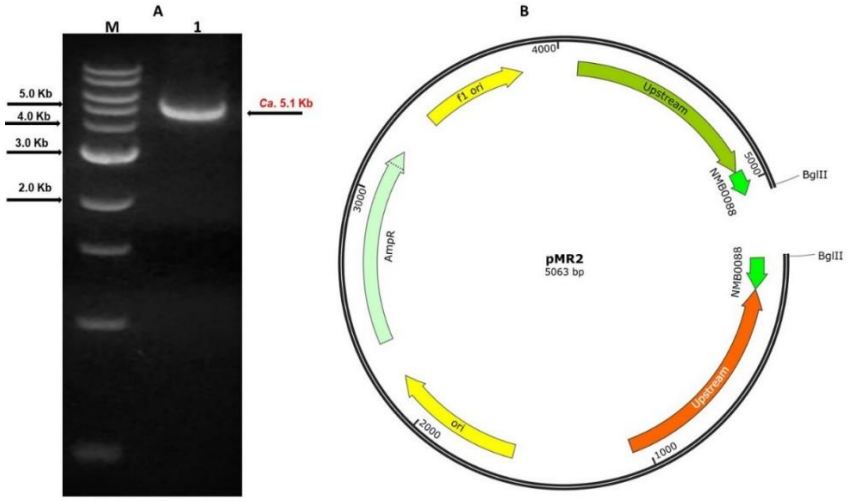

Figure 3.9: Analysis by 1% agarose gel electrophoresis, demonstrating that NMB0088 was successfully deleted from the DNA sequences of pMR1 to give construct pMR2. (A) Lane M: 1 kb DNA marker; Lane 1: inverse PCR product from pMR1 as template, representing *ca.* 5.1 kb fragment: 3.0 kb pGEM-T Easy vector backbone and 2.1 kb flanking DNA regions of *fadL* (NMB0088). (B) Map of pMR2 showing inverse PCR after deletion of *fadL* from plasmid pMR1.

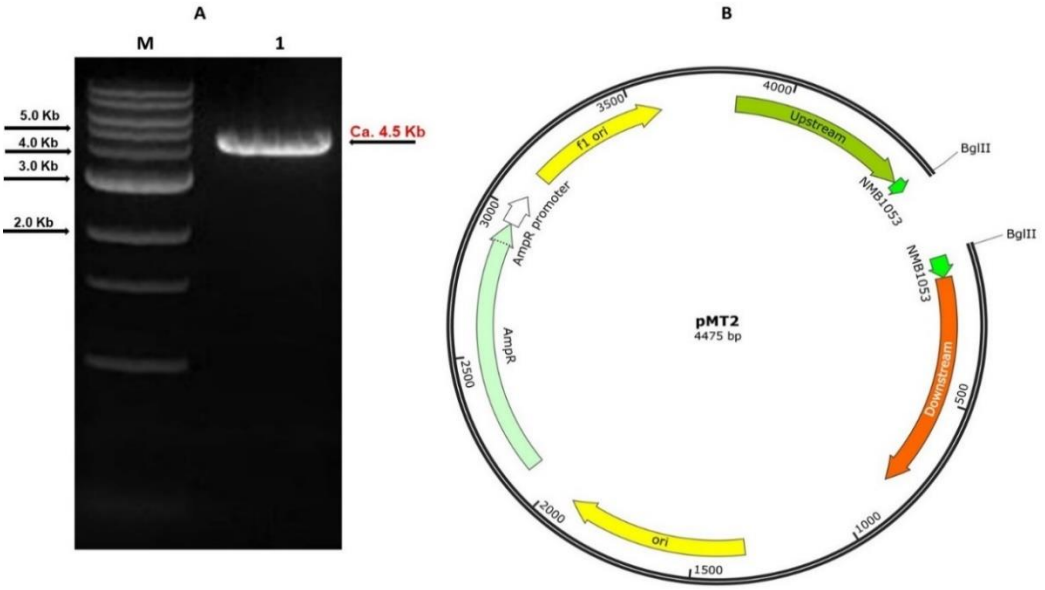

Figure 3.10: Analysis by 1% agarose gel electrophoresis, demonstrating that NMB1053 was successfully deleted from the DNA sequences of pMT1 to give construct pMT2. (A) Lane M: 1 kb marker; Lane 1: an inverse PCR product from pMT1 as template, representing *ca.* 4.5 kb fragment: 3.0 kb pGEM-T Easy vector backbone and 1.5 kb flanking DNA regions of NMB1053 (*opc5)*. (B) Map of pMT2 showing inverse PCR after deletion of *opc5* from plasmid pMT1.

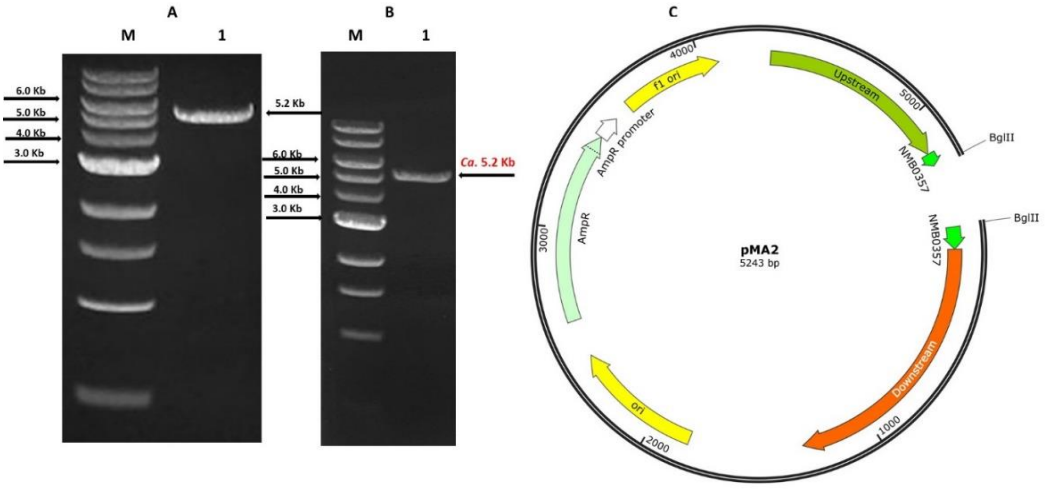

Figure 3.11: Analysis by 1% agarose gel electrophoresis, demonstrating that NMB0375 was successfully deleted from the DNA sequences of pMA1 to give construct pMA2. (A) Lane M: 1 kb DNA marker; Lane 1: inverse PCR product from pMA1 as template, representing *ca.* 5.2 kb fragment: 3.0 kb pGEM-T vector backbone and 2.2 kb NMB0375 (*mafA*), flanking DNA regions. (B) Lane M: 1 kb DNA marker; Lane 1: *SalI* digestion of pMA2 (*mafA*) potential clones yielded one bands at *ca.* 5.2 kb. (C) Map of pMA2 showing inverse PCR after deletion *mafA* from plasmid pMA1.

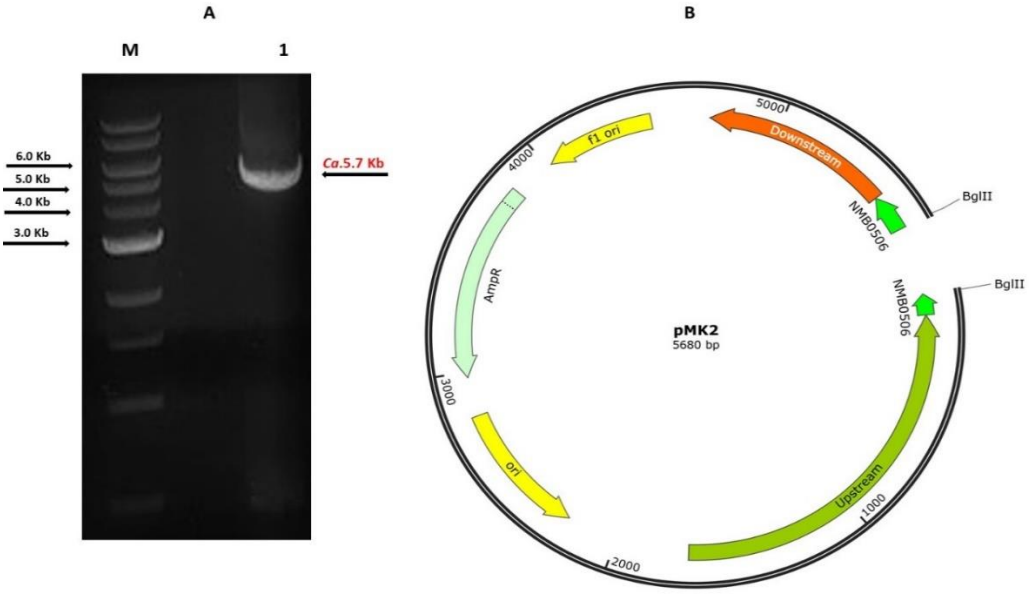

Figure 3.12: Analysis by 1% agarose gel electrophoresis, demonstrating that NMB0506 was successfully deleted from the DNA sequences of pMK1 to give construct pMK2. (A) Lane M: 1 kb DNA marker; Lane 1: inverse PCR product from pMK1 as template, representing *ca.* 5.7 kb fragment: 3.0 kb pGEM-T Easy vector backbone and 2.7 kb of *NMB0506* DNA flanking regions. (B) Map of pMK2 showing inverse PCR after deletion *NMB0506* from plasmid pMK1.

3.2.5 Preparation of antibiotic resistance cassette for cloning into pMA2, pMT2, pMR2 and pMK2 plasmids

Plasmids containing the Omega (streptomycin/spectinomycin resistance) cassette and kanamycin resistance (kan) cassette were obtained (see Table 2.1). After DNA extraction of the respective plasmids (pJMK30 and pHP45Ω) they were digested with *BamHI*. The kan cassette was obtained by digestion of pJMK30, yielding the expected product of 1.5 kb, whereas the Omega cassette was acquired from plasmid pHP45Ω, yielding the expected product of 2.0 kb. The Omega (Ω) sequence contains an aminoglycoside antibiotic resistance gene and also has two inverted repeat sequences at either end that act as transcription termination signals, preventing the transcription of all downstream genes. Therefore, this cassette is transcriptionally isolated (Wooldridge et al., 2005). However, since the kan cassette does not contain transcription termination signals, it is capable of restoring transcription of downstream genes when cloned in the same orientation as the

disrupted genes (Van Vliet et al., 1998). Before ligation into the pMA2, pMT2, pMR2 and pMK2 plasmids, both cassettes were purified from the above *BamHI* digests by agarose gel electrophoresis, followed by band excision and DNA isolation using a gel extraction kit as shown in Figure 3.13.

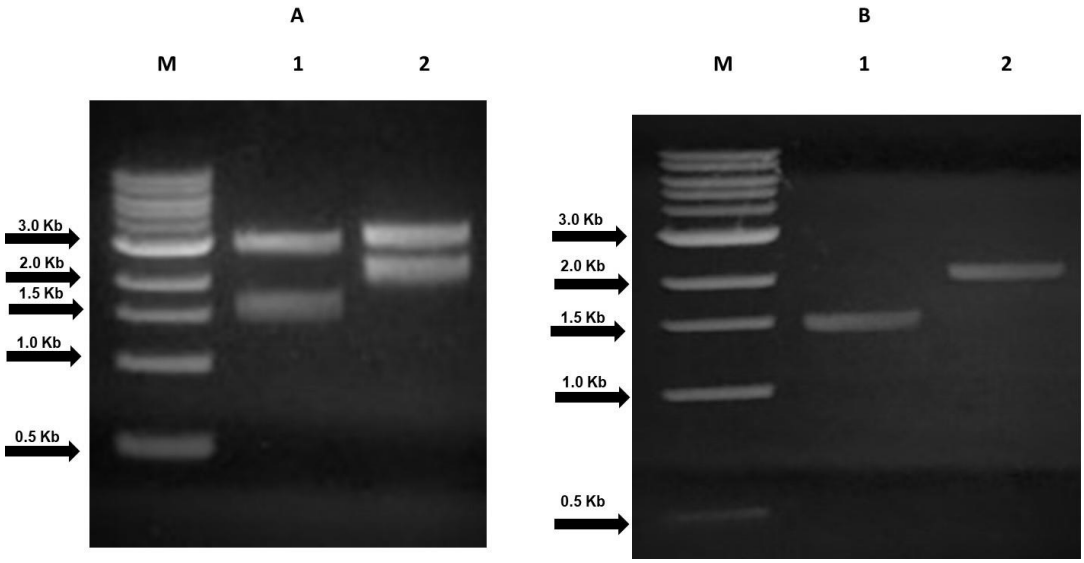

Figure 3.13: Analysis by 1% agarose gel electrophoresis, showing that the pJMK30 and pHP45Ω vectors were successfully digested and purified with *BamHI*. *BamHI* sites are present at both ends of the kan cassette in pJMK30, and of the Omega cassette in pHP45Ω. (A) Lane M: 1 kb marker; Lane 1: restriction digest of pJMK30 with *BamHI* to obtain a kan cassette, where the lower band of *ca*.1.5 kb represents the kan cassette, and the upper band corresponds to the vector backbone; Lane 2: restriction digest of pHP45Ω with *BamHI* to obtain an Omega resistance cassette, where the lower band of *ca*.2.0 kb represents the Omega cassette, and the upper band corresponds to the vector backbone. (B) Lane M: 1 kb marker; Lane 1: kan cassette after purification by gel extraction, showing a band at *ca*. 1.5 kb; Lane 2: Omega cassette after purification by gel extraction, showing a band at *ca*. 2.0 kb.

3.2.6 Construction of pMT3 and pMK3 utilizing the kan cassette

The kan cassette obtained by *BamHI* digestion of pJMK30 (which contains *BamHI* sites on either side of the insert) was ligated into dephosphorylated, *BglII* digested pMT2 and pMK2, to create the new constructs pMT3 and pMK3, respectively.

Successful cloning of pMT3 was confirmed by restriction digestion of the isolated plasmid with *SalI*, resulting in fragments of *ca*. 2.3 kb (kan cassette plus upstream DNA flanking *opc5*) and *ca.* 3.7 kb (downstream sequence flanking *opc5* plus pGEM-T easy vector backbone) as shown in Figure 3.14. Successful cloning of pMK3 was confirmed likewise, resulting in fragments of *ca*. 3.1 kb (part of the kan cassette plus upstream flanking DNA *NMB0506*) and *ca.* 4.1 kb (remainder of kan cassette, downstream region plus pGEM-T easy vector backbone) as shown in Figure 3.15. Two internal primers (30-KAN-CTERM and 30-KAN-NTERM) targeting sites within the kan cassette were used to confirm its successful ligation into pMT3 and pMK3 by DNA sequencing.

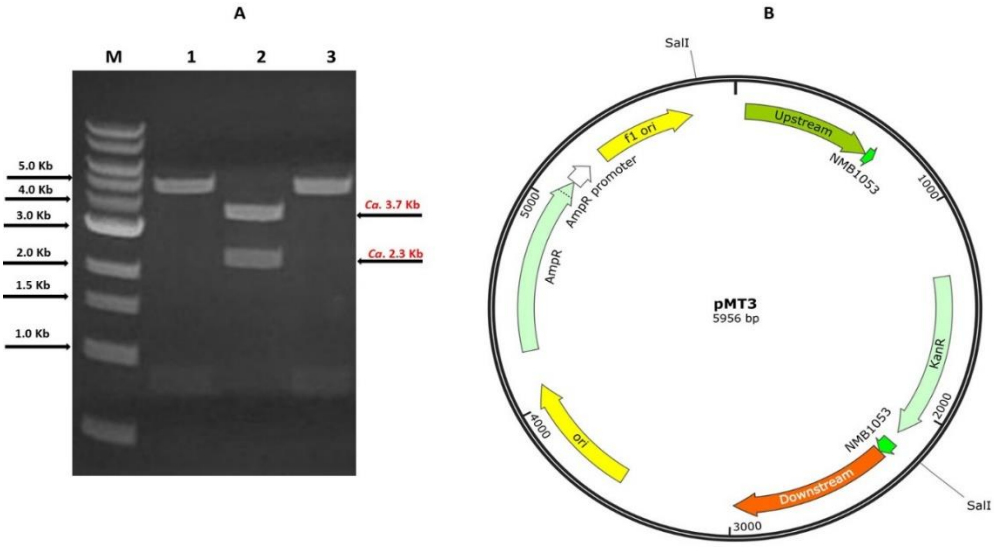

Figure 3.14: 1% agarose gel electrophoresis following restriction digestion of pMT3 by *SalI*, confirming the presence of the kan cassette. (A) *SalI* digestion of pMT3. Lane M: 1 kb marker; Lanes 1 and 3: The observed bands at *ca*. 0.9 kb and *ca.* 5.1 kb indicated that the kan cassette was inserted into pMT2 vector in a different orientation than intended; Lane 2: Bands of *ca*. 2.3 kb and *ca*. 3.7 kb, corresponding to the intended construct with kan cassette inserted in the correct orientation. (B) Map of pMT3 showing features of interest and *SalI* restriction sites.

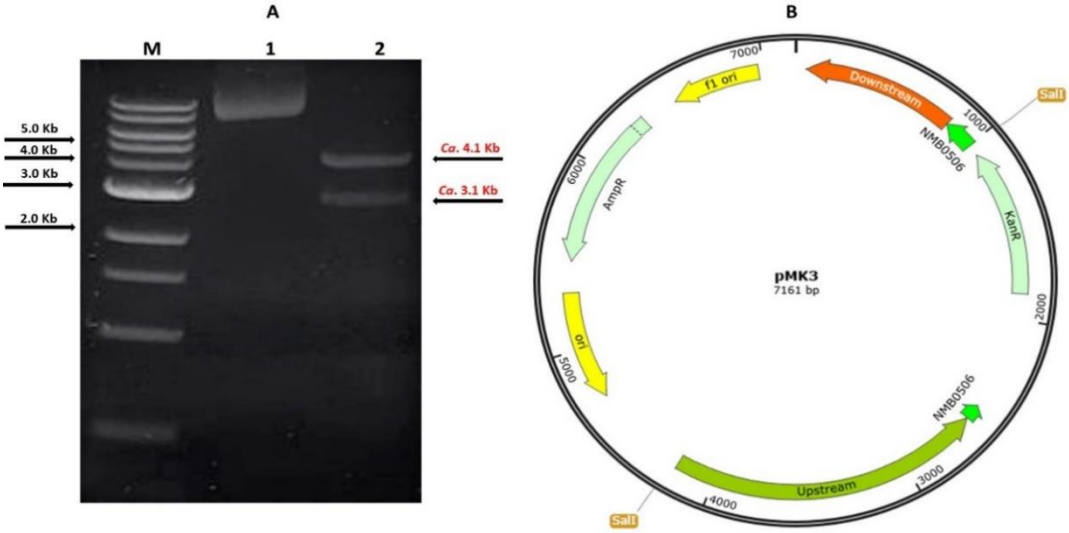

Figure 3.15: 1% agarose gel electrophoresis following restriction digestion of pMK3 by *SalI*, confirming the presence of the kan cassette. (A) Lane M: 1 kb marker; Lane 1: DNA without restriction enzyme; Lane 2: *SalI* was used to digest pMK3, confirming ligation of the kan cassette as revealed by the expected two fragments at *ca*. 4.1 kb (downstream sequence flanking NMB0506 plus pGEM-T easy vector backbone and small part of the kan cassette) and *ca*. 3.1 kb (kan cassette plus upstream flanking region). (B) Map of pMK3 showing features of interest and *SalI* restriction sites.

3.2.7 Construction of pMA4 and pMR4 utilizing the Omega cassette

Similarly, the Omega cassette obtained by *BamHI* digestion of pHP45Ω was ligated into dephosphorylated, *BglII*-digested pMA2 and pMR2 to create the new constructs pMA4 and pMR4.

Putative clones were selected using ampicillin, streptomycin and spectinomycin. Successful cloning was confirmed for the extracted pMA4 vector by restriction digestion with *SphI,* which resulted in two fragments. The first of these was *ca*. 2.7 kb in size (upstream region of *mafA* plus part of the Omega cassette) and the second was *ca*. 4.6 kb (remainder of the Omega cassette, downstream flanking sequence of *mafA* plus pGEM-T vector backbone) as shown in Figure 3.16. Successful cloning was confirmed for pMR4 by restriction digestion with *SphI,* which resulted in two fragments. The first band was observed at *ca*. 2.7 kb (upstream region of *fadL* plus part of the Omega cassette) and the second at *ca*. 4.4 kb (remainder of the Omega cassette, downstream flanking sequence of *fadL* plus pGEM-T easy vector backbone) as shown in Figure 3.17. DNA sequencing was again conducted to confirm the successful ligation into pMA2 and pMR2.

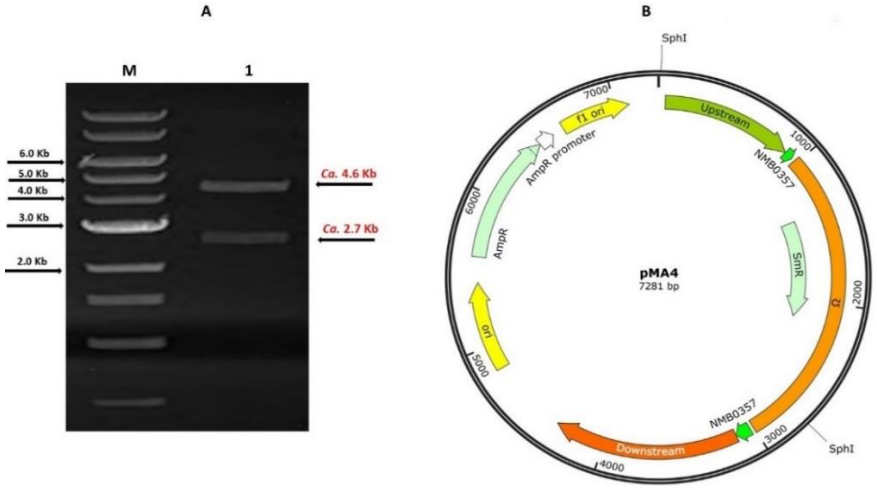

Figure 3.16: 1% agarose gel electrophoresis following restriction digestion of pMA4 by *SphI* confirming the presence of the Omega resistance cassette. The Omega cassette was successfully ligated into pMA2. (A) Lane M: 1 kb marker; Lane 1: *SphI* digestion of pMA4 produced two fragments of *ca.* 4.6 kb including part of the Omega cassette, the downstream flanking region of *mafA* and the pGEM-T vector backbone and *ca*. 2.7 kb, which includes the upstream region of *mafA* and the majority of the Omega cassette. (B) Map of pMA4 showing relevant features and *SphI* sites.

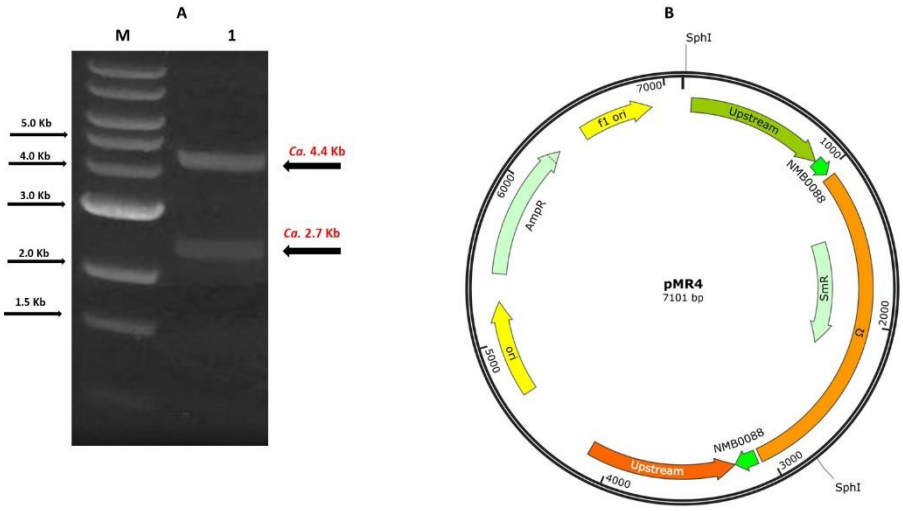

Figure 3.17: 1% agarose gel electrophoresis following restriction digestion of pMR4 by *SphI* confirming the presence of the Omega resistance cassette. The Omega cassette was successfully ligated into pMR2. (A) Lane M: 1 kb marker; Lane 1: *SphI* digestion of pMR4 yielded two fragments of the expected sizes: *ca.* 4.4 kb, which includes part of the Omega cassette, the downstream flanking region of *fadL* and the pGEM-T Easy vector backbone and *ca.* 2.7 kb, which includes the upstream region of *fadL* and the majority of the Omega cassette. (B) Map of pMR4 showing relevant features and *SphI* sites.

3.2.8 Natural transformation of MC58 and verification of *opc5* and *NMB0506* mutagenesis:

Plasmids pMT3 and pMK3 were used to naturally transform *N. meningitidis* MC58 with transformants selected using kanamycin. Mutation of *opc5* or *NMB0506* was confirmed by screening for the presence of the kan cassette at the desired location and orientation in the chromosome, using PCR analysis of extracted chromosomal DNA from putative mutants. In the case of *NMB0506* mutation, PCR experiment using the primers NMB0502-seqF and Kan-NTERM would give a *ca.* 1.9 kb PCR product if the kan cassette had successfully replaced the deleted gene. This expected band was observed with DNA samples from five out of six putative mutants (Figure 3.18), indicating successful replacement of *NMB0506* in the putative mutants. These mutant strains were designated as MC58Δ*NMB0506-kan*.

Verification of *opc5* mutants was achieved similarly, using primers NMB1051-seqR and NMB1054-seqF to verify the presence of the kan cassette in place of *opc5*. In this case, the expected PCR product was *ca* 3.0 kb for the required mutants, and the expected band was observed in five out of six DNA samples extracted from putative mutants (Figure 3.19). This suggested that replacement of *opc5* with the kan cassette had occurred, and the successfully mutated strains were designated as MC58Δ*NMB1053-kan.*

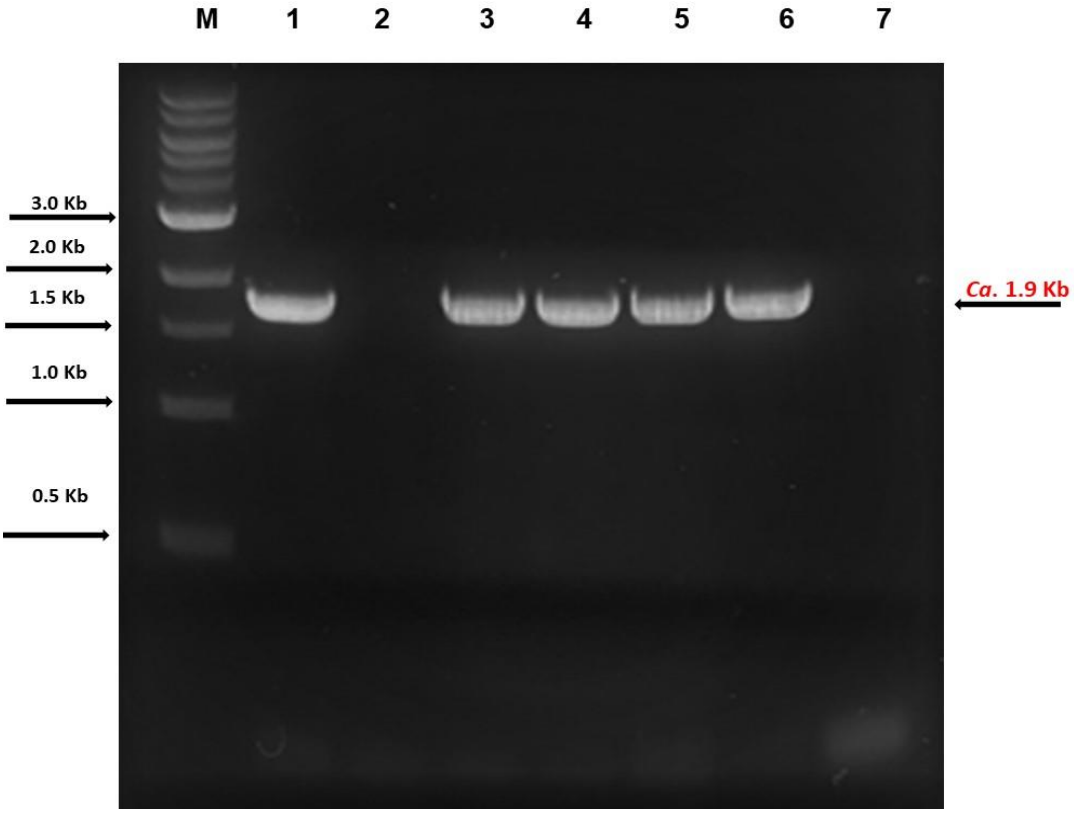

Figure 3.18. Analysis by 1% agarose gel electrophoresis of PCR amplicons confirming the correct generation of MC58 mutants lacking *NMB0506*. Chromosomal DNA was extracted from putative mutants and used in PCR experiments to confirm the position and orientation of the kan cassette, using the primers NMB0502-seqF and Kan-NTERM. This was expected to produce a *ca.* 1.9 kb PCR product only if the kan cassette was in the same orientation as the deleted *NMB0506*. Lane M: DNA marker; Lanes 1, 3–6: PCR amplification from putative *NMB0506* mutant DNA. A band of the expected size was observed, confirming successful replacement of *NMB0506* with the kan cassette in the same orientation; Lane 2: failed to produce any band, presumably due to the absence of the cassette or a failed reaction; Lane 7: negative control, with no chromosomal DNA.

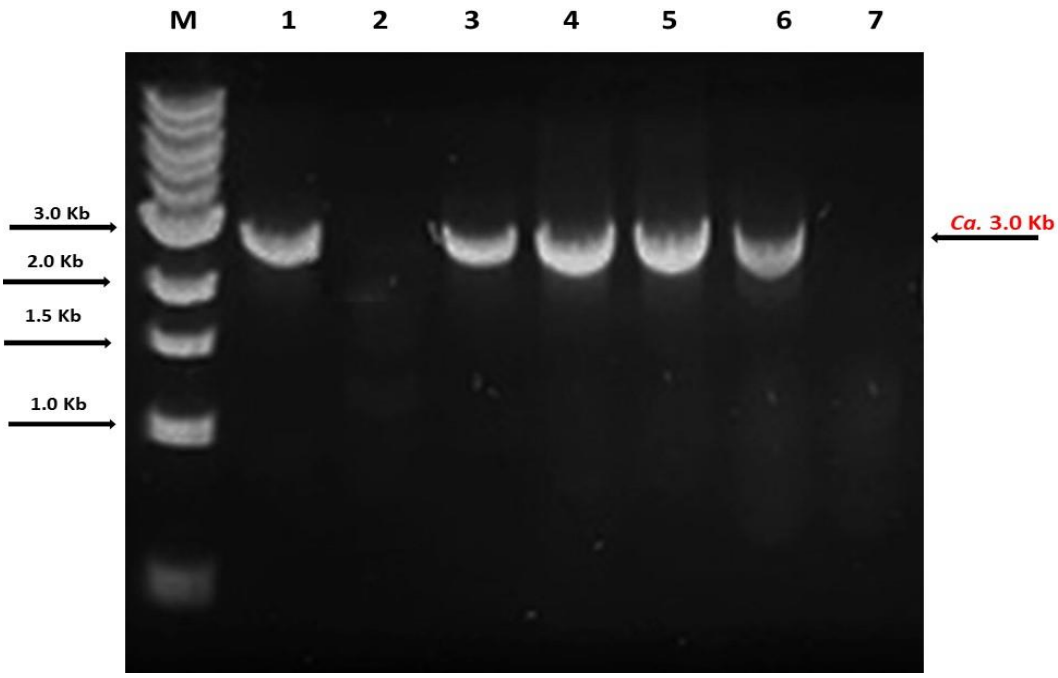

Figure 3.19. Analysis by 1% agarose gel electrophoresis of PCR amplicons confirming the correct generation of MC58 mutants lacking *opc5*. Chromosomal DNA was extracted from putative mutants and used in PCR experiments to confirm the position and orientation of the kan cassette using primers NMB1051-seqR and NMB1054-seqF and the band is different from the WT sized band because deleted a gene of *ca.* 700 bp and replaced it with the 1.5 kb kan cassette. This was expected to produce a *ca.* 3.0 kb product in the presence of the kan cassette if inserted in the same orientation as that of *opc5*. Lane M: DNA markers; Lanes 1, 3–6: PCR amplification of putative *opc5* mutant DNA. A band of the expected size was observed, confirming successful replacement of *opc5* with the kan cassette in the same orientation; Lanes 2: with no band suggesting the Kan cassette in the wrong orientation; Lane 7: negative control, with no chromosomal DNA.

3.2.9 Natural transformation of MC58 and verification of *mafA* (NMB0375) and *fadL* (NMB0088) mutagenesis

Mutation of *mafA* (NMB0375) and *fadL (NMB0088)* was similarly assessed by PCR following natural transformation of meningococcal strain MC58 with pMA4 and pMR4, respectively. Putative *mafA* and *fadL* clones were initially screened for the presence of the cloned Omega cassette, at the proper location and with the correct orientation, by PCR using *mafA* and *fadL* region-specific primer pairs. In the case of *mafA* deletion, these PCR reactions were performed using the primers Omega-F

and NMB0374-seqR with chromosomal DNA extracted from putative *mafA* mutants as template. The expected *ca*. 1.6 kb PCR product was observed for six out of seven DNA samples from putative mutants, as shown in Figure 3.20, suggesting successful mutation of *mafA* in all but one of the strains chosen. The verified *mafA* clones were designated as MC58Δ*NMB0375-Omega.*

For *fadL* mutants, the presence and orientation of the Omega cassette was confirmed by the same method using the gene-specific primers Omega-R and NMB0089-seqF. A PCR product of *ca.* 1.6 kb was expected where the Omega cassette was present instead of *fadL*, and this product was obtained from the DNA sample of all six putative mutants screened (Figure 3.21). Thus, successful mutation of *fadL* had been achieved in all of the putative mutants, which were designated as MC58Δ*NMB0088-Omega.*

Therefore, the combined PCR results from this and the previous section (1.2.8) confirm successful substitution of the targeted genes in all cases, giving *opc5* and *NMB0506* meningococcal strains containing the kan cassette in place of the targeted genes, and *mafA* and *fadL* strains with the Omega cassette substituted for the targeted genes.

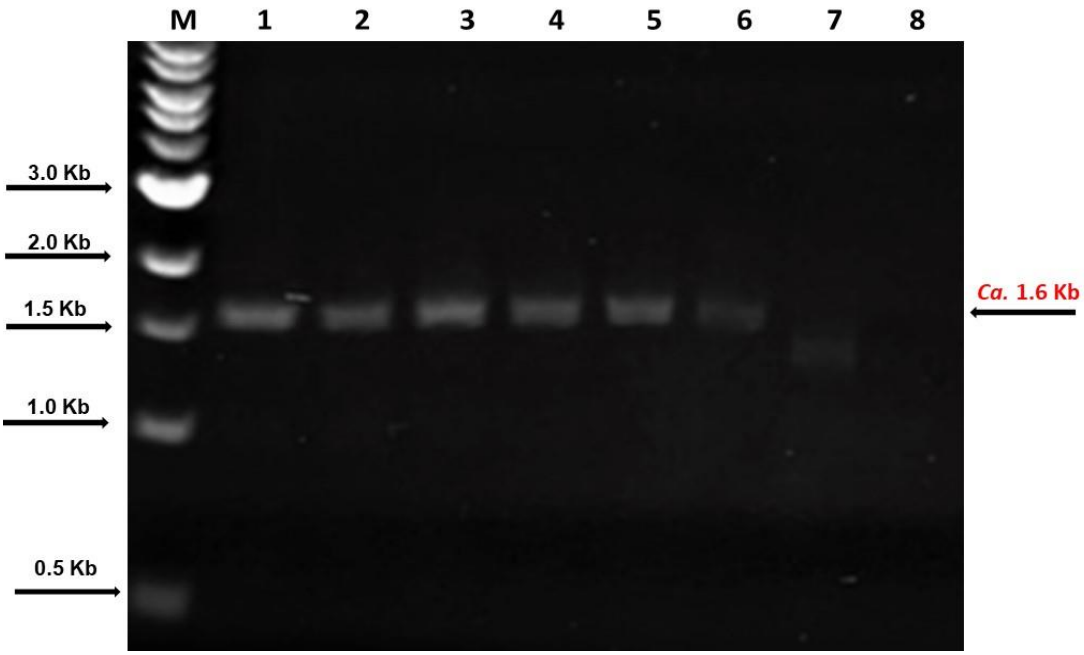

Figure 3.20: Analysis by 1% agarose gel electrophoresis showing PCR amplification from *N. meningitidis mafA* mutants. Chromosomal DNA was extracted from putative *mafA* mutants and used in PCR experiments to confirm the insertion and orientation of the Omega cassette, using the primers Omega-F and NMB0374-seqR. This was expected to produce a *ca.* 1.6 kb PCR product if the Omega cassette had correctly replaced *mafA*. Lane M: DNA markers; Lane 1-6 putative *mafA* mutant DNA. Lane 7, which failed to produce any band suggesting the cassette in the wrong orientation, lane 8 as a negative control without chromosome DNA. A band of the expected size was observed, confirming successful replacement of *mafA* with the Omega cassette in the same orientation.

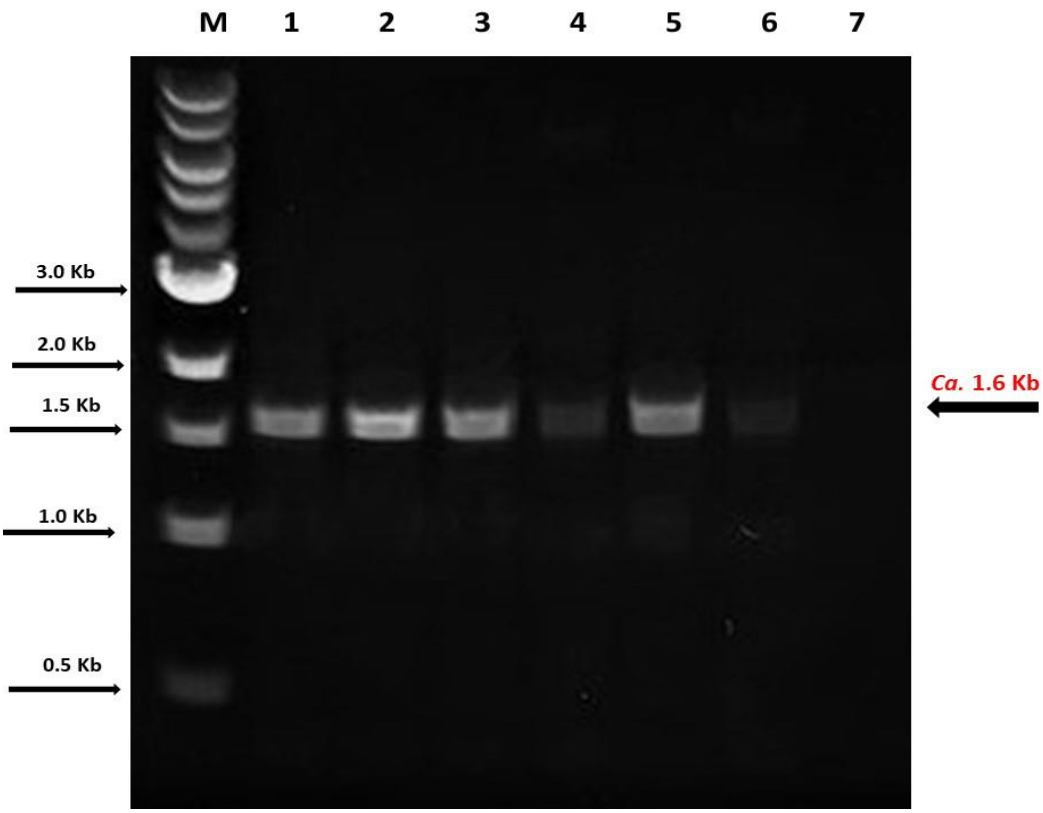

Figure 3.21: Analysis by 1% agarose gel electrophoresis showing PCR amplification from *N. meningitidis fadL* mutants. Chromosomal DNA was extracted from putative mutants and used in PCR experiments to confirm the insertion and orientation of the Omega cassette using primers Omega-R and NMB0089-seqF. This was expected to produce a *ca*. 1.6 kb PCR product in the presence of the Omega cassette in the same orientation as the deleted *fadL*. Lane M: DNA markers; Lanes, 1-6, putative *fadL* mutant DNA, lane 7 as a negative control, whereas a band of expected size was observed in 1-6 lanes, confirming the successful replacement of *fadL* with the Omega in the same orientation.

3.2.10 Comparison of the growth characteristics of MC58-WT, MC58Δ*NMB0375-Omega*, MC58Δ*NMB1053-kan*, MC58Δ*NMB0506-kan* and MC58Δ*NMB0088-Omega*

With the required knockout strains confirmed, it was necessary to first demonstrate that mutation of the targeted genes did not significantly affect the growth rate of the *N. meningitidis* mutants, before moving on to further analysis. Growth profiles were therefore determined for the constructed mutants (MC58Δ*NMB0375-Omega,* MC58Δ*NMB1053-kan,* MC58Δ*NMB0506-kan and* MC58Δ*NMB0088-Omega),* comparing them to wild-type strain MC58. The rate of growth was monitored in liquid culture, and colony morphology was also assessed visually on chocolate agar plates. The mutants all showed similar morphology and colour to wild type MC58 on chocolate agar (data not shown). All strains were grown in BHI broth supplemented with 1% Vitox, with an equivalent starting OD_{600} of 0.05. Growth was assessed by measuring the OD_{600} of aliquots removed from each culture at hourly intervals. Experiments were performed in triplicate, and the results are presented in Figure 3.22. All of the mutants displayed growth profiles that were very similar to that of their wild type of strain.

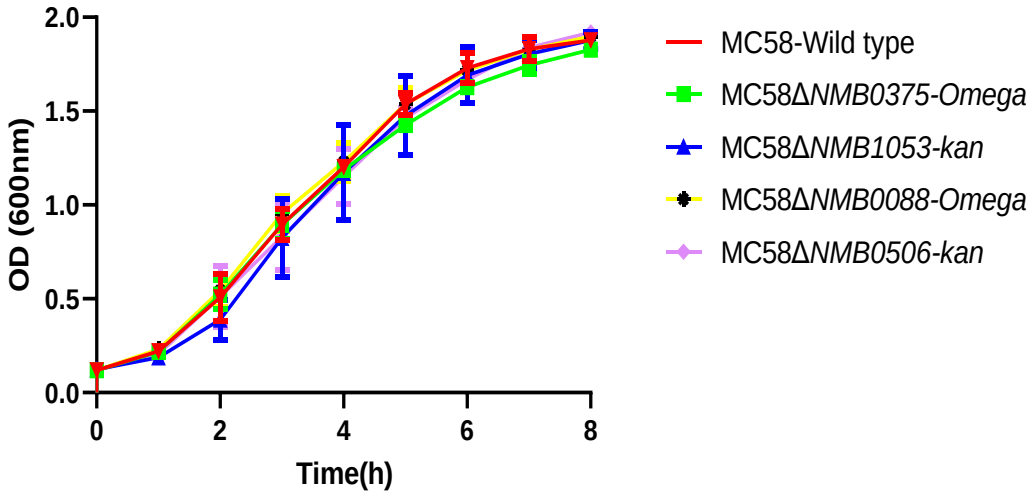

Figure 3.22. Growth profiles of MC58-Wild type, MC58Δ*NMB0375-Omega*, MC58Δ*NMB1053-kan*, MC58Δ*NMB0506-kan* and MC58Δ*NMB0088-Omega* strains of *N. meningitidis* in BHI + 1% Vitox. Optical density (OD) of cultures was measured at 600 nm at the indicated time points. The mean values for the MC58Δ*NMB1053-kan*, MC58Δ*NMB0375-Omega*, MC58Δ*NMB0506-kan and* MC58Δ*NMB0088-Omega* were not statistically different from the wild-type ($p > 0.05$). Error bars indicating SEM.

3.2.11 Comparison of *N. meningitidis* (MC58) and *N. lactamica* in cell adhesion and cell invasion assays

Before beginning association and invasion assays for the various mutant strains, and moving on to investigate the possible effects of inhibiting FGFR1 activation during meningococcal infections, it was first necessary to confirm the differential ability of *N. lactamica* ATCC 23970 and *N. meningitidis* MC58 to adhere to and invade HBMECs. These experiments were repeated independently four times, and demonstrated that whilst both *N. lactamica* and *N. meningitidis* can adhere to and invade HBMECs to some degree, *N. lactamica* exhibits significantly reduced adhesion and invasion compared to MC58 (Figure 3.23). Since these results were in line with expectations, they established the usefulness of the experimental setup and suggested it was suitable to investigate the effects of inhibiting FGFR1 (SU5402) of activation during meningococcal infections, using *N. meningitidis* (MC58) with *N. lactamica* as an appropriate negative control. In addition, the results shown also

indicate that these the experimental conditions used are valid for comparison of wild-type MC58 was valid to using as a wild type, to determine the function of MC58Δ*NMB0375-Omega*, MC58Δ*NMB1053-kan*, MC58Δ*NMB0506-kan* and MC58Δ*NMB0088-Omega* to determine whether the targeted genes play functional roles in meningococcal adhesion to, and invasion of, human epithelial cells.

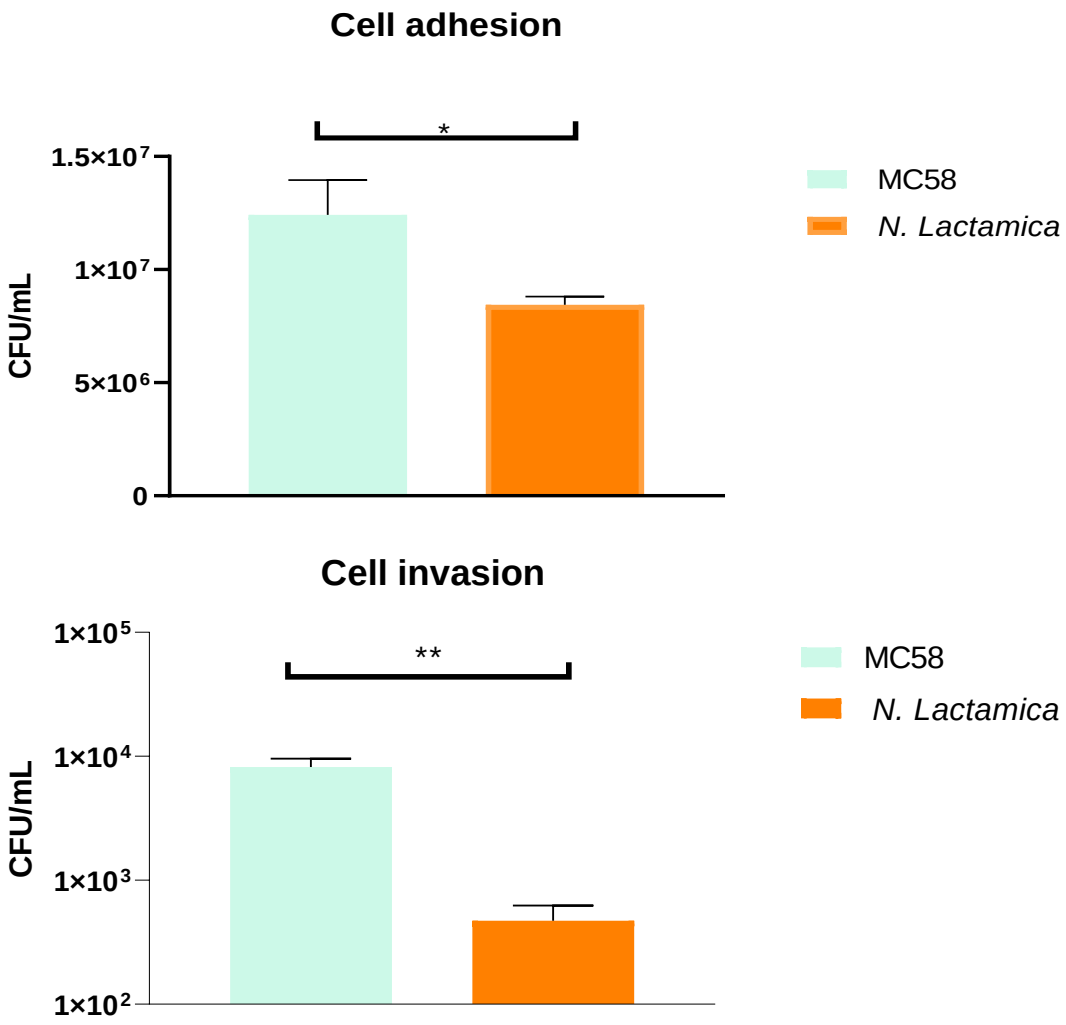

Figure 3.23: Interaction of *N. meningitidis* MC58 and *N. lactamica* ATCC 23970 with HBMECs, at 4 h (cell adhesion assay) and 1 h (cell invasion assay). The results show that association with, and invasion of, HBMECs are significantly different between *N. lactamica* and *N. meningitidis* at 4 h post infection. Cells were washed, lysed, homogenised and then serial dilutions were plated onto chocolate agar plates to allow the number of CFUs to be calculated. For invasion experiments, gentamicin was added in fresh medium, and incubation continued for a further 1 h before processing as above. It was observed that *N. meningitidis* associates with and invades HBMECs to a significantly greater extent than *N. lactamica*. The value for *N. lactamica* were lower than the *N. meningitidis* and the differences were statistically significant (*p < 0.05, ** p <0.01) for cell adhesion and cell invasion respectively. Mean values are shown from four independent experiments, each using quadruplicate wells with error bars indicating SEM. This analysis done by t-tests, unpaired.

3.2.12 Inhibition of FGFR1 by SU5402 does not affect meningococcal adhesion or invasion to HBMECs

A chemical inhibitor (SU5402) was used to investigate the possible effects of inhibiting FGFR1 activation during meningococcal infections. Confluent HBMECs were serum-starved and treated with different concentrations of SU5402 for 1 h at 37°C in an atmosphere of 5% CO_2. The media was then removed before bacterial suspensions were added and incubated for 4 h to allow for bacterial attachment. After washing, cells were lysed and serial 10-fold dilutions in PBS were made (down to 10^{-4}), plated out, and cultured to allow for assessment of bacterial adhesion. Alternatively, after the 4 h incubation step for bacterial adhesion, a cellular invasion assay could be performed instead. This is also referred to as a gentamicin protection assay, since an antibiotic (gentamicin) is added to the growth medium, stimulating the attached bacteria to internalise into the HMBECs to avoid being killed. For this assay, the growth medium from the initial 4 h incubation step was exchanged for fresh medium containing gentamicin. After incubation for a further 1 h, the cells were washed and lysed as above, and serial dilutions made in PBS for plating out. Culturing these plates allows for the extent of bacterial internalisation (invasion) to be measured, since in the presence of gentamicin, any bacteria that remained extracellular would have been killed and removed during the wash step. In cells treated with SU5402, the number of bacterial cells that associated with or invaded into HBMECs was not significantly reduced for either *N. meningitidis* (MC58) or *N. lactamica*, as shown in Figures 3.24 and 3.25.

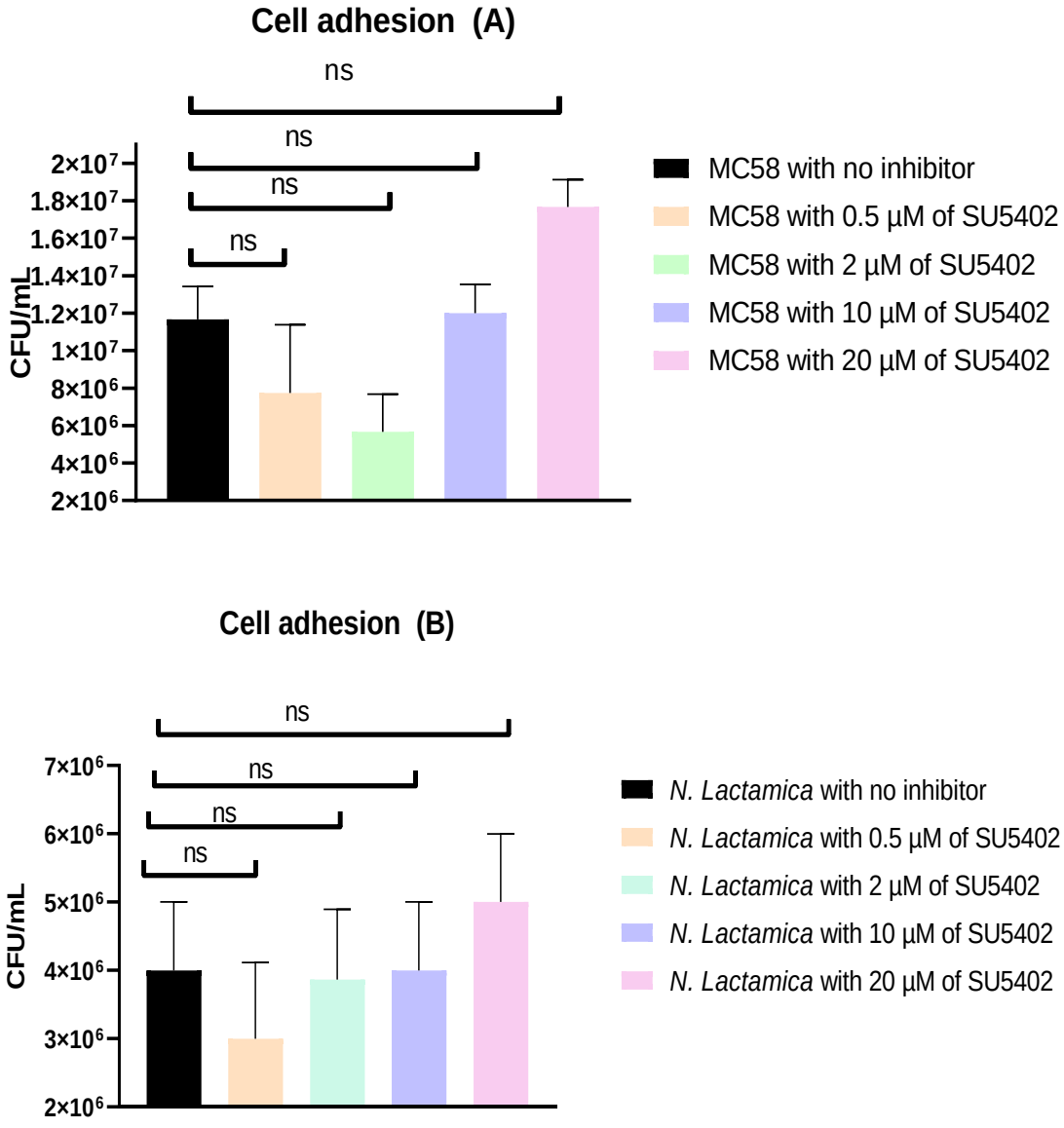

Figure 3.24. Attachment of *N. meningitidis* MC58 and *N. lactamica* ATCC 23970 to HBMECs in the presence of an FGFR1 inhibitor (SU5402). HBMECs were infected with **(A).** *N. meningitidis* MC58 or **(B).** *N. lactamica* ATCC 23970 for 4 h (MOI: 10). There was no significant ($p > 0.05$) reduction in the number of either meningococcal cells or *N. lactamica* associated with HBMECs at any concentration of the inhibitor (SU5402) when compared to control (no inhibitor). Experiments were performed in four independent wells and the values shown represent the mean of three independent experiments. Error bars indicate SEM. This analysis done by one-way ANOVA.

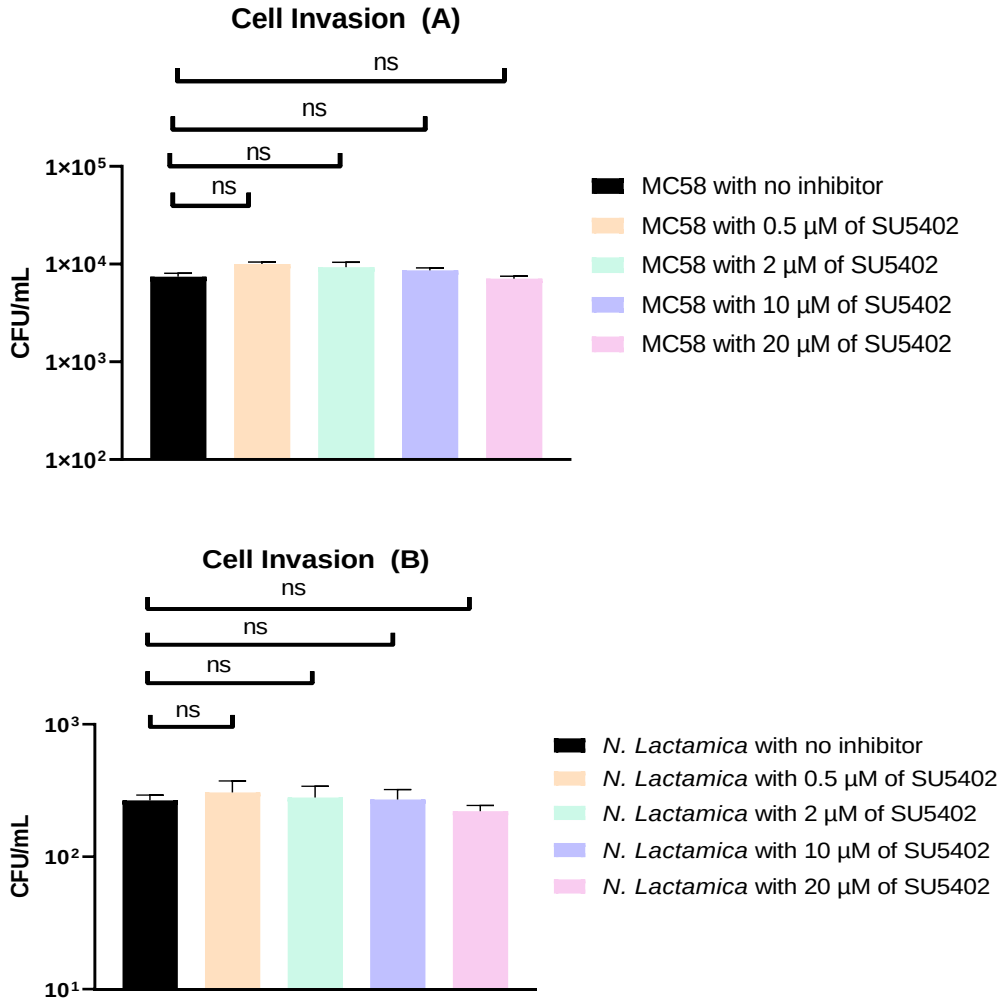

Figure 3.25. Invasion of HBMECs by *N. meningitidis* MC58 and *N. lactamica* ATCC 23970 in the presence of an FGFR1 inhibitor (SU5402). HBMECs infected with **(A).** *N. meningitidis* MC58 or **(B).** *N. lactamica* after 4 h of adhesion (MOI: 10) and then incubated for a further 1 h in the presence of gentamicin. Homogenised lysates were prepared and serially diluted as above, then aliquots applied to chocolate agar plates. There was no significant ($p > 0.05$) difference between the number of internalised meningococcal cells and *N. lactamica* and between treated HBMECs and untreated as a control. Experiments were performed in four independent wells and the values shown represent the mean of three independent experiments. Error bars indicate SEM. This analysis done by one-way ANOVA

3.2.13 Adhesion assays of MC58Δ*NMB0375-Omega*, MC58Δ*NMB1053-kan*, MC58Δ*NMB0506-kan* and MC58Δ*NMB0088-Omega* using HBMECs

To determine whether MafA, Opc5, FadL or NMB0506 contribute to cell adhesion and/or invasion of HBMECs, MC58-WT and mutant strains were compared. An MC58Δ*pilQ/*Δ*porA* mutant was also included, as this strain has previously been shown to exhibit significantly reduced adhesion and invasion (Virji et al., 1993, Orihuela et al., 2009). These experiments were carried out as two different sets of experiments due to the availability of strains at different times. There were not any statistically significant differences between MC58-WT and MC58Δ*NMB1053-kan* or MC58Δ*NMB0375-Omega* (Figure 3.26A), although the number of colonies was noticeably reduced with the Δ*NMB0375* mutant despite not reaching statistical significance. At this point, it is important to note that *N. meningitidis* strain MC58 contains duplicate *mafA* genes, denoted *mafA1* and *mafA2*, at loci *NMB0375* and *NMB0652*, respectively (Grifantini et al., 2002a, Grifantini et al., 2002b). It is possible that *MC58ΔNMB0375-Omega* has lower MafA expression relative to MC58-WT but retains some expression of the protein via *mafA2*, since both genes encode identical MafA proteins. Thus, although the results of the adhesion assay do suggest a role for MafA, it might be necessary to make a double knockout strain to observe a statistically significant effect. There was also no statistically significant difference between MC58-WT and MC58Δ*NMB0506-kan* in adhesion ability (Figure 3.26B), but significantly reduced adhesion was observed for MC58Δ*NMB0088-Omega* relative to wild-type, with the effect almost as strong as for the control mutant, MC58Δ*pilQ/*Δ*porA.*

As noted above, these experiments were carried out as two separate sets due to strain availability, which might have influenced the results. However, the data obtained suggested that adhesion of the mutant strains MC58Δ*NMB1053-kan*, MC58Δ*NMB0375-Omega* and MC58Δ*NMB0506-kan* was not significantly different relative to wild type MC58 (although in the case of *MC58ΔNMB0375-Omega*, the *mafA* gene duplication mentioned above should be taken into

consideration). However, MC58Δ*NMB0088-Omega* did display significantly attenuated adhesion ability relative to MC58 WT, and was compromised to nearly the same extent as MC58Δ*pilQ/*Δ*porA* control mutant. Thus, NMB0088 might play an important role in meningococcal attachment to HBMECs.

3.2.14 Invasion assay of MC58Δ*NMB0375-Omega,* MC58Δ*NMB1053-kan,* MC58Δ*NMB0506-kan* and MC58Δ*NMB0088-Omega* using HBMECs

To determine whether MC58Δ*NMB0375-Omega,* MC58Δ*NMB1053-kan,* MC58Δ*NMB0506-kan* and MC58Δ*NMB0088-Omega* contribute to cellular invasion of the exposed monolayer of HBMECs, an invasion assay was carried out according to the above procedure, after the initial 4 h incubation step for attachment. As before, the medium was exchanged for fresh medium containing gentamicin and incubation continued for 1 h. Samples were then processed as for the association assay.

There were statistically significant differences for MC58Δ*NMB1053-kan* and MC58Δ*NMB0375-Omega* relative to MC58-WT. Thus, significantly less invasion ($p < 0.05$) was seen for the NMB0375 (*mafA*) and NMB1053 (*opc5)* mutants than for the strain MC58-WT. The control mutant, MC58Δ*pilQ/*Δ*porA*, also showed significantly reduced invasion compared to wild type (Figure 3.27A). The other mutant strains, MC58Δ*NMB0506-kan* and *MC58ΔNMB0088-Omega*, also displayed statistically significantly lowered invasion ability relative to MC58-WT, and the reduction in cell number close to that seen for the control mutant, MC58Δ*pilQ/*Δ*porA* (Figure 3.27B).

As for the attachment assay, these results might be affected by the fact that these experiments were carried out in two different sets because of the availability of strains at different times. Nonetheless, all of the mutant strains (MC58Δ*NMB1053- kan,* MC58Δ*NMB0375-Omega,* MC58Δ*NMB0506-kan* and MC58Δ*NMB0088-Omega*) gave statistically fewer colonies compared to MC58-WT, suggesting that all of these genes are involved in meningococcal invasion of HBMECs. All of the knockout strains showed reduced invasion, even

though there were varying effects on their interaction with HBMECs in terms of initial attachment. In the case of *MC58ΔNMB0375-Omega*, it would be interesting to find out whether a double *mafA* knockout would show a stronger difference in invasion ability relative to MC58-WT.

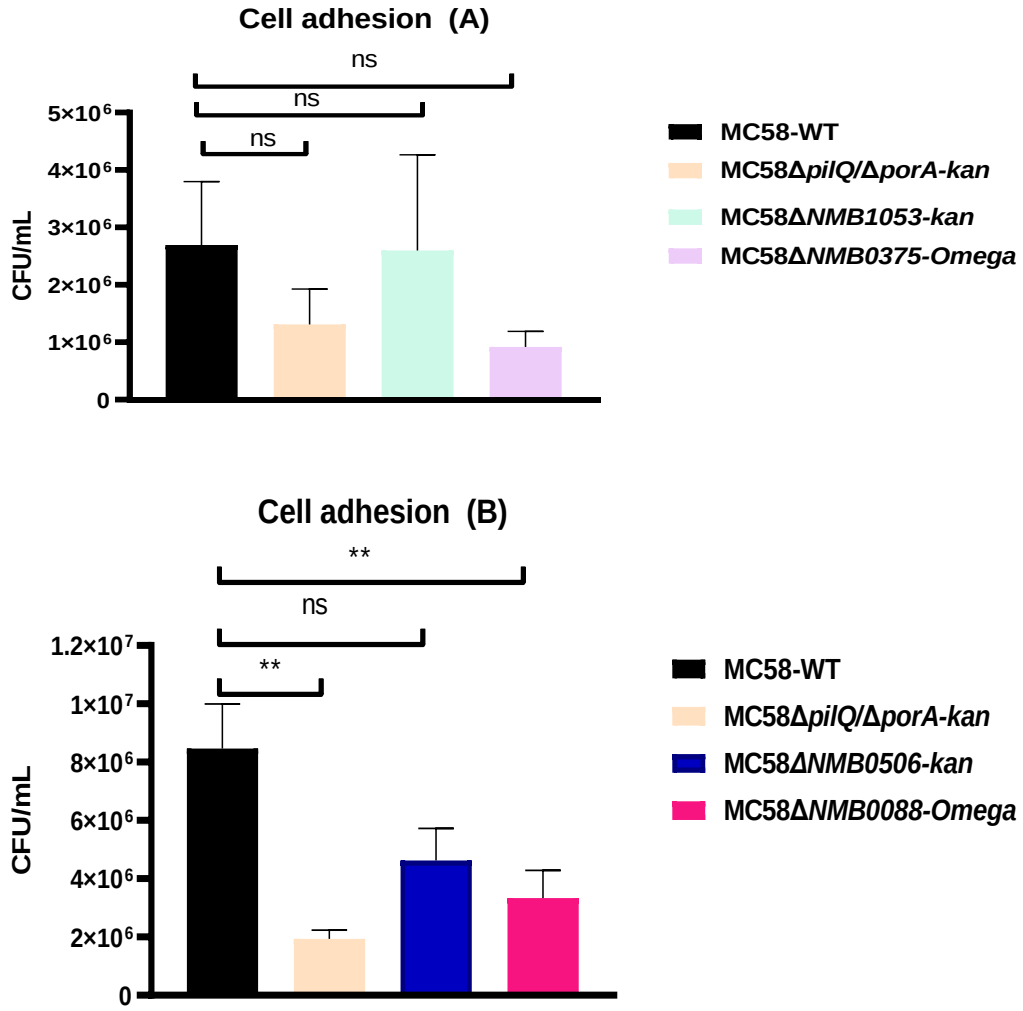

Figure 3.26 Adhesion of meningococcal mutants to HBMECs. (A) The number of colonies of MC58-WT, MC58Δ*pilQ/*Δ*porA*, MC58Δ*NMB1053-kan* and MC58Δ*NMB0375-Omega*, respectively, which adhered to HBMECs. The value for the MC58Δ*NMB0375-Omega* was lower than the wild type, but the difference was not statistically significant ($p > 0.05$). MC58Δ*pilQ/*Δ*porA*, used as a control, showed no significantly reduced adhesion compared to MC58-WT ($p > 0.05$). Mean values are shown from five independent experiments, each using quadruplicate wells. 'CFU' denotes colony forming units. Error bars denote SEM. **(B)** The number of colonies of MC58-WT, MC58Δ*pilQ/*Δ*porA*, MC58Δ*NMB0506-kan* and MC58Δ*NMB0088-Omega*, respectively, which adhered to HBMECs. Values for the MC58Δ*NMB0506-kan* was lower than wild type, but the differences were not statistically significant ($p > 0.05$), however, MC58Δ*NMB0088-Omega* mutants was statistically significant when compared with wild type (**$p < 0.0098$). MC58Δ*pilQ/*Δ*porA* used as a control, showed a significantly reduced adhesion compared to MC58-WT (**$p < 0.0014$). Mean values are shown from five independent experiments, each using quadruplicate wells. 'CFU' denotes colony forming units. Error bars denote SEM.

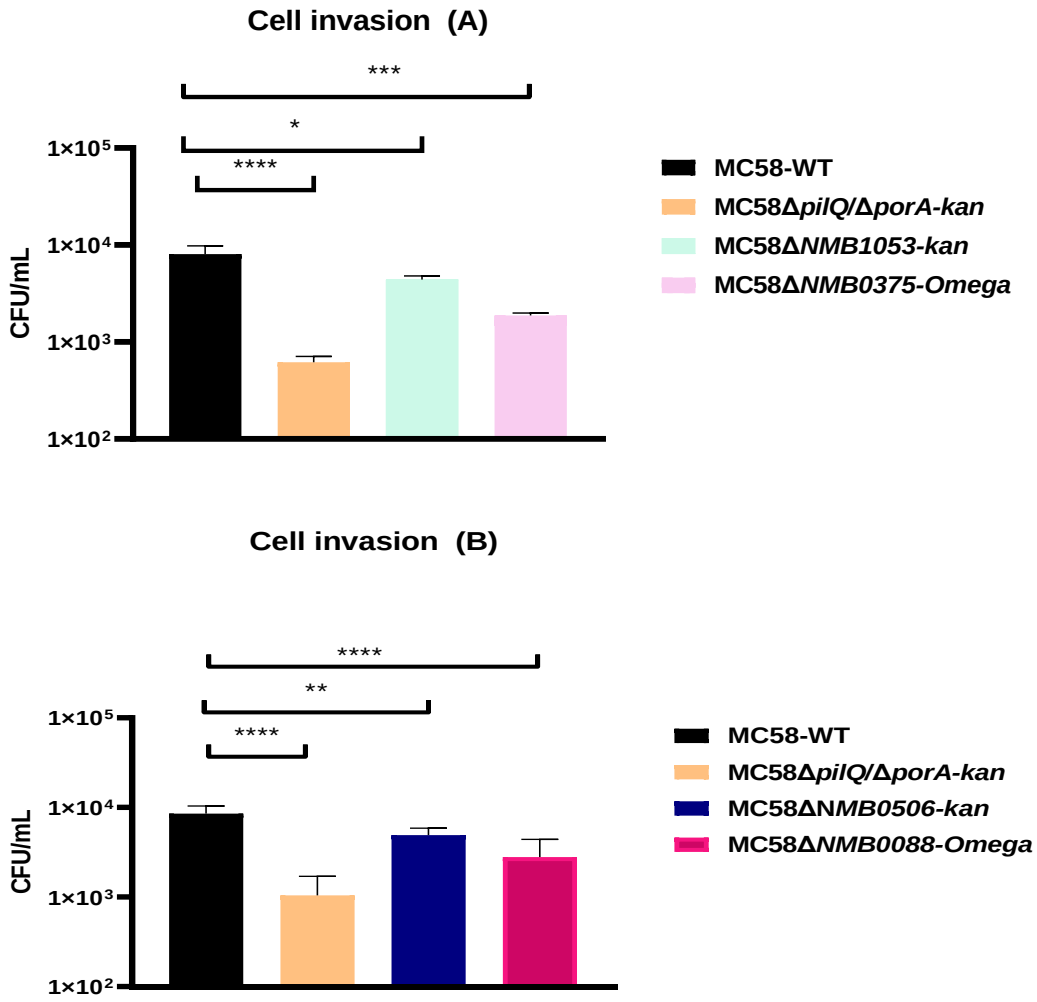

Figure 3.27: Invasion of HBMECs by meningococcal mutants. (A) The number of invading colonies of MC58-WT, MC58Δ*NMB1053-kan* and MC58Δ*NMB0375-Omega*, respectively, into HBMECs. A significant reduction (*$p < 0.05$ and ***$p < 0.001$) was found for invasion of the NMB0375 (*mafA*) and NMB1053 (*opc5*) mutants relative to MC58-WT respectively. The control mutant, MC58Δ*pilQ/*Δ*porA*, also showed significantly reduced invasion compared to wild type. Mean values are shown from five independent experiments, each using quadruplicate wells. 'CFU' denotes colony forming units. Error bars denote standard errors. **(B)** The number of invading MC58-WT, MC58Δ*NMB0506-kan* and MC58Δ*NMB0088-Omega*, respectively, into HBMECs. A significant reduction (**$p < 0.01$ and ****$p < 0.0001$) was found relative to MC58-WT for invasion of the *NMB0506* and *fadL* mutants respectively. The MC58Δ*pilQ/*Δ*porA* mutant, used as a control, also showed significantly reduced invasion compared to wild type. HBMECs were infected with the different mutants for 4 h (MOI: 10). Gentamicin was then added, in fresh medium, and incubation continued for a further 1 h. Mean values are shown from five independent experiments, each using quadruplicate wells. 'CFU' denotes colony forming units. Error bars denote SEM.

3.3 Discussion

Interaction between pathogenic bacteria and their host is important for causing a disease, but *N. meningitidis* interactions with host tissues are complex and incompletely understood, and therefore remain under investigation. There remains an ongoing need to identify additional virulence factors in order to improve disease treatment and management; for example, through the discovery of novel vaccine antigens. Previous work carried out in our laboratory found evidence for a direct and specific interaction between *N. meningitidis* and FGFR1 IIIc as a new cellular receptor for pathogenic meningococci. For example, it was found that activated FGFR1 is recruited by internalised meningococci inside HBMECs, and that knockdown of FGFR1 significantly attenuates bacterial attachment and invasion. Thus, FGFR1 expression and activation were demonstrated to be necessary for optimal adhesion and invasion of *N. meningitidis* to HBMECs, and interaction of FGFR1 IIIc with the bacterial cells was confirmed by ELISA (Azimi, 2014, Azimi et al., 2020).

In addition, laboratory work included ELISA screening a number of *N. meningitidis* MC58 mutants in an attempt to find possible ligands for FGFR1 on the surface of the bacteria (Azimi et al., 2020). One of the meningococcal mutants used in that study was a PilQ-deficient strain (Δ*pilQ*). PilQ is the secretin component of the type IV pilus export machinery. Importantly, PilQ-deficient strains are not piliated: pilus subunits are still expressed, but they are not exported across the outer membrane (Carbonnelle et al., 2006, Berry et al., 2012).

Previous work in our group has therefore shown, via mutation of PilQ, that meningococcal TFP are important for FGFR1-mediated adhesion of *N. meningitidis* to host endothelial cells (Azimi et al., 2020). Whereas TFP have broad involvement in bacterial adhesion, they often form low-affinity interactions, as illustrated by the examples of the CD147 and β2AR receptors mentioned above (Bernard et al., 2014, Le Guennec et al., 2020). Many other bacterial adhesins have been implicated in invasion of the host, and multiple surface-exposed meningococcal factors are evidently involved in the invasion of host tissues that occurs in meningococcal

disease. In fact, it is well recognised that minor adhesins might play important roles in the pathogenesis of meningococcal disease (Hill et al., 2010). In this project, it was therefore hypothesised that other specific, high-affinity bacterial ligands for FGFR1 may be present on the surface of disease-associated meningococci.

Previous work in our laboratory compared the binding properties of *N. meningitidis*, *N. gonorrhoeae*, *N. polysaccharea* and *N. lactamica* to FGFR1 IIIc, and revealed that the two pathogenic species (*N. meningitidis* and *N. gonorrhoeae*) bound to the receptor to a significantly greater extent than the commensal species. In contrast, the commensal species that frequently inhabit the nasopharyngeal mucosa and rarely, cause disease. This suggests that binding to FGFR1 IIIc might be important for the pathogenesis of invasive *Neisseria*, possibly permitting them to access deeper tissues. Furthermore, the above observations suggest that the bacterial ligand for FGFR1 IIIc might: (1) be expressed only by both *N. meningitidis* and *N. gonorrhoeae*, but not the commensal species; (2) be expressed at much higher levels in the pathogenic than the commensal species; or (3) be structurally different between the pathogenic and commensal species (Azimi, 2014).

To identify other potential FGFR1 ligands, an experimentally-determined meningococcal interactome with HBMECs disclosed by Kánová et al. (2018) was taken as the starting point to search for new candidates of interest. These authors did not use *N. meningitidis* strain MC58 in their study, but rather "isolate M1/03", a serogroup B strain not listed in PubMLST, and for which little sequence data is available. However, they did partially sequence the *mafA* gene of this strain (GenBank MK940370) and found 99.8% sequence homology with *mafA* of MC58 (Kánová et al., 2019), which corresponds to 100% identity at the amino acid level (present analysis; data not shown). For the purposes of this study, it was therefore assumed that candidate adhesins identified in *N. meningitidis* isolate M1/03 would have identical homologues in strain MC58.

Taking the unfiltered set of 41 candidate meningococcal ligands reported by Kánová et al. (2018) and searching for homologues in the commensal *N. lactamica* allowed for identification of several potentially important novel meningococcal

ligands. As described above, the initial list (Table 3.1) was filtered down to seven candidate proteins as the focus of further study: the four that were ultimately pursued in this project (*mafA*, *fadL*, *opc5* and *NMB0506*), along with NadA (NMB1994), NMB1533 and NMB1126/1164, which all have homologues in *N. lactamica* but with low sequence identities (64.1%, 85.6% and 86.6%, respectively). Interestingly, Kánová et al. (2018) found evidence for involvement of two of these three additional proteins (NadA and NMB1126/1164) in meningococcal adhesion to HBMECs. Cloning of *N. meningitidis* NadA and NMB1533 was therefore attempted in this project, but proved unsuccessful (for example, mutations were found in the plasmids after cloning of *nadA*). For NMB1126/1164, both loci encode an identical protein, perhaps due to a gene duplication event, and are separated by only ~10 kb in the bacterial genome. Since these loci could not be targeted individually, cloning them was not attempted during this project.

Overall, efforts to assemble the plasmids required for gene inactivation proved successful. Knockout strains of *N. meningitidis* were generated for all four target genes using natural transformation. However, the identity of the inserted antibiotic resistance cassette varied between knockouts: the kan cassette for mutation of *opc5* and *NMB0506*, and the Omega cassette for *mafA* and *fadL*. It was initially intended to make knockout strains with both cassettes for each gene, but constraints of time ultimately prevented this. However, the requisite plasmids were prepared for three of the four incomplete experiments (*opc5* and *NMB0506* with the Omega cassette inserted, and *mafA* with the kan cassette), so mutants could be generated using these plasmids in future work, if required.

Before moving on to investigate the properties of the mutant strains in attachment and invasion assays, experiments to validate the role of FGFR1 in these processes were initially attempted. Pre-treatment of HBMECs with the FGFR1 inhibitor SU5402 did not alter the adhesion or invasion behaviour of either *N. meningitidis* or *N. lactamica* (Figures 3.24, 3.25), which stands in contrast to previous results from our group (Azimi, 2014), where significant differences were observed in the presence of SU5402. In subsequent work, it might be useful to repeat these

experiments according to the earlier protocol but also to use a different inhibitor than SU5402.

One recent study also designated it as a multi-kinase inhibitor, and identified other off-targets including ABL and JAK3 (Gudernova et al., 2016). Thus, SU5402 does not have good specificity for FGFR1. All known FGFR inhibitors target more than one family member (albeit with different activities). At present, there does not seem to be an FGFR1 inhibitor available that has high selectivity over other FGFR family members (i.e., does not inhibit FGFR2–4). However, compounds with much reduced off-target activity (outside the FGFR family) have been developed, and some of these should serve as more suitable tool compounds for future work building on this study. For example, the investigational drugs AZD4547 and PRN1371, which inhibit FGFR1–3 and FGFR1–4, respectively, might be useful alternatives, because both compounds show their highest potency against FGFR1 (Dai et al., 2019).

To investigate the functions of the four targeted genes in meningococcal adhesion and invasion with HBMECs, the interaction of mutant strains with these human cells was compared to the wild-type strain, and adhesion and invasion assay data was generated for all four strains along with a positive control. Of the four genes targeted as potential FGFR1 ligands, only MC58Δ*NMB0088-Omega* showed a significant contribution towards attachment of *N. meningitidis* MC58 to HBMECs in the present study (Figure 3.26). Interestingly, this identification of NMB0088 (FadL) as a meningococcal adhesin appears to be a novel finding not reported before. The FadL protein has, however, previously been analysed in terms of its strain variation (Yero et al., 2010), and proposed as a potential serogroup B vaccine antigen given its abundance in OMVs (Sardinas et al., 2009). FadL is discussed in more detail below.

More broadly, the results shown in Figure 3.26 draw attention to some important limitations of the present experiments (noting the large standard errors). Firstly, due to practical considerations, these experiments were run in two parts on different days (i.e., the *ΔmafA* and *Δopc5* mutants were run in a separate experiment to the *ΔfadL*

and *ΔNMB0506* mutants). Secondly, it is known that there can be phenotypic variation between different batches of the MC58 strain of *N. meningitidis*, and this seemingly needs to be better controlled for. These limitations could be mitigated in future by: (i) varying the mutant pairings between experiments, and (ii) increasing the number of repeats.

Furthermore, in some experiments in this study, the difference in binding between MC58-WT and the MC58Δ*pilQ/*Δ*porA* control mutant did not reach statistical significance as would be expected. This strongly suggests that additional repeats (e.g., N = 10) would have been useful to reduce standard errors, as suggested above, enabling more confident conclusions to be drawn about which results were significant and which were not. In future work, combining this possibility with the 'mixed pairings' approach mentioned above would likely give much more conclusive results.

Although statistical significance was not reached here for the *ΔmafA* mutant relative to MC58-WT for attachment to HBMECs, it did show noticeably reduced levels of adhesion (Figure 3.26A) that might prove significant with a suitably modified experimental design to overcome the current limitations. This might in turn overcome the unexpected failure to confirm a statistically significant role for Δ*mafA* in adhesion to HBMECs, given the findings reported in the literature (Kánová et al., 2018, Kánová et al., 2019). However, in the particular case of *mafA*, there is a gene duplication in *N. meningitidis* MC58, and the importance of this has already been noted above. Thus, making and evaluating a double *mafA* knockout strain might well resolve the discrepancy in this case. Furthermore, the inconsistency with previous results might also be due to differences in experimental approach. Kánová et al. (2018) measured the interaction of purified recombinant MafA protein with protein extract from HBMECs (not whole cells) by ELISA, and with whole HBMECs using immunocytochemistry. They did not conduct any binding assays with whole bacterial cells as was done here, where the adhesion properties of MC58-WT and *ΔmafA* meningococcal strains were compared directly. Another possibility

concerns the experimental variability encountered in the present study, as addressed above.

The observation here of a role for *ΔmafA* in invasion suggests functional significance for the protein in meningococcal disease. The MafB protein is a secreted toxin involved in fratricide, or contact-dependent inhibition (CDI), an activity which is a feature of all major bacterial lineages (Arenas et al., 2015, Arenas et al., 2020). In meningococci, export of MafB is known to depend on MafA with the pair seemingly functioning as a TPSS, so it is likely that the two proteins are functionally interdependent in host cell attachment, especially given that *mafA* and *mafB* genes usually localise together on genomic islands (Arenas et al., 2020).

In contrast to the differences seen for adhesion, all four genes of interest were found to play a significant role in meningococcal invasion of HBMECs (Figure 3.27). Continuing to focus on *ΔmafA*, Kánová et al. (2019) suggested it is likely involved in neuroinvasion and carried out a transcriptomic analysis of HBMECs challenged with the protein. In common with whole meningococci, purified MafA was able to induce host genes associated with cellular remodelling and endocytosis (in addition to an inflammatory response), suggesting a functional role in invasion of host tissues. The results obtained in the present study apparently confirm such a role for MafA.

Hypothetical protein *NMB0506* is a hemagglutinin-related protein and contact-dependent inhibition (CDI), an activity which is common to all major bacterial lineages (García et al., 2012, Arenas et al., 2013, Jamet and Nassif, 2015). In CDI, bacterial toxins are secreted via T5SS, with the CdiA protein (more generically, TpsA) being the toxin whose secretion relies on the CdiB/TpsB partner (Jamet and Nassif, 2015). In *Neisseria* species, *tpsA*/*tpsB* gene pairs are situated on specific genomic islands with several downstream *tpsA*-like cassettes, designated as *tpsC*, which possibly represent a source of antigenic variation of TpsA through recombination events (Arenas et al., 2013). The *NMB0506* locus of *N. meningitidis* strain MC58 encodes such a CdiA-like toxin and was previously annotated as *tpsC3*, one of six *tpsC* genes positioned downstream of a primary *tpsA* locus, *NMB0497*

(Arenas et al., 2013). In this project, the discovery of the NMB0506 protein as a functional invasion appears to be a novel finding for such a gene, and might inspire further efforts to search for previously unanticipated functional roles of other *tpsC*-encoded proteins.

The FadL protein (also known as OmpP1) is a fatty acid transporter originally discovered in *E. coli* (Nunn and Simons, 1978). Intriguingly, FadL is a recognised adhesin/invasin in *H. influenzae* where it mediates invasion of host tissues via the CEACAM1 receptor (Tchoupa et al., 2015, Moleres et al., 2018), but does not seem to have been characterised as a neisserial virulence factor to date. The above results (Figures 3.26, 3.27) therefore appear to represent the first demonstration of roles for FadL in adhesion and invasion behaviours of *N. meningitidis.*

Finally, Opc/Opc5 was also found to promote invasion of HBMECs in this work. This protein is an established adhesin, as discussed in general introduction, and binds directly to HSPGs on the surface of host cells. It also two serum factors, fibronectin and vitronectin, to bind to the integrin receptors for these ligands, leading to internalisation of the bacterium by HBMECs (Unkmeir et al., 2002). However, this process reportedly requires the human serum factors to promote invasion, but the assay done here (Figure 3.27) used serum-free medium. This suggests that the effect of Opc in promoting invasion of HBMECs seen here must be due to an alternative receptor other than integrins, such as FGFR1.

At this point, it is important to note that additional characterisation of the mutants would help support the proposed roles of the target genes in adhesion/invasion. For example, knockout of protein expression could be established using western blot, and qPCR could be used to confirm that the target genes are not transcribed in the mutants. Wider genotyping might consider whether known phase variable or antigenic genes, such as *nalP* and *mspA*, were affected by the mutations (e.g., by using PCR and sequencing). If more comprehensive genotyping is required, whole-genome sequencing could be undertaken.

In summary, successful inactivation/knockout was achieved for all four genes targeted as potential meningococcal FGFR1 ligands: *mafA*, *fadL*, *opc5* and

NMB0506. Cellular assays with HBMECs implicated all four of the encoded proteins as important for invasion of host endothelial cells, and FadL was also established as a potential novel outer membrane adhesin of *N. meningitidis*. The next step was to investigate direct interaction of these bacterial proteins, and of whole meningococci, with the purified extracellular ligand-binding domain of FGFR1.

Chapter 4: Binding of *N. meningitidis* to Fibroblast growth factor receptor 1 (FGFR1)

4.1 Introduction

The ability of bacteria to adhere to cellular surfaces is key to their ability to colonise and infect host organisms (Ribet and Cossart, 2015). An important function of this bacterial cell surface adhesion is the activation and delivery of virulence factors; however, signalling within host cells may also be affected, which can additionally facilitate the spread and prolongation of disease (Kim et al., 2010). During bacterial adhesion to host cells, multiple pathogenic adhesion molecules bind to target host receptors. These adhesins play a particularly crucial role in infection, especially due to the physical stress exerted on host cells during their involvement in the early steps of bacterial attachment (Berne et al., 2018, Dufrene and Persat, 2020).

It is clear that bacteria have evolved a variety of strategies in order to colonise and invade human organs and tissues despite the presence of multiple host defence mechanisms against these pathogens (Ribet and Cossart, 2015). The initial adhesion process involves a wide variety of microbial adhesins and proceeds in a sequential manner, wherein these bacterial adhesins bind to their host receptors one by one in a defined sequence. Binding of adhesins to host receptors also follows the cooperativity principle, in the meaning that initial interaction induces expression of further host cell receptors, promoting binding of additional adhesin molecules (Virji, 2008). For most bacteria, initial attachment occurs via binding of adhesins to external cellular proteins. Following such attachment to surface receptors, host cell responses typically include internalisation of the pathogen, or tight attachment after initialisation of specific intracellular signalling (Van Sorge and Doran, 2012, Doran et al., 2016).

At the subcellular level, different cell types respond differently to surface attachment of bacteria; for example, some cells remodel the actin cytoskeleton in response to the activation of specific signalling pathways (Haglund and Welch, 2011, Alto and Orth, 2012). Pathogens including *Salmonella* and *Shigella* are known to achieve this by introducing effector proteins directly into the

cytoplasm of host cells via a type III secretion pathway and inducing reorganisation of actin polymers (Zhou and Galán, 2001, Davis et al., 2008, Alto and Orth, 2012). Other pathogens such as *Neisseria*, *Yersinia* or *Listeria* induce a unique signalling pathway involving growth factor induced host cell membrane ruffling, cell migration and cell adhesion. In this way, these pathogens are taken up by non-professional phagocytic host cells (Rottner et al., 2005).

Some bacterial pathogens avoid host immune responses by exploiting various pathways that enable them to survive within host cells; for example, bacteria are able to display OMPs on their surface that shield recognisable antigen epitopes to avoid recognition by the host immune response. Other immune evasion mechanisms include forming niches in the host cytoplasm to allow successful replication, or resisting host immune responses (Ribet and Cossart, 2015).

For *N. meningitidis*, haematogenous spread after penetration through the nasopharyngeal mucosa is a well-known pathogenic mechanism, but the means by which this microorganism crosses the blood–cerebrospinal fluid (B-CSF) barrier are incompletely understood and remain under investigation (Sokolova et al., 2004, Join-Lambert et al., 2010). Nonetheless, *N. meningitidis* appears to be well suited to survive the environmental challenges faced during its travel from the upper respiratory tract to eventually cross the B-CSF barrier (Schoen et al., 2014, Simonis and Schubert-Unkmeir, 2016). Surface structures of *N. meningitidis* can influence adhesin interactions with receptor molecules of the host, and one such vital structure is the capsule (Simonis and Schubert-Unkmeir, 2016), that can mask surface proteins from aspects of the immune system (such as immunoglobulin). There is convincing evidence from several studies that the capsule of *N. meningitidis* is also helpful for its survival within human cells, and as mentioned in the introduction, the capsule contributes to immune evasion and survival in the bloodstream. It has also been found that genes encoding elements of the capsule formation pathway are upregulated following penetration of host cells (Spinosa et al., 2007).

The capsule is also involved in HBMECs infection and interaction with host cell microtubules, and is therefore important for bacterial replication and survival at the

intracellular stage of infection (Kim et al., 2003, Nikulin et al., 2006, Talà et al., 2014). Structures known as membrane protrusions, similar to epithelial microvilli, form as a result of *N. meningitidis* adhesion to the endothelial cells. This process results in formation of protein complexes, or cortical plaques, under the pathogenic colonies within cells and these processes facilitate bacterial internalisation into intracellular vacuoles (Merz et al., 1999, Eugène et al., 2002, Miller et al., 2013). Exactly how *N. meningitidis* initiates interaction with, and attaches to, host cells are still under investigation. In order to facilitate initial attachment and invasion, bacteria typically bind to a variety of extracellular matrix proteins, including laminin, collagen, and fibronectin (Vaca et al., 2020). As another example, *N. meningitidis* has the ability to bind to members of the human carcinoembryonic antigen-related cell adhesion molecules (CEACAM) family of membrane proteins, which act as surface receptors for adhesion of the bacterium (Griffiths et al., 2007, Virji, 2009). Bacterial adhesins may bind to specific receptors on host cells that cause signal transduction, consequentially resulting in tight attachment of bacteria or their internalisation by the host cells (Coureuil et al., 2012, Doran et al., 2016). The human laminin receptor is a key binding site for many neuroinvasive bacterial species including *H. influenzae*, *N. meningitidis* and *S. pneumoniae*, and their binding facilitates the host–pathogen interaction (Orihuela et al., 2009, Coureuil et al., 2012, Herold et al., 2019). Studies have demonstrated that interaction between host HBMECs and *N. meningitidis* through the laminin receptor is facilitated by involvement of the PilQ component of type IV pili (TFP) and PorA. In addition, there is evidence for interaction between host HBMECs and pneumococcal choline binding protein A (CbpA), and for binding of outer membrane protein P2 (OmpP2) of *H. influenzae* to the laminin receptor (Orihuela et al., 2009, Abouseada et al., 2012, Dando et al., 2014, Herold et al., 2019).

Multiple mechanisms have been described of invasion of HBMECs by *N. meningitidis*, for example mediated by the PilC1 subunit of TFP which undergoes phase variation that contributes to the host cell adhesion process (Rytkönen et al., 2004, Morand et al., 2009). PilC1-triggered endothelial cellular

infection induces EGFR depletion in cells, possibly due to recycling of receptors and degradation (Morand et al., 2009). In addition, previous studies on meningococcal invasion have demonstrated recruitment of ErbB2 (an EGFR family member) upon colonisation of endothelial cells. This results in ErbB2 homo-dimerisation and downstream activation of the actin-binding adapter protein cortactin, which subsequently triggers actin rearrangement leading to its polymerisation in cortical plaques underneath the bacterial colonies at the endothelial cell surface (Hoffmann et al., 2001, Slanina et al., 2014). Members of the EGFR family have been proposed as additional host molecules involved in invasion, and hence in the process by which *N. meningitidis* crosses the BBB (Slanina et al., 2014).

Another class of receptor tyrosine kinases, fibroblast growth factor receptors (FGFRs) together with their ligands (fibroblast growth factors, or FGFs) play a critical role in proliferation, metazoan development, survival capability and differentiation throughout early and late development stages (Lemmon and Schlessinger, 2010, Wesche et al., 2011). The FGFRs are individual, multifunctional transmembrane receptors located at the surface of human cells. They are involved in migration, cell differentiation and proliferation during early embryogenesis and also contribute to wound healing, tumour angiogenesis and tissue repair during adulthood (Presta et al., 2005, Lemmon and Schlessinger, 2010). These receptors have a transmembrane region, a C-terminal cytoplasmic region and an N-terminal extracellular region, which contains three immunoglobulin (Ig)-like domains and functions as the ligand-binding domain due to its ‘acidic box’ motif that interacts with cell adhesion molecules and heparin sulphate proteoglycans (HSPGs) (Lemmon and Schlessinger, 2010, Azimi et al., 2020). The transmembrane and cytoplasmic regions contain tyrosine residues which are phosphorylated in order to activate the downstream signalling pathway (Slanina et al., 2014). The extracellular ligand-binding domain of FGFRs contains three Ig-like domains, here designated D1, D2 and D3. The first of these domains is involved in receptor autoinhibition, while the second and third mediate ligand (FGF) binding (Ibrahimi et al., 2004, Haugsten et al., 2010, Lemmon and Schlessinger, 2010). Different receptor

isoforms, including variations in the Ig-like domains D1–D3, are produced by alternative splicing of transcribed genes (Olsen et al., 2004, Eswarakumar et al., 2005). The 'acidic box' is a conserved, negatively-charged motif positioned between domains D1 and D2 and acting as binding site for divalent cations that enhance interaction of the adjacent heparin binding domain with its sulphated proteoglycan ligands Figure 4.1 (Olsen et al., 2004, Eswarakumar et al., 2005).

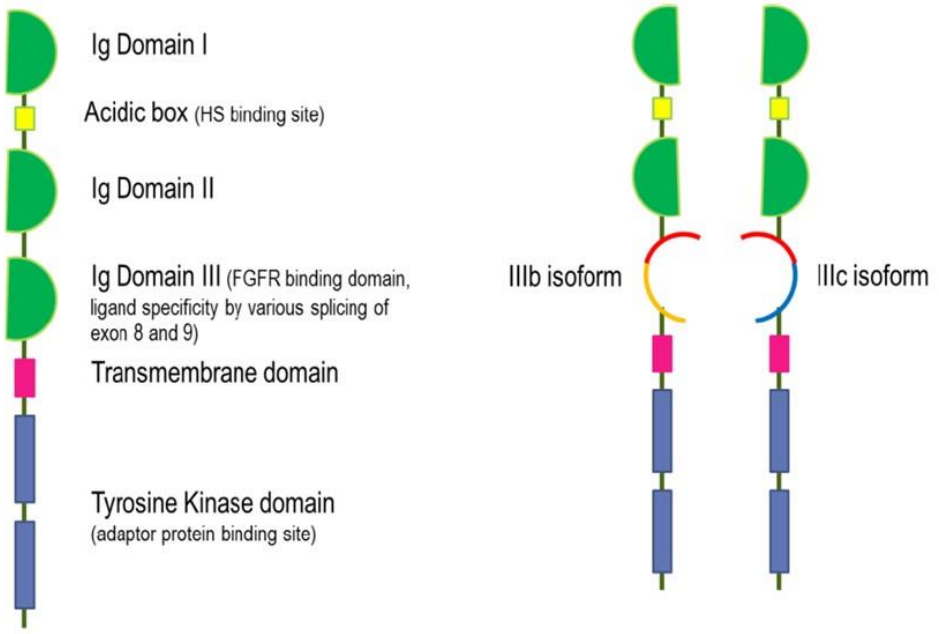

Figure 4.1 Schematic overview of the prototypical FGFR structure. FGFR consists of one transmembrane domain, three IgG-like domains in the N-terminal half, and an acidic box between Ig-like domains (Ig-D) I and II (where heparin sulphate binds). FGFR1 is expressed in alternative isoforms based on alternative splicing of the second half of the third Ig-like domain. This results in a higher affinity for ligands and a higher specificity for receptor ligands. Obtained from (Azimi, 2014).

The FGF signalling pathway was first discovered in 1939 by Trowell and Willmer, via the pro-proliferative effects of bovine brain extracts on cultured fibroblast cells (Trowell and Willmer, 1939, Kim et al., 2020). Initial characterisation of this

mitogenic activity assigned it to 'basic FGF' (bFGF), a 15 kDa FGF molecule so named because of its high isoelectric point (pI). Later, another molecule with FGF activity was found in brain extracts and termed 'acidic FGF' (aFGF) due to its low pI (Mohammadi et al., 2005, Ornitz and Itoh, 2015). It was subsequently found that mitogenic activity is additionally mediated by sulphated glycosaminoglycans (heparin) through FGF binding (Mohammadi et al., 2005). It is now known that 22 ligands make up the human FGF family, and that they bind directly to four homologous, high-affinity FGFRs (FGFR1–FGFR4) (Laestander and Engström, 2014, Sarabipour and Hristova, 2016). Regardless of variation in size between the FGFs (17–34 kDa), they all share the same conserved sequence of 120 amino acids with 16–65% sequence homology (Eswarakumar et al., 2005), and possess distinct generic characteristics, including an N-terminal signal sequence and a core region responsible for FGFR and glycosaminoglycan binding (Mohammadi et al., 2005).

The FGFR proteins are involved in the pathogenesis of certain microorganisms, although a detailed understanding of their specific roles in infectious diseases requires further investigation. Nonetheless, they have been implicated in the pathogenesis of *Rickettsia*, where they mediate internalisation of the bacterium into endothelial cells, with recent work directly implicating HSPG-associated FGFR1 in internalisation of *Rickettsia rickettsii* by human microvascular endothelial cells (Sahni et al., 2017). The same study found that administration of an FGFR inhibitor (AZD4547) reduced the rickettsial burden in a murine model of *Rickettsia conorii* endothelial target spotted fever rickettsiosis. FGFRs also play a role in the pathogenesis of *Chlamydia trachomatis*, where they are involved in the penetration of epithelial cells via the FGF2 pathway (Kim et al., 2011, Sahni et al., 2017). In this case, *C. trachomatis* infection is associated with binding and uptake of the bacterium into epithelial cells mediated either by upregulated FGF2 expression, or direct binding to FGF2 (Kim et al., 2011, Mehlitz and Rudel, 2013). These events result in binding of FGF2–bacteria–HSPGs to FGFRs, inducing internalisation of bacterial elementary bodies; consequently, *C. trachomatis* infection in HeLa cells relies on enhanced expression of FGF2 mediated by ERK1/2 stimulation, in turn driven by activation of FRS2 (Kim et al., 2011).

The events triggered by FGF ligand binding to FGFRs have attracted much attention over the last few decades. It was initially found that each cell type contains low- and high-affinity FGF receptors, with two binding sites that can be differentiated on the heparin-independent site and ionic strength (Zhou et al., 1997, Laestander and Engström, 2014). The FGFs primarily form ternary complexes (FGF–FGFR–HSPG) involving an FGF ligand, a receptor (FGFR) and heparan sulfate proteoglycans (HSPG) (Ibrahimi et al., 2004, Xie et al., 2020). The observation that *C. trachomatis* pathogenesis involves binding of the bacterium to both FGF2 and HSPGs, as noted above (Kim et al., 2011, Mehlitz and Rudel, 2013), has implications for meningococcal behaviour in IMD that have perhaps been overlooked. These earlier findings with *C. trachomatis* suggest that pathogenic *N. meningitidis* might also form FGF–bacteria–HSPG complexes as part of the internalisation mechanism via FGFRs; an especially intriguing possibility given the known affinity of meningococcal Opc for HSPGs.

Binding of an FGF to its receptor stimulates dimerisation of the FGFR, which in turn induces conformational changes in the cytoplasmic domain of the receptor. It can then form complexes with other kinases for example, through the cytoplasmic juxtamembrane domain and tyrosine phosphorylation is also activated (Schlessinger, 2000, Yokote et al., 2005, Lemmon and Schlessinger, 2010). This recruitment of signalling proteins upon stimulation by FGF assists tyrosine autophosphorylation at specific residues of activated FGFRs, which then serve as docking sites for adapter proteins to initiate downstream signalling (Eswarakumar et al., 2005, Lemmon and Schlessinger, 2010). Multiple intracellular adapter proteins are phosphorylated by active FGFRs including FRS2 (fibroblast growth factor receptor substrate 2), which binds to the activated FGFR through its phosphor tyrosine binding (PTB) domain and is subsequently phosphorylated (Ong et al., 2001, Yokote et al., 2005, Gotoh, 2008).

By related mechanisms, several downstream signalling pathways can be induced by activated FGFRs, including the trans-autophosphorylation of the receptor tyrosine kinase (RTK) domain. More specifically, four major signalling pathways are

activated by FGF/FGFRs: the Ras/MAPK and Ras/Raf/MAPK; PI3K/Akt; PLC- γ/PKC; and JAK/STAT pathways (Li et al., 1999, Knights and Cook, 2010, Ornitz and Itoh, 2015).

FGFR1 contains seven autophosphorylation sites (Y463, Y583, Y585, Y653, Y654, Y730 and Y766), which have been analysed for their involvement in different FGFR1-mediated cellular responses; however, it is not always clear which signal transduction pathways are associated with which site(s), and FGFR autophosphorylation is tightly regulated. Nonetheless, phosphorylation of Y653 and Y654 is known to be crucial for phosphorylation of adapter proteins to activate downstream signalling, and phosphorylation of Y766 is also important (Mohammadi et al., 1996, Hart et al., 2000, Furdui et al., 2006).

Two distinct mechanisms govern FGFR regulation of the phospholipase C (PLC) pathway: FGFR can bind directly to PLC-γ or can be bound by PLC-ε via Ras, in a ternary complex (Mohammadi et al., 1991, Vázquez-Manrique et al., 2008). Either way, this results in the release of two secondary messengers, diacylglycerol (DAG) and inositol-1,4,5-triphosphate (IP3), produced by the PLC enzymes via hydrolysis of phosphatidylinositol-l-4,5-bisphosphate (Cross et al., 2002, Lyon and Tesmer, 2013). In cell mitogenesis, only PLC-γ has been shown to interact with activated FGFRs, through a specific binding site for the PLC-γ SH2 domain is created upon autophosphorylation of Tyr766 in the C-terminal tail of FGFR1 (Mohammadi et al., 1991, Mohammadi et al., 1996, Cross et al., 2002, Haugsten et al., 2010).

Signalling pathways involving FGFR1 are required to maintain the integrity, and ensure differentiation, of endothelial cells within the microvasculature (Kanda et al., 1996, Murakami et al., 2008, Azimi et al., 2020), with FGFR1 also known to play roles in BBB angiogenesis and maintenance of barrier integrity, suggesting that it might be utilised by *N. meningitidis* to cross the BBB and cause meningitis (Azimi et al., 2020). Indeed, the entry of *N. meningitidis* into HBMECs is known to be dependent upon interaction with FGFR1 that is recruited upon pathogen binding (Slanina et al., 2014, Azimi et al., 2020), in addition to being

mediated by EGFR, which accumulates close to sites of bacterial attachment as mentioned above. Furthermore, bFGF was found to exert a protective effect on cultured HBMECs, since it significantly rescued monolayer permeability induced by reoxygenation and glucose deprivation (Lin et al., 2018).

Invading bacterial cells were found to co-localise with activated FGFR1 molecules and α-actinin, consistent with earlier findings that FGFR1 is trafficked into early endosomes in a clathrin-independent process regulated by Syndecan 4 (Elfenbein and Simons, 2013, Azimi et al., 2020). Azimi et al. (2020) also found that FGFR1 is completely internalised into the cytoplasm, together with the bacterium, during *N. meningitidis* invasion of HBMECs. The foregoing considerations suggest that *N. meningitidis* utilises the transcellular pathway while invading HBMECs, which does not compromise the integrity of the monolayer.

Previously, the region encoding the extracellular ligand-binding domain of FGFR1 has been amplified from cDNA and cloned to create a plasmid (pEf-Bos-ss-Fc-extFGFR1IIIc-ires-TPZ) encoding an FGFR1 IIIc human immunoglobulin Fc fusion protein (Azimi et al., 2020). This chapter describes work where the same plasmid was used to express recombinant FGFR1 in HEK293T cells, which was then purified and used in ELISA experiments to confirm its interaction with meningococci. The immunoglobulin portion alone, encoded by pEF-Bos-ss-Fc-stop-LRP-ires-TPZ construct, was utilised as a control. This portion (the Fc-tag) corresponds to the Fc domain, or constant region, of immunoglobulin (IgG) heavy-chains. To further investigate the FGFR1-binding properties of the proposed bacterial ligands (MafA, Opc5, FadL and NMB0506), expression of recombinant forms of these proteins was undertaken. Various experiments, such as ELISA assays and far-western blotting, were utilized as additional means of establishing which, if any, of these four proteins of interest are capable of interacting strongly with the ligand-binding domain of FGFR1.

4.2 Results

4.2.1 Expression of Fc-FGFR1 IIIc and Fc-stop in HEK293T cells by transient transfection using calcium phosphate reagent

A variety of methods can be used to deliver genetic materials such as DNA, RNA, and siRNA into eukaryotic cells. These include chemical, physical, lipid or viral vector-mediated methods (Kim and Eberwine, 2010), and it is possible to study the function and expression of a gene using such delivery technologies (Hawley-Nelson et al., 2008). In addition, these technologies are useful for the expression of correctly folded recombinant proteins, including glycoproteins such as FGFR1, which require specific post-translational modifications for structural studies or physiological purposes; for example, in diagnostic or therapeutic applications (Chan et al., 2002, Duchesne et al., 2006).

Transfection of HEK293T cells for protein expression was therefore investigated with plasmid pEf-Bos-ss-Fc-extFGFR1IIIc-ires-TPZ and pEF-Bos-ss-Fc-stop-LRP-ires-TPZ constructs. Initially, cells were transfected with both plasmids using the calcium phosphate ($CaPO_4$) precipitation method employed previously in our group (Azimi, 2014). Transfection efficiency was evaluated using medium-scale transfection (MST) experiments in T-75 flasks, monitored by the fluorescence level from GFP-topaz (which is co-expressed by the pEf-Bos-based constructs using an internal ribosome binding site), as measured by a fluorescence microscope at different time points (typically 24, 48 and 72 h post-transfection). To determine transfection efficiencies, phase images were evaluated, and the percentages of GFP-expressing cells and non-GFP-expressing cells were determined manually. Unfortunately, in this study below 20% of cells showed GFP expression three days post-transfection (Figure 4.2). However, it is important to note that the efficiency of transfection using $CaPO_4$ precipitation is recognised as being very sensitive to any inconsistencies in reagent quality or working pH of materials (ThermoFisher Scientific). Attempts were made to optimise the procedure by varying the plasmid DNA concentration (1–3 μg/mL); however, this still failed to achieve successful transfection and protein expression (result not shown).

Attempts to express both proteins via transfection using $CaPO_4$ precipitation were also verified as unsuccessful by running the supernatant on SDS–PAGE and immunoblotting, as a result of which no expression could be identified (result not shown). Also, transfected cells detached from the flask when incubated for more than three days, suggesting extensive cell death. Therefore, although $CaPO_4$ can be a cost-effective method, its efficiency here with HEK293T cells was too low, meaning that the efficiency of the procedure was unsuitable for protein production (based on GFP-topaz expression), and was therefore lower than required for recombinant protein production. Rather than undertake potentially extensive and time-consuming optimisation of the $CaPO_4$-based procedure, alternative transfection reagents were explored instead to increase the efficiency of protein expression.

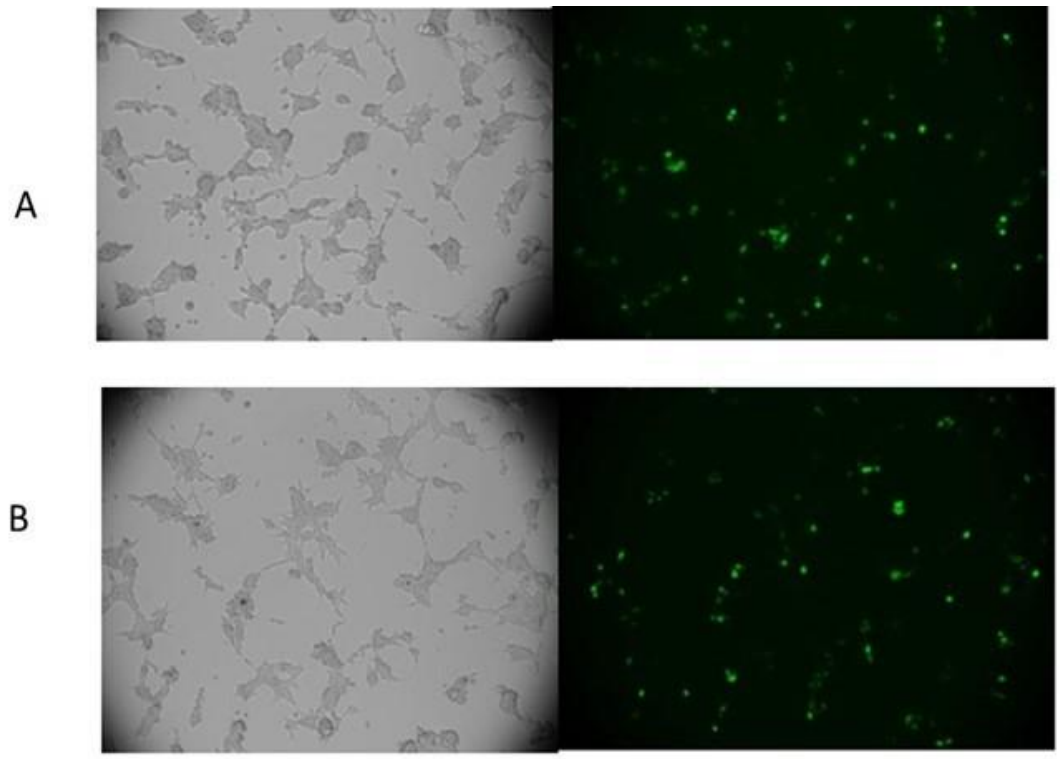

Figure 4.2: Transfection of HEK293T cells with pEf-Bos-ss-Fc-extFGFR1IIIc-ires-TPZ or pEF-Bos-ss-Fc-stop-LRP-ires-TPZ by $CaPO_4$. HEK293T cells were grown to 30% confluence and transfected with 1 μg ml^{-1} of pEf-Bos-ss-Fc-extFGFR1IIIc-ires-TPZ (A) or pEF-Bos-ss-Fc-stop-LRP-ires-TPZ (B) using $CaPO_4$. Cells were visualised after 72 h using a fluorescence microscope. The right-hand panels show fluorescence, and the corresponding panels on the left show bright field images. For transfections using $CaPO_4$ precipitation, cells were grown in a T-75 flask until 30% confluent, then transfection mixes were prepared by mixing 1 μg ml^{-1} of plasmid DNA with 155μL of 2 M $CaCl_2$, then dH_2O was added to a final volume of 1.5 ml. After mixing thoroughly, 1.5 ml of 2× HBS was added to form the DNA/$CaPO_4$ precipitate followed by incubation at room temperature for 10 min to form the transfection mix, following which the transfection mix was added dropwise to the cells in flasks. The cells were then incubated at 37°C in a 5% CO_2 incubator for 24 h. Next day, the growth medium was replaced by Ultra CHO cell medium, and the cells incubated for a further 48 h.

4.2.2 Optimising transfection, expression, and purification of Fc-FGFR1 IIIc and Fc-stop in HEK293T cells

A review of the literature revealed that HEK293T cells have been successfully transfected using the Lipofectamine 3000 reagent in addition to $CaPO_4$ precipitation (González-González et al., 2020, Hasan et al., 2021). The first alternative transfection reagent evaluated for transfection efficiency in this work was

Lipofectamine 3000, for optimisation of the expression of Fc-FGFR1 IIIc and Fc-stop in HEK293T cells. For this method, GFP-topaz expression, used to determine transfection efficiency, indicated successful transfection of HEK293T cells, reaching its highest level (60%) at three days post-transfection. During this experiment, non-transfected cells were used as a negative control. For small-scale transfection (SST) experiments, the expression plasmid pEf-Bos-ss-Fc-extFGFR1IIIc-ires-TPZ and pEF-Bos-ss-Fc-stop-LRP-ires-TPZ were again used to transiently transfect HEK293T cells for expression of the fusion protein Fc-FGFR1 IIIc and Fc-stop, respectively.

4.2.2.1 Expression of Fc-FGFR1 IIIc and Fc-stop in HEK293T cells by transient transfection using Lipofectamine 3000 reagent

For transfection using Lipofectamine 3000, expression of Fc-FGFR1 IIIc and Fc-stop in HEK293T cells was achieved successfully using the plasmids pEf-Bos-ss-Fc-extFGFR1IIIc-ires-TPZ and pEF-Bos-ss-Fc-stop-LRP-ires-TPZ, based on the observed expression of GFP-topaz. Cells were incubated for 72 h post-transfection, and the progress of protein expression was monitored by GFP fluorescence microscopy (Figure 4.3). To confirm expression of target proteins of the expected size, media was collected at the end of the 72-h incubation, and cells were lysed in RIPA buffer supplemented with phosphatase and protease inhibitors and analysed by SDS–PAGE and immunoblotting. Following transfection with expression constructs for Fc-stop, and the Fc-FGFR1 IIIc fusion protein, the transfection was shown to be successful by fluorescence microscopy since expression of GFP-topaz was observed. A faint band corresponding to the expected fusion protein was seen on the western blot in lysates of cells transfected using Lipofectamine 3000, but not in the supernatant media for Fc-FGFR1 IIIc and Fc-stop (Figure 4.4 and Figure 4.5) respectively, confirming expression of both proteins in HEK293T cells transfected using Lipofectamine 3000. Although the transfection efficiency was improved using this reagent, the fusion protein was not secreted in the supernatant and most of the expressed protein remained inside the cells. Furthermore, after more than three days post-transfection, the cells died and detached from the flask. In conclusion, the

transfection efficiency of HEK293T cells using Lipofectamine 3000 was satisfactory, but both of the expressed proteins remained intracellular and were not secreted in the supernatant as expected. This anticipated secretion is a property of the Fc-tag, which typically carries an N-terminal signal sequence when used in protein expression constructs to ensure secretion of the expressed protein into the supernatant. In this case, secretion was unsuccessful, so an alternative transfection reagent was therefore tried, but it was also decided to go forward with large-scale transfection (LST) experiments and purify the expressed proteins from cell lysates.

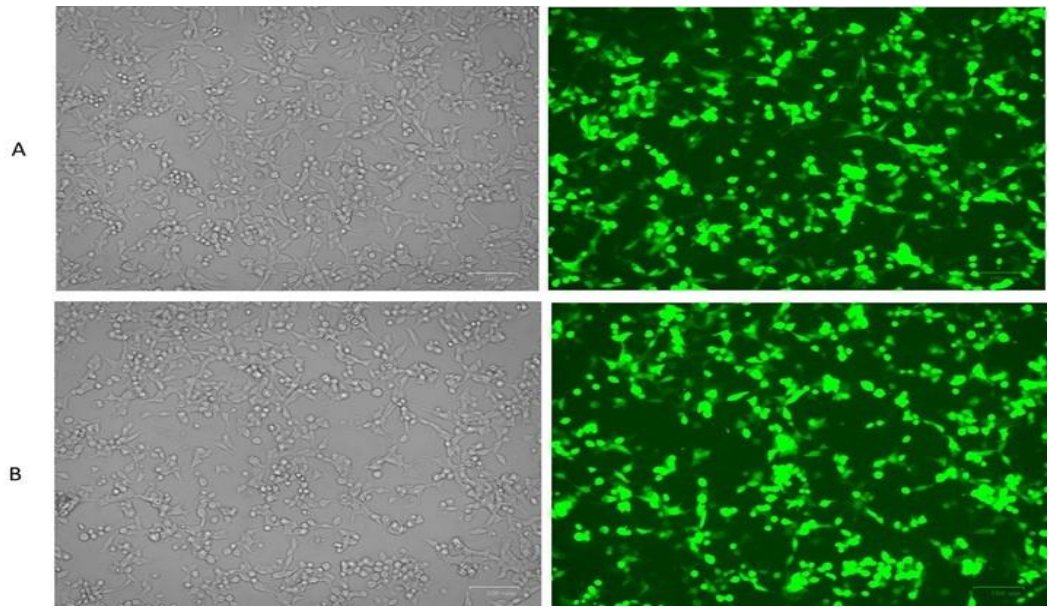

Figure 4.3: Transfection of HEK293T cells with pEf-Bos-ss-Fc-extFGFR1IIIc-ires-TPZ or pEF-Bos-ss-Fc-stop-LRP-ires-TPZ by lipofectamine 3000. HEK293T cells were grown to 90% confluence and transfected with 6 µg of pEf-Bos-ss-Fc-extFGFR1IIIc-ires-TPZ (A) or pEF-Bos-ss-Fc-stop-LRP-ires-TPZ (B) using Lipofectamine 3000. Cells were visualised after 72 h by fluorescence microscope. The right-hand panels show fluorescence, and the corresponding panels on the left show bright field images. HEK293T transfection using Lipofectamine 3000 was as follows. Cells were grown in T-25 flasks until 70–90% confluence was reached, then transfection mixes were prepared consisting of 11 µl Lipofectamine 3000 reagent and 500 µl Opti-MEM medium. In a separate microcentrifuge tube, 6 µg plasmid DNA was mixed with 8 µl of the diluted Lipofectamine 3000 reagent and 500 µl Opti-MEM, then incubated at room temperature for 5 min. This was then added to original Opti-MEM solution containing the Lipofectamine reagent and incubated for 45 min, following which the transfection mix was added dropwise to the cells in T-25 flasks. The cells were then incubated at 37°C in a 5% CO_2 incubator for 18 h. Next, the growth medium was replaced by DMEM with antibiotics and without added FBS, and the cells incubated for a further 48 h.

4.2.2.1.1 Purification of recombinant Fc-tagged Fc-FGFR1 and Fc-stop proteins after transfection with Lipofectamine 3000

The Fc-tagged extracellular domain of FGFR1 (Fc-FGFR1 IIIc) and Fc-stop were expressed by transient transfection of HEK293T cells as described above. With Lipofectamine 3000-mediated transient transfection, the growth medium and whole cell lysate were collected 72 h post-transfection and analysed. The expressed proteins contained the Fc portion of immunoglobulin, which was therefore predicted to direct them into the secretion pathway; however, Fc-FGFR1 IIIc and Fc-stop were not observed in the culture supernatant. Therefore, RIPA buffer was used to lyse the cells and clarified cell lysates were collected and analysed. To purify Fc-FGFR1 IIIc and Fc-stop, protein A/G Sepharose was employed (since this will capture the Fc-tag). Purification was carried out at 4°C to prevent protein precipitation and degradation. A/G-Sepharose was added to the cleared cell lysate after diluted 1:1 (v/v) with binding buffer and the contents incubated with shaking at 4°C overnight. An empty column was prepared by washing 5× with binding buffer to prepare the filter for binding the Fc-tag. The cell lysate with the beads was then added to the column and incubated for 10 min. And then, the flow-through was collected and the column was washed 3 times with sodium chloride binding buffer to removed weak binding. Fc-tagged proteins were eluted at low pH (0.1 M glycine pH 2.5), which works by weakening the interaction between the Fc-tag and the column, then neutralised with Tris–HCl.

Purified whole cell lysates were probed by SDS–PAGE to separate proteins, then immunoblotting was undertaken to identify the Fc fragment of IgG for both Fc-FGFR1 and Fc-stop, which resulted in the identification of Fc-tagged Fc-FGFR1 IIIc and Fc-stop. An anti-FGFR1 antibody was also selected to verify purification of the extracellular domain of Fc-FGFR1 IIIc (results not shown). For the Fc-FGFR1 IIIc fusion protein in whole cell lysates, a band was observed at *ca.* 50 kDa, which is somewhat lower than the expected value of 62 kDa (the estimated size of the Fc-tagged FGFR1 IIIc domain) (Figure 4.4). The extracellular IIIc domain of FGFR1 has a molecular weight of *ca.* 33 kDa, and the Fc-tag is *ca*. 29 kDa, such that the

combined molecular weight of the expressed construct should be 62 kDa. However, the FGFR1 portion of the fusion protein (Fc-FGFR1 IIIc) has a low theoretical pI value of 5.50, which likely explains why its mobility on SDS–PAGE and immunoblotting is lower than expected based on size. For the Fc-stop protein in whole cell lysates, a band was observed at *ca.* 29 kDa (Figure 4.5), matching the expected molecular weight. It is important to note that when immunoblotting for these proteins, the anti-Fc antibody (alkaline phosphatase conjugate) only gave a faint band. An anti-goat IgG (secondary antibody–alkaline phosphatase conjugate) was also used to improve detection of the Fc-tag (used at 1:30,000 in 5% skimmed milk in PBST). The nitrocellulose membrane was incubated with both of these antibodies in sequence, resulting in a stronger band.

Nonetheless, the protein expression results suggested the need to find another transfection reagent: firstly, because the protein had not been secreted in the supernatant, and secondly because the amount of protein after purification was very low, making the process inefficient since the transfection reagent is expensive. We decided to find out a suitable collaborator within our university, to find advice on alternative transfection methods. The Martinez-Pomares group work with the same tag (Fc-tag) and have carried out optimisation of their transfection protocols for expression of Fc-tagged proteins. Through this work, they found that the GeneJuice reagent was the best-performing transfection reagent for protein expression.

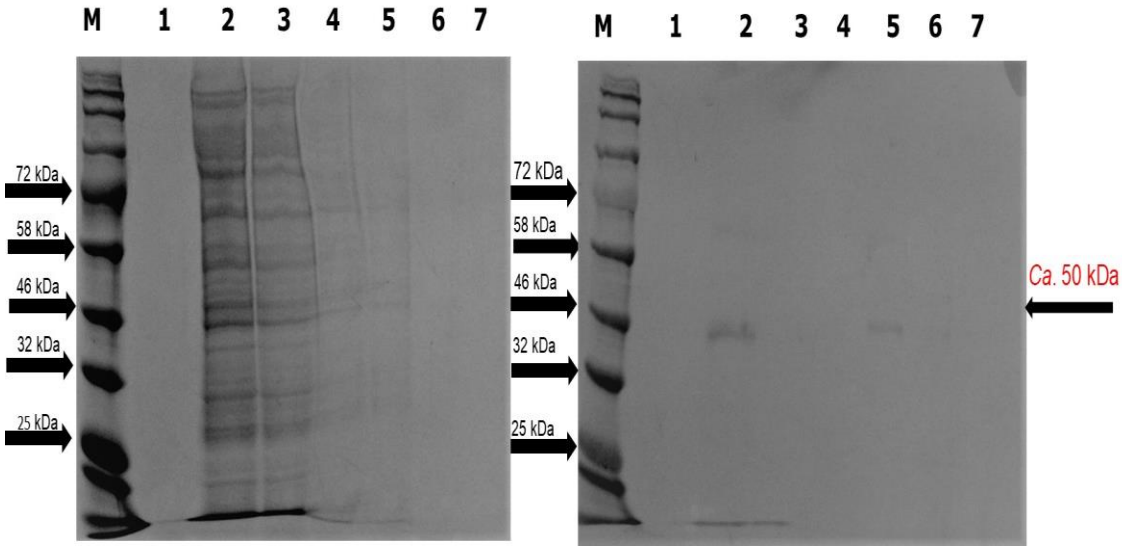

Figure 4.4: 8% SDS-PAGE and immunoblotting analysis for the presence of Fc-FGFR1 IIIc in whole cell lysates (WCL) of HEK293T cells 72 h post-transfection. HEK293T cells were grown to 90% confluence and transfected with 6 µg of pEf-Bos-ss-Fc-extFGFR1IIIc-ires-TPZ using Lipofectamine 3000. Proteins were analysed by SDS-PAGE (left), or by immunoblotting (right) after transfer to a nitrocellulose membrane and probing with anti-Fc antibody and anti-goat IgG (as described in the main text). M: protein size ladder; 1: column filtrate after purification; 2: clarified cell lysate; 3: clarified cell lysate after passing through column (flow-through from loading step); 4: column washes (3× with binding buffer); 5: first fraction collected during elution (0.1 M glycine pH 2.5 followed by neutralisation with 1 M Tris–HCl pH 9); 6: second eluted fraction; 7: third eluted fraction.

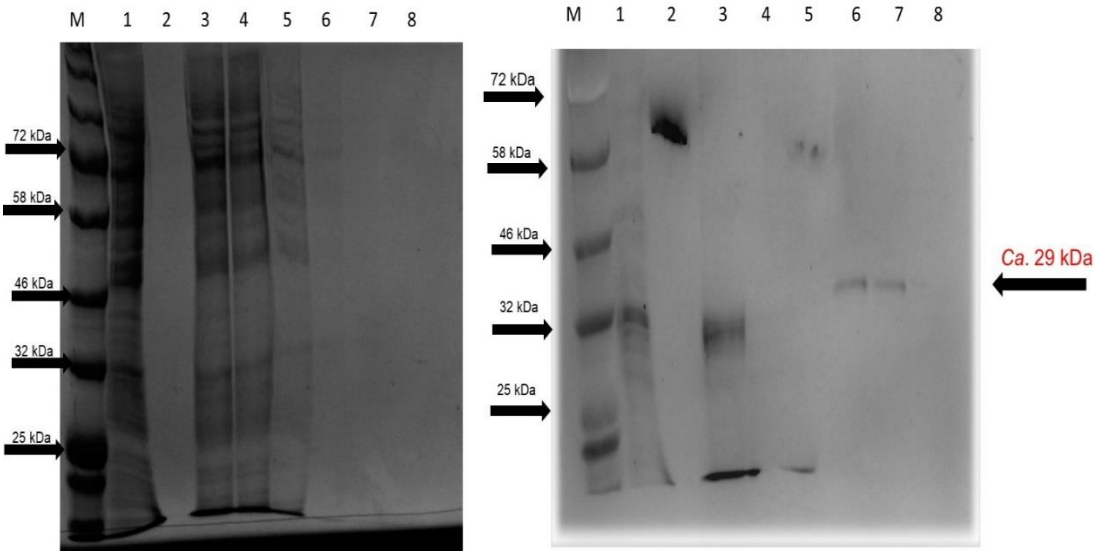

Figure 4.5: 8% SDS-PAGE and immunoblotting analysis for the presence of Fc-stop in whole cell lysates (WCL) of HEK293T cells 72 h post-transfection. HEK293T cells were grown to 90 % confluence and transfected with 6 µg of pEF-Bos-ss-Fc-stop-LRP-ires-TPZ using Lipofectamine 3000. Proteins were analysed by SDS-PAGE (left), or by immunoblotting (right) after transfer to a nitrocellulose membrane and probing with anti-Fc antibody and anti-goat IgG (as described in the main text). M: protein size ladder; 1: clarified cell lysate from (small scale transfections); 2: Filter of column after purification; 3: clarified cell lysate before loading to column from (large scale); 4: clarified cell lysate after passing through column (flow-through from loading step); 5: column washes (3× with binding buffer); 5: first fraction collected during elution (0.1 M glycine pH 2.5 followed by neutralisation with 1 M Tris–HCl pH 9); 6: second eluted fraction; 7: third eluted fraction; 8: fourth eluted fraction.

4.2.2.2 Expression of Fc-FGFR1 IIIc and Fc-stop in HEK293T cells by transient transfection using GeneJuice reagent

An alternative transfection reagent, GeneJuice, was tried for optimisation of transfection efficiency in this work, for expression of Fc-FGFR1 IIIc and Fc-stop in HEK293T cells. The GeneJuice reagent was compared, and transfection efficiency was monitored by GFP fluorescence as before. For this method, GFP-topaz expression indicated successful transfection of HEK293T cells, reaching its highest levels (80%) at five to eight days post-transfection. During this experiment, non-transfected cells were used as a negative control. For large-scale transfection (LST) experiments, the expression plasmids pEf-Bos-ss-Fc-extFGFR1IIIc-ires-TPZ and pEF-Bos-ss-Fc-stop-LRP-ires-TPZ were again used to transiently transfect HEK293T cells for expression of the fusion protein Fc-FGFR1 IIIc and Fc-stop, respectively.

With transfection using the GeneJuice reagent, expression of Fc-FGFR1 IIIc and Fc-stop in HEK293T cells was achieved successfully using the plasmids pEf-Bos-ss-Fc-extFGFR1IIIc-ires-TPZ and pEF-Bos-ss-Fc-stop-LRP-ires-TPZ, respectively, based on the observed expression of GFP-topaz. Cells were incubated for eight days (Fc-FGFR1 IIIc) or five days (Fc-stop) post-transfection, and the progress of protein expression was monitored by GFP ZOE microscopy (Figure 4.6). This was followed by confirmation of protein expression and determination of the size of the expressed proteins by SDS–PAGE and immunoblotting (result not shown). A faint band for the expected fusion protein was observed in the corresponding SDS–PAGE and immunoblotting analyses of the supernatant of cells transfected with Fc-FGFR1 IIIc and Fc-stop. This suggested that the transfection efficiency of HEK293T cells using the GeneJuice reagent was satisfactory, because of the high percentage of GFP-positive cells (more than for $CaPO_4$ precipitation or Lipofectamine 3000), and because both proteins were observed in the supernatant post-transfection. Thus, this method was accepted as the best source of recombinant protein and subsequent purification.

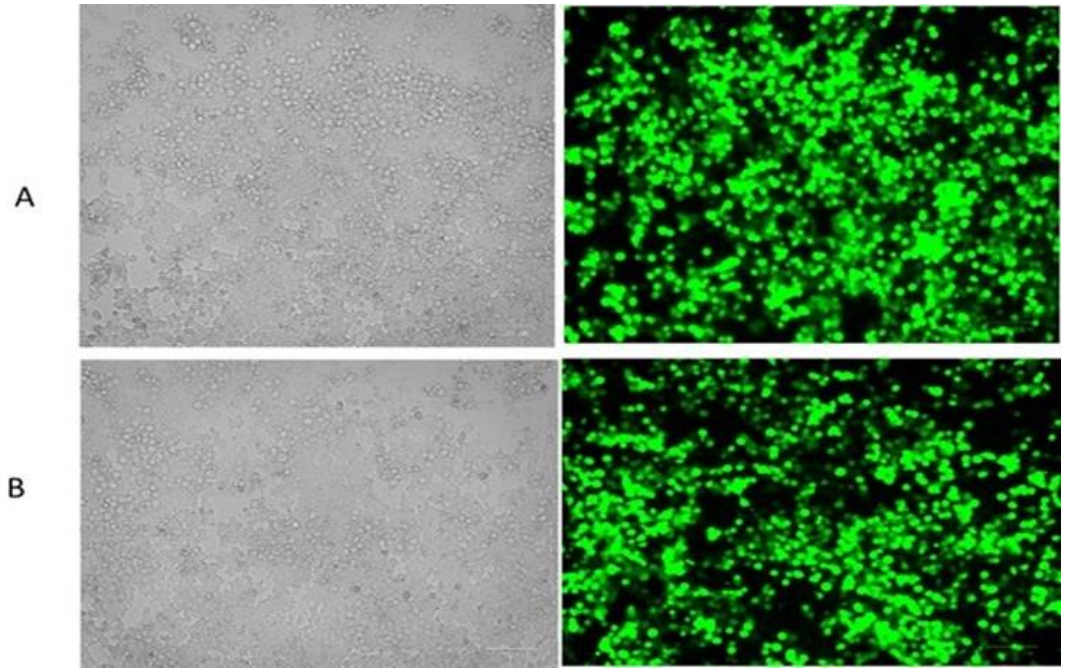

Figure 4.6: Transfection of HEK293T cells with pEf-Bos-ss-Fc-extFGFR1IIIc-ires-TPZ or pEF-Bos-ss-Fc-stop-LRP-ires-TPZ plasmids using the GeneJuice reagent. Expression from pEf-Bos-ss-Fc-extFGFR1IIIc-ires-TPZ (A) and pEF-Bos-ss-Fc-stop-LRP-ires-TPZ (B) after transfection into HEK293T cells. Transfection efficiency was determined five-eight days post-transfection by measuring the fluorescence intensity using a ZOE microscope. The right-hand panels show fluorescence, and the corresponding panels on the left show images acquired using bright field illumination. HEK293T cells were transfected using the GeneJuice regent as follows. Cells were grown in a T-225 flask until 60% confluence was reached, then the growth medium was exchanged with DMEM (low glucose) supplemented with penicillin/streptomycin and 10% FBS (18 mL). Following this, transfection mixes were prepared consisting of 54 µl GeneJuice reagent and 1.8 mL Opti-MEM. The mixture was incubated for 10 min at room temperature then 23 µg of plasmid DNA was added, followed by incubation for a further 15 min. The transfection mixture was next added dropwise to the flask and mixed into the growth medium gently by rocking back and forth, and side-to-side, a few times. The cells were then incubated at 37°C in a 5% CO_2 incubator for 18 h. Next, the growth medium was replaced by 35 mL of Opti-MEM with antibiotics and without added FBS, and the cells incubated for a further eight days (Fc-FGFR1 IIIc) or five days (Fc-stop). The supernatant was collected in a Falcon tube and centrifuged at 3000 × *g* for 15 min at 4°C, then filtered through a 0.22 µM filter and stored at 4°C until beginning the purification process.

4.2.2.2.1 Purification of Fc-tagged recombinant FGFR1 (Fc-FGFR1 IIIc) and Fc-stop expressed by transient transfection with the GeneJuice reagent

As noted above, the Fc-tagged FGFR1 (Fc-FGFR1 IIIc) and Fc-stop proteins were expected to be secreted, and therefore attempts were made to purify them from the supernatant. Cells were harvested before any significant cell death/detachment was observed, and the supernatant was collected in a Falcon tube and centrifuged. Recombinant proteins were purified manually, and the procedure was carried out at 4°C to prevent protein precipitation and degradation. An empty column was filled with protein A/G-Sepharose up to the pre-marked level and washed with PBS to prepare for binding of the Fc-tag. The culture supernatant, processed as above, was prefiltered through a 0.22 μM filter to remove any remaining cells and cellular debris, then applied to the column at a flow rate of approximately 1 mL/min. The column was washed with PBS to remove any remaining cells and weakly-bound proteins. Then, bound (Fc-tagged) proteins were eluted with 0.1 M glycine pH 2.8, collecting 10 drops of eluent in each tube. Each eluted fraction was neutralised immediately with one drop of Tris–HCl, which was essential to prevent protein degradation.

Protein samples were again analysed using SDS–PAGE, and the Fc fragments of IgG were detected using antibodies. This verified the presence of the tagged FGFR1 extracellular domain (Fc-FGFR1 IIIc), given that a band was observed above 58 kDa. This is the expected size of the Fc-tagged FGFR1 IIIc protein, as illustrated (Figure 4.7), and purified Fc-stop (Fc-tag alone) showed the expected size of 29 kDa (Figure 4.8). For each final fraction from the purification, protein concentration was quantified by UV absorbance (A_{280}) using a NanoDrop instrument. All purified protein fractions were stored at -80°C. For the subsequent experiments described below (ELISA experiments and far-western blotting to determine whether the IIIc domain of FGFR1 interacts directly with *N. meningitidis*), fraction number 3 was used for Fc-stop, and fraction number 4 for Fc-FGFR1 IIIc.

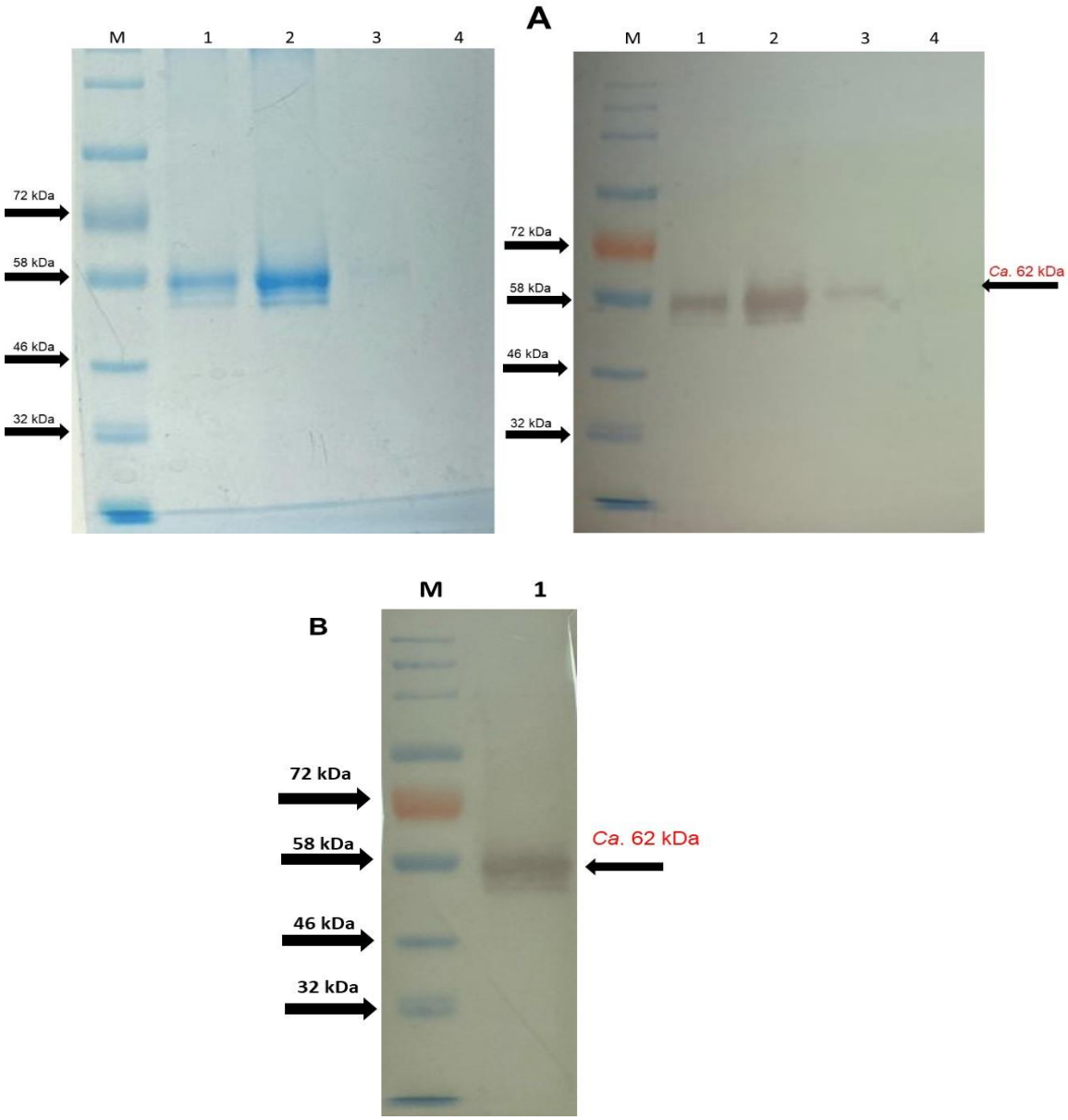

Figure 4.7: 10% SDS-PAGE and immunoblotting analysis of expression and purification of Fc-FGFR1 IIIc from culture supernatants after transfection of HEK293T cells using the GeneJuice reagent. A: SDS-PAGE analysis (left) shows expression and purification of the extracellular domain of FGFR1 (Fc-FGFR1 IIIc); and immunoblotting analysis (right) shows the same, analysed using an anti-Fc-tag antibody and anti-goat IgG (alkaline phosphatase conjugate, 1:30,000 in 5% skimmed milk in PBST). M: protein size markers; 1: fourth fraction of protein (after elution with 0.1 M glycine and neutralisation by Tris-HCl); 2: fifth eluted fraction; 3: sixth eluted fraction; 4: seventh eluted fraction; B: Immunoblotting analysis of purified Fc-FGFR1 IIIc with an anti-FGFR1 antibody. M: protein size markers; 1: fourth fraction of protein (after elution with 0.1 M glycine and neutralisation by Tris−HCl).

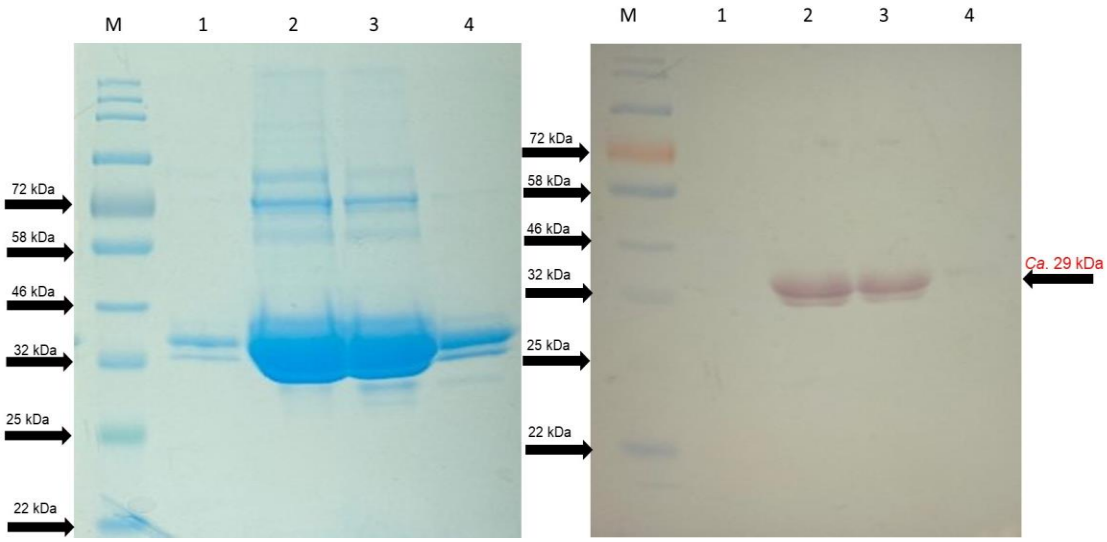

Figure 4.8: 10% SDS-PAGE and immunoblotting analysis of expression and purification of Fc-stop from culture supernatants after transfection of HEK293T cells using the GeneJuice reagent. 10% SDS-PAGE analysis (left) shows expression and purification of Fc-stop; and immunoblotting analysis (right) shows the same using an anti-Fc-tag antibody and anti-goat IgG (alkaline phosphatase conjugate, 1:30,000 in 5% skimmed milk in PBST). M: protein size markers; 1: third fraction of protein (after elution with 0.1 M glycine and neutralisation by Tris-HCl); 2: fraction number four; 3: fraction number five; 4: fraction number six.

4.2.3 There is a direct interaction between meningococci and the extracellular domain of FGFR1 (IIIc ligand-binding domain)

Following successful purification of Fc-FGFR1 IIIc and Fc-stop, ELISA experiments were carried out to confirm interaction between FGFR1 and *N. meningitidis* surface structures. Briefly, *N. meningitidis* was grown at 37°C with shaking until the OD_{600} reached 0.5, at which point the bacteria were collected by centrifugation and washed twice with PBS. The bacteria were fixed using formaldehyde and then centrifuged again, washed with PBS, and the pellets resuspended in sodium carbonate buffer (pH 7.4). Microplate wells were uniformly coated with the appropriate formaldehyde-fixed whole meningococcal cell suspension, with triplicate wells for each MC58 concentration. Following incubation overnight, unbound bacteria were removed, and the wells washed and blocked. Different concentrations of Fc-FGFR1 IIIc were screened in order to choose the optimal concentration for measuring binding to the immobilised meningococci. Specifically, Fc-FGFR1 IIIc (1, 2, 3, or 4 μg ml^{-1}) and Fc-stop (1 μg ml^{-1}) in 1% w/v BSA/PBS were then added to the appropriate wells, and the plate incubated at 4°C overnight with gentle agitation. Interaction of the bacteria with recombinant proteins was probed using an anti-Fc-tag antibody. In each experiment, wells coated with 1% BSA/PBS were used as controls in order to measure background levels of binding. The Fc-tag only construct served as a negative control, which had been cloned into the same vector and purified using the same method as for Fc-FGFR1 IIIc, as described above.

The results of this experiment are shown in Figure 4.9, and indicate that all the different concentrations of Fc-FGFR1 IIIc screened showed a statistically significant difference in binding relative to control; 1% BSA/PBS+Fc-FGFR1 IIIc. Thus, direct interaction was detected between the FGFR1 extracellular IIIc domain and *N. meningitidis* (MC58) at all protein concentrations tested. This interaction was not due to affinity of the bacteria for the Fc-tag, because the Fc-tag-only control (Fc-stop) showed less significant interaction with MC58 than for Fc-FGFR1 IIIc. As a result of this optimisation experiment, the best concentration of Fc-FGFR1 IIIc

to use for whole cell ELISA was determined as 2 µg ml^{-1}, because this gave the maximum binding signal that was not increased by using more protein (i.e., binding saturation was reached). The appropriate concentration for Fc-stop was therefore 1 µg/mL, considering their relative molecular weights (62 kDa and 29 kDa for Fc-FGFR1 IIIc and Fc-stop, respectively).

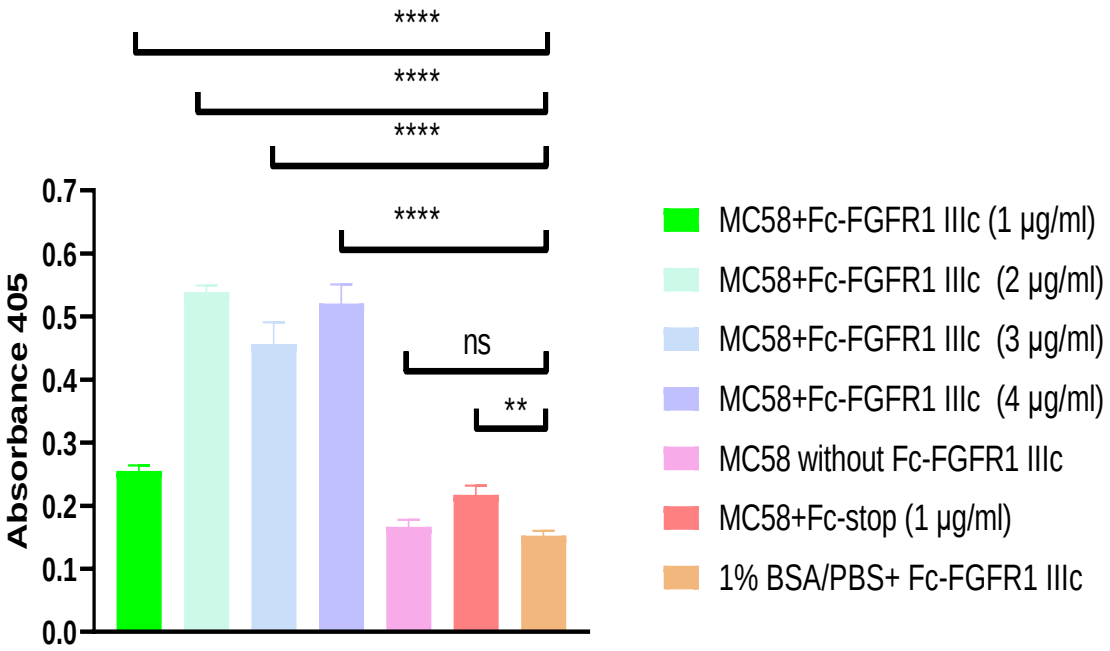

Figure 4.9: *N. meningitidis* interacts directly with the extracellular IIIc domain of FGFR1. Microplate wells were evenly coated with formaldehyde-fixed whole meningococci. Absorbance readings were made after 40 min (based on initial optimisation done by reading the plate every 10 min). Substrate was added and absorbance was measured at 405 nm in a microplate reader (GloMax). These results represent the mean of three independent experiments, each carried out in triplicate and analysed used a one-way ANOVA. The error bars indicate SEM. Direct interaction was detected between the FGFR1 extracellular IIIc domain and *N. meningitidis* (MC58); this interaction was not caused by MC58 interacting with the Fc-tag, because there was a statistically significant difference between bacterial binding to Fc only (** $P \leq 0.01$) and Fc-FGFR1 IIIc (**** $P \leq 0.0001$). In this experiment, different concentrations of Fc-FGFR1 IIIc were screened in order to choose the optimal concentration for binding to MC58. There were statistically significant differences between 1% BSA/PBS+Fc-FGFR1 IIIc and MC58+Fc-FGFR1 IIIc (1 µg ml^{-1}, 2 µg ml^{-1}, 3 µg ml^{-1}, and 4 µg ml^{-1}) **** $P \leq 0.0001$.

4.2.4 Assessment of interaction between mutant *N. meningitidis* strains and Fc-FGFR1 IIIc and Fc-stop by whole-cell ELISA

The aim of this experiment was to compare interactions between FGFR1 IIIc and the following bacterial strains: *N. meningitidis* MC58; MC58Δ*NMB0375-Omega*; MC58Δ*NMB1053-kan;* MC58Δ*NMB0506-kan;* MC58Δ*NMB0088-Omega* and MC58Δ*pilQ/*Δ*porA*, as well as with the commensal species *N. lactamica*.

Microplate wells were homogenously coated with the appropriate formaldehyde-fixed bacterial cell suspension, as before. Following overnight incubation with gentle agitation, the wells were washed three times (PBST), followed by a blocking step (1% BSA/PBS) to reduce nonspecific binding. The wash steps with PBST were repeated, then Fc-FGFR1 IIIc (2 $\mu g\, ml^{-1}$) and Fc-stop (1 $\mu g\, ml^{-1}$) in 1% w/v BSA/PBS were added to the appropriate wells, and the plate incubated at 4°C overnight with gentle agitation. Following this, the wells were washed three times with PBST, then an alkaline phosphatase-conjugated anti-Fc antibody (anti-FC-tag) in 1% BSA/PBS was added followed by overnight incubation at 4°C with gentle agitation. After an additional three PBST washes, colour was finally developed by addition of alkaline phosphatase substrate. A GloMax microplate reader was used for data acquisition, at an absorbance wavelength of 405 nm.

The results, presented in Figure 4.10, showed significantly less binding of *N. lactamica* and MC58Δ*pilQ/*Δ*porA* to Fc-FGFR1 IIIc than for MC58-WT. However, no significant difference was evident for interaction of the mutants lacking *mafA*, *fadL*, *opc5* or *NMB0506* with Fc-FGFR1 IIIc compared to MC58-WT. In addition (Figure 4.11), no significant binding to Fc-stop was observed for *N. lactamica* or any of the different *N. meningitidis* MC58 strains, was evident compared to MC58-WT. Therefore, the results indicated that pure Fc-FGFR1 IIIc still bound to *N. meningitidis* even after knockout of the target genes, which indicates that Fc-FGFR1 IIIc interacts with other outer membrane proteins or that there is considerable redundancy in FGFR1 IIIc ligands with multiple knockouts required in order for a difference in FGFR1 IIIc binding to be discernible. For a more specific assessment of the interactions involved, we decided to purify the

protein products of the four targeted genes in order to evaluate their specific interactions with FGFR1 IIIc in protein–protein interaction experiments.

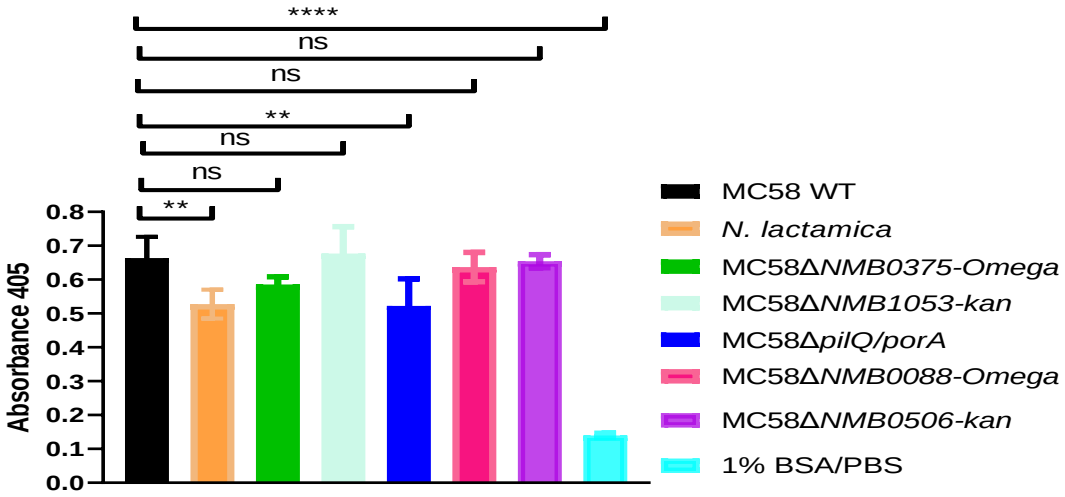

Figure 4.10: ELISA data showing the binding of Fc-FGFR1 IIIc to Neisserial strains. Significantly reduced binding was seen for *N. lactamica* and MC58Δ*pilQ*/Δ*porA* (** $P \leq 0.01$) compared to wild-type MC58, but there was no significant difference between the MafA, FadL, Opc5 and NMB0506 mutants and Fc-FGFR1 IIIc compared to MC58-WT ($p > 0.05$). Absorbance readings were made after 40 min. Substrate was added and absorbance was measured at 405 nm in a microplate reader (GloMax). Experiments were repeated five times, i.e., the values presented are the mean of five independent assays (each performed in triplicate) and used a one-way ANOVA. The error bars indicate SEM.

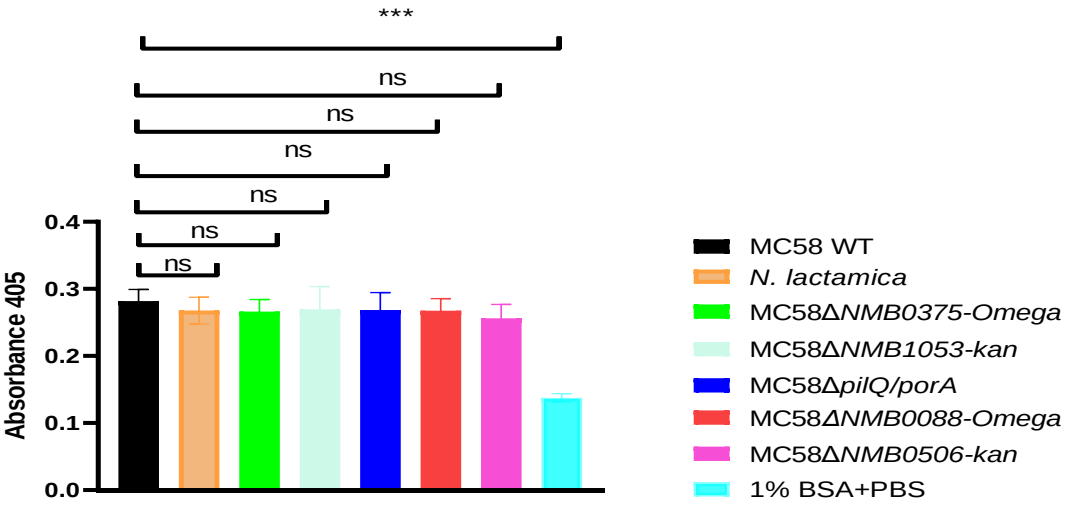

Figure 4.11: ELISA data showing the binding of Fc-stop to Neisserial strains. There was no significant difference between the binding of *N. lactamica* or the different *N. meningitidis* MC58 strains to Fc-stop, compared to binding exhibited by the wild-type MC58 ($p > 0.05$). Absorbance readings were made after 40 min. Substrate was added and absorbance was measured at 405 nm in a microplate reader (GloMax). Experiments were repeated five times, i.e., the values presented are the mean of five independent assays (each performed in triplicate) and used a one-way ANOVA. The error bars indicate SEM.

4.2.5 Cloning of the *mafA*, *opc5* and *fadL* genes into pQE-30

Previously in this study (Figure 3.26 and 3.27), cell adhesion and invasion assays successfully demonstrated interaction between *N. meningitidis* and HBMECs; an interaction that was shown to depend on FGFR1 in earlier work from our group (Azimi, 2014). However, the whole-cell ELISA experiments described above indicated that meningococci still bound to purified recombinant Fc-FGFR1 IIIc even after knockout of the targeted genes, which were proposed to encode bacterial ligands for FGFR1. This encouraged us to express and purify three of the four target proteins for further investigation: MafA, Opc5 and FadL. Unfortunately, there was not enough time available during this project for cloning, expression, and purification of the NMB0506 protein.

According to the SignalP 4.1 prediction tool, the predicted cleavage site for posttranslational removal of the MafA signal peptide is between amino acids 14 and 15 (0.9920 probability). Amplification of the region of *mafA* encoding amino acids 16–313 was therefore targeted, and *BamHI* restriction sites were introduced via overhangs in both the forward and reverse primers to enable cloning of amplicon into the pQE-30 vector. Thus, primers MafAQE30-F and MafAQE30-R were designed for amplification of *mafA* minus its N-terminal signal peptide-encoding region based on the nucleotide sequence of the corresponding open reading frame in the genome of *N. meningitidis* strain MC58 (Table 2.3).

Similarly, the targeted region of FadL consisted of amino acids 26–466 of the protein sequence since N-terminal signal peptide cleavage was predicted to occur between amino acids 24 and 25 in this case (0.9065 probability). Primers FadLPQE30-F and FadLPQE30-R (Table 2.3) were designed for amplification of *fadL* (26–466), as the method used for *mafA.*

The same approach was adopted for *opc5*, in this case targeting amino acids 22–272 for amplification since N-terminal signal peptide cleavage was predicted to occur between amino acids 20 and 21 this time, although with lower confidence

(0.5145 probability). Primers Opc5PQE30-F and Opc5PQE30-R (Table 2.3) were designed to amplify *opc5* (22–272), and introduce *BamHI* sites, as above.

In all cases, chromosomal DNA from *N. meningitidis* strain MC58 was used as the template for PCR reactions, which were carried out. Products of the expected sizes were obtained in all cases: 0.9 kb for *mafA* (Figure 4.12A), 0.76 kb for *opc5* (Figure 4.12B) and 1.3 kb for *fadL* (Figure 4.12C).

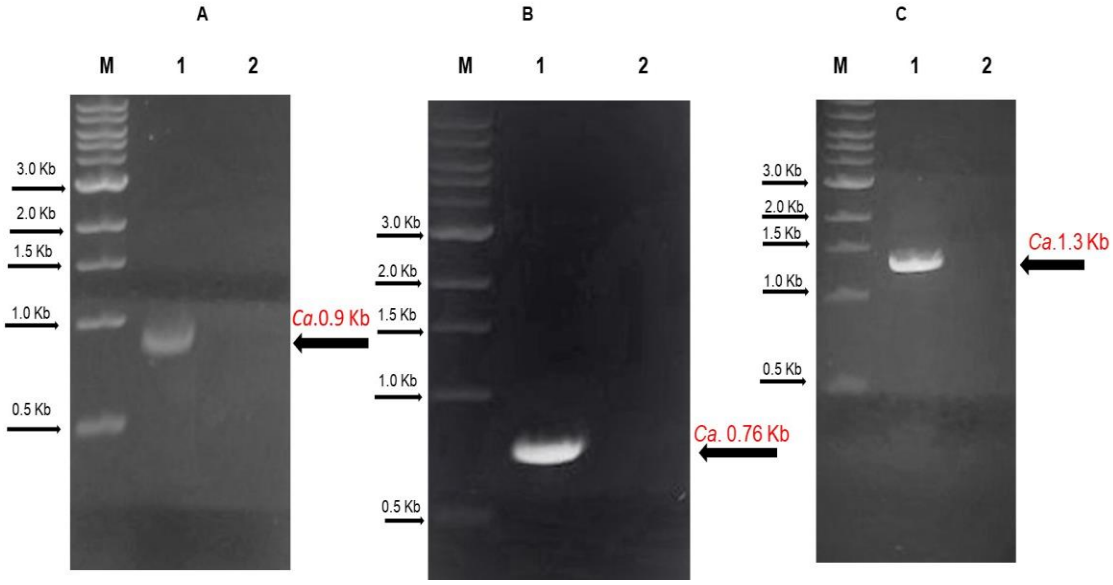

Figure 4.12. Analysis by 1% agarose gel electrophoresis showing PCR amplification of the three targeted genes (*mafA*, *opc5* and *fadL*) from *N. meningitidis* MC58 chromosomal DNA. (A) Lane M: 1 kb DNA ladder; Lane 1: PCR product of *mafA* (0.9 kb amplicon); Lane 2: negative control (no template DNA). (B) Lane M: 1 kb DNA ladder; Lane 1: PCR product of *opc5* (0.76 kb amplicon); Lane 2: negative control. (C) Lane M: 1 kb DNA ladder; Lane 1: PCR product of *fadL* (1.3 kb amplicon); Lane 2: negative control.

After analysing the PCR products by agarose gel electrophoresis to confirm that bands of the expected sizes were present, all three PCR products were purified and digested with *BamHI*. The pQE-30 vector was also *BamHI* digested, then in order to prevent its self-ligation (re-circularisation), it was dephosphorylated before ligation reactions with the inserts.

Ligation products were then used to transform into *E. coli* JM109 and the transformation mixture was aliquoted onto LB agar plates containing ampicillin, which were then incubated at 37°C for 16 h. Plasmid DNA was subsequently

extracted from liquid cultures of the resulting transformants using a DNA plasmid extraction kit for screening.

From the above transformations, seven colonies were screened for successful cloning of *mafA* into pQE-30 vector using *BamHI* digestion. One of the seven contained the expected size of insert (Figure 4.13) and the resultant plasmid construct, pMA5, encodes a His_6-tagged truncated MafA protein starting with the amino acid sequence MRGSHHHHHHGS (encoded by pQE-30), followed by MafA residues 16–313. Similar screening showed that two out of eight colonies contained the *opc5* insert (Figure 4.14) and the resulting construct, pMT5, encodes full-length Opc5, minus the N-terminal signal peptide, together with the same vector-encoded N-terminal His_6-tag as above. For *fadL*, five colonies were screened to confirm successful cloning by the same procedure. The results indicated cloning success for one of the five colonies (Figure 4.15) and giving the resultant plasmid pMR5 that encodes the full-length FadL, minus its N-terminal signal peptide, and preceded by the same vector-encoded His_6-tag sequence as before. Additional expression constructs were made for pMA5, pMT5 and pMR5 in which the N-terminal- signal peptide of each protein was removed. This strategy was suggesting that removal of the signal sequence leads to more efficient protein expression and purification.

For further analysis of correct cloning of the required inserts into pQE-30, one clone was selected for each gene to perform DNA sequencing, and the results were analysed to confirm the presence of the correct sequence and verify the absence of any PCR-generated errors.

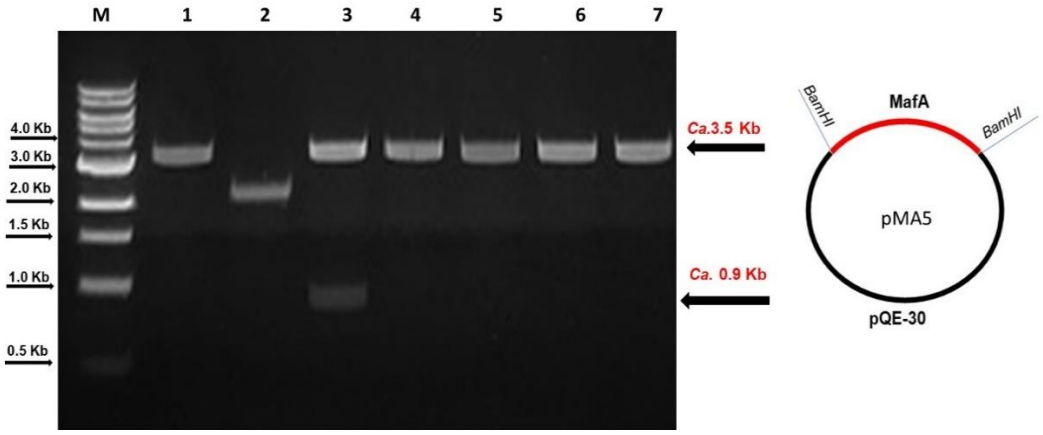

Figure 4.13: 1% agarose gel electrophoresis showing the cloned *mafA* insert in the pQE-30 vector, as verified by restriction digestion with *BamHI*. Lane M: 1 kb DNA ladder; Lanes 1, 4–7: putative *mafA* clones after restriction digest with *BamHI*, showing a band for the pQE-30 vector backbone only but no insert corresponding to the cloned *mafA* gene; Lane 2: no insert corresponding to the cloned *mafA* gene; Lane 3: successful clone showing two bands, corresponding to the vector backbone (3.5 kb) and *mafA* insert (0.9 kb).

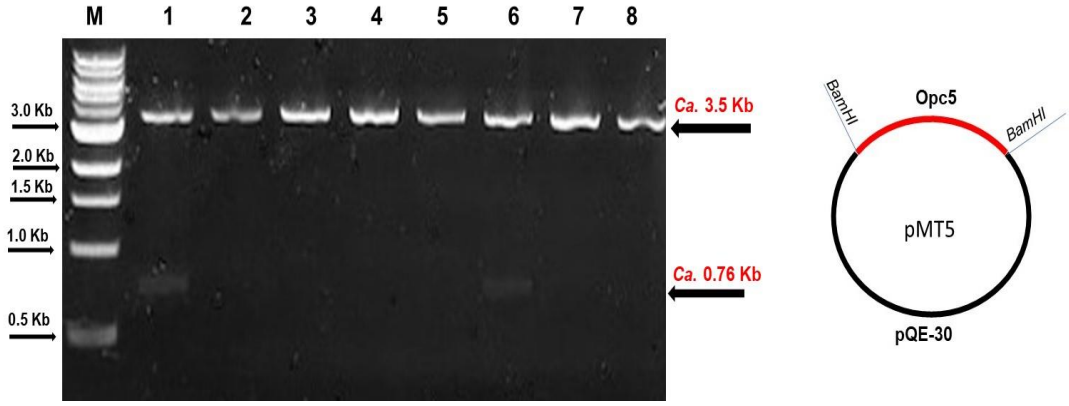

Figure 4.14: 1% agarose gel electrophoresis showing the cloned *opc5* insert in the pQE-30 vector, as verified by restriction digest with *BamHI*. Lane M: 1 kb DNA ladder; Lanes 1 and 6: successful clones, as demonstrated by the presence of two bands corresponding to the pQE-30 vector backbone and *opc5* insert at 3.5 kb and 0.76 kb, respectively; Lanes 2–5,7,8: putative clones lacking the *opc5* insert and containing a band for the pQE-30 vector backbone only.

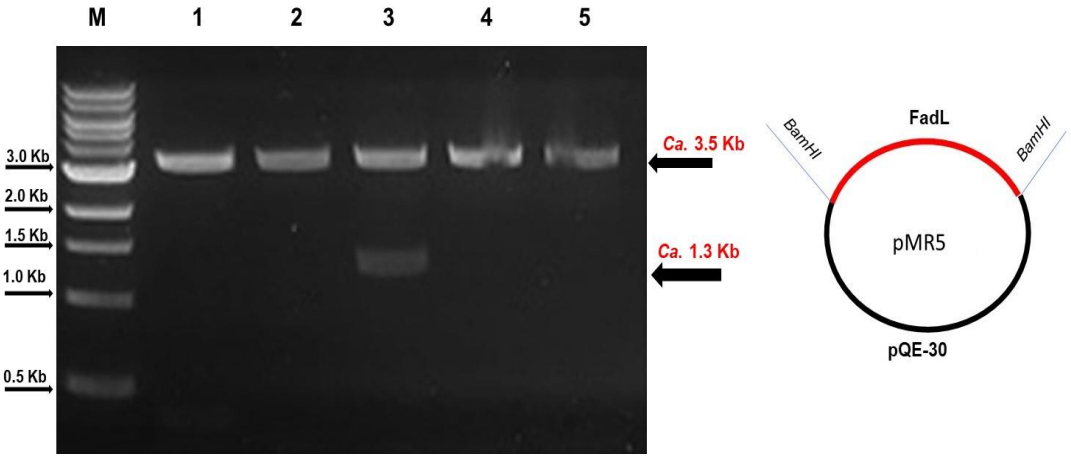

Figure 4.15: 1% agarose gel electrophoresis showing the cloned *fadL* insert in the pQE-30 vector, as verified by restriction digest with *BamHI*. Lane M: 1 kb DNA ladder; Lanes 1,2,4,5: bands corresponding to the pQE-30 vector backbone only; Lane 3: successful clone showing two bands at 3.5 kb (pQE-30 vector backbone) and 1.3 kb (cloned insert from the *fadL* gene).

4.2.6 Small-scale expression of MafA, Opc5 and FadL

Expression of MafA, Opc5 and FadL from pMA5, pMT5 and pMR5, respectively, was evaluated by preparing whole cell lysates extracted from IPTG-induced cultures. These were analysed by SDS-PAGE followed by immunoblotting using monoclonal antibodies raised against the anti-His_6 tag. Expression was initially tested on small scale cultures which were grown at 37°C until exponential phase was reached (OD_{600} = 0.6). Expression from the vectors was induced by adding 1 mM IPTG followed by culturing for a further 4 h, with aliquots removed at hourly intervals. Samples were centrifuged then cell pellets were resuspended in 1× SDS sample buffer.

Samples were then run on 10% SDS–polyacrylamide gels. This revealed expressed protein bands at approximately *ca.* 36 kDa, *ca.* 31 kDa and *ca.* 51 kDa for MafA, Opc5 and FadL, respectively, corresponding to the predicted sizes of the His_6-tagged fusion proteins. Immunoblots with an anti-His_6-tag monoclonal antibody confirmed that the over-expressed bands were His_6-tagged proteins.

For MafA, all of the induced samples (1–4 h) contained good yields of an immunoreactive band at the expected size. These observations indicated that

successful purification of MafA could likely be achieved from large scale cultures, since a good level of protein was identified in the IPTG-induced test cultures.

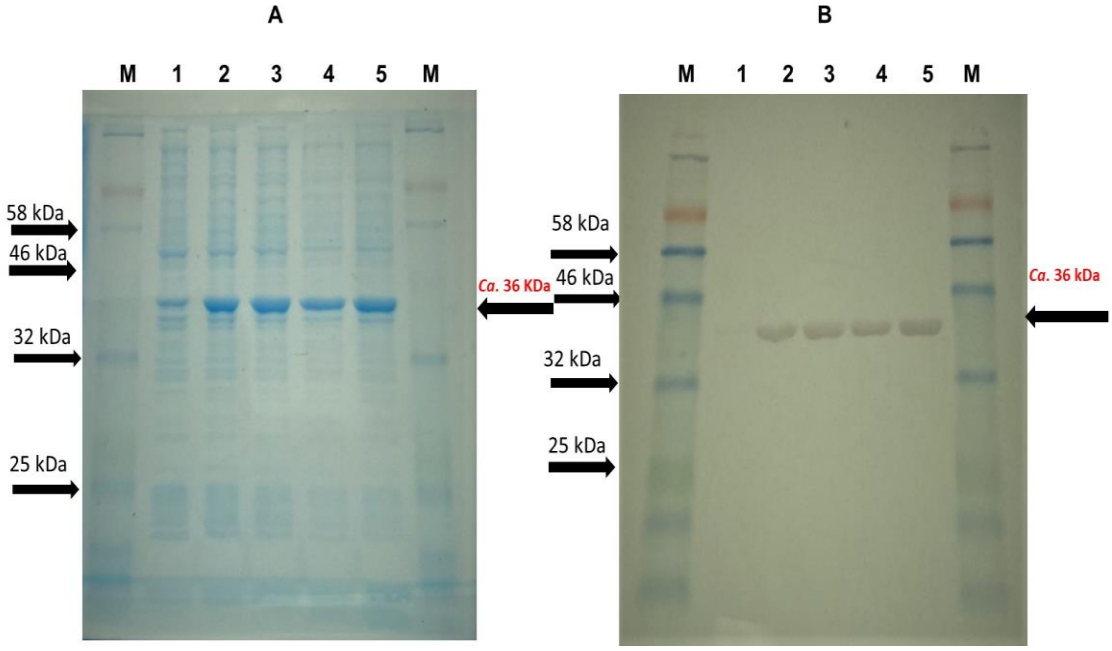

Figure 4.16: SDS–PAGE and immunoblot analysis of the His$_6$-MafA fusion protein expressed from pMA5 on a small scale. (A) 10% SDS–PAGE analysis. (B) Immunoblot assay. Lane M: protein markers; Lane 1: cell lysate of non-induced JM109 (pMA5); Lanes 2–5: whole cell lysates of cultures induced with 1 mM IPTG, incubated at 37°C for 1 h, 2 h, 3 h and 4 h respectively. Lanes B1–B5 were incubated with an anti-His$_6$-tag primary antibody. After washing the membrane and incubating with a secondary antibody (anti-mouse IgG-alkaline phosphatase), and washing again, the blot was developed by adding alkaline phosphatase substrate. The results of both analytical procedures indicated the presence of the expected fusion protein band at *ca.* 36 kDa (His$_6$-MafA) in all IPTG-induced cell lysates.

The results for Opc5 and FadL were less satisfactory, and the expression level of both proteins was very low under these conditions (data not shown). Growing the *E. coli* at a lower temperature (18°C) and culturing for longer post-induction (16 h) failed to improve the results (data not shown).

As an alternative approach, a change of growth medium was explored. The Opc5 and FadL recombinant proteins were expressed in *E. coli* JM109 cultures grown in Terrific Broth (TB) and induced by IPTG for up to 3 h. As before, pre-induction and induced samples were denatured and then analysed by 10 % SDS–PAGE, alongside the same negative control sample described above. This analysis showed bands with an apparent molecular weight of *ca.* 31 kDa for Opc5 and *ca.* 51 kDa for FadL, corresponding to the expected sizes of these His_6-tagged proteins (Figures 4.17 and 4.18, respectively). Immunoblot analysis confirmed that these proteins were his-tagged, with all induced samples showing an immune-reactive band of the expected size, whereas a faint band was observed in the pre-induced samples. Subsequently, applying the same method, Opc5 and FadL were expressed successfully on a larger scale.

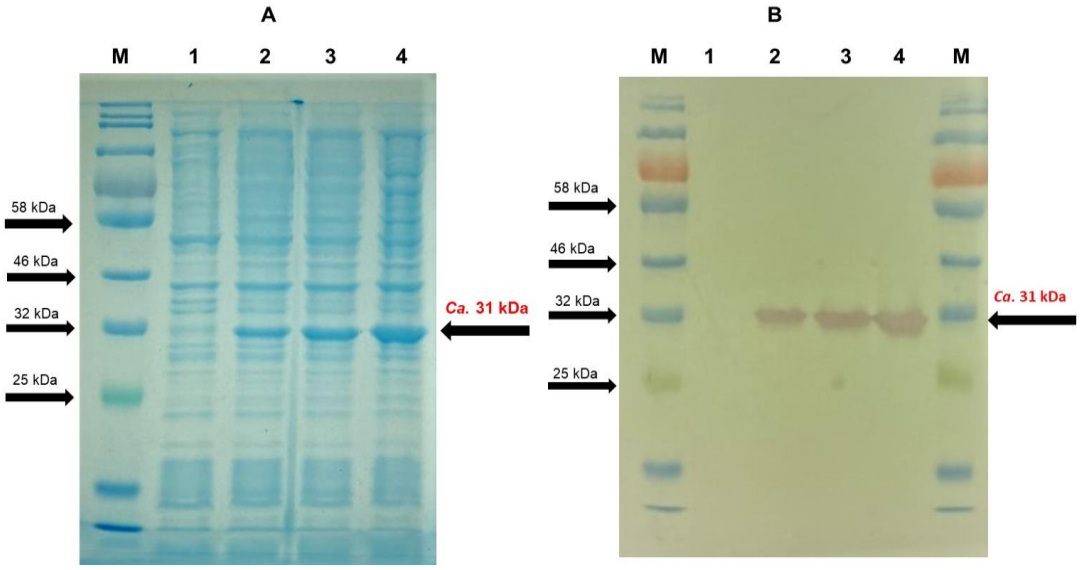

Figure 4.17: SDS–PAGE and immunoblot analysis of the His_6-Opc5 fusion protein expressed from pMT5 on a small scale. (A) 10% SDS–PAGE analysis. (B) Immunoblot assay. Lane M: protein markers; Lane 1: cell lysate of non-induced (pMT5) transformed *E. coli* cultures; Lanes 2–4: whole cell lysates of cultures induced with 1 mM IPTG, incubated at 37°C for 1 h, 2 h and 3 h time points respectively. Lanes B1–B4 were incubated with an anti-His_6-tag primary antibody. After washing the membrane and incubating with a secondary antibody (anti-mouse IgG-alkaline phosphatase), and washing again, the blot was developed by adding alkaline phosphatase substrate. The results of both analytical procedures indicated the presence of the expected fusion protein band at *ca*. 31 kDa (His_6-Opc5) in all IPTG-induced cell lysates.

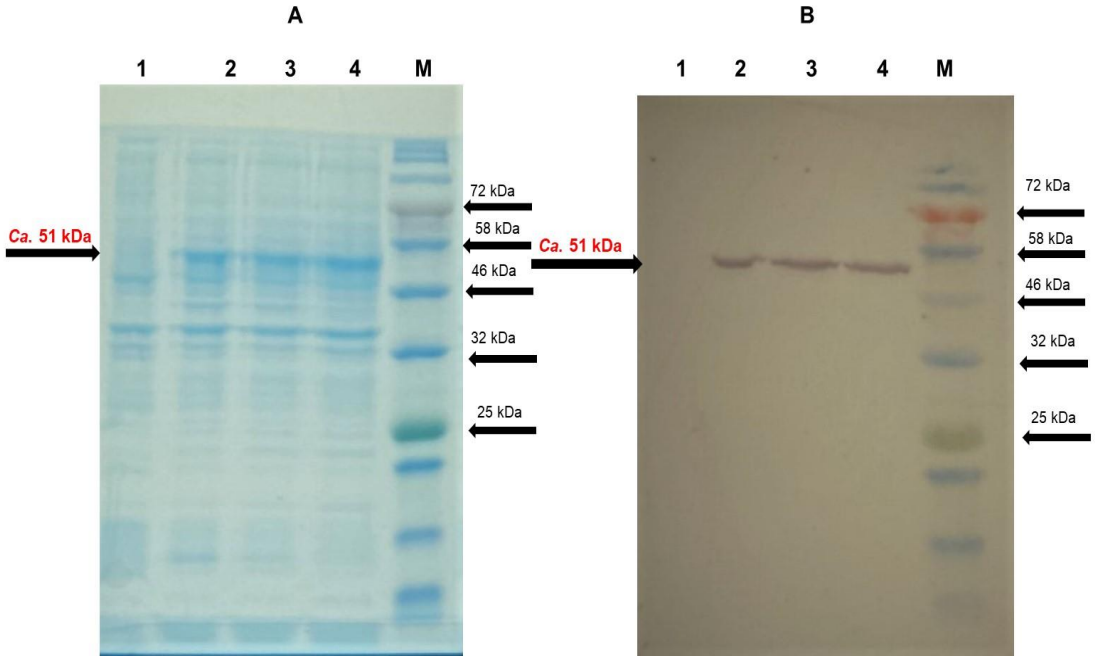

Figure 4.18: SDS–PAGE and immunoblot analysis of the His_6-FadL fusion protein expressed from pMR5 on a small scale. (A) 10% SDS–PAGE analysis. (B) Immunoblot assay. Lane M: protein markers; Lane 1: cell lysate of non-induced (pMR5) transformed *E. coli* cultures; Lanes 2–4: whole cell lysates of cultures induced with 1 mM IPTG, incubated at 37°C for 1 h, 2 h and 3 h time points respectively. Lanes B1–B4 were incubated with an anti-His_6-tag primary antibody. After washing the membrane and incubating with a secondary antibody (anti-mouse IgG-alkaline phosphatase), and washing again, the blot was developed by adding alkaline phosphatase substrate. The results of both analytical procedures indicated the presence of the expected fusion protein band at *ca*. 51 kDa (His_6-FadL) in all IPTG-induced cell lysates.

4.2.7 Large scale expression of His6-MafA

After confirming expression on a small scale, MafA was expressed from the pMA5 construct on a larger scale to obtain material for protein purification. Protein content of the cell lysate was confirmed by SDS–PAGE followed by immunoblotting using an anti-His_6-tag monoclonal antibody as shown in Figure 4.19, as before.

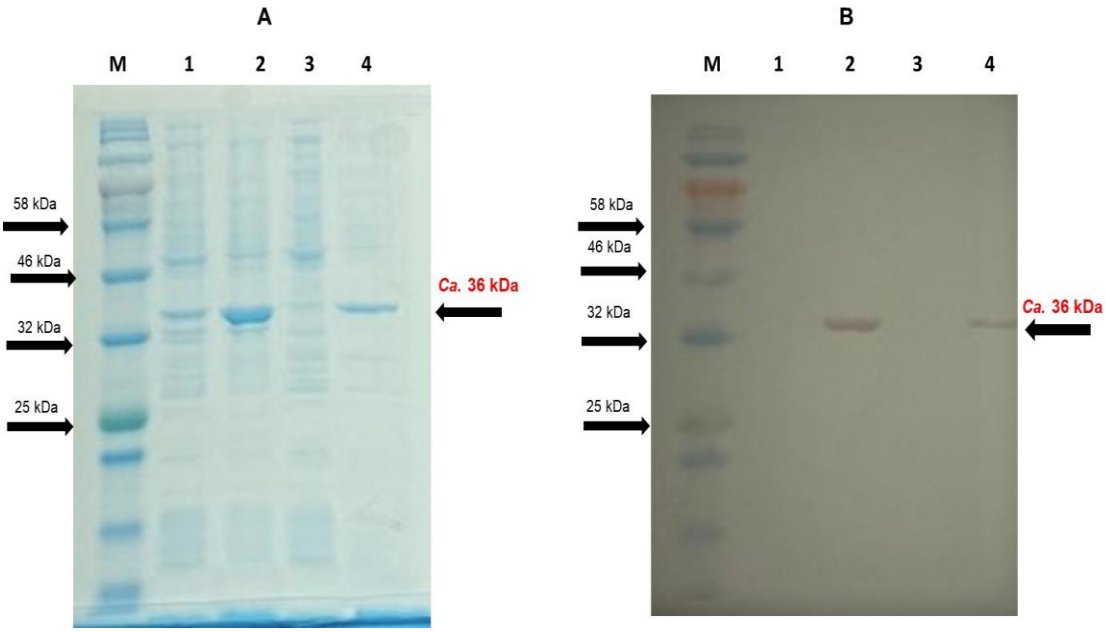

Figure 4.19: SDS–PAGE and immunoblot assay of the His_6-MafA fusion protein expressed from pMA5 on a large scale. (A) 10% SDS-PAGE analysis. (B) Immunoblot assay. Lane M: protein markers; Lane 1: cell lysate of non-induced pMA5 transformed *E. coli* culture (on a small scale); Lane 2: whole cell lysate of culture induced with 1 mM IPTG (on a small scale); Lane 3: cell lysate from large-scale culture of non-induced pMA5 transformed *E. coli*; Lane 4: cell lysate from large-scale culture induced with 1 mM IPTG and incubated at 37°C for 3 h. Lanes B1–B4 were incubated with an anti-His_6-tag primary antibody. After washing the membrane and incubating with a secondary antibody (anti-mouse IgG-alkaline phosphatase), and washing again, the blot was developed by adding alkaline phosphatase substrate. The two analytical procedures confirmed expression of the expected *ca.* 36 kDa fusion protein in induced cultures of *E. coli* transformed with the pMA5 plasmid.

4.2.7.1 Purification of MafA under native conditions

Cells harvested from 500 mL of *E. coli* IPTG-induced culture were resuspended in lysis buffer, sonicated on ice, then the lysate clarified by centrifugation. The supernatant (cleared lysate) was then loaded onto a 5 mL HisTrap FF Crude column using an ÄKTA Prime Plus FPLC system pre-washed with a low imidazole buffer. During sample application, the flow through was collected, and the column was then washed to remove loosely-bound proteins. Elution of the strongly-bound His_6-tagged protein was then carried out with elution buffer (high concentration of imidazole), using an elution gradient that was monitored via the chromatogram. Eluted fractions were stored at 4°C for further analysis was carried out before subsequent concentration and desalting. Samples taken during the purification process were analysed by SDS–PAGE and immunoblot analysis. Only MafA was purified by this method (Figures 4.20 and 4.21).

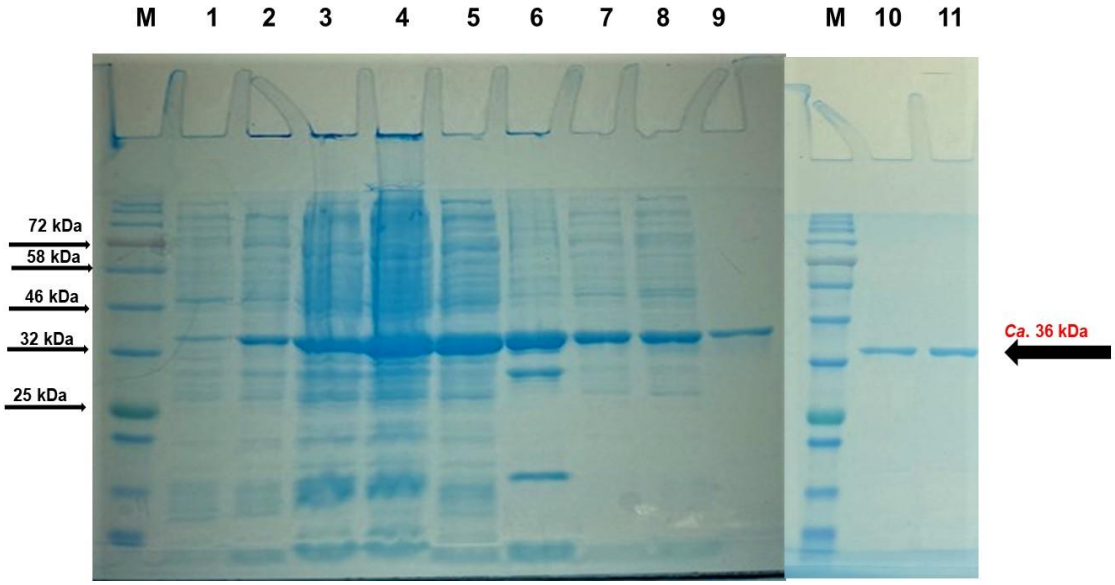

Figure 4.20: 10% SDS–PAGE analysis of IMAC purification of MafA. Lane M: pre-stained protein markers; Lane 1: control lysate (non-induced cells); Lane 2: cell lysate of culture induced with 1 mM IPTG, incubated at 37°C for 3 h; Lane 3: cell pellets after resuspension in lysis buffer and before sonication; Lane 4: cell pellets after sonication; Lane 5: after centrifugation at 10,000 × *g* and 0.22 µm filtration, soluble proteins (clarified lysate); Lane 6: sample after centrifugation at 10,000 × *g* (pellet); Lane 7: protein that precipitated in the Falcon tube and was not loaded onto the IMAC column; Lane 8: flow-through from IMAC column loading step; Lanes 9–11: eluted fractions number 5, 6 and 7, respectively.

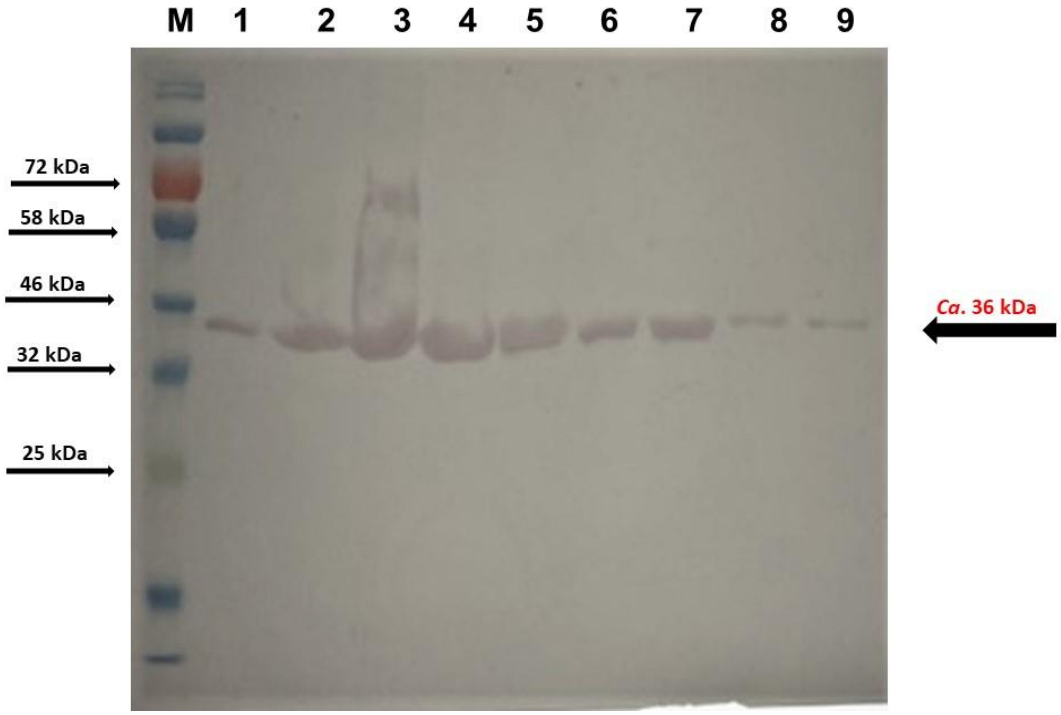

Figure 4.21: Immunoblot analysis of IMAC purification of MafA. Lane M: pre-stained protein markers; Lane 1: cell lysate of culture induced with 1 mM IPTG, incubated at 37°C for 3 h; Lane 2: cell pellets after resuspended in lysis buffer and before sonication; Lane 3: cell pellets after sonication for 10 min (20 s on/off) on ice, Lane 4: after centrifugation and 0.22 μm filtration, soluble proteins (clarified lysate) that were passed onto the IMAC column; Lane 5: sample after centrifugation at 10,000 × *g* (pellet); Lane 6: protein that precipitated in the Falcon tube and was not loaded on the IMAC column; Lane 7: flow-through from IMAC column loading step; Lanes 8, 9: eluted fractions number 5 and 6, respectively. Lanes 1–9 were then incubated with an anti-His6-tag primary antibody. After washing the membrane and incubating with a secondary antibody (anti-mouse IgG-alkaline phosphatase), and washing again, the blot was developed by adding alkaline phosphatase substrate.

4.2.7.2 Concentration and desalting of MafA

Fractions (F5, F6 and F7) containing the highest amounts of pure MafA protein were concentrated by centrifugation and dialysed to yield the final purified His_6-MafA protein as shown in Figure 4.22. The protein content was quantified using a UV absorbance (A_{280}) using a NanoDrop instrument, and the concentration of the final protein preparation was determined to be 0.24 mg/mL. The protein was aliquoted and stored at -80°C until further use. After purifying and desalting MafA, this was used to evaluate protein-protein interactions by ELISA.

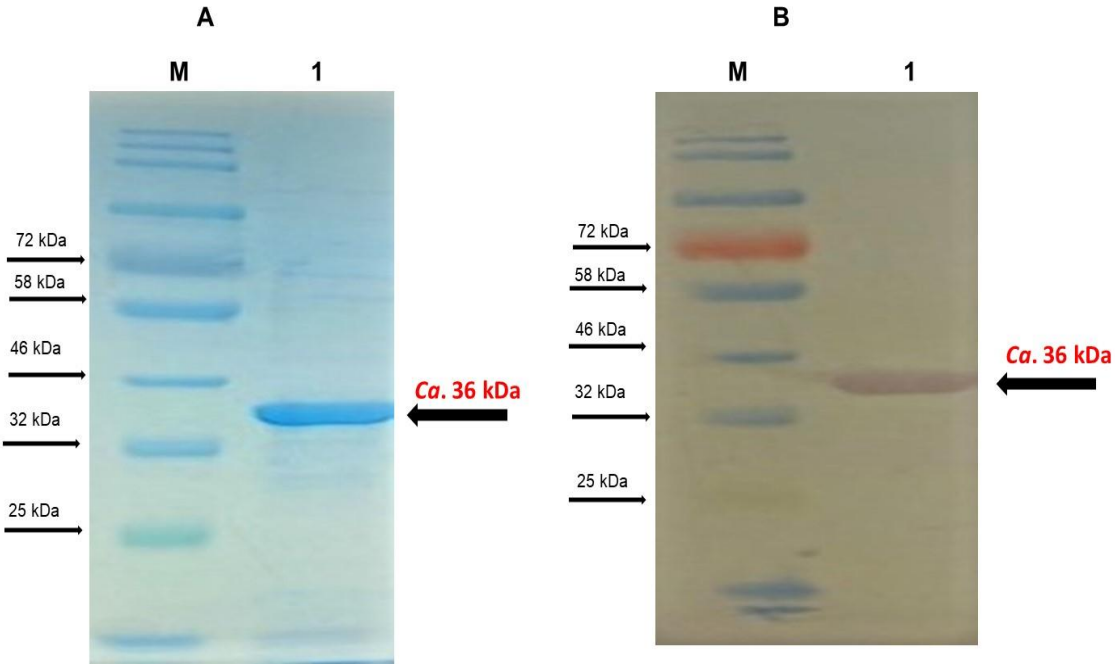

Figured 4.22: SDS–PAGE and immunoblot analysis of His_6-MafA after concentration and desalting. (A) 10% SDS–PAGE analysis. (B) Immunoblot assay with an anti-His6-tag primary antibody. Lane M: protein markers; Lane 1: MafA after concentration, before dialysis. A desalting step (dialysis) was then performed to exchange the high-imidazole buffer with PBS, containing 20% glycerol (for protein stability). Finally, the protein was concentrated and stored at -80°C until further use.

4.2.8 Large scale expression of Opc5 and FadL

Following the confirmation of expression on a small scale (Section 4.2.6), Opc5 and FadL were expressed from the pMT5 and pMR5 plasmids, respectively, on a large scale in an attempt to provide sufficient quantities for protein purification. As was the case for MafA, cell lysates were prepared and analysed by SDS–PAGE, protein staining followed by immunoblotting using anti-His_6-tag monoclonal antibodies, as shown in Figures 4.23 and 4.24 for Opc5 and FadL, respectively. In both cases, a band was seen that indicated the presence of the expressed protein at the expected molecular weight (*ca.* 31 kDa for Opc5 and *ca.* 51 kDa for FadL, respectively), in the lysates of induced cells transformed with plasmids pMT5 (for Opc5) and pMR5 (for FadL). These results suggested that the two proteins could be purified by the same method as MafA (expressed from pMA5).

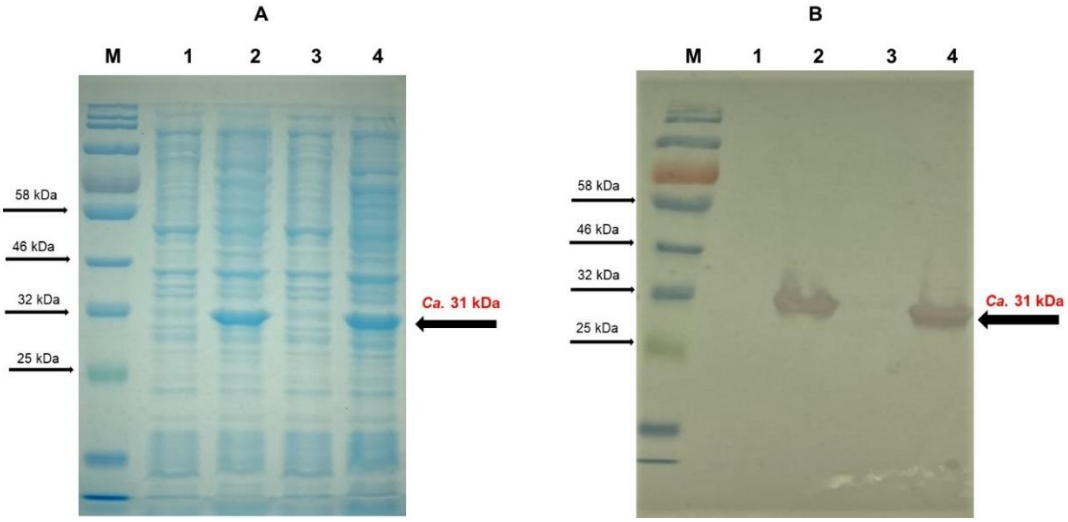

Figure 4.23: SDS–PAGE and immunoblot assay of the His_6-Opc5 fusion protein expressed on a large scale. (A) 10% SDS-PAGE analysis. (B) Immunoblot assay. Lane M: protein markers; Lane 1: cell lysate of small-scale, non-induced pMT5 transformed *E. coli* culture pre-incubated at 37°C for 2 h; Lane 2: cell lysate of small-scale culture induced with 1 mM IPTG, incubated at 37°C for 3 h; Lane 3: cell lysate of large-scale, non-induced pMT5 transformed *E. coli*; Lane 4: cell lysate of large-scale cultures induced with 1 mM IPTG, incubated at 37°C for 3 h. Lanes B1–B4 were incubated with an anti-His_6-tag primary antibody. After washing the membrane and incubating with a secondary antibody (anti-mouse IgG-alkaline phosphatase), and washing again, the blot was developed by adding alkaline phosphatase substrate. The results of both analytical procedures indicated the presence of the presumed *ca.* 31 kDa band corresponding to His_6-Opc5 in all lysates of induced cells transformed with the pMT5 plasmid.

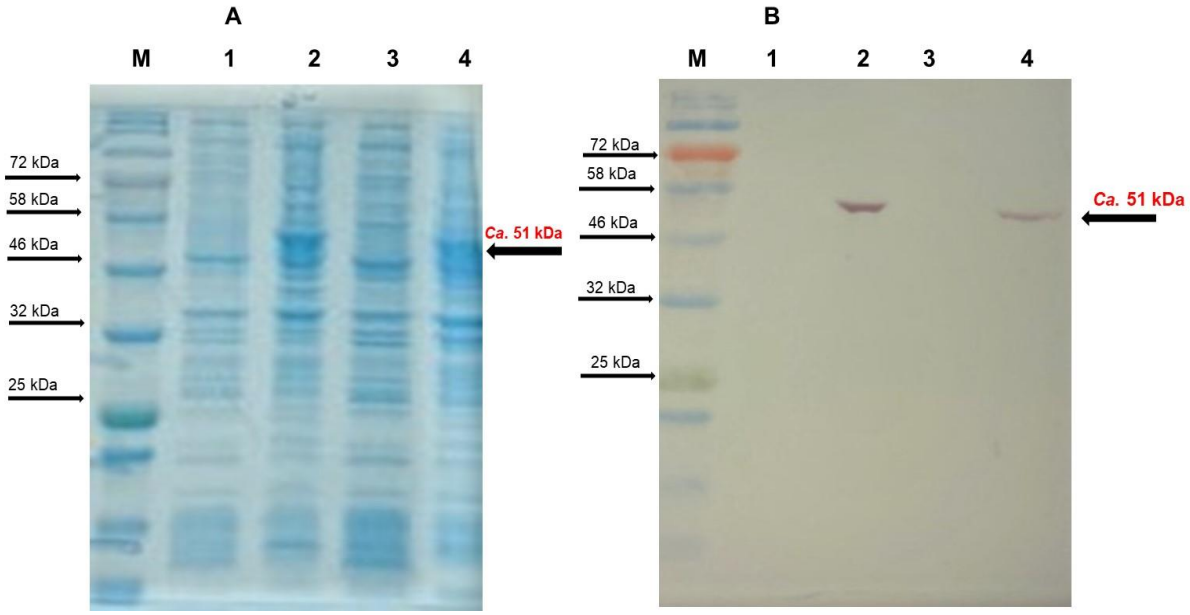

Figure 4.24: SDS–PAGE and immunoblot assay of the His_6-FadL fusion protein expressed on a large scale. (A) 10% SDS-PAGE analysis. (B) Immunoblot assay. Lane M: protein markers; Lane 1: cell lysate of small-scale, non-induced pMR5 transformed *E. coli* culture pre-incubated at 37°C for 2 h; Lane 2: cell lysates of small-scale culture induced with 1 mM IPTG, incubated at 37°C for 3 h; Lane 3: cell lysate of large-scale, non-induced pMR5 transformed *E. coli*; Lane 4: cell lysate of large-scale cultures induced with 1 mM IPTG, incubated at 37°C for 3 h. Lanes B1–B4 were incubated with an anti-His_6-tag primary antibody. After washing the membrane and incubating with a secondary antibody (anti-mouse IgG-alkaline phosphatase), and washing again, the blot was developed by adding alkaline phosphatase substrate. Both analytical procedures confirmed the presence of the presumed *ca.* 51 kDa molecular weight band corresponding to His_6-FadL in lysates of induced cells transformed with the pMR5 plasmid.

4.2.8.1 Purification of Opc5 and FadL under native conditions

Cells harvested from 500 mL of induced culture were resuspended in lysis buffer, sonicated on ice, then the lysate was clarified by centrifugation. In both cases (Opc5 and FadL), the protein was found mainly in the insoluble pellet. Attempts were made to solubilise these recombinant proteins using Triton X-100 with extraction by disruption of the pellets. For both Opc5 and FadL, fractions were collected separately and analysed by SDS–PAGE and protein staining, or immunoblotting using anti-His6-tag monoclonal antibodies, but the solubilising attempts proved unsuccessful for both Opc5 (Figures 4.25 and 4.26) and FadL (Figures 4.27 and 4.28). The corresponding protein band was detected strongly in the insoluble fraction, whereas only a weak band was present in the soluble fraction. Thus, it seemed apparent that the Opc5 and FadL proteins were expressed mostly in an insoluble form which would prevent purification.

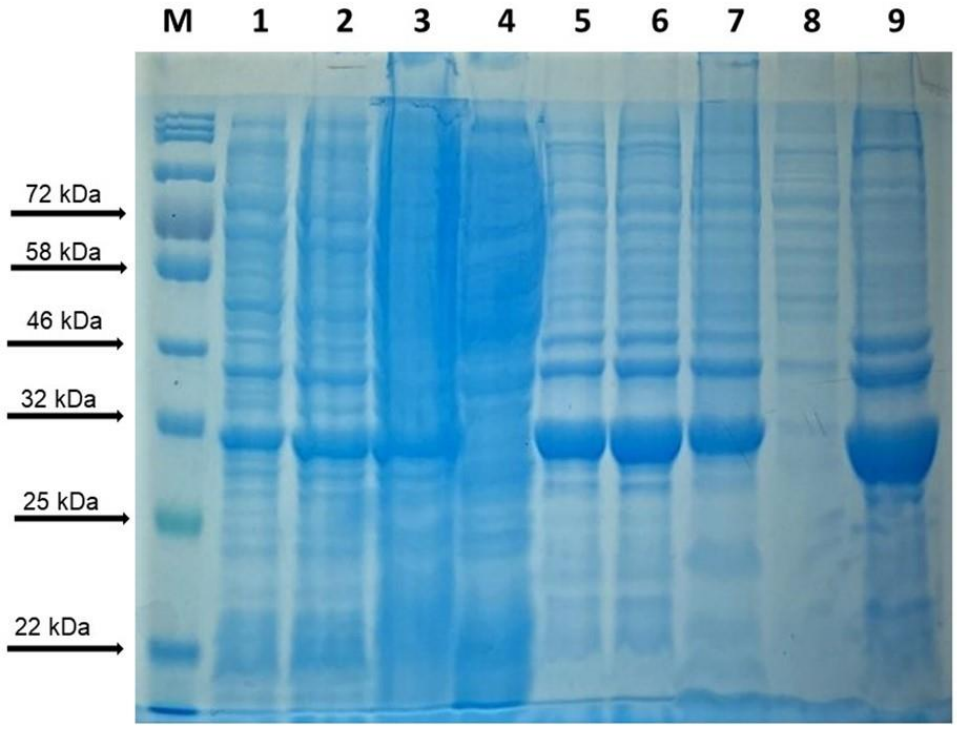

Figure 4.25: Purification of Opc5 from a cell pellet of IPTG-induced *E. coli* JM109 containing pMT5. 10% SDS–PAGE analysis. Lane M: pre-stained protein markers; Lane 1: cell lysate of culture induced with 1 mM IPTG, incubated at 37°C for 3 h (large scale); Lane 2: cell pellets after centrifugation at 4,500 × *g* for 15 min at 4°C and then resuspended in 5 mL of lysis buffer, but before sonication; Lane 3: cell pellets after sonication for 10 min (20 s on/off) on ice; Lane 4: after centrifugation at 10,000 × *g* (insoluble); Lane 5: pellet after centrifugation at 10,000 × *g*; Lane 6: pellet in 5 mL of lysis buffer again and after additional sonication for 10 min (20 s on/off) on ice; Lane 7: sample after 1 h incubation with 0.05% (v/v) Triton X-100 at room temperature; Lane 8: supernatant after centrifugation again at 10,000 × *g* for 30 min at 4°C; Lane 9: sample after centrifugation at 10,000 × *g* (pellet).

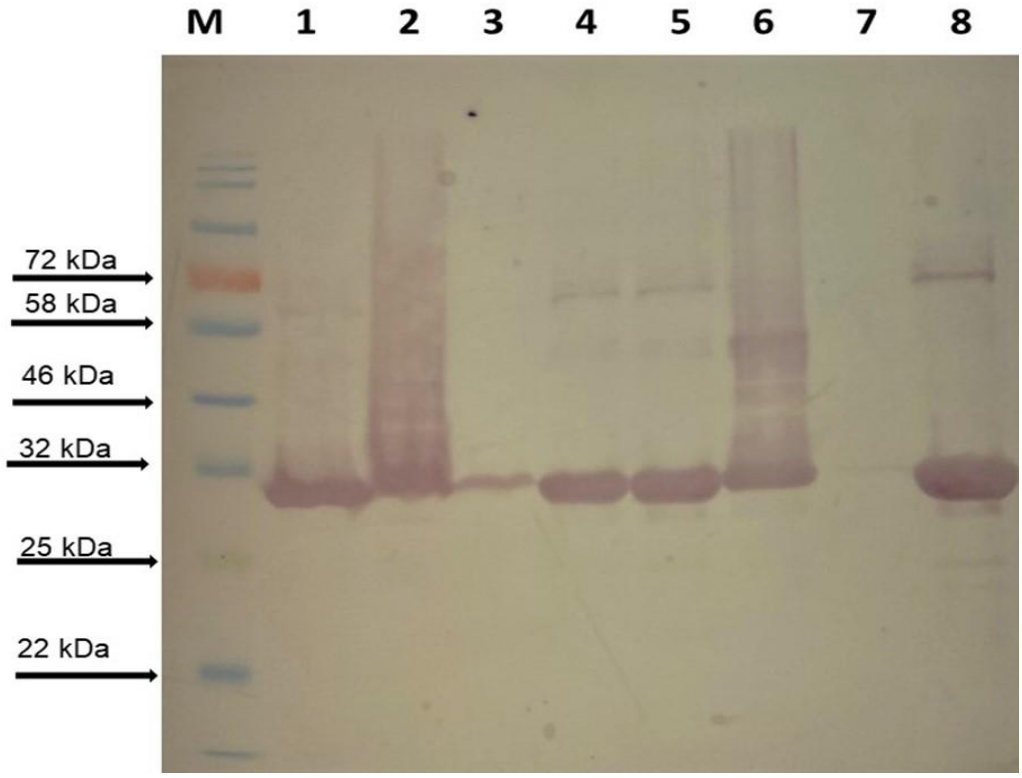

Figure 4.26: Purification of Opc5 from a cell pellet of IPTG-induced *E. coli* JM109 containing pMT5. Western blotting. Lane M: pre-stained protein markers; Lane 1: cell lysate of cultures induced with 1 mM IPTG, incubated at 37°C for 3 h, and after resuspended in 5 mL of lysis buffer and before sonication; Lane 2: sample after sonication for 10 min (20 s on/off) on ice; Lane 3: supernatant after centrifugation at 10,000 × *g* for 30 min at 4°C; Lane 4: pellet after centrifugation at 10,000 × *g*; Lane 5: pellet in 5 mL of lysis buffer and after additional sonication for 10 min (20 s on/off) on ice; Lane 6: sample after 1 h incubation with 0.05% (v/v) Triton X-100; Lane 7: supernatant after centrifugation again at 10,000 × *g* for 30 min at 4°C; Lane 8: pellet after centrifugation at 10,000 × *g*. Lanes 1–9 were incubated with an anti-His6-tag primary antibody. After washing the membrane and incubating with a secondary antibody (anti-mouse IgG-alkaline phosphatase), and washing again, the blot was developed by adding alkaline phosphatase substrate.

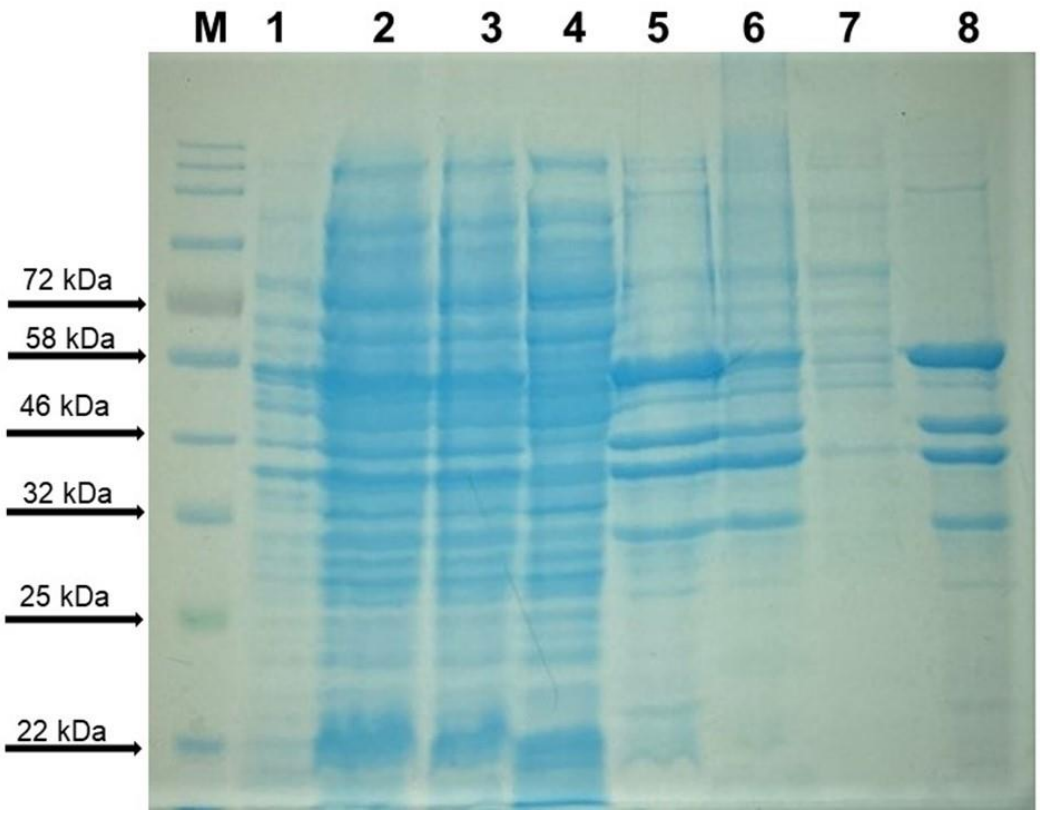

Figure 4.27: Purification of FadL from a cell pellet harvested from IPTG-induced *E. coli* JM109 containing pMR5. 10% SDS–PAGE analysis. Lane M: pre-stained protein markers; Lane 1: cell lysate of cultures induced with 1 mM IPTG, incubated at 37°C for 3 h, cell pellets harvested by centrifugation at 4,500 × *g* for 15 min at 4°C and then resuspended in 5 mL of lysis buffer before sonication; Lane 2: cell pellet after sonication for 10 min (20 s on/off) on ice; Lane 3: pellet after centrifugation at 10,000 × *g*; Lane 4: after centrifugation at 10,000 × *g* (insoluble); Lane 5: pellet in 5 mL of lysis buffer and after further sonication for 10 min (20 s on/off) on ice; Lane 6: sample after 1 h incubation with 0.05% (v/v) Triton X-100; Lane 7: supernatant after centrifugation at 10,000 × *g* for 30 min at 4°C; Lane 8: pellet after centrifugation at 10,000 × *g*.

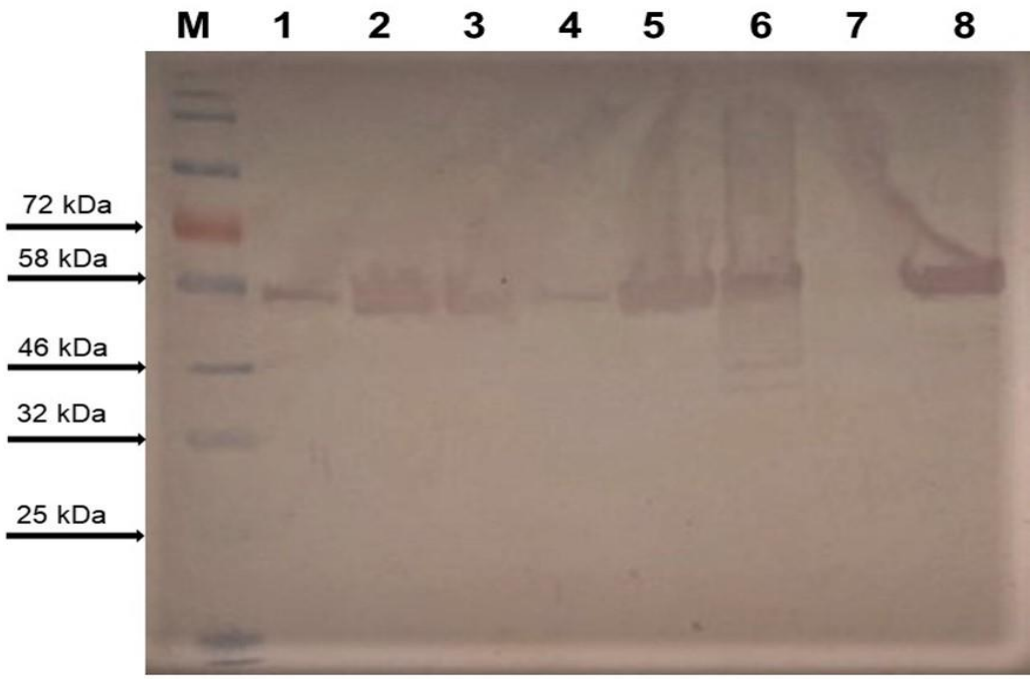

Figure 4.28: Purification of FadL from a cell pellet harvested from IPTG-induced *E. coli* JM109 containing pMR5. Western blotting. Lane M: pre-stained protein markers; Lane 1: cell lysate of cultures induced with 1 mM IPTG, incubated at 37°C for 3 h, cell pellets harvested by centrifugation at 4,500 × g for 15 min at 4°C and then resuspended in 5 mL of lysis buffer before sonication; Lane 2: cell pellet after sonication for 10 min (20 s on/off) on ice; 3: pellet after centrifugation at 10,000 × *g*; Lane 4: after centrifugation at 10,000 × *g* (insoluble); Lane; Lane 5: pellet in 5 mL of lysis buffer and after further sonication for 10 min (20 s on/off) on ice; Lane 6: sample after 1 h incubation with 0.05% (v/v) Triton X-100; Lane 7: supernatant after centrifugation at 10,000 × *g* for 30 min at 4°C; Lane 8: pellet after centrifugation at 10,000 × *g*. Lanes 1–9 were incubated with an anti-His6-tag primary antibody. After washing the membrane and incubating with a secondary antibody (anti-mouse IgG-alkaline phosphatase), and washing again, the blot was developed by adding alkaline phosphatase substrate.

In summary, expression of recombinant His_6-tagged MafA in *E. coli* proved straightforward, and the protein was successfully obtained in pure form after a single affinity (IMAC) purification step. In contrast, Opc5 and FadL were not readily expressed in soluble form and were instead found in inclusion bodies, from which attempts to solubilise them proved unsuccessful. Due to the time constraints of the present project, further work to optimise the solubilisation of Opc5 and FadL was not possible, and purification of these recombinant proteins could therefore not be achieved as part of this study.

4.2.9 Identification of interaction between whole cell lysates of MafA, Opc5 and FadL and Fc-FGFR1 IIIc and Fc-stop by far-western blotting

As targets, whole cell lysates of *E. coli* were used that had been transformed with the protein expression constructs pMA5 (MafA), pMT5 (Opc5) and pMR5 (FadL) and induced with IPTG. As bait, the purified mammalian proteins Fc-FGFR1 IIIc and Fc-stop were used, both of which contained Fc-tags. It was important to ensure sufficient quantities of target bacterial proteins in crude lysates (10–100 μg) and in purified form in the case of MafA (0.2–1 μg) and of the purified recombinant bait proteins (1–10 μg). To meet these criteria, approximately 20 μg/mL was used for cell lysates and 2 μg/mL for purified proteins. Samples were loaded into the gel wells, along with negative control. A protein ladder was also used. After separation by SDS–PAGE, proteins were transferred to a nitrocellulose membrane, denatured in (denaturing and renaturing buffer) containing 6 M guanidine–HCl at room temperature for 30 min, and renatured by slowly decreasing the guanidine–HCl concentration. The membrane was incubated with denaturing and renaturing buffer containing 3 M, 1 M then 0.1 M guanidine–HCl for 30 min at room temperature for each concentration respectively, and finally with denaturing and renaturing buffer containing no guanidine–HCl at 4°C overnight.

Membrane blocking was performed with 5% skimmed milk powder in PBST overnight at 4°C. Next day, the membrane was incubated with purified bait protein (Fc-FGFR1 IIIc) (2 $\mu g\ ml^{-1}$), and Fc-stop as a negative control (2 $\mu g\ ml^{-1}$), in protein-binding buffer overnight at 4°C. The membrane was washed with PBST to remove unbound bait proteins and the blot was incubated with the appropriate antibody: anti-Fc-tag secondary antibody to detect bait proteins. Next, the membrane was washed with PBST then incubated with anti-goat IgG (alkaline phosphatase conjugate, in 5% skimmed milk in PBST). After additional PBST washes, detection of the bound bait proteins was performed using alkaline phosphatase substrate with imaging as before.

The results, presented in Figure 4.29, showed that lysates of *E. coli* overexpressing MafA, Opc5 and FadL were successfully separated by SDS–PAGE and the proteins

transferred onto nitrocellulose membrane. Bands for all three of the overexpressed proteins were seen at the correct sizes. MafA might interact with Fc-FGFR1 IIIc, because a far-western band was detected at the expected size of MafA that was not detected for the negative control, as shown in Figure 4.30A. Thus, an interaction was successfully observed since Fc-FGFR1 IIIc was detected in a band at the molecular weight of MafA, not the Fc-FGFR1 IIIc protein, and in the case of no interaction, a band would not be observed.

However, *E. coli* overexpression lysates allowed us to probe the interaction of Opc5 and FadL with pure Fc-FGFR1 IIIc as an alternative to using the purified proteins, which were not obtained successfully as explained above. Their interaction with pure Fc-FGFR1 IIIc was therefore assessed by far-western blotting, as well as comparing MafA in lysate form, and using lysate from *E. coli* transformed with empty vector (pQE-30 without insert) as a negative control. The results indicated no apparent interaction between Fc-FGFR1 IIIc and Opc5 or FadL, since no far-western band was observed and the result for both proteins was the same as for the negative control (results not shown).

In addition, a similar far-western blotting experiment was carried out using cell lysates from *N. meningitidis* MC58 and the *mafA* mutant strain (MC58Δ*NMB0375-Omega*), following the same procedure, to look for interaction of pure Fc-FGFR1 IIIc with MafA in meningococci. It was expected that a difference would be seen between MC58-WT and the *mafA* mutant, due to knockout of the gene. The results (Figure 4.30B) did not show an interaction between pure Fc-FGFR1 IIIc and MafA in *N. meningitidis* MC58 cell lysate, because no band corresponding to the molecular weight of MafA was seen. However, a band was seen at higher molecular weight, and the cell lysate of the *mafA* mutant strain (MC58Δ*NMB0375-Omega*) also gave a band, therefore, no difference was thus observed between lysates of *N. meningitidis* MC58 and the *mafA* mutant strain (MC58Δ*NMB0375-Omega)*, in terms of interaction with purified Fc-FGFR1 IIIc.

To confirm the observed interaction was with FGFR1 IIIc and not the Fc-tag, the experiment was repeated as above, but with purified Fc-stop added instead of Fc-

FGFR1 IIIc. No interaction was observed between Fc-stop and MafA, as shown in Figure 4.31A. Also, the results indicated no interaction between cell lysates of *N. meningitidis* MC58 and the *mafA* mutant strain (MC58Δ*NMB0375-Omega*) and Fc-stop, as shown in Figure 4.31B. In the case of interaction between Fc-stop and MafA, a band would be detected located according to the molecular weight of MafA, but an interaction between them was not present and no interaction band was observed.

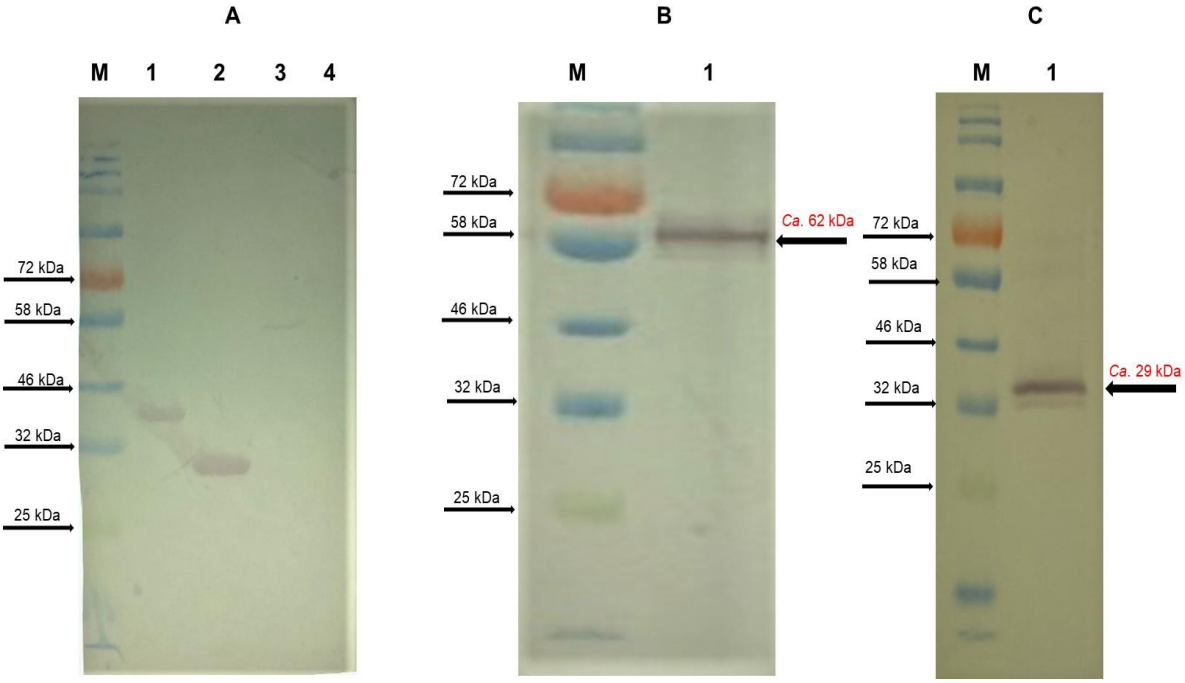

Figure 4.29: Western blotting showing whole cell lysates of transformed *E. coli* (overexpressing MafA, Opc5 or FadL) and purified Fc-FGFR1 IIIc and Fc-stop. Lane M: protein markers; Lane A1: whole cell lysate of pMA5 (MafA) transformed *E. coli*; Lane A2: pMT5 (Opc5) transformed cells, Lane A3: pMR5 (FadL) transformed cells; Lane A4: *E. coli* transformed with empty vector (pQE-30 without insert) as a negative control; Lane B1: Fc-FGFR1 IIIc; Lane C1: Fc-stop. Lysates of *E. coli* overexpressing MafA, Opc5, FadL, Fc-FGFR1 IIIc and Fc-stop were separated by SDS–PAGE and proteins transferred onto nitrocellulose membrane. Proteins were denatured and renatured on the membrane. Lanes A1–A4 were then incubated with an anti-His_6-tag primary antibody, whereas lanes B1 and C1 were incubated with an anti-Fc-tag antibody. After washing the membrane and incubating with a secondary antibody (anti-mouse for lanes A1–A4 and anti-goat for lanes B1 and C1), and washing again, the blot was developed by adding alkaline phosphatase substrate.

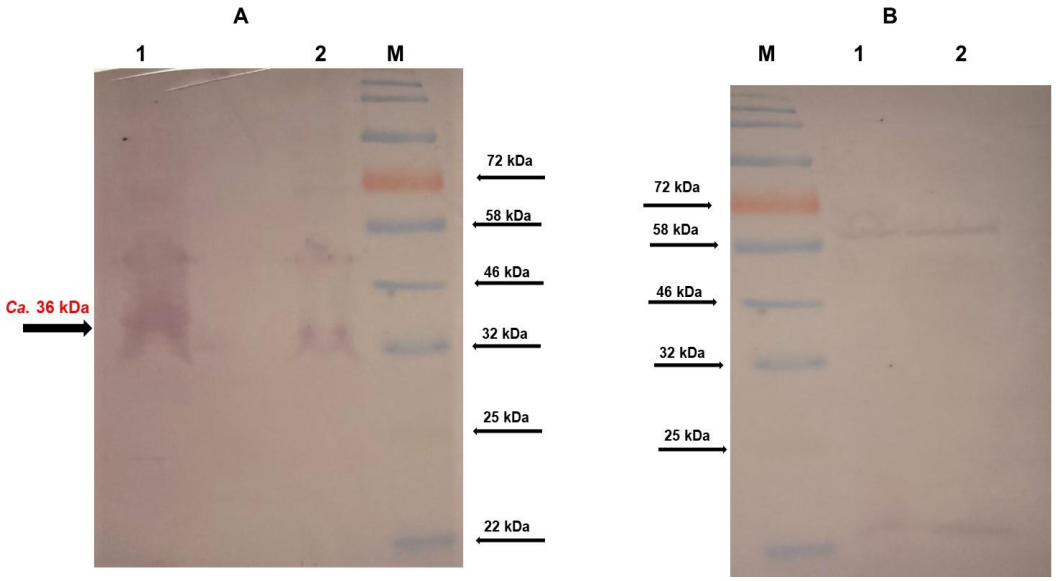

Figure 4.30: Far-Western blotting showing interaction of whole cell lysates (pMA5) with Fc-FGFR1 IIIc. Cell lysates were separated by SDS–PAGE and proteins were transferred onto nitrocellulose membrane, then denatured and renatured on the membrane. Blots were incubated with purified Fc-FGFR1 IIIc. After further incubation overnight with an anti-Fc-tag antibody, washing three times with PBST, incubating with an anti-goat secondary antibody, and washing again, bound proteins were detected by adding alkaline phosphatase substrate. Lane A1: cell lysate of *E. coli* transformed with pMA5 (MafA); Lane A2: *E. coli* transformed with empty vector (pQE-30 without insert), as a negative control; Lane B1: *N. meningitidis* MC58 cell lysate; Lane B2: cell lysate of *mafA* mutant strain (MC58Δ*NMB0375-Omega*). A successful far-Western blot appears similar to a standard Western blot, but where a band for Fc-FGFR1 IIIc is detected corresponding to the molecular weight of MafA, not the Fc-FGFR1 IIIc protein, thereby providing evidence of an interaction.

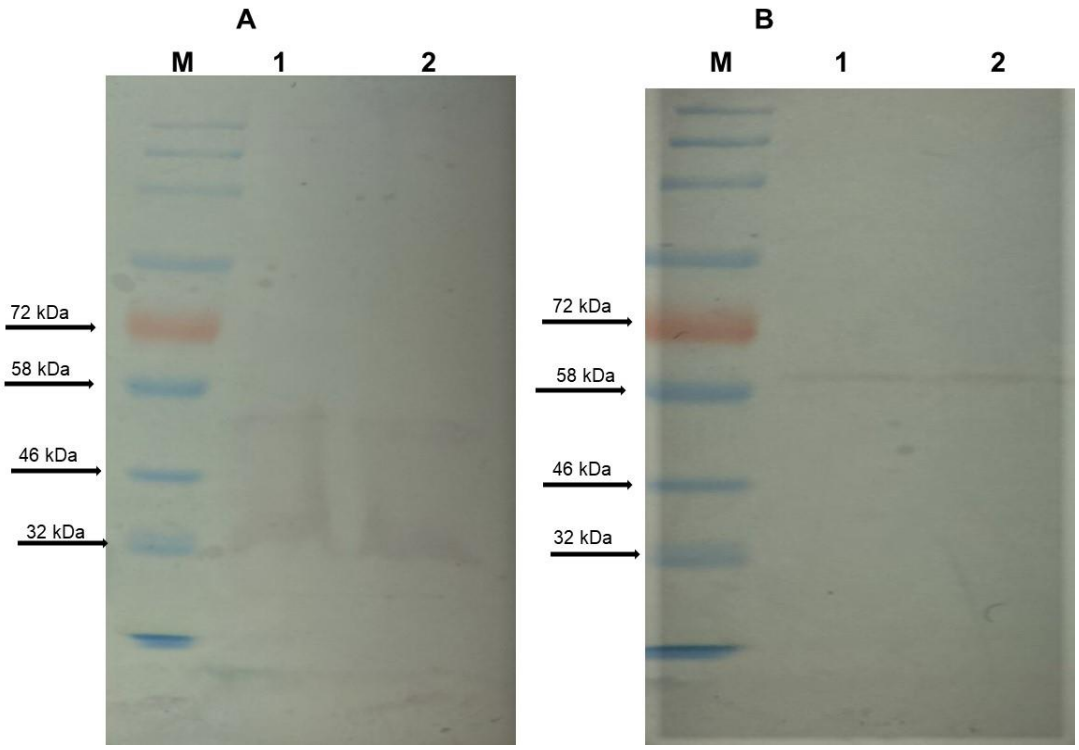

Figure 4.31: Far-Western blotting to assess interaction of Fc-stop with whole cell lysates (pMA5*).* Lane A1: Whole cell lysates were separated by SDS–PAGE and proteins transferred onto nitrocellulose membrane. The bound proteins were denatured and renatured on the membrane, then incubated with purified Fc-stop. After further incubation overnight with an anti-Fc-tag antibody, washing three times with PBST, incubating with an anti-goat antibody, and washing again, bound proteins were detected by adding alkaline phosphatase substrate. Lane A1:cell lysate of *E. coli* transformed with pMA5 (MafA); Lane A2: *E. coli* transformed with empty vector (pQE-30 without insert), as a negative control; Lane B1: cell lysate of *N. meningitidis* MC58; Lane B2: *mafA* mutant (MC58Δ*NMB0375-Omega)*. Bands would be located according to the molecular weight of MafA if an interaction with bait protein (Fc-stop) was present, but no interaction was observed between them.

4.2.10 Interaction between MafA and the extracellular IIIc domain of FGFR1

An ELISA experiment was conducted to confirm whether purified Fc-FGFR1 IIIc interacts with purified MafA, given the above tentative evidence of interaction between these two proteins from far-western blotting experiments. When microplate wells are coated with Fc-tagged recombinant proteins, the Fc-tag will attach to the well surface, thereby giving optimal display of immobilised capture proteins attached to the tag. Different concentrations of Fc-FGFR1 IIIc and Fc-stop (2, 1, 0.5, 0.25 and 0.125 μg ml^{-1}) were first screened to find the optimum concentration for each. In addition, it was confirmed by western blotting that no interaction occurs between the Fc-containing proteins (Fc-FGFR1 IIIc and Fc-stop) and the anti-His_6-tag primary antibody used. In this confirmatory experiment, no band was seen on the nitrocellulose membrane (corresponding to anti-His_6-tag) and MafA was used as a positive control; thus, the ELISA assay was assumed to only detect direct interaction between Fc-FGFR1 IIIc and MafA, and the antibody (anti-His_6-tag) was assumed to be specific for MafA.

In addition, pyocin S3 (from *Pseudomonas aeruginosa*) was obtained from the Kim Hardie group and used as a negative control. Before using this sample in ELISA assays, western blotting was done to confirm the interaction between pyocin S3 and the anti-His_6-tag primary antibody, and after following the protocol for western blotting a band was seen at the assumed molecular weight of pyocin S3. In addition, different concentrations of MafA and pyocin S3 (2, 1, 0.5, 0.25 and 0.125 μg ml^{-1}) were first screened to find the optimum concentration for each, before doing protein–protein interaction (ELISA) assays. The best concentration for pyocin S3 (2 μg ml^{-1} in 1% BSA/PBS) and MafA (1 μg ml^{-1} in 1% BSA/PBS). The ELISA plate was read at 10 min intervals after adding alkaline phosphatase substrate, and the best time point for reading the results was determined as 40 min.

The ELISA interaction assays were performed using microplate wells coated with purified Fc-stop (0.3 μg ml^{-1} in PBS) and Fc-FGFR1 IIIc (1 μg ml^{-1} in PBS) in triplicate, by overnight incubation at 4°C. Next, the wells were washed with PBST,

blocked and then incubated with purified MafA (1 μg ml^{-1} in 1% BSA/PBS) that was added to both Fc-FGFR1 IIIc and Fc-stop wells, and pyocin S3 (2 μg ml^{-1} in 1% BSA/PBS) as a negative control for both Fc-FGFR1 IIIc and Fc-stop. After this, the plate was washed three times with PBST then a primary antibody (anti-His_6-tag was added and the plate incubated overnight at 4°C. After washing, a secondary antibody solution was then added (anti-mouse IgG alkaline phosphatase), followed by a 2 h incubation at room temperature. Finally, colour was developed by the addition of alkaline phosphatase substrate. A GloMax instrument was used for reading the plates, at an absorbance wavelength of 405 nm, 40 min after addition of the substrate.

The results of this experiment indicated no significant binding of Fc-FGFR1 IIIc and Fc-stop to purified MafA and S3 after 40 min compared to control (1% BSA/PBS + MafA). At this point, a difference was expected between the background and test protein wells due to binding. Therefore, it was decided to take a reading each hour, and after 10 h incubation with detection reagent, significant binding between Fc-FGFR1 IIIc and MafA was observed compared to control (1% BSA/PBS + MafA), also, no significant interaction was found between MafA and Fc-stop, or between pyocin S3 and both Fc-FGFR1 IIIc and Fc-stop as shown in Figure 4.32. Specific binding of MafA to Fc-FGFR1 IIIc was significantly higher than binding of MafA to Fc-stop, which was not significantly higher than binding of MafA to wells coated with 1% BSA/PBS + MafA.

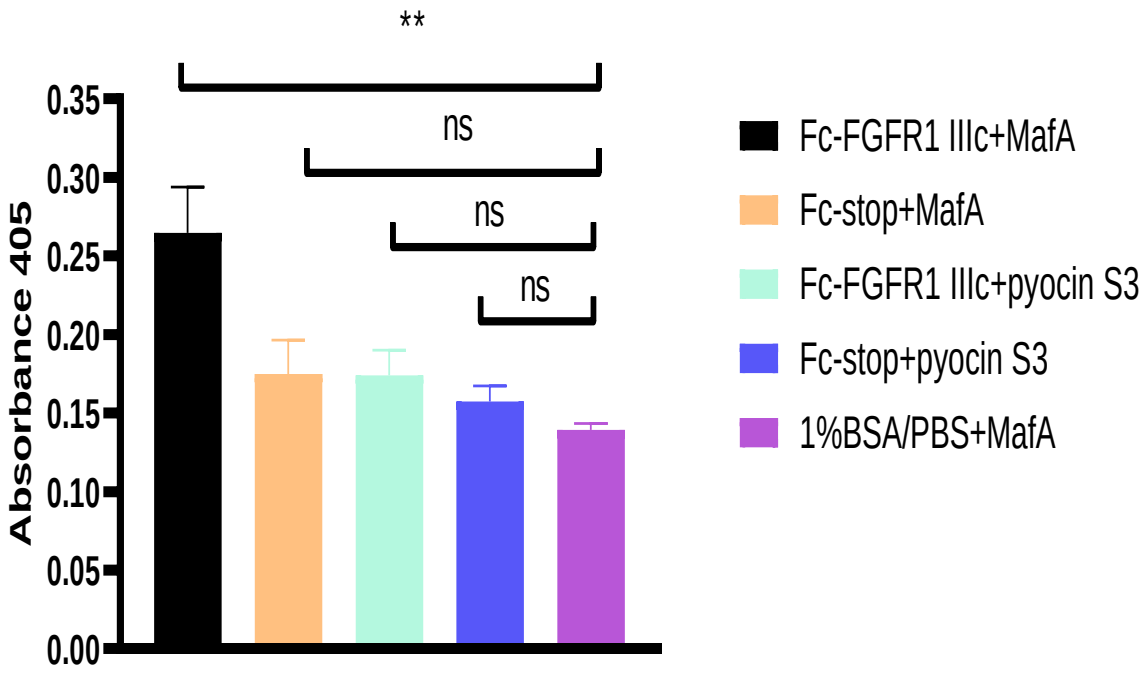

Figure 4.32: Identifying binding of Fc-FGFR1 IIIc and Fc-stop to purified MafA. Plates were coated with purified Fc-stop (0.3 μg ml^{-1} in PBS) and Fc-FGFR1 IIIc (1 μg ml^{-1} in PBS), and then the plate was incubated overnight with purified MafA (1 μg ml^{-1} in 1% BSA/PBS) that was added to both Fc-FGFR1 IIIc and Fc-stop wells, with pyocin S3 (2 μg ml^{-1} in 1% BSA/PBS) also included as a negative control for both Fc-FGFR1 IIIc and Fc-stop. A primary antibody (anti-His_6-tag, 1:2,000) in 1% BSA/PBS was used, then a secondary antibody solution was then added (anti-mouse IgG, 1:5,000 in 1% BSA/PBS). Absorbance readings were taken 10 h after addition of alkaline phosphatase substrate. Error bars denote standard error of the mean (SEM). Experiments were repeated independently three times, each in triplicate. A significant interaction between Fc-FGFR1 IIIc and MafA was apparent, which was statistically significant when compared with 1% BSA/PBS+MafA (** $p < 0.01$) and this done by one-way ANOVA. However, no significant binding was detected between Fc-stop and MafA. Also, pyocin S3 did not interact with either Fc-FGFR1 IIIc or Fc-stop ($p > 0.05$) when compared with 1% BSA/PBS+MafA.

4.3 Discussion

This chapter set out to build on previous work carried out in our laboratory, which offered a direct and specific interaction between pathogenic *N. meningitidis* and the extracellular IIIc domain of FGFR1 (Azimi, 2014, Azimi et al., 2020). The studies described in the previous chapter identified a role for all four current meningococcal genes of interest (*mafA, fadL, opc5* and *NMB0506*) in invasion of HBMECs, and also characterised *fadL* as a novel adhesin of *N. meningitidis*. The next step was therefore to assess the possible involvement of FGFR1 IIIc interactions in the bacterial processes mediated by these proteins. To do this, recombinant forms of FGFR1 IIIc (extracellular domain) and the putative bacterial ligands were required.

In order to achieve functional of protein, human FGFR1 IIIc was expressed in mammalian cells (HEK293T) as previously, using an expression plasmid constructed within our group (pEF-Bos-ss-FC-extFGFR1 IIIc-ires-TPZ) that encodes an N-terminally Fc-tagged form of the extracellular domain of FGFR1 IIIc. A plasmid encoding Fc-stop (pEF-Bos-ss-Fc-stop-ires-TPZ) was also used, to express the Fc-tag alone for control purposes. Transient transfections were used for protein expression, with their efficiency monitored by GFP fluorescence resulting from co-expression of the GFP-topaz protein via an IRES motif included in the expression construct. Both proteins were expected to be secreted into the supernatant, helping to facilitate affinity purification. Transfections carried out using both $CaPO_4$ precipitation or Lipofectamine 3000 proceeded with low efficiency and failed to produce sufficient recombinant protein in the supernatant. Instead, the best method leading to secretion of soluble Fc-FGFR1 IIIc was found to be the use of GeneJuice transfection reagent. Expression of both of Fc-FGFR1 IIIc and Fc-stop was confirmed by SDS–PAGE analysis and immunoblotting. Affinity purification, using Protein A/G Sepharose to capture the Fc-tag, yielded near-homogenous samples of recombinant Fc-FGFR1 IIIc and Fc-stop respectively, containing minimal impurities and suitable for direct use in binding experiments with potential bacterial ligands.

The full-length meningococcal MafA, Opc5 and FadL coding sequences, lacking just their signal peptides, were successfully cloned into the pQE-30 vector for protein expression with N-terminal hexahistidine tags. Due to time constraints, the fourth gene of interest, *NMB0506*, was not cloned in this project, although this is suggested as future work given the newly established function in host cell invasion as discussed in chapter three. The other three proteins of interest all showed good expression in *E. coli* JM109 cells following IPTG induction, as determined by immunoblot analysis using anti-His_6-tag monoclonal antibodies. The MafA protein was successfully purified by IMAC affinity chromatography from the soluble fraction of the whole cell lysate (Figures 4.20 and 4.21), providing a near-homogenous sample after this purification step. However, recombinant Opc5 and FadL were not purified successfully despite several attempts. They were not present in the induced cultures as soluble protein, but were rather found in insoluble form, in the pellet (i.e., in bacterial inclusion bodies).

This is a known issue for both proteins. FadL has been purified from inclusion bodies in previous studies (Yero et al., 2006, Castellanos et al., 2007, Sardinas et al., 2009) as has Opc5 (Musacchio et al., 1997, Jolley et al., 2001). In these cases, proteins were generally solubilised from the pellet with urea, although guanidine–HCl was used for Opc5 in one case (Musacchio et al., 1997). Attempts to use the detergent Triton X-100 to solubilise the recombinant protein were not successful; other solubilising agents might have been tried but, although it is also important to note that time constraints in this project did not allow for extensive investigations to optimise these protocols. This could be explored in future work, perhaps based on the literature procedures cited, although recombinant protein recovered from inclusion bodies is not ideal for functional studies and a number of alternative approaches could be tried to obtain soluble protein. Nonetheless, purification from bacterial inclusion bodies might ultimately prove necessary and it would certainly be useful to adopt this approach at some point for the comparison. Inclusion bodies are dynamic structures that can contain both amyloid and native-like forms of the expressed protein (Cano-Garrido et al., 2013, Singh et al., 2015), and although refolding into the native form is often possible, there is not necessarily any guarantee

that this will be achieved for any given protein. Understanding this, non-denaturing methods have been developed for harvesting recombinant protein from inclusion bodies (Singh et al., 2015), and these could certainly be tried if soluble protein cannot be obtained after optimisation, or if the more conventional denaturation/refolding approach from inclusion bodies fails to give functional protein. Overall, successful expression and purification of natively folded FadL and Opc5 should be possible in future, given sufficient optimisation attempts. Such development work might help to enable production of recombinant NMB0506 (if it also tends to form inclusion bodies).

As noted earlier, the Fc-FGFR1_IIIc protein showed a lower molecular weight than expected on SDS–PAGE gels (observed 50 kDa, calculated 62 kDa). Analysing the sequence of this fusion protein showed that it has a low theoretical pI value of 6.04, which is mainly due to the properties of the FGFR1_IIIc portion (theoretical pI 5.50). Therefore, at the running pH of SDS–PAGE (approximately pH 8), the Fc-FGFR1_IIIc fusion protein will have more negative charge than average, and will consequently migrate faster towards the anode than most other proteins of similar molecular weight. This explains why the observed molecular weight was lower than expected.

In future work it might be helpful, by using appropriate assays where possible, to also verify that the recombinant proteins were obtained in functional form. For Fc-FGFR1_IIIc, an FGF1 binding assay could be used; for example, by gel shift (EMSA) assay (Wu et al., 2003), or ELISA experiments using the immobilised fusion protein to capture FGF ligand(s), with immunological detection of the latter. For MafA, functional validation might prove more challenging since it has not been widely studied, and it is only found in pathogenic *Neisseria* species; however, it is important to note that functionality has been demonstrated for the recombinant protein in a previous transcriptomic study (Kánová et al., 2019). Gonococcal MafA has previously been characterised as a glycolipid binding protein (Paruchuri et al., 1990), although a similar role has yet to be confirmed for the meningococcal protein. Nevertheless, a glycolipid binding assay could be investigated for MafA, perhaps

taking the ELISA-based approach of Karve and Weiss (2014) as a starting point, and beginning by assessing binding of *N. meningitidis* MafA to the glycolipid types specifically identified as ligands for the gonococcal protein (Paruchuri et al., 1990). As a more in-depth approach, a transcriptomic study mirroring that of Kánová et al. (2019) could be undertaken. In that work, overlapping transcriptional responses were identified in HBMECs challenged with either wild type meningococci, or recombinant MafA protein. However, the proposed glycolipid binding assay should prove much less demanding, and is therefore preferable as a starting point.

If recombinant forms of the other bacterial ligands are successfully obtained in future work, it will also be important to verify that they are functional, especially if purification from bacterial inclusion bodies is required. For Opc, a fibronectin binding assay adapted from that of Sa E Cunha et al. (2010) might prove suitable. For FadL, assuming that it functions as a fatty acid transporter in common with the *E. coli* homologue, the [^{3}H]oleate binding assay developed by Black and Zhang (1995) could be adapted to use recombinant protein rather than whole cells, perhaps by immobilising the protein via its His_6-tag and using it to capture ligand, followed by quantification using scintillation counting. Alternatively, it might be possible to develop an SPR assay using unlabelled oleate; or to quantify the FadL oleate interaction using ITC, which is perhaps the best option if sufficient quantities of the protein are obtained. Little is known about NMB0506, since it is expressed from a locus not previously assumed to encode a functional protein. Here, the best approach might be to adopt the strategy of Kánová et al. (2019) for MafA, comparing the transcriptional response of HMBECs on challenge with NMB0506 protein, wild type *N. meningitidis* MC58, and the *ΔNMB0506* strain. If an overlap in cellular responses can be identified between the recombinant protein and wild type (but not mutant) meningococci, then the recombinant protein could likely be assumed to be functional.

The recombinant proteins that were successfully obtained during this study (Fc-FGFR1 IIIc, Fc-stop and MafA) did prove useful in carrying out a range of assays to investigate interactions. However, whole-cell ELISA with fixed meningococci

unexpectedly failed to show any statistically significant differences in Fc-FGFR1 IIIc binding ability between MC58-WT and the knockout strains. Since we obtained evidence that MafA, at least, interacts with Fc-FGFR1 IIIc, there are possible follow-up experiments that could be done to potentially improve our understanding of these results. For example, doing the ELISA experiment differently by immobilising Fc-FGFR1 IIIc and looking for binding by fixed bacteria in suspension would be useful to try, to see if the results are any different.

However, there are some possible limitations of the whole-cell ELISA assay. Fixing the bacteria with formaldehyde will chemically modify their surface structures, including the ligands that might bind to host receptors such as FGFR1. This could impact the results of binding assays and potentially create both false negatives and false positives. The difference seen between MC58-WT and the control mutant, MC58*ΔpilQ/*Δ*porA*, might argue against a negative impact in the present case (Figure 4.10), but the influence of the fixation process on any particular interaction of interest will depend on the reactivity of the specific ligand(s) involved, which may or may not have reactive amino acid sidechains in critical binding regions. Therefore, the results of assays that use fixation should be interpreted with caution. Whole-cell ELISA experiments are a useful starting point, but because of these limitations due to the fixing process, any results of interest should be followed up and confirmed by other methods. It may also be the case that Fc-FGFR1 IIIc binds to other and/or multiple bacterial ligands. To explore this possibility, multiple mutants could be made to see if combining gene knockouts gives any noticeable impact upon binding. For example, the target genes could be mutated in the MC58Δ*pilQ/*Δ*porA* (e.g., to make MC58*ΔmafAΔpilQΔporA*), to see if there is any further reduction in binding ability due to introducing the extra mutations.

The protein–protein interaction experiments by far-western blotting did provide tentative evidence for an interaction between Fc-FGFR1 IIIc and MafA, but not with FadL or Opc5. The far-western blotting results for FadL and Opc5, although negative, should be explained. Both proteins were blotted from whole-cell *E. coli* lysates where they were present in inclusion bodies, as mentioned earlier. Thus, even

though they were denatured and refolded on the membrane, it is not certain that their true native conformation was presented to binding protein (Fc-FGFR1 IIIc) in these experiments, and the far-western blotting results should therefore be verified by additional experiments before reaching any final conclusions. This limitation is a disadvantage of the far-western blotting technique, and means that there is no guarantee that the interaction sites of the bacterial proteins with Fc-FGFR1 IIIc will be present in the correct conformation on the membrane, and available for efficient binding of the specific protein.

The protein–protein interaction ELISA experiments also offered evidence of an interaction between MafA and Fc-FGFR1 IIIc, since a signal was seen with MafA that was not present in background wells (Fc-stop), or with pyocin S3 (used as a negative control). However, a statistically significant difference in the observed signal did not develop until 10 h after addition of the substrate, and this is a very long timescale for such an experiment. Over that length of time, nonspecific effects such as protein aggregation or oxidation could become significant and cannot be ruled out at this stage. Fc-FGFR1 IIIc has multiple (14) cysteine residues that might therefore oxidise slowly under the assay conditions.

Conformation of the interaction might be by two options, first, the strength of the MafA–Fc-FGFR1 IIIc interaction is unknown, and it might simply be that a higher concentration of MafA was required to give a more conclusive result. So, following any necessary optimisation of the assay conditions, a dose response interaction ELISA should be done using a range of different concentrations of MafA (e.g., 1, 4, 8 and 12 μg ml^{-1}). This would hopefully provide better evidence for an interaction between MafA and Fc-FGFR1 IIIc. Second, binding between these proteins should be confirmed by at least one additional technique, ideally using more quantitative methods of characterising the binding interaction such as isothermal titration calorimetry (ITC).

Taken together, the results from this and the previous chapter suggest some interesting conclusions, as well as offering useful guidance for future research in this area. However, there are also some apparent inconsistencies that remain to be

resolved. For example, while all four proteins of interest (MafA, Opc5, FadL and NMB0506) demonstrated a role in meningococcal invasion of HBMECs, only the MafA protein was found to interact with Fc-FGFR1 IIIc, the hypothesised receptor for all four bacterial ligands. Furthermore, despite the involvement of all four proteins in invasion, only FadL was found to be involved in initial attachment to host cells, but no evidence for a direct interaction between FadL and Fc-FGFR1 IIIc was obtained by far-western blotting suggesting that FadL binds to an alternative HBMEC receptor.

In addition to the improved assessment of MafA– Fc-FGFR1 IIIc interactions suggested earlier, it would be useful to obtain purified FadL (and perhaps Opc5 as well), to complete a more thorough assessment of the hypothesis that these bacterial proteins bind to FGFR1 on the surface of host cells. Production of recombinant NMB0506 and binding assessment with FGFR1 IIIc should be an important for future work, given the novel and unexpected functional relevance of this protein discovered in the host cell invasion assay. Moreover, the attachment and invasion assays could be repeated with or without FGFR1 siRNA knockdown, to better characterise the most likely FGFR1 ligand(s) among the current proteins of interest. Whether they all bind to FGFR1 or not, it is possible that other host cell receptors are involved in the function of these bacterial ligands in pathogenesis. For example, FadL of *H. influenzae* is known to interact with host tissues via the CEACAM1 receptor (Tchoupa et al., 2015, Moleres et al., 2018), as noted in the previous chapter. Therefore, the possibility that meningococcal FadL also interacts with CEACAM1 should be investigated, especially given that Kuespert et al. (2011), inferred the presence of a second, unidentified, meningococcal invasion other than Opa that binds to this host receptor.

Chapter 5: General discussion and future works

N. meningitidis remains the most common causative agent of bacterial meningitis (Mahmoud and Harhara, 2020). The human nasopharynx is the only known reservoir for *N. meningitidis*, with between 3–20% of the general population having colonisation by this organism but no detectable symptoms (Tzeng and Stephens, 2021). Furthermore, the mechanisms responsible for nasopharyngeal colonisation remain incompletely understood, as do the factors that influence the progression from commensal colonisation (asymptomatic carriage) to IMD (invasive disease), although a number of factors are thought to be involved (Gasparini et al., 2012).

It is assumed that *N. meningitidis* crosses the nasopharyngeal mucosa relatively frequently but is normally killed by the complement system. This is evident by the frequency with which people with complement deficiencies are susceptible to repeated cases of meningococcal disease (Lewis and Ram, 2014), but encapsulated meningococci have the potential to proliferate uncontrollably in this environment and be disseminated to other areas of the body, which can result in inflammation, sepsis and purpuric rash (Coureuil et al., 2013). Thus, one aspect of pathogenesis is evasion of host immune responses. Meningococci have developed several such mechanisms, and multiple virulence factors play significant roles in resisting immune response, including the capsule, OMPs, LOS and fHbp. In some cases, *N. meningitidis* crosses the BBB, reaches the CSF, and crosses the meninges, where it can cause meningitis (Virji, 2009).

It is important to note that despite recent advances in the field of disease prevention, many aspects of meningococcal pathogenesis remain poorly defined. For example, it is still unclear how the bacteria cross the BBB even though progress has been made in understanding the mechanisms used by these bacteria to bind to and penetrate endothelial cells. A better understanding the pathogenic mechanisms of IMD, and identification of novel antigens against emerging pathogenic strains, are therefore important emphases of continuing work in the field.

The work in this study involved screening for potential new meningococcal ligands, with a particular focus on the host FGFR1 receptor that was shown to play a role in bacterial adhesion and invasion by previous work in our group. When activated, the FGFR1 receptor is trafficked and recruited to internalised *N. meningitidis* within HBMECs, and ELISA experiments verified a direct interaction of the extracellular domain of Fc-FGFR1 IIIc with meningococcal strain MC58, but not with the commensal *N. lactamica* strain ATCC 23970 (Azimi et al., 2020).

Through mutation of PilQ, the same earlier study also established an important role for meningococcal TFP in FGFR1-mediated adhesion of *N. meningitidis* to host endothelial cells (Azimi et al., 2020). However, many other bacterial adhesins have been implicated in invasion of the host, and multiple surface-exposed meningococcal factors are apparently involved in the invasion of host tissues that occurs in IMD. Therefore, it was hypothesised that other specific, high-affinity bacterial ligands for FGFR1 are present on the surface of disease-associated meningococci. It is well appreciated that minor adhesins might play important roles in the pathogenesis of meningococcal disease (Hill et al., 2010), and some such interactions have been explored; for example, between HBMECs and MafA (Kánová et al., 2018, Kánová et al., 2019), which was one of the *N. meningitidis* proteins investigated in this study. Given the previous findings from our group regarding TFP, a PilQ-deficient strain (Δ*pilQ*/Δ*porA*) was used as a positive control when evaluating the roles of potential novel adhesins.

Four meningococcal proteins were identified as candidate FGFR1 ligands by bioinformatic analysis of an experimentally determined interactome (Kánová et al., 2018). Mutation of these four genes (*mafA*, *opc5*, *fadL* and *NMB0506*) was carried out in *N. meningitidis* strain MC58, to allow for screening of their functional roles in attachment and invasion with HBMECs, and to permit assessment of interaction of their encoded surface-exposed proteins with recombinant FGFR1. Mutagenic plasmids were generated by cloning the meningococcal *mafA*, *opc5*, *fadL* and *NMB0506* genes, along with flanking DNA regions that contained at least one natural Neisserial uptake sequence, into the

pGEM-T Easy or pGEM-T vectors. Constructs for inactivation/knockout of target genes were then generated via suitable deletions using INPCR followed by ligation of different antibiotic resistance cassettes. To investigate the functions of the four genes of interest in meningococcal adhesion and invasion with HBMECs, the interaction of mutant strains with these human cells was compared to that of the wild type of strain, and adhesion and invasion assay data was generated for all four strains along with (Δ*pilQ*/Δ*porA*) as a positive control. Although each of the four meningococcal mutants had some effect on meningococcal invasion, the level of significance was higher for the *mafA* and *fadL* mutants. Furthermore, only the *fadL* mutant was significantly less able to bind to HBMECs.

Next, the role of FGFR1 in mediating the attachment and invasion processes with HBMECs was investigated. The extracellular domain of the human FGFR1 IIIc protein was expressed in a functional form in mammalian cells (HEK293T), using an expression plasmid constructed within our group (pEF-Bos-ss-FC-extFGFR1 IIIc-ires-TPZ) that encodes an N-terminally Fc-tagged form of the protein (Azimi, 2014). Expression of the protein using transient transfection proved challenging, but use of the GeneJuice reagent was found to be the most suitable approach for secretion of soluble Fc-FGFR1 IIIc. For the candidate bacterial ligands, the full-length meningococcal MafA, Opc5 and FadL coding sequences (lacking their signal peptides) were successfully cloned into the pQE-30 vector for protein expression with N-terminal hexahistidine tags. These three proteins all showed good expression in *E. coli* (JM109) cells following IPTG induction, as determined by immunoblot analysis using anti-His_6-tag monoclonal antibodies, and MafA was successfully purified by IMAC affinity chromatography. However, recombinant Opc5 and FadL were not purified successfully despite several attempts, since the expressed proteins were found in the insoluble fraction. It is likely that with sufficient optimisation work, successful expression and purification of natively-folded FadL and Opc5 should be possible in future, as discussed in Chapter 4.

Protein–protein interaction experiments using far-western blotting provided tentative evidence for an interaction between Fc-FGFR1 IIIc and MafA, but not with

FadL or Opc5. But this experiment had some limitations, an aspect that was considered in Chapter 4, meaning that the results are not conclusive and appropriate follow-up experiments would be a useful part of any subsequent extension of this work. Investigation of protein–protein interactions by ELISA also offered evidence of an interaction between MafA and Fc-FGFR1 IIIc. Taken together, the presented results suggest that if MafA of meningococci does interact with FGFR1 of HBMECs, this interaction is involved in invasion rather than initial attachment. For future work, it would be beneficial to confirm binding between these proteins by at least one additional technique, ideally using more quantitative methods such as ITC, which could also be applied to obtain more definitive answers for FadL and Opc5.

In addition, evidence for direct binding to FGFR1 was demonstrated for MafA. It should be noted that the *mafA* (NMB0375) gene of *N. meningitidis* strain MC58 is duplicated at locus *NMB0652*, and these loci have been designated as *mafA1* and *mafA2*, respectively (Grifantini et al., 2002a, Grifantini et al., 2002b). The two genes encode identical proteins and downstream gene (*mafB*) but have different upstream flanking regions. In the present study, only *mafA1* was inactivated, and it is therefore possible that the knockout strain used here retains some level of MafA expression via *mafA2*. In future work, a double knockout should be made, which has in fact been previously reported for *N. meningitidis* strain MC58 (Grifantini et al., 2002a, Grifantini et al., 2002b). MafA has been identified as a minor constituent of the OMV component of the Bexsero vaccine (Semchenko et al., 2019), and *mafA* (NMB0652) which is duplicated on the MC58 genome and was itself shown to elicit bactericidal antibodies against *N. meningitidis* strain MC58 in mice (Grifantini et al., 2002a, Grifantini et al., 2002b). It is likely that this approach would provide more convincing evidence for the role of MafA in host cell adhesion and invasion.

The functional significance of FadL in attachment of *N. meningitidis* to HBMECs does not seem to involve FGFR1 in whole cell ELISA, but it might bind to an alternative receptor. As discussed in Chapter 4, this could possibly be CEACAM1, and follow-up experiments to investigate this possibility are recommended. Furthermore, the apparent role of meningococcal FadL as a bacterial adhesin which

is already known for its homologue in *H. influenzae* (Tchoupa et al., 2015, Moleres et al., 2018) as discussed in Chapter 3 is particularly interesting given that it has previously been suggested as a candidate vaccine antigen (Sardiñas et al., 2009, Yero et al., 2010). Sardiñas et al. (2009) noted that FadL seems to be abundant in serogroup B meningococcal OMVs and demonstrated production of bactericidal antibodies after immunisation in mice. It seems surprising that following these initial assessments, FadL does not seem to have been actively trialled as an experimental vaccine candidate, although there was some concern over strain coverage given the level of antigenic variation; specifically, high variability in the variable regions of the protein (Sardiñas et al., 2009). It was suggested that a multivalent vaccine with four variants would be necessary for good coverage (Yero et al., 2010). Considering the present results, it might be useful to determine whether FadL plays a role in host cell attachment of other meningococcal strains, since this might provide support for further investigating the protein as a potential vaccine antigen.

However, like FadL, it does not seem that MafA has been actively pursued as a candidate vaccine antigen. The results of the present study indicate that further investigation might be necessary, since eliciting antibodies against MafA would not only aid bacterial killing and inhibit meningococcal interaction with host cells, but would also be expected to block direct interaction of MafA with FGFR1. If so, this would prevent receptor activation and downstream signalling, and therefore avoid the subsequent events that apparently contribute to invasion of host tissues.

To set this discussion in a wider context, it seems pertinent to consider the level of conservation in homologues of *mafA* and *fadL*. As noted already, MafA has classically been viewed as unique to pathogenic *Neisseria* species. Arenas et al. (2015) found that neisserial *mafA* genes cluster into two distinct phylogenetic groups, one with high sequence identity (>95%), and the other with much lower identity (<70%). The implications of this for pathogenesis do not appear to be well understood at present, and in a recent analysis of gonorrhoeal vaccine candidates, Baarda et al. (2021) did not place MafA among their priority candidates. It was

suggested that both *mafA* subtypes would have to be used if this protein were to be pursued as an antigen, clearly placing it at a disadvantage compared to other possibilities.

Thus, MafA remains relatively understudied, and future work should investigate the binding properties of this adhesin from multiple neisserial strains, particularly aiming to distinguish between the two major genetic lineages. This is necessary to establish which domain(s) of the protein are essential for binding to host cells, and to better understand sequence variations. Beyond pathogenic neisserial species, Arenas et al. (2020) intriguingly and perhaps unexpectedly identified close homologues of *mafA* in the wider *Neisseraceae* family, including *Bergeriella denitrificans* (99.4% identity) and *Kingella potus* (94.1%), along with evidence for the occurrence of other, albeit less closely related, homologues distributed more widely among protobacteria.

Structurally, MafA is predicted to embed in the bacterial outer membrane by forming oligomers, rather than having a β-barrel structure (Arenas et al., 2020), suggesting a functional resemblance to pore-forming toxins. The same authors concluded that these MafA oligomers do not present large surface-exposed regions, suggesting that host cell adhesion is conferred by small, and possibly highly variable, extracellular loop regions. This should be investigated in future work, and if confirmed, it would show interesting similarities to what is already known for *fadL*.

Importantly, FadL/OmpP1 has already been studied as a virulence factor in *H. influenzae*. The *E. coli* homologue is a 14-stranded β-barrel membrane transporter, the structure of which was solved in 2004 (van den Berg et al., 2004). Tchoupa et al. (2015) modelled FadL from *H. influenzae* based on this structure, and found generally high sequence conservation across multiple isolates, with a notable exception being three surface-exposed loops that displayed high variability. They speculated that sequence variations in these loop regions are responsible for inter-strain variation in CEACAM receptor binding properties. In subsequent work, Moleres et al. (2018) highlighted the importance of these surface-exposed loops for

CEACAM1 binding by using molecular dynamics simulations with FadL homologues from multiple *H. influenzae* strains.

Although meningococcal FadL has low amino acid sequence identity with the *E. coli* homologue, studies by Sardiñas et al. (2009) and Yero et al. (2010) to assess its vaccine potential concluded that the overall structure is likely similar, and putatively identified three extracellular loop regions which showed the anticipated variability between meningococcal strains. Four main variants were identified, and some association of these with serogroup and/or clonal complex was also found. Although neither study ruled out the pursuit of FadL as a vaccine antigen, both seemed cautious, with Sardiñas et al. (2010) hinting that multiple variants would likely be required for sufficient strain coverage. Future work should consider CEACAM receptors as binding targets for meningococcal FadL proteins, perhaps looking at the receptor specificity of the four main *fadL* clusters described above. Importantly, it also seems unclear at present whether the neisserial homologues encode functional fatty acid transporters, and this aspect also ideally requires clarification.

Finally, although time limitations prevented expression, purification and binding assessment of NMB0506, this should be for future work. As described in Chapter 3, the *NMB0506* locus was previously characterised by Arenas et al. (2013) The present discovery that this gene encodes a functional invasin is therefore of considerable potential significance, and further efforts should be made to confirm its involvement in meningococcal invasion of HBMECs and identify the host cellular receptor(s) involved.

Table 5.1. Summary the most significant findings for each of the gene studied by the different experiments undertaken in this research project.

		Mutants interacting with HBMECs		Whole cell binding	far-western blotting binding	(ELISA) Binding
protein/mutant		Invasion	Adhesion			
pilQ/porA	Positive control	(****$p \leq 0.0001$)	(**$p \leq 0.01$)	(**$p \leq 0.01$)		
NMB0375	*mafA*	(***$p \leq 0.001$)	>0.05	>0.05	Possible binding	(**$p \leq 0.01$)
NMB1053	*opc5*	(*$p \leq 0.05$)	>0.05	>0.05	Not binding	Not experimented yet
NMB0088	*fadL*	(****$p \leq 0.0001$)	(**$p \leq 0.01$)	>0.05	Not binding	Not experimented yet
NMB0506	*Hypothetical Protein*	(**$p \leq 0.01$)	> 0.05	>0.05	Not experimented yet	Not experimented yet
N. lactamica		(**$p \leq 0.01$)	(*$p \leq 0.05$)	(**$p \leq 0.01$)		

References

ABBOTT, N. J. 2002. Astrocyte–endothelial interactions and blood–brain barrier permeability. *Journal of Anatomy*, 200, 523–534.

ABBOTT, N. J., PATABENDIGE, A. A., DOLMAN, D. E., YUSOF, S. R. & BEGLEY, D. J. 2010. Structure and function of the blood–brain barrier. *Neurobiology of Disease*, 37, 13–25.

ABIO, A., NEAL, K. R. & BECK, C. R. 2013. An epidemiological review of changes in meningococcal biology during the last 100 years. *Pathogens and Global Health*, 107, 373–380.

ABOUSEADA, N. M., ASSAFI, M. S. A., MAHDAVI, J., OLDFIELD, N. J., WHELDON, L. M., WOOLDRIDGE, K. G. & ALA'ALDEEN, D. A. 2012. Mapping the laminin receptor binding domains of *Neisseria meningitidis* PorA and *Haemophilus influenzae* OmpP2. *PLoS One*, 7(9) (article e46233).

ADEEB, N., MORTAZAVI, M. M., TUBBS, R. S. & COHEN-GADOL, A. A. 2012. The cranial dura mater: a review of its history, embryology, and anatomy. *Child's Nervous System*, 28, 827–837.

AGIER, L., MARTINY, N., THIONGANE, O., MUELLER, J. E., PAIREAU, J., WATKINS, E. R., IRVING, T. J., KOUTANGNI, T. & BROUTIN, H. 2017. Towards understanding the epidemiology of *Neisseria meningitidis* in the African meningitis belt: a multi-disciplinary overview. *International Journal of Infectious Diseases*, 54, 103–112.

AGRAWAL, S. & NADEL, S. 2011. Acute bacterial meningitis in infants and children. *Pediatric Drugs*, 13, 385–400.

AHO, E., DEMPSEY, J., HOBBS, M., KLAPPER, D. & CANNON, J. 1991. Characterization of the opa (class 5) gene family of *Neisseria meningitidis*. *Molecular Microbiology*, 5, 1429–1437.

AKKAYA, O., GUVENC, H. I., YUKSEKKAYA, S., OPUS, A., GUZELANT, A., KAYA, M., KURTOGLU, M. G. & KAYA, N. 2017. Real-time PCR detection of the most common bacteria and viruses causing meningitis. *Clinical Laboratory*, 63, 827–832.

ALA'ALDEEN, D. A. & TURNER, D. P. 2006. *Neisseria meningitidis*, in GILLESPIE, S. & HAWKEY, P. M. (eds.) *Principles and Practice of Clinical Bacteriology*. Chichester: John Wiley & Sons, 205–220.

ALMEIDA, S. M. D., NOGUEIRA, M. B., RABONI, S. M. & VIDAL, L. R. 2007. Laboratorial diagnosis of lymphocytic meningitis. *Brazilian Journal of Infectious Diseases*, 11, 489–495.

AL-OBAIDI, M. M. J. & DESA, M. N. M. 2018. Mechanisms of blood–brain barrier disruption by different types of bacteria, and bacterial–host interactions facilitate the bacterial pathogen invading the brain. *Cellular and Molecular Neurobiology*, 38, 1349–1368.

ALTO, N. M. & ORTH, K. 2012. Subversion of cell signaling by pathogens. *Cold Spring Harbor Perspectives in Biology*, 4(article a006114), 1–17.

ANDERSEN, C. 2003. Channel-tunnels: outer membrane components of type I secretion systems and multidrug efflux pumps of Gram-negative bacteria, in AMARA, S. G., BAMBERG, E., BLAUSTEIN, M. P., GRUNICKE, H., JAHN, R., LDERER, W. J., MIYAJIMA, A., MURER, H., OFFERMANNS, S., PFANNER, N., SCHULTZ, G. & SCHWEIGER, M. (eds.) *Reviews of Physiology, Biochemistry and Pharmacology*. Berlin: Springer, 122–165.

ANDERSON, J. E., SPARLING, P. F. & CORNELISSEN, C. N. 1994. Gonococcal transferrin-binding protein 2 facilitates but is not essential for transferrin utilization. *Journal of Bacteriology*, 176, 3162–3170.

ANDREWS, N. J., WAIGHT, P. A., GEORGE, R. C., SLACK, M. P. & MILLER, E. 2012. Impact and effectiveness of 23-valent pneumococcal polysaccharide vaccine against invasive pneumococcal disease in the elderly in England and Wales. *Vaccine*, 30, 6802–6808.

ARENAS, J., CATÓN, L., VAN DEN HOEVEN, T., DE MAAT, V., CRUZ HERRERO, J. & TOMMASSEN, J. 2020. The outer-membrane protein MafA of *Neisseria meningitidis* constitutes a novel protein secretion pathway specific for the fratricide protein MafB. *Virulence*, 11, 1701–1715.

ARENAS, J., DE MAAT, V., CATÓN, L., KREKORIAN, M., HERRERO, J. C., FERRARA, F. & TOMMASSEN, J. 2015. Fratricide activity of MafB protein of *N. meningitidis* strain B16B6. *BMC Microbiology*, 15(article 156), 1–11. ARENAS, J., NIJLAND, R., RODRIGUEZ, F. J., BOSMA, T. N. & TOMMASSEN, J. 2013. Involvement of three meningococcal surface-exposed proteins, the heparin-binding protein NhbA, the α-peptide of IgA protease and the autotransporter protease NalP, in initiation of biofilm formation. *Molecular Microbiology*, 87, 254–268.

ARENAS, J., SCHIPPER, K., VAN ULSEN, P., VAN DER ENDE, A. & TOMMASSEN, J. 2013. Domain exchange at the 3′ end of the gene encoding the fratricide meningococcal two-partner secretion protein A. *BMC Genomics*, 14(article 622), 1–14.

ARKING, D., TONG, Y. & STEIN, D. C. 2001. Analysis of lipooligosaccharide biosynthesis in the *Neisseriaceae*. *Journal of Bacteriology*, 183, 934–941.

ARTENSTEIN, M. S., GOLD, R., ZIMMERLY, J. G., WYLE, F. A., SCHNEIDER, H. & HARKINS, C. 1970. Prevention of meningococcal disease by group C polysaccharide vaccine. *New England Journal of Medicine*, 282, 417–420.

ASMAT, T. M., TENENBAUM, T., JONSSON, A.-B., SCHWERK, C. & SCHROTEN, H. 2014. Impact of calcium signaling during infection of *Neisseria meningitidis* to human brain microvascular endothelial cells. *PLoS One*, 9(article e114474), 1–24.

AZIMI, S. 2014. Interactions between the *Neisseria meningitidis* and its human host. PhD Thesis. University of Nottingham.

AZIMI, S., WHELDON, L. M., OLDFIELD, N. J., ALA'ALDEEN, D. A. & WOOLDRIDGE, K. G. 2020. A role for fibroblast growth factor receptor 1 in the pathogenesis of *Neisseria meningitidis*. *Microbial Pathogenesis*, 149(article 104534).

BACKERT, S. & MEYER, T. F. 2006. Type IV secretion systems and their effectors in bacterial pathogenesis. *Current Opinion in Microbiology*, 9, 207–217.

BALHUIZEN, M. D., VELDHUIZEN, E. J. & HAAGSMAN, H. P. 2021. Outer membrane vesicle induction and isolation for vaccine development. *Frontiers in Microbiology*, 12(article 629090), 1–14.

BALLABH, P., BRAUN, A. & NEDERGAARD, M. 2004. The blood–brain barrier: an overview: structure, regulation, and clinical implications. *Neurobiology of Disease*, 16(1), 1–13.

BALMER, P., BORROW, R. & MILLER, E. 2002. Impact of meningococcal C conjugate vaccine in the UK. *Journal of Medical Microbiology*, 51, 717–722.

BANKS, W. A. 2015. The blood–brain barrier in neuroimmunology: tales of separation and assimilation. *Brain, Behavior, and Immunity*, 44, 1–8.

BARNIER, J.-P., EUPHRASIE, D., JOIN-LAMBERT, O., AUDRY, M., SCHONHERR-HELLEC, S., SCHMITT, T., BOURDOULOUS, S., COUREUIL, M., NASSIF, X. & EL BEHI, M. 2021. Type IV pilus retraction enables sustained bacteremia and

plays a key role in the outcome of meningococcal sepsis in a humanized mouse model. *PLoS Pathogens*, 17(article e1009299), 1–21.

BARRILE, R., KASENDRA, M., ROSSI-PACCANI, S., MEROLA, M., PIZZA, M., BALDARI, C., SORIANI, M. & ARICÒ, B. 2015. *Neisseria meningitidis* subverts the polarized organization and intracellular trafficking of host cells to cross the epithelial barrier. *Cellular Microbiology*, 17, 1365–1375.

BARTLEY, S. N., MOWLABOCCUS, S., MULLALLY, C. A., STUBBS, K. A., VRIELINK, A., MAIDEN, M. C., HARRISON, O. B., PERKINS, T. T. & KAHLER, C. M. 2017. Acquisition of the capsule locus by horizontal gene transfer in *Neisseria meningitidis* is often accompanied by the loss of UDP-GalNAc synthesis. *Scientific Reports*, 7(article 44442), 1–14.

BEESLAAR, J., ABSALON, J., BALMER, P., SRIVASTAVA, A., MAANSSON, R., YORK, L. J. & PEREZ, J. L. 2018. Clinical data supporting a 2-dose schedule of MenB-FHbp, a bivalent meningococcal serogroup B vaccine, in adolescents and young adults. *Vaccine*, 36, 4004–4013.

BEG, A. A. 2002. Endogenous ligands of Toll-like receptors: implications for regulating inflammatory and immune responses. *Trends in Immunology*, 23, 509–512.

BENNETT, J. S., JOLLEY, K. A., EARLE, S. G., CORTON, C., BENTLEY, S. D., PARKHILL, J. & MAIDEN, M. C. 2012. A genomic approach to bacterial taxonomy: an examination and proposed reclassification of species within the genus Neisseria. *Microbiology*, 158, 1570–1580.

BENZ, I. & SCHMIDT, M. A. 1989. Cloning and expression of an adhesin (AIDA-I) involved in diffuse adherence of enteropathogenic *Escherichia coli*. *Infection and Immunity*, 57, 1506–1511.

BENZ, I. & SCHMIDT, M. A. 1992. AIDA-I, the adhesin involved in diffuse adherence of the diarrhoeagenic *Escherichia coli* strain 2787 (O126:H27), is synthesized via a precursor molecule. *Molecular Microbiology*, 6, 1539–1546.

BERGOUNIOUX, J., COUREUIL, M., BELLI, E., LY, M., CAMBILLAU, M., GOUDIN, N., NASSIF, X. & JOIN-LAMBERT, O. 2016. Experimental evidence of bacterial colonization of human coronary microvasculature and myocardial tissue during meningococcemia. *Infection and Immunity*, 84**,** 3017–3023.

BERNARD, S. C., SIMPSON, N., JOIN-LAMBERT, O., FEDERICI, C., LARAN-CHICH, M.-P., MAÏSSA, N., BOUZINBA-SÉGARD, H., MORAND, P. C., CHRETIEN,

F. & TAOUJI, S. 2014. Pathogenic *Neisseria meningitidis* utilizes CD147 for vascular colonization. *Nature Medicine*, 20, 725–731.

BERNDSEN, M., ERLENDSDÓTTIR, H. & GOTTFREDSSON, M. 2012. Evolving epidemiology of invasive *Haemophilus* infections in the post-vaccination era: results from a long-term population-based study. *Clinical Microbiology and Infection*, 18, 918–923.

BERNE, C., ELLISON, C. K., DUCRET, A. & BRUN, Y. V. 2018. Bacterial adhesion at the single-cell level. *Nature Reviews Microbiology*, 16, 616–627.

BERRINGTON, A., TAN, Y.-C., SRIKHANTA, Y., KUIPERS, B., VAN DER LEY, P., PEAK, I. & JENNINGS, M. 2002. Phase variation in meningococcal lipooligosaccharide biosynthesis genes. *FEMS Immunology & Medical Microbiology*, 34, 267–275.

BERRY, J.-L., PHELAN, M. M., COLLINS, R. F., ADOMAVICIUS, T., TØNJUM, T., FRYE, S. A., BIRD, L., OWENS, R., FORD, R. C. & LIAN, L.-Y. 2012. Structure and assembly of a trans-periplasmic channel for type IV pili in *Neisseria meningitidis*. *PLoS Pathogens*, 8(article e1002923), 1–15.

BIAGINI, M., SPINSANTI, M., DE ANGELIS, G., TOMEI, S., FERLENGHI, I., SCARSELLI, M., RIGAT, F., MESSUTI, N., BIOLCHI, A. & MUZZI, A. 2016. Expression of factor H binding protein in meningococcal strains can vary at least 15-fold and is genetically determined. *Proceedings of the National Academy of Sciences*, 113, 2714–2719.

BIAIS, N., HIGASHI, D. L., BRUJIĆ, J., SO, M. & SHEETZ, M. P. 2010. Force-dependent polymorphism in type IV pili reveals hidden epitopes. *Proceedings of the National Academy of Sciences*, 107, 11358–11363.

BILLE, E., ZAHAR, J.-R., PERRIN, A., MORELLE, S., KRIZ, P., JOLLEY, K. A., MAIDEN, M. C., DERVIN, C., NASSIF, X. & TINSLEY, C. R. 2005. A chromosomally integrated bacteriophage in invasive meningococci. *The Journal of Experimental Medicine*, 201, 1905–1913.

BILUKHA, O. & ROSENSTEIN, N. E. 2005. Prevention and control of meningococcal disease: recommendations of the Advisory Committee on Immunization Practices (ACIP). Centers for Disease Control and Prevention.

BINET, R., LÉTOFFÉ, S., GHIGO, J. M., DELEPELAIRE, P. & WANDERSMAN, C. 1997. Protein secretion by Gram-negative bacterial ABC exporters – a review. *Gene*, 192, 7–11.

BIRTLES, A., HARDY, K., GRAY, S. J., HANDFORD, S., KACZMARSKI, E. B., EDWARDS-JONES, V. & FOX, A. J. 2005. Multilocus sequence typing of *Neisseria meningitidis* directly from clinical samples and application of the method to the investigation of meningococcal disease case clusters. *Journal of Clinical Microbiology*, 43, 6007–6014.

BISCARDI, J. S., MAA, M.-C., TICE, D. A., COX, M. E., LEU, T.-H. & PARSONS, S. J. 1999. c-Src-mediated phosphorylation of the epidermal growth factor receptor on Tyr845 and Tyr1101 is associated with modulation of receptor function. *Journal of Biological Chemistry*, 274, 8335–8343.

BJERRE, A., BRUSLETTO, B., ØVSTEBØ, R., JOØ, G. B., KIERULF, P. & BRANDTZAEG, P. 2003. Identification of meningococcal LPS as a major monocyte activator in IL-10 depleted shock plasmas and CSF by blocking the CD14-TLR4 receptor complex. *Journal of Endotoxin Research*, 9, 155–163.

BLACK, P. N. & ZHANG, Q. 1995. Evidence that His110 of the protein FadL in the outer membrane of *Escherichia coli* is involved in the binding and uptake of long-chain fatty acids: possible role of this residue in carboxylate binding. *Biochemical Journal*, 310, 389–394.

BOISIER, P., NICOLAS, P., DJIBO, S., TAHA, M.-K., JEANNE, I., MAÍNASSARA, H. B., TENEBRAY, B., KAIRO, K. K., GIORGINI, D. & CHANTEAU, S. 2007. Meningococcal meningitis: unprecedented incidence of serogroup X—related cases in 2006 in Niger. *Clinical Infectious Diseases*, 44(5), 657–663.

BONNAH, R. A., HOELTER, J., STEEGHS, L., ENNS, C. A., SO, M. & MUCKENTHALER, M. U. 2005. Lipooligosaccharide-independent alteration of cellular homeostasis in *Neisseria meningitidis*-infected epithelial cells. *Cellular Microbiology*, 7, 869–885.

BOOY, R., GENTILE, A., NISSEN, M., WHELAN, J. & ABITBOL, V. 2019. Recent changes in the epidemiology of *Neisseria meningitidis* serogroup W across the world, current vaccination policy choices and possible future strategies. *Human Vaccines & Immunotherapeutics*, 15, 470–480.

BORKOWSKI, J., LI, L., STEINMANN, U., QUEDNAU, N., STUMP-GUTHIER, C., WEISS, C., FINDEISEN, P., GRETZ, N., ISHIKAWA, H. & TENENBAUM, T. 2014. *Neisseria meningitidis* elicits a pro-inflammatory response involving IκBζ in a human blood–cerebrospinal fluid barrier model. *Journal of Neuroinflammation*, 11(article 163), 1–18.

BORKOWSKI, J., SCHROTEN, H. & SCHWERK, C. 2020. Interactions and signal transduction pathways involved during central nervous system entry by *Neisseria meningitidis* across the blood–brain barriers. *International Journal of Molecular Sciences*, 21(article 8788), 1–24.

BORROW, R., ABAD, R., TROTTER, C., VAN DER KLIS, F. R. & VAZQUEZ, J. A. 2013. Effectiveness of meningococcal serogroup C vaccine programmes. *Vaccine*, 31, 4477–4486.

BORROW, R., ALARCÓN, P., CARLOS, J., CAUGANT, D. A., CHRISTENSEN, H., DEBBAG, R., DE WALS, P., ECHÁNIZ-AVILES, G., FINDLOW, J. & HEAD, C. 2017. The Global Meningococcal Initiative: global epidemiology, the impact of vaccines on meningococcal disease and the importance of herd protection. *Expert Review of Vaccines*, 16, 313–328.

BOSIS, S., MAYER, A. & ESPOSITO, S. 2015. Meningococcal disease in childhood: epidemiology, clinical features and prevention. *Journal of Preventive Medicine and Hygiene*, 56(3), E121–E124.

BOSLEGO, J., GARCIA, J., CRUZ, C., ZOLLINGER, W., BRANDT, B., RUIZ, S., MARTINEZ, M., ARTHUR, J., UNDERWOOD, P. & SILVA, W. 1995. Efficacy, safety, and immunogenicity of a meningococcal group B (15:P1.3) outer membrane protein vaccine in Iquique, Chile. *Vaccine*, 13, 821–829.

BOULTON, I. C., GORRINGE, A. R., ALLISON, N., ROBINSON, A., GORINSKY, B., JOANNOU, C. L. & EVANS, R. W. 1998. Transferrin-binding protein B isolated from *Neisseria meningitidis* discriminates between apo and diferric human transferrin. *Biochemical Journal*, 334, 269–273.

BRADLEY, C. J., GRIFFITHS, N. J., ROWE, H. A., HEYDERMAN, R. S. & VIRJI, M. 2005. Critical determinants of the interactions of capsule-expressing *Neisseria meningitidis* with host cells: the role of receptor density in increased cellular targeting via the outer membrane Opa proteins. *Cellular Microbiology*, 7, 1490–1503.

BRANDTZAEG, P. & VAN DEUREN, M. 2012. Classification and pathogenesis of meningococcal infections, in CHRISTODOULIDES, M. (ed.) *Neisseria meningitidis: Advanced Methods and Protocols*. Totowa, NJ: Humana, 21–35.

BRANDTZAEG, P., BJERRE, A., ØVSTEBØ, R., BRUSLETTO, B., JOØ, G. B. & KIERULF, P. 2001. Invited review: *Neisseria meningitidis* lipopolysaccharides in human pathology. *Journal of Endotoxin Research*, 7, 401–420.

BRANDTZAEG, P., KIERULF, P., GAUSTAD, P., SKULBERG, A., BRUUN, J. N., HALVORSEN, S. & SØRENSEN, E. 1989. Plasma endotoxin as a predictor of multiple organ failure and death in systemic meningococcal disease. *Journal of Infectious Diseases*, 159, 195–204.

BRAUN, J. M., BLACKWELL, C. C., POXTON, I. R., EL AHMER, O., GORDON, A. E., AL MADANI, O. M., WEIR, D. M., GIERSEN, S. & BEUTH, J. 2002. Proinflammatory responses to lipo-oligosaccharide of *Neisseria meningitidis* immunotype strains in relation to virulence and disease. *Journal of Infectious Diseases*, 185, 1431–1438.

BREHONY, C., JOLLEY, K. A. & MAIDEN, M. C. 2007. Multilocus sequence typing for global surveillance of meningococcal disease. *FEMS Microbiology Reviews*, 31, 15–26.

BRIGHTBILL, H. & MODLIN, R. 2000. Toll-like receptors: molecular mechanisms of the mammalian immune response. *Immunology*, 101(1), 1–10.

BRÖKER, M., EMONET, S., FAZIO, C., JACOBSSON, S., KOLIOU, M., KUUSI, M., PACE, D., PARAGI, M., PYSIK, A. & SIMÕES, M. J. 2015. Meningococcal serogroup Y disease in Europe: continuation of high importance in some European regions in 2013. *Human Vaccines & Immunotherapeutics*, 11, 2281–2286.

BROOKS, A. N., KILGOUR, E. & SMITH, P. D. 2012. Molecular pathways: fibroblast growth factor signaling: a new therapeutic opportunity in cancer. *Clinical Cancer Research*, 18, 1855–1862.

BROUWER, M. C., DE GANS, J., HECKENBERG, S. G., ZWINDERMAN, A. H., VAN DER POLL, T. & VAN DE BEEK, D. 2009. Host genetic susceptibility to pneumococcal and meningococcal disease: a systematic review and meta-analysis. *The Lancet Infectious Diseases*, 9, 31–44.

BROUWER, M. C., MCINTYRE, P., DE GANS, J., PRASAD, K. & VAN DE BEEK, D. 2010. Corticosteroids for acute bacterial meningitis. *Cochrane Database of Systematic Reviews*, article CD004405.

BROWN, D. R., HELAINE, S., CARBONNELLE, E. & PELICIC, V. 2010. Systematic functional analysis reveals that a set of seven genes is involved in fine-tuning of the multiple functions mediated by type IV pili in *Neisseria meningitidis*. *Infection and Immunity*, 78, 3053–3063.

BRUGE, J., BOUVERET-LE CAM, N., DANVE, B., ROUGON, G. & SCHULZ, D. 2004. Clinical evaluation of a group B meningococcal *N*-propionylated polysaccharide conjugate vaccine in adult, male volunteers. *Vaccine*, 22, 1087–1096.

BRUNET, F. G., VOLFF, J.-N. & SCHARTL, M. 2016. Whole genome duplications shaped the receptor tyrosine kinase repertoire of jawed vertebrates. *Genome Biology and Evolution*, 8, 1600–1613.

BRUSLETTO, B. S., LØBERG, E. M., HELLERUD, B. C., GOVERUD, I. L., BERG, J. P., OLSTAD, O. K., GOPINATHAN, U., BRANDTZAEG, P. & ØVSTEBØ, R. 2020. Extensive changes in transcriptomic "fingerprints" and immunological cells in the large organs of patients dying of acute septic shock and multiple organ failure caused by *Neisseria meningitidis*. *Frontiers in Cellular and Infection Microbiology*, 10(article 42), 1–30.

BURMAN, C., SERRA, L., NUTTENS, C., PRESA, J., BALMER, P. & YORK, L. 2019. Meningococcal disease in adolescents and young adults: a review of the rationale for prevention through vaccination. *Human Vaccines & Immunotherapeutics*, 15, 459–469.

CAIN, M. D., SALIMI, H., DIAMOND, M. S. & KLEIN, R. S. 2019. Mechanisms of pathogen invasion into the central nervous system. *Neuron*, 103, 771–783.

CANO-GARRIDO, O., RODRÍGUEZ-CARMONA, E., DÍEZ-GIL, C., VÁZQUEZ, E., ELIZONDO, E., CUBARSI, R., SERAS-FRANZOSO, J., CORCHERO, J. L., RINAS, U. & RATERA, I. 2013. Supramolecular organization of protein-releasing functional amyloids solved in bacterial inclusion bodies. *Acta Biomaterialia*, 9, 6134–6142.

CAPECCHI, B., ADU-BOBIE, J., DI MARCELLO, F., CIUCCHI, L., MASIGNANI, V., TADDEI, A., RAPPUOLI, R., PIZZA, M. & ARICÒ, B. 2005. *Neisseria meningitidis* NadA is a new invasin which promotes bacterial adhesion to and penetration into human epithelial cells. *Molecular Microbiology*, 55, 687–698.

CARBONNELLE, E., HELAINE, S., NASSIF, X. & PELICIC, V. 2006. A systematic genetic analysis in *Neisseria meningitidis* defines the Pil proteins required for assembly, functionality, stabilization and export of type IV pili. *Molecular Microbiology*, 61, 1510–1522.

CARBONNELLE, E., HILL, D. J., MORAND, P., GRIFFITHS, N. J., BOURDOULOUS, S., MURILLO, I., NASSIF, X. & VIRJI, M. 2009. Meningococcal interactions with the host. *Vaccine*, 27(supplement 2), B78–B89.

CARRILLO, J. L. M., GARCÍA, F. P. C., CORONADO, O. G., GARCÍA, M. A. M. & CORDERO, J. F. C. 2017. Physiology and pathology of innate immune response against pathogens, in REZAEI, N. (ed.) *Physiology and Pathology of Immunology*. London: IntechOpen.

CASEY, R., NEWCOMBE, J., MCFADDEN, J. & BODMAN-SMITH, K. B. 2008. The acute-phase reactant C-reactive protein binds to phosphorylcholine-expressing *Neisseria meningitidis* and increases uptake by human phagocytes. *Infection and Immunity*, 76, 1298–1304.

CASTELLANOS, L., BETANCOURT, L., SARDIÑAS, G., PERERA, Y., NIEBLA, O., GARCÍA, D., CABALLERO, E., COBAS, K., GONZÁLEZ, S. & GUILLÉN, G. 2007. Characterization of *N. meningitidis* proteoliposome proteins. Consistency and reproducibility among batches of VA-MENGOC-BC, assessed by proteomic techniques. *Biotecnología Aplicada*, 24(2), 168–171.

CASTILLO, D., HARCOURT, B., HATCHER, C., JACKSON, M., KATZ, L., MAIR R., MAYER, L., NOVAK, R., RAHALISON, L., SCHMINK, S. et al. 2011a. Identification and characterization of *Neisseria meningitidis*, in *Laboratory Methods for the Diagnosis of Meningitis Caused by Neisseria meningitidis, Streptococcus pneumoniae, and Haemophilus influenzae WHO Manual*. 2nd edn. Centers for Disease Control and Prevention, 57–72. Retrieved from: https://stacks.cdc.gov/view/cdc/11632

CASTILLO, D., HARCOURT, B., HATCHER, C., JACKSON, M., KATZ, L., MAIR R., MAYER, L., NOVAK, R., RAHALISON, L., SCHMINK, S. et al. 2011b. Primary culture and presumptive identification of *Neisseria meningitidis*, *Streptococcus pneumoniae*, and *Haemophilus influenzae*, in *Laboratory Methods for the Diagnosis of Meningitis Caused by Neisseria meningitidis, Streptococcus pneumoniae, and Haemophilus influenzae WHO Manual*. 2nd edn. Centers for Disease Control and Prevention, 32–56. Retrieved from: https://stacks.cdc.gov/view/cdc/11632

CAUGANT, D. A. & BRYNILDSRUD, O. B. 2020. *Neisseria meningitidis*: using genomics to understand diversity, evolution and pathogenesis. *Nature Reviews Microbiology*, 18, 84–96.

CAUGANT, D. A. & MAIDEN, M. C. 2009. Meningococcal carriage and disease Population biology and evolution. *Vaccine*, 27(supplement 2), B64–B70.

CAUGANT, D. A., HØIBY, E., MAGNUS, P., SCHEEL, O., HOEL, T., BJUNE, G., WEDEGE, E., ENG, J. & FRØHOLM, L. 1994. Asymptomatic carriage of *Neisseria meningitidis* in a randomly sampled population. *Journal of Clinical Microbiology*, 32, 323–330.

CHAMBERS, C. A., LACEY, C. A., BROWN, D. C. & SKYBERG, J. A. 2021. Nitric oxide inhibits interleukin-1-mediated protection against *Escherichia coli* K1-induced sepsis and meningitis in a neonatal murine model. *Immunology and Cell Biology*, 99, 596–610.

CHAN, L. C., YOUNG, P. R., BLETCHLY, C. & REID, S. 2002. Production of the baculovirus-expressed dengue virus glycoprotein NS1 can be improved dramatically with optimised regimes for fed-batch cultures and the addition of the insect moulting hormone, 20-Hydroxyecdysone. *Journal of Virological Methods*, 105, 87–98.

CHANG, Q., TZENG, Y.-L. & STEPHENS, D. S. 2012. Meningococcal disease: changes in epidemiology and prevention. *Clinical Epidemiology*, 4, 237–245.

CHÁVEZ-BUENO, S. & MCCRACKEN, G. H. 2005. Bacterial meningitis in children. *Pediatric Clinics*, 52, 795–810.

CHEN, I. & DUBNAU, D. 2004. DNA uptake during bacterial transformation. *Nature Reviews Microbiology*, 2, 241–249.

CHOW, J. C., YOUNG, D. W., GOLENBOCK, D. T., CHRIST, W. J. & GUSOVSKY, F. 1999. Toll-like receptor-4 mediates lipopolysaccharide-induced signal transduction. *Journal of Biological Chemistry*, 274, 10689–10692.

CIESIELSKA, A., MATYJEK, M. & KWIATKOWSKA, K. 2021. TLR4 and CD14 trafficking and its influence on LPS-induced pro-inflammatory signaling. *Cellular and Molecular Life Sciences*, 78, 1233–1261.

COHN, A. C., MACNEIL, J. R., CLARK, T. A., ORTEGA-SANCHEZ, I. R., BRIERE, E. Z., MEISSNER, H. C., BAKER, C. J. & MESSONNIER, N. E. 2013. Prevention and control of meningococcal disease: recommendations of the Advisory Committee on Immunization Practices (ACIP). *Morbidity and Mortality Weekly Report: Recommendations and Reports*, 62(2), 1–28.

COLLINS, R. F., DAVIDSEN, L., DERRICK, J. P., FORD, R. C. & TØNJUM, T. 2001. Analysis of the PilQ secretin from *Neisseria meningitidis* by transmission electron microscopy reveals a dodecameric quaternary structure. *Journal of Bacteriology*, 183, 3825–3832.

COLLINS, R. F., FORD, R. C., KITMITTO, A., OLSEN, R. O., TØNJUM, T. & DERRICK, J. P. 2003. Three-dimensional structure of the *Neisseria meningitidis* secretin PilQ determined from negative-stain transmission electron microscopy. *Journal of Bacteriology*, 185, 2611–2617.

COLLINS, R. F., FRYE, S. A., BALASINGHAM, S., FORD, R. C., TØNJUM, T. & DERRICK, J. P. 2005. Interaction with type IV pili induces structural changes in the bacterial outer membrane secretin PilQ. *Journal of Biological Chemistry*, 280, 18923–18930.

COMANDUCCI, M., BAMBINI, S., BRUNELLI, B., ADU-BOBIE, J., ARICÒ, B., CAPECCHI, B., GIULIANI, M. M., MASIGNANI, V., SANTINI, L. & SAVINO, S. 2002. NadA, a novel vaccine candidate of *Neisseria meningitidis*. *Journal of Experimental Medicine*, 195, 1445–1454.

CORNELISSEN, C. N. & HOLLANDER, A. 2011. TonB-dependent transporters expressed by *Neisseria gonorrhoeae*. *Frontiers in Microbiology*, 2(article 117), 1–13.

CORNELISSEN, C. N. 2018. Subversion of nutritional immunity by the pathogenic *Neisseriae*. *Pathogens and Disease*, 76(article ftx112), 1–14.

COUREUIL, M., JOIN-LAMBERT, O., LÉCUYER, H., BOURDOULOUS, S., MARULLO, S. & NASSIF, X. 2012. Mechanism of meningeal invasion by *Neisseria meningitidis*. *Virulence*, 3, 164–172.

COUREUIL, M., JOIN-LAMBERT, O., LÉCUYER, H., BOURDOULOUS, S., MARULLO, S. & NASSIF, X. 2013. Pathogenesis of meningococcemia. *Cold Spring Harbor Perspectives in Medicine*, 3(article a012393), 1–15.

COUREUIL, M., LECUYER, H., BOURDOULOUS, S. & NASSIF, X. 2017. A journey into the brain: insight into how bacterial pathogens cross blood–brain barriers. *Nature Reviews Microbiology*, 15, 149–159.

COUREUIL, M., LÉCUYER, H., SCOTT, M. G., BOULARAN, C., ENSLEN, H., SOYER, M., MIKATY, G., BOURDOULOUS, S., NASSIF, X. & MARULLO, S. 2010. Meningococcus hijacks a β2-adrenoceptor/β-arrestin pathway to cross brain microvasculature endothelium. *Cell*, 143, 1149–1160.

COUREUIL, M., MIKATY, G., MILLER, F., LÉCUYER, H., BERNARD, C., BOURDOULOUS, S., DUMÉNIL, G., MÈGE, R.-M., WEKSLER, B. B. & ROMERO, I. A. 2009. Meningococcal type IV pili recruit the polarity complex to cross the brain endothelium. *Science*, 325, 83–87.

CRAIG, L. & LI, J. 2008. Type IV pili: paradoxes in form and function. *Current Opinion in Structural Biology*, 18, 267–277.

CRAIG, L., VOLKMANN, N., ARVAI, A. S., PIQUE, M. E., YEAGER, M., EGELMAN, E. H. & TAINER, J. A. 2006. Type IV pilus structure by cryo-electron microscopy and crystallography: implications for pilus assembly and functions. *Molecular Cell*, 23, 651–662.

CROSS, M. J., LU, L., MAGNUSSON, P., NYQVIST, D., HOLMQVIST, K., WELSH, M. & CLAESSON-WELSH, L. 2002. The Shb adaptor protein binds to tyrosine 766 in the FGFR-1 and regulates the Ras/MEK/MAPK pathway via FRS2 phosphorylation in endothelial cells. *Molecular Biology of the Cell*, 13(8), 2881–2893.

CRUM-CIANFLONE, N. & SULLIVAN, E. 2016. Meningococcal vaccinations. *Infectious diseases and therapy*, 5**,** 89-112.

CUNHA, C. S. E., GRIFFITHS, N. J. & VIRJI, M. 2010. *Neisseria meningitidis* Opc invasin binds to the sulphated tyrosines of activated vitronectin to attach to and invade human brain endothelial cells. *PLoS Pathogens*, 6(article e1000911), 1–18.

CUNHA, S. E., GRIFFITHS, N. J., MURILLO, I. & VIRJI, M. 2009. *Neisseria meningitidis* Opc invasin binds to the cytoskeletal protein α-actinin. *Cellular Microbiology*, 11, 389–405.

DA SILVA, R. A., KARLYSHEV, A. V., OLDFIELD, N. J., WOOLDRIDGE, K. G., BAYLISS, C. D., RYAN, A. & GRIFFIN, R. 2019. Variant signal peptides of vaccine antigen, FHbp, impair processing affecting surface localization and antibody-mediated killing in most meningococcal isolates. *Frontiers in Microbiology*, 10(article 2847), 1–20.

DAI, S., ZHOU, Z., CHEN, Z., XU, G. & CHEN, Y. 2019. Fibroblast growth factor receptors (FGFRs): structures and small molecule inhibitors. *Cells*, 8(article 614), 1–15.

DALBEY, R. E. & KUHN, A. 2012. Protein traffic in Gram-negative bacteria–how exported and secreted proteins find their way. *FEMS Microbiology Reviews*, 36, 1023–1045.

DANDO, S. J., MACKAY-SIM, A., NORTON, R., CURRIE, B. J., JOHN, J. A. S., EKBERG, J. A., BATZLOFF, M., ULETT, G. C. & BEACHAM, I. R. 2014. Pathogens penetrating the central nervous system: infection pathways and the

cellular and molecular mechanisms of invasion. *Clinical Microbiology Reviews*, 27, 691–726.

DANIELS, C. C., ROGERS, P. D. & SHELTON, C. M. 2016. A review of pneumococcal vaccines: current polysaccharide vaccine recommendations and future protein antigens. *Journal of Pediatric Pharmacology and Therapeutics*, 21, 27–35.

DAUTIN, N. & BERNSTEIN, H. D. 2007. Protein secretion in Gram-negative bacteria via the autotransporter pathway. *Annual Review of Microbiology*, 61, 89–112.

DAVIS, J., WANG, J., TROPEA, J. E., ZHANG, D., DAUTER, Z., WAUGH, D. S. & WLODAWER, A. 2008. Novel fold of VirA, a type III secretion system effector protein from *Shigella flexneri*. *Protein Science*, 17, 2167–2173.

DE CASTRO, M. C. R. & RAMOS-E-SILVA, M. 2020. The rash with mucosal ulceration. *Clinics in Dermatology*, 38, 35–41.

DE FILIPPIS, I., DE LEMOS, A. P. S., HOSTETLER, J. B., WOLLENBERG, K., SACCHI, C. T., HARRISON, L. H., BASH, M. C. & PREVOTS, D. R. 2012. Molecular epidemiology of *Neisseria meningitidis* serogroup B in Brazil. *PLoS One*, 7(article e33016), 1–10.

DE JONGE, M., VIDARSSON, G., VAN DIJKEN, H., HOOGERHOUT, P., VAN ALPHEN, L., DANKERT, J. & VAN DER LEY, P. 2003. Functional activity of antibodies against the recombinant OpaJ protein from *Neisseria meningitidis*. *Infection and Immunity*, 71, 2331–2340.

DE SOUZA, A. L. & SEGURO, A. C. 2008. Two centuries of meningococcal infection: from Vieusseux to the cellular and molecular basis of disease. *Journal of Medical Microbiology*, 57, 1313–1321.

DE VRIES, F. P., COLE, R., DANKERT, J., FROSCH, M. & VAN PUTTEN, J. P. 1998. *Neisseria meningitidis* producing the Opc adhesin binds epithelial cell proteoglycan receptors. *Molecular Microbiology*, 27, 1203–1212.

DEGHMANE, A. E., GIORGINI, D., LARRIBE, M., ALONSO, J. M. & TAHA, M. K. 2002. Down-regulation of pili and capsule of *Neisseria meningitidis* upon contact with epithelial cells is mediated by CrgA regulatory protein. *Molecular Microbiology*, 43, 1555–1564.

DEGHMANE, A.-E., VECKERLÉ, C., GIORGINI, D., HONG, E., RUCKLY, C. & TAHA, M.-K. 2009. Differential modulation of TNF-α–induced apoptosis by *Neisseria meningitidis*. *PLoS Pathogens*, 5(article e1000405), 1–17.

DEL TORDELLO, E., VACCA, I., RAM, S., RAPPUOLI, R. & SERRUTO, D. 2014. *Neisseria meningitidis* NalP cleaves human complement C3, facilitating degradation of C3b and survival in human serum. *Proceedings of the National Academy of Sciences*, 111, 427–432.

DELEPELAIRE, P. 2004. Type I secretion in gram-negative bacteria. *Biochimica et Biophysica Acta (BBA) - Molecular Cell Research*, 1694, 149–161.

DESVAUX, M., HÉBRAUD, M., TALON, R. & HENDERSON, I. R. 2009. Secretion and subcellular localizations of bacterial proteins: a semantic awareness issue. *Trends in Microbiology*, 17, 139–145.

DESVAUX, M., PARHAM, N. J. & HENDERSON, I. R. 2004. The autotransporter secretion system. *Research in Microbiology*, 155, 53–60.

DEVOY, A., DYET, K. & MARTIN, D. 2005. Stability of PorA during a meningococcal disease epidemic. *Journal of Clinical Microbiology*, 43, 832–837.

DJINGAREY, M. H., BARRY, R., BONKOUNGOU, M., TIENDREBEOGO, S., SEBGO, R., KANDOLO, D., LINGANI, C., PREZIOSI, M.-P., ZUBER, P. L. & PEREA, W. 2012. Effectively introducing a new meningococcal A conjugate vaccine in Africa: the Burkina Faso experience. *Vaccine*, 30(supplement 2), B40–B45.

DORAN, K. S., FULDE, M., GRATZ, N., KIM, B. J., NAU, R., PRASADARAO, N., SCHUBERT-UNKMEIR, A., TUOMANEN, E. I. & VALENTIN-WEIGAND, P. 2016. Host–pathogen interactions in bacterial meningitis. *Acta Neuropathologica*, 131, 185–209.

DORSETT, M. & LIANG, S. Y. 2016. Diagnosis and treatment of central nervous system infections in the emergency department. *Emergency Medicine Clinics*, 34, 917–942.

DOS SANTOS SOUZA, I., MAÏSSA, N., ZIVERI, J., MORAND, P. C., COUREUIL, M., NASSIF, X. & BOURDOULOUS, S. 2020. Meningococcal disease: A paradigm of type-IV pilus dependent pathogenesis. *Cellular Microbiology*, 22(article e13185), 1–10.

DRETLER, A., ROUPHAEL, N. & STEPHENS, D. 2018. Progress toward the global control of *Neisseria meningitidis*: 21st century vaccines, current guidelines, and challenges for future vaccine development. *Human Vaccines & Immunotherapeutics*, 14, 1146–1160.

DUCHESNE, L., TISSOT, B., RUDD, T. R., DELL, A. & FERNIG, D. G. 2006. *N*-Glycosylation of fibroblast growth factor receptor 1 regulates ligand and heparan sulfate co-receptor binding. *Journal of Biological Chemistry*, 281, 27178–27189.

DUCHESNE, L., TISSOT, B., RUDD, T. R., DELL, A. & FERNIG, D. G. 2006. *N*-Glycosylation of fibroblast growth factor receptor 1 regulates ligand and heparan sulfate co-receptor binding. *Journal of Biological Chemistry*, 281, 27178–27189.

DUFAILU, O. A., MAHDAVI, J., ALA'ALDEEN, D. A., WOOLDRIDGE, K. G. & OLDFIELD, N. J. 2018. Uptake of Neisserial autotransporter lipoprotein (NalP) promotes an increase in human brain microvascular endothelial cell metabolic activity. *Microbial Pathogenesis*, 124, 70–75.

DUFRENE, Y. F. & PERSAT, A. 2020. Mechanomicrobiology: how bacteria sense and respond to forces. *Nature Reviews Microbiology*, 18, 227–240.

DUMENIL, G. 2011. Revisiting the extracellular lifestyle. *Cellular Microbiology*, 13, 1114–1121.

DUNN, K. L., VIRJI, M. & MOXON, E. R. 1995. Investigations into the molecular basis of meningococcal toxicity for human endothelial and epithelial cells: the synergistic effect of LPS and pili. *Microbial Pathogenesis*, 18, 81–96.

DURANDO, P., FAUST, S. N. & TORRES, A. 2015. Immunological features and clinical benefits of conjugate vaccines against bacteria. *Journal of Immunology Research*, 2015(article 934504), 1–3.

DWILOW, R. & FANELLA, S. 2015. Invasive meningococcal disease in the 21st century—an update for the clinician. *Current Neurology and Neuroscience Reports*, 15(article 2), 1–9.

EADIE, M. J. 2003. A pathology of the animal spirits – the clinical neurology of Thomas Willis (1621–1675) Part II – Disorders of intrinsically abnormal animal spirits. *Journal of Clinical Neuroscience*, 10(2), 146–157.

ELFENBEIN, A. & SIMONS, M. 2013. Syndecan-4 signaling at a glance. *Journal of Cell Science*, 126, 3799–3804.

ENGELHARDT, B. 2008. The blood–central nervous system barriers actively control immune cell entry into the central nervous system. *Current Pharmaceutical Design*, 14, 1555–1565.

ENGSTRÖM, P. E., NORHAGEN, G., BOTTARO, A., CARBONARA, A. O., LEFRANC, G., STEINITZ, M., SÖDER, P., SMITH, C. & HAMMARSTRÖM, L. 1990. Subclass distribution of antigen-specific IgA antibodies in normal donors and

individuals with homozygous C alpha 1 or C alpha 2 gene deletions. *Journal of Immunology*, 145, 109–116.

ERLICH, K. S. & CONGENI, B. L. 2012. Importance of circulating antibodies in protection against meningococcal disease. *Human Vaccines & Immunotherapeutics*, 8, 1029–1035.

ESWARAKUMAR, V., LAX, I. & SCHLESSINGER, J. 2005. Cellular signaling by fibroblast growth factor receptors. *Cytokine & Growth Factor Reviews*, 16, 139–149.

EUGÈNE, E., HOFFMANN, I., PUJOL, C., COURAUD, P.-O., BOURDOULOUS, S. & NASSIF, X. 2002. Microvilli-like structures are associated with the internalization of virulent capsulated *Neisseria meningitidis* into vascular endothelial cells. *Journal of Cell Science*, 115, 1231–1241.

FAELLA, F., PAGLIANO, P., FUSCO, U., ATTANASIO, V. & CONTE, M. 2006. Combined treatment with ceftriaxone and linezolid of pneumococcal meningitis: a case series including penicillin-resistant strains. *Clinical Microbiology and Infection*, 12, 391–394.

FEAVERS, I. M. & MAIDEN, M. C. 2017. Recent progress in the prevention of serogroup B meningococcal disease. *Clinical and Vaccine Immunology*, 24(article e00566-16), 1–13.

FEAVERS, I. M., GRAY, S. J., URWIN, R., RUSSELL, J. E., BYGRAVES, J. A., KACZMARSKI, E. B. & MAIDEN, M. C. 1999. Multilocus sequence typing and antigen gene sequencing in the investigation of a meningococcal disease outbreak. *Journal of Clinical Microbiology*, 37, 3883–3887.

FERNÁNDEZ, L. A. & BERENGUER, J. 2000. Secretion and assembly of regular surface structures in Gram-negative bacteria. *FEMS Microbiology Reviews*, 24, 21–44.

FERREIRA, V. P., PANGBURN, M. K. & CORTÉS, C. 2010. Complement control protein factor H: the good, the bad, and the inadequate. *Molecular Immunology*, 47, 2187–2197.

FIGUEROA, J. & DENSEN, P. 1991. Infectious diseases associated with complement deficiencies. *Clinical microbiology reviews*, 4**,** 359-395.

FINDLOW, H., CAMPBELL, H., LUCIDARME, J., ANDREWS, N., LINLEY, E., LADHANI, S. & BORROW, R. 2019. Serogroup C *Neisseria meningitidis* disease epidemiology, seroprevalence, vaccine effectiveness and waning immunity, England, 1998/99 to 2015/16. *Eurosurveillance*, 24(article 1700818), 1–11.

FINNE, J., BITTER-SUERMANN, D., GORIDIS, C. & FINNE, U. 1987. An IgG monoclonal antibody to group B meningococci cross-reacts with developmentally regulated polysialic acid units of glycoproteins in neural and extraneural tissues. *Journal of Immunology*, 138, 4402–4407.

FLEXNER, S. 1913. The results of the serum treatment in thirteen hundred cases of epidemic meningitis. *Journal of Experimental Medicine*, 17, 553–576.

FRANZOSO, S., MAZZON, C., SZTUKOWSKA, M., CECCHINI, P., KASIC, T., CAPECCHI, B., TAVANO, R. & PAPINI, E. 2008. Human monocytes/macrophages are a target of *Neisseria meningitidis* Adhesin A (NadA). *Journal of Leukocyte Biology*, 83, 1100–1110.

FRASCH, C. E., ZOLLINGER, W. D. & POOLMAN, J. T. 1985. Serotype antigens of *Neisseria meningitidis* and a proposed Scbemefor designation of serotypes. *Reviews of Infectious Diseases*, 7, 504–510.

FROSCH, M., WEISGERBER, C. & MEYER, T. F. 1989. Molecular characterization and expression in Escherichia coli of the gene complex encoding the polysaccharide capsule of *Neisseria meningitidis* group B. *Proceedings of the National Academy of Sciences*, 86, 1669–1673.

FU, J., LI, L., YANG, X., YANG, R., AMJAD, N., LIU, L., TAN, C., CHEN, H. & WANG, X. 2019. Transactivated epidermal growth factor receptor recruitment of α-actinin-4 from F-actin contributes to invasion of brain microvascular endothelial cells by meningitic *Escherichia coli*. *Frontiers in Cellular and Infection Microbiology*, 8(article 448), 1–16.

FURDUI, C. M., LEW, E. D., SCHLESSINGER, J. & ANDERSON, K. S. 2006. Autophosphorylation of FGFR1 kinase is mediated by a sequential and precisely ordered reaction. *Molecular Cell*, 21, 711–717.

GABUTTI, G., STEFANATI, A. & KUHDARI, P. 2015. Epidemiology of *Neisseria meningitidis* infections: case distribution by age and relevance of carriage. *Journal of Preventive Medicine and Hygiene*, 56(3), E116–E120.

GAGNEUX, S., WIRTH, T., HODGSON, A., EHRHARD, I., MORELLI, G., KRIZ, P., GENTON, B., SMITH, T., BINKA, F. & PLUSCHKE, G. 2002. Clonal groupings in serogroup X *Neisseria meningitidis*. *Emerging Infectious Diseases*, 8(5), 462–466.

GANDHI, A., BALMER, P. & YORK, L. J. 2016. Characteristics of a new meningococcal serogroup B vaccine, bivalent rLP2086 (MenB-FHbp; Trumenba®). *Postgraduate Medicine*, 128, 548–556.

GARCÍA, D., YERO, D., NIEBLA, O., COBAS, K., PERERA, Y., CABALLERO, E., DELGADO, M. & PAJÓN, R. 2012. Predicted proteins of *Neisseria meningitidis* as potential vaccine candidates: from in silico analyses to experimental corroboration. *Biotecnología Aplicada*, 29, 22–28.

GARRITY, G. M., BELL, J. A. & LILBURN, T. 2005. Class II. Betaproteobacteria *class. nov.*, in BRENNER, D. J., KRIEG, N. R. & STALEY, G. T. (eds.) *Bergey's Manual of Systematic Bacteriology*. Boston, MA: Springer, 575–922.

GASPARINI, R. & PANATTO, D. 2011. Meningococcal glycoconjugate vaccines. *Human Vaccines*, 7, 170–182.

GASPARINI, R., AMICIZIA, D., LAI, P. L. & PANATTO, D. 2012. *Neisseria meningitidis*, pathogenetic mechanisms to overcome the human immune defences. *Journal of Preventive Medicine and Hygiene*, 53, 50–55.

GASPARINI, R., PANATTO, D., BRAGAZZI, N., LAI, P., BECHINI, A., LEVI, M., DURANDO, P. & AMICIZIA, D. 2015. How the knowledge of interactions between meningococcus and the human immune system has been used to prepare effective *Neisseria meningitidis* vaccines. *Journal of Immunology Research*, 2015(article 189153), 1–27.

GAULT, J., FERBER, M., MACHATA, S., IMHAUS, A.-F., MALOSSE, C., CHARLES-ORSZAG, A., MILLIEN, C., BOUVIER, G., BARDIAUX, B. & PÉHAU-ARNAUDET, G. 2015. *Neisseria meningitidis* type IV pili composed of sequence invariable pilins are masked by multisite glycosylation. *PLoS Pathogens*, 11(article e1005162), 1–24.

GENEVROIS, S., STEEGHS, L., ROHOLL, P., LETESSON, J. J. & VAN DER LEY, P. 2003. The Omp85 protein of *Neisseria meningitidis* is required for lipid export to the outer membrane. *EMBO Journal*, 22, 1780–1789.

GEOFFROY, M.-C., FLOQUET, S., MÉTAIS, A., NASSIF, X. & PELICIC, V. 2003. Large-scale analysis of the meningococcus genome by gene disruption: resistance to complement-mediated lysis. *Genome Research*, 13, 391–398.

GHANNAM, J. Y. & AL KHARAZI, K. A. 2019. Neuroanatomy, cranial meninges, in *StatPearls*. Treasure Island, FL: StatPearls Publishing. Available from: https://www.ncbi.nlm.nih.gov/books/NBK539882/

GIUFRÈ, M., CARDINES, R., CAPORALI, M. G., ACCOGLI, M., D'ANCONA, F. & CERQUETTI, M. 2011. Ten years of Hib vaccination in Italy: prevalence of non-encapsulated *Haemophilus influenzae* among invasive isolates and the possible impact on antibiotic resistance. *Vaccine*, 29, 3857–3862.

GOLD, R., LEPOW, M. L., GOLDSCHNEIDER, I. & GOTSCHLICH, E. C. 1977. Immune response of human infants to polysaccharide vaccines of groups A and C *Neisseria meningitidis*. *Journal of Infectious Diseases*, 136(supplement 1), S31–S35.

GOLD, R., LEPOW, M. L., GOLDSCHNEIDER, I., DRAPER, T. & GOTSCHLICH, E. 1975. Clinical evaluation of group A and group C meningococcal polysaccharide vaccines in infants. *Journal of Clinical Investigation*, 56, 1536–1547.

GONZÁLEZ-GONZÁLEZ, E., PALESTINO-DÍAZ, I., LÓPEZ-PACHECO, F., MÁRQUEZ-IPIÑA, A. R., LARA-MAYORGA, I. M., TRUJILLO-DE SANTIAGO, G. & ALVAREZ, M. M. 2020. Rapid and cost-effective development of stable clones for the production of anti-Ebola monoclonal antibodies in HEK293T cells. *bioRxiv*. Available from :https://doi.org/10.1101/2020.04.21.054429

GORRINGE, A. R. & PAJÓN, R. 2012. Bexsero: a multicomponent vaccine for prevention of meningococcal disease. *Human Vaccines & Immunotherapeutics*, 8, 174–183.

GOTOH, N. 2008. Regulation of growth factor signaling by FRS2 family docking/scaffold adaptor proteins. *Cancer science,* 99**,** 1319-1325.

GOTSCHLICH, E. C., GOLDSCHNEIDER, I. & ARTENSTEIN, M. S. 1969. Human immunity to the meningococcus: IV. Immunogenicity of group A and group C meningococcal polysaccharides in human volunteers. *Journal of Experimental Medicine*, 129, 1367–1384.

GRAY-OWEN, S. D. & BLUMBERG, R. S. 2006. CEACAM1: contact-dependent control of immunity. *Nature Reviews Immunology*, 6, 433–446.

GREEN, E. R. & MECSAS, J. 2016. Bacterial secretion systems: an overview. *Microbiology Spectrum*, 4(article VMBF-0012-2015), 1–19.

GRIFANTINI, R., BARTOLINI, E., MUZZI, A., DRAGHI, M., FRIGIMELICA, E., BERGER, J., RANDAZZO, F. & GRANDI, G. 2002a. Gene expression profile in *Neisseria meningitidis* and *Neisseria lactamica* upon host-cell contact: from basic

research to vaccine development. *Annals of the New York Academy of Sciences,* 975**,** 202-216.

GRIFANTINI, R., BARTOLINI, E., MUZZI, A., DRAGHI, M., FRIGIMELICA, E., BERGER, J., RATTI, G., PETRACCA, R., GALLI, G. & AGNUSDEI, M. 2002b. Previously unrecognized vaccine candidates against group B meningococcus identified by DNA microarrays. *Nature biotechnology,* 20**,** 914-921.

GRIFFISS, J. M., YAMASAKI, R., ESTABROOK, M. & KIM, J. J. 1991. Meningococcal molecular mimicry and the search for an ideal vaccine. *Transactions of the Royal Society of Tropical Medicine and Hygiene*, 85, 32–36.

GRIFFITHS, M. J., MCGILL, F. & SOLOMON, T. 2018. Management of acute meningitis. *Clinical Medicine*, 18, 164–169.

GRIFFITHS, N. J., BRADLEY, C. J., HEYDERMAN, R. S. & VIRJI, M. 2007. IFN-γ amplifies NFκB-dependent *Neisseria meningitidis* invasion of epithelial cells via specific upregulation of CEA-related cell adhesion molecule 1. *Cellular Microbiology*, 9, 2968–2983.

GUDERNOVA, I., VESELA, I., BALEK, L., BUCHTOVA, M., DOSEDELOVA, H., KUNOVA, M., PIVNICKA, J., JELINKOVA, I., ROUBALOVA, L. & KOZUBIK, A. 2016. Multikinase activity of fibroblast growth factor receptor (FGFR) inhibitors SU5402, PD173074, AZD1480, AZD4547 and BGJ398 compromises the use of small chemicals targeting FGFR catalytic activity for therapy of short-stature syndromes. *Human Molecular Genetics*, 25, 9–23.

HADI, H. A., WOOLDRIDGE, K. G., ROBINSON, K. & ALA'ALDEEN, D. A. 2001. Identification and characterization of App: an immunogenic autotransporter protein of *Neisseria meningitidis*. *Molecular Microbiology*, 41, 611–623.

HAGLUND, C. M. & WELCH, M. D. 2011. Pathogens and polymers: microbe–host interactions illuminate the cytoskeleton. *Journal of Cell Biology*, 195, 7–17.

HARRIS, S. L., ZHU, D., MURPHY, E., MCNEIL, L. K., WANG, X., MAYER, L. W., HARRISON, L. H., JANSEN, K. U. & ANDERSON, A. S. 2011. Preclinical evidence for the potential of a bivalent fHBP vaccine to prevent *Neisseria meningitidis* serogroup C disease. *Human Vaccines*, 7, 68–74.

HARRISON, L. H. 2006. Prospects for vaccine prevention of meningococcal infection. *Clinical Microbiology Reviews*, 19, 142–164.

HARRISON, L. H., MOHAN, N. & KIRKPATRICK, P. 2010. Meningococcal group A, C, Y and W-135 conjugate vaccine. *Nature reviews. Drug discovery*, 9**,** 429.

HARRISON, L. H., TROTTER, C. L. & RAMSAY, M. E. 2009. Global epidemiology of meningococcal disease. *Vaccine*, 27(supplement 2), B51–B63.

HARRISON, O. B., CLAUS, H., JIANG, Y., BENNETT, J. S., BRATCHER, H. B., JOLLEY, K. A., CORTON, C., CARE, R., POOLMAN, J. T. & ZOLLINGER, W. D. 2013. Description and nomenclature of *Neisseria meningitidis* capsule locus. *Emerging Infectious Diseases*, 19(4), 566–573.

HART, K. C., ROBERTSON, S. C., KANEMITSU, M. Y., MEYER, A. N., TYNAN, J. A. & DONOGHUE, D. J. 2000. Transformation and Stat activation by derivatives of FGFR1, FGFR3, and FGFR4. *Oncogene*, 19, 3309–3320.

HARVEY, D., HOLT, D. E. & BEDFORD, H. 1999. Bacterial meningitis in the newborn: a prospective study of mortality and morbidity. *Seminars in Perinatology*, 23(3), 218–225.

HASAN, M. M., RAGNARSSON, L., CARDOSO, F. C. & LEWIS, R. J. 2021. Transfection methods for high-throughput cellular assays of voltage-gated calcium and sodium channels involved in pain. *PLoS One*, 16(article e0243645), 1–18.

HAUGSTEN, E. M., WIEDLOCHA, A., OLSNES, S. & WESCHE, J. 2010. Roles of fibroblast growth factor receptors in carcinogenesis. *Molecular Cancer Research*, 8, 1439–1452.

HAWLEY-NELSON, P., CICCARONE, V. & MOORE, M. L. 2008. Transfection of cultured eukaryotic cells using cationic lipid reagents. *Current Protocols in Molecular Biology*, 81, 9.4.1–9.4.17.

HEDARI, C. P., KHINKARLY, R. W. & DBAIBO, G. S. 2014. Meningococcal serogroups A, C, W-135, and Y tetanus toxoid conjugate vaccine: a new conjugate vaccine against invasive meningococcal disease. *Infection and Drug Resistance*, 7, 85–99.

HEISE, T. & DERSCH, P. 2006. Identification of a domain in *Yersinia* virulence factor YadA that is crucial for extracellular matrix-specific cell adhesion and uptake. *Proceedings of the National Academy of Sciences*, 103, 3375–3380.

HÉLAINE, S., CARBONNELLE, E., PROUVENSIER, L., BERETTI, J. L., NASSIF, X. & PELICIC, V. 2005. PilX, a pilus-associated protein essential for bacterial aggregation, is a key to pilus-facilitated attachment of *Neisseria meningitidis* to human cells. *Molecular Microbiology*, 55, 65–77.

HELLERUD, B. C., AASE, A., HERSTAD, T. K., NÆSS, L. M., KRISTIANSEN, L. H., TRØSEID, A.-M. S., HARBOE, M., LAPPEGÅRD, K. T., BRANDTZÆG, P. & HØIBY, E. A. 2010. Critical roles of complement and antibodies in host defense mechanisms against *Neisseria meningitidis* as revealed by human complement genetic deficiencies. *Infection and Immunity*, 78, 802–809.

HENDERSON, I. R., CAPPELLO, R. & NATARO, J. P. 2000. Autotransporter proteins, evolution and redefining protein secretion. *Trends in Microbiology*, 8, 529–532.

HENDERSON, I. R., NAVARRO-GARCIA, F. & NATARO, J. P. 1998. The great escape: structure and function of the autotransporter proteins. *Trends in Microbiology*, 6, 370–378.

HENDERSON, I. R., NAVARRO-GARCIA, F., DESVAUX, M., FERNANDEZ, R. C. & ALA'ALDEEN, D. 2004. Type V protein secretion pathway: the autotransporter story. *Microbiology and Molecular Biology Reviews*, 68(4), 692–744.

HENRIQUES-NORMARK, B. & TUOMANEN, E. I. 2013. The pneumococcus: epidemiology, microbiology, and pathogenesis. *Cold Spring Harbor Perspectives in Medicine*, 3(article a010215), 1–16.

HEROLD, R., SCHROTEN, H. & SCHWERK, C. 2019. Virulence factors of meningitis-causing bacteria: enabling brain entry across the blood–brain barrier. *International Journal of Molecular Sciences*, 20(article 5393), 1–28.

HILL, D. J., GRIFFITHS, N. J., BORODINA, E. & VIRJI, M. 2010. Cellular and molecular biology of *Neisseria meningitidis* colonization and invasive disease. *Clinical Science*, 118, 547–564.

HITCHCOCK, P. J. 1989. Unified nomenclature for pathogenic *Neisseria* species. *Clinical Microbiology Reviews*, 2(supplement), S64–S65.

HODEIB, S., HERBERG, J. A., LEVIN, M. & SANCHO-SHIMIZU, V. 2020. Human genetics of meningococcal infections. *Human Genetics*, 139, 961–980.

HOFFMAN, O. & WEBER, J. R. 2009. Pathophysiology and treatment of bacterial meningitis. *Therapeutic Advances in Neurological Disorders*, 2, 401–412.

HOFFMANN, I., EUGÈNE, E., NASSIF, X., COURAUD, P.-O. & BOURDOULOUS, S. 2001. Activation of ErbB2 receptor tyrosine kinase supports invasion of endothelial cells by *Neisseria meningitidis*. *Journal of Cell Biology*, 155, 133–144.

HOLST, J., MARTIN, D., ARNOLD, R., HUERGO, C. C., OSTER, P., O'HALLAHAN, J. & ROSENQVIST, E. 2009. Properties and clinical performance of vaccines

containing outer membrane vesicles from *Neisseria meningitidis*. *Vaccine*, 27(supplement 2), B3–B12.

HUANG, S.-H. & JONG, A. 2009. Evolving role of laminin receptors in microbial pathogenesis and therapeutics of CNS infection. *Future Microbiology*, 4, 959–962.

HUMPHRIES, H. E., TRIANTAFILOU, M., MAKEPEACE, B. L., HECKELS, J. E., TRIANTAFILOU, K. & CHRISTODOULIDES, M. 2005. Activation of human meningeal cells is modulated by lipopolysaccharide (LPS) and non-LPS components of *Neisseria meningitidis* and is independent of Toll-like receptor (TLR) 4 and TLR2 signalling. *Cellular Microbiology*, 7, 415–430.

HUNG, M.-C. & CHRISTODOULIDES, M. 2013. The biology of *Neisseria* adhesins. *Biology*, 2, 1054–1109.

HUNG, M.-C., HECKELS, J. E. & CHRISTODOULIDES, M. 2013. The adhesin complex protein (ACP) of *Neisseria meningitidis* is a new adhesin with vaccine potential. *mBio*, 4(article e00041-13), 1–10.

HUNTER, T. 1998. The Croonian Lecture 1997. The phosphorylation of proteins on tyrosine: its role in cell growth and disease. *Philosophical Transactions of the Royal Society of London. Series B: Biological Sciences*, 353, 583–605.

HURTADO-ALVARADO, G., VELÁZQUEZ-MOCTEZUMA, J. & GÓMEZ-GONZÁLEZ, B. 2017. Chronic sleep restriction disrupts interendothelial junctions in the hippocampus and increases blood–brain barrier permeability. *Journal of Microscopy*, 268, 28–38.

HUSSAIN, S., PETERSON, J. H. & BERNSTEIN, H. D. 2020. Bam complex-mediated assembly of bacterial outer membrane proteins synthesized in an in vitro translation system. *Scientific Reports*, 10(article 4557), 1–8.

IBRAHIMI, O. A., ZHANG, F., LANG HRSTKA, S. C., MOHAMMADI, M. & LINHARDT, R. J. 2004. Kinetic model for FGF, FGFR, and proteoglycan signal transduction complex assembly. *Biochemistry*, 43, 4724–4730.

IDOSA, B. A., KELLY, A., JACOBSSON, S., DEMIREL, I., FREDLUND, H., SÄRNDAHL, E. & PERSSON, A. 2019. *Neisseria meningitidis*-induced caspase-1 activation in human innate immune cells is LOS-dependent. *Journal of Immunology Research*, 2019(article 6193186), 1–13.

IMHAUS, A. F. & DUMÉNIL, G. 2014. The number of *Neisseria meningitidis* type IV pili determines host cell interaction. *EMBO Journal*, 33, 1767–1783.

IRWIN, S. W., AVERIL, N., CHENG, C. Y. & SCHRYVERS, A. B. 1993. Preparation and analysis of isogenic mutants in the transferrin receptor protein genes, tbpA and tbpB, from *Neisseria meningitidis*. *Molecular Microbiology*, 8, 1125–1133.

JACOB-DUBUISSON, F., GUÉRIN, J., BAELEN, S. & CLANTIN, B. 2013. Two-partner secretion: as simple as it sounds? *Research in Microbiology*, 164, 583–595.

JACOB-DUBUISSON, F., LOCHT, C. & ANTOINE, R. 2001. Two-partner secretion in Gram-negative bacteria: a thrifty, specific pathway for large virulence proteins. *Molecular Microbiology*, 40, 306–313.

JAFRI, R. Z., ALI, A., MESSONNIER, N. E., TEVI-BENISSAN, C., DURRHEIM, D., ESKOLA, J., FERMON, F., KLUGMAN, K. P., RAMSAY, M. & SOW, S. 2013. Global epidemiology of invasive meningococcal disease. *Population Health Metrics*, 11(article 17), 1–9.

JAMET, A. & NASSIF, X. 2015. New players in the toxin field: polymorphic toxin systems in bacteria. *mBio*, 6(article e00285-15), 1–8.

JANEWAY, JR., C. A. & MEDZHITOV, R. 2002. Innate immune recognition. *Annual Review of Immunology*, 20, 197–216.

JANEWAY, JR., C. A. 1989. Approaching the asymptote? Evolution and revolution in immunology. *Cold Spring Harbor Symposia on Quantitative Biology*, 54, 1–13.

JARVA, H., RAM, S., VOGEL, U., BLOM, A. M. & MERI, S. 2005. Binding of the complement inhibitor C4bp to serogroup B *Neisseria meningitidis*. *Journal of Immunology*, 174, 6299–6307.

JENNINGS, M. P., SRIKHANTA, Y. N., MOXON, E. R., KRAMER, M., POOLMAN, J. T., KUIPERS, B. & VAN DER LEY, P. 1999. The genetic basis of the phase variation repertoire of lipopolysaccharide immunotypes in *Neisseria meningitidis*. The GenBank accession number for the sequence reported in this paper is U65788. *Microbiology*, 145, 3013–3021.

JÓDAR, L., FEAVERS, I. M., SALISBURY, D. & GRANOFF, D. M. 2002. Development of vaccines against meningococcal disease. *The Lancet*, 359, 1499–1508.

JOHN, C. C. 1994. Treatment failure with use of a third-generation cephalosporin for penicillin-resistant pneumococcal meningitis: case report and review. *Clinical Infectious Diseases*, 18, 188–193.

JOHNSON, J. R., OSWALD, E., O'BRYAN, T. T., KUSKOWSKI, M. A. & SPANJAARD, L. 2002. Phylogenetic distribution of virulence-associated genes among

Escherichia coli isolates associated with neonatal bacterial meningitis in the Netherlands. *Journal of Infectious Diseases*, 185, 774–784.

JOHSWICH, K. 2017. Innate immune recognition and inflammation in *Neisseria meningitidis* infection. *Pathogens and Disease*, 75(article ftx022), 1–17.

JOHSWICH, K. O., ZHOU, J., LAW, D. K., ST. MICHAEL, F., MCCAW, S. E., JAMIESON, F. B., COX, A. D., TSANG, R. S. & GRAY-OWEN, S. D. 2012. Invasive potential of nonencapsulated disease isolates of *Neisseria meningitidis*. *Infection and Immunity*, 80, 2346–2353.

JOIN-LAMBERT, O., MORAND, P. C., CARBONNELLE, E., COUREUIL, M., BILLE, E., BOURDOULOUS, S. & NASSIF, X. 2010. Mechanisms of meningeal invasion by a bacterial extracellular pathogen, the example of *Neisseria meningitidis*. *Progress in Neurobiology*, 91, 130–139.

JOLLEY, K. A., APPLEBY, L., WRIGHT, J. C., CHRISTODOULIDES, M. & HECKELS, J. E. 2001. Immunization with recombinant Opc outer membrane protein from *Neisseria meningitidis*: influence of sequence variation and levels of expression on the bactericidal immune response against meningococci. *Infection and Immunity*, 69, 3809–3816.

JONES, D. M., BORROW, R., FOX, A. J., GRAY, S., CARTWRIGHT, K. A. & POOLMAN, J. T. 1992. The lipooligosaccharide immunotype as a virulence determinant in *Neisseria meningitidis*. *Microbial Pathogenesis*, 13, 219–224.

JOSE, J., JÄHNIG, F. & MEYER, T. F. 1995. Common structural features of IgA1 protease-like outer membrane protein autotransporters. *Molecular Microbiology*, 18, 378–380.

JUDELSOHN, R. & MARSHALL, G. 2012. The burden of infant meningococcal disease in the United States. *Journal of the Pediatric Infectious Diseases Society*, 1, 64–73.

KAHLER, C. M. & STEPHENS, D. S. 1998. Genetic basis for biosynthesis, structure, and function of meningococcal lipooligosaccharide (endotoxin). *Critical Reviews in Microbiology*, 24, 281–334.

KAHLER, C. M., CARLSON, R. W., RAHMAN, M. M., MARTIN, L. E. & STEPHENS, D. S. 1996. Inner core biosynthesis of lipooligosaccharide (LOS) in *Neisseria meningitidis* serogroup B: identification and role in LOS assembly of the α1,2 *N*-acetylglucosamine transferase (RfaK). *Journal of Bacteriology*, 178, 1265–1273.

KAHLER, C. M., LYONS-SCHINDLER, S., CHOUDHURY, B., GLUSHKA, J., CARLSON, R. W. & STEPHENS, D. S. 2006. *O*-Acetylation of the terminal *N*-

acetylglucosamine of the lipooligosaccharide inner core in *Neisseria meningitidis*: influence on inner core structure and assembly. *Journal of Biological Chemistry*, 281, 19939–19948.

KAHLER, C. M., MARTIN, L. E., TZENG, Y.-L., MILLER, Y. K., SHARKEY, K., STEPHENS, D. S. & DAVIES, J. K. 2001. Polymorphisms in pilin glycosylation locus of *Neisseria meningitidis* expressing class II pili. *Infection and Immunity*, 69, 3597–3604.

KAHLER, C. M., NAWROCKI, K., ANANDAN, A., VRIELINK, A. & SHAFER, W. M. 2018. Structure–function relationships of the Neisserial EptA enzyme responsible for phosphoethanolamine decoration of lipid A: rationale for drug targeting. *Frontiers in Microbiology*, 9(article 1922), 1–11.

KAHLER, C., MARTIN, L., SHIH, G., RAHMAN, M., CARLSON, R. & STEPHENS, D. 1998. The (α2→8)-linked polysialic acid capsule and lipooligosaccharide structure both contribute to the ability of serogroup B *Neisseria meningitidis* to resist the bactericidal activity of normal human serum. *Infection and Immunity*, 66, 5939–5947.

KÄLLSTRÖM, H., ISLAM, M. S., BERGGREN, P.-O. & JONSSON, A.-B. 1998. Cell signaling by the type IV pili of pathogenic *Neisseria*. *Journal of Biological Chemistry*, 273, 21777–21782.

KÄLLSTRÖM, H., LISZEWSKI, M. K., ATKINSON, J. P. & JONSSON, A. B. 1997. Membrane cofactor protein (MCP or CD46) is a cellular pilus receptor for pathogenic *Neisseria*. *Molecular Microbiology*, 25, 639–647.

KANDA, S., LANDGREN, E., LJUNGSTRÖM, M. & CLAESSON-WELSH, L. 1996. Fibroblast growth factor receptor 1-induced differentiation of endothelial cell line established from tsA58 large T transgenic mice. *Cell Growth & Differentiation: The Molecular Biology Journal of the American Association for Cancer Research*, 7(3), 383–395.

KANONENBERG, K., SCHWARZ, C. K. & SCHMITT, L. 2013. Type I secretion systems–a story of appendices. *Research in Microbiology*, 164, 596–604.

KÁŇOVÁ, E., JIMÉNEZ-MUNGUÍA, I., MAJEROVÁ, P., TKÁČOVÁ, Z., BHIDE, K., MERTINKOVÁ, P., PULZOVÁ, L., KOVÁČ, A. & BHIDE, M. 2018. Deciphering the interactome of *Neisseria meningitidis* with human brain microvascular endothelial cells. *Frontiers in Microbiology*, 9(article 2294), 1–13.

KÁŇOVÁ, E., TKÁČOVÁ, Z., BHIDE, K., KULKARNI, A., JIMÉNEZ-MUNGUÍA, I., MERTINKOVÁ, P., DRÁŽOVSKÁ, M., TYAGI, P. & BHIDE, M. 2019. Transcriptome analysis of human brain microvascular endothelial cells response to *Neisseria meningitidis* and its antigen MafA using RNA-seq. *Scientific Reports*, 9(article 18763), 1–16.

KANY, S., VOLLRATH, J. T. & RELJA, B. 2019. Cytokines in inflammatory disease. *International Journal of Molecular Sciences*, 20(article 6008), 1–31.

KARVE, S. S. & WEISS, A. A. 2014. Glycolipid binding preferences of Shiga toxin variants. *PLoS One*, 9(article e101173), 1–10.

KAWAI, T. & AKIRA, S. 2010. The role of pattern-recognition receptors in innate immunity: update on Toll-like receptors. *Nature Immunology*, 11, 373–384.

KAWASAKI, T. & KAWAI, T. 2014. Toll-like receptor signaling pathways. *Frontiers in Immunology*, 5(article 461), 1–8.

KHAIRALLA, A. S., OMER, S. A., MAHDAVI, J., ASLAM, A., DUFAILU, O. A., SELF, T., JONSSON, A. B., GEÖRG, M., SJÖLINDER, H. & ROYER, P. J. 2015. Nuclear trafficking, histone cleavage and induction of apoptosis by the meningococcal App and MspA autotransporters. *Cellular Microbiology*, 17, 1008–1020.

KHASAWNEH, A. H., GARLING, R. J. & HARRIS, C. A. 2018. Cerebrospinal fluid circulation: What do we know and how do we know it? *Brain Circulation*, 4(1), 14–18.

KIM, D. H., HUEGEL, J., TAYLOR, B. L., NUSS, C. A., WEISS, S. N., SOSLOWSKY, L. J., MAUCK, R. L. & KUNTZ, A. F. 2020. Biocompatibility and bioactivity of an FGF-loaded microsphere-based bilayer delivery system. *Acta Biomaterialia*, 111, 341–348.

KIM, J. H., JIANG, S., ELWELL, C. A. & ENGEL, J. N. 2011. *Chlamydia trachomatis* co-opts the FGF2 signaling pathway to enhance infection. *PLoS Pathogens*, 7(article e1002285), 1–18.

KIM, K. J., ELLIOTT, S. J., DI CELLO, F., STINS, M. F. & KIM, K. S. 2003. The K1 capsule modulates trafficking of *E. coli*-containing vacuoles and enhances intracellular bacterial survival in human brain microvascular endothelial cells. *Cellular Microbiology*, 5, 245–252.

KIM, K. S. 2006. Microbial translocation of the blood–brain barrier. *International Journal for Parasitology*, 36, 607–614.

KIM, K. S. 2008. Mechanisms of microbial traversal of the blood–brain barrier. *Nature Reviews Microbiology*, 6, 625–634.

KIM, K. S. 2010. Acute bacterial meningitis in infants and children. *The Lancet Infectious Diseases*, 10, 32–42.

KIM, M., ASHIDA, H., OGAWA, M., YOSHIKAWA, Y., MIMURO, H. & SASAKAWA, C. 2010. Bacterial interactions with the host epithelium. *Cell host & microbe*, 8**,** 20-35.

KIM, T. K. & EBERWINE, J. H. 2010. Mammalian cell transfection: the present and the future. *Analytical and Bioanalytical Chemistry*, 397, 3173–3178.

KIM, W. M., HUANG, Y.-H., GANDHI, A. & BLUMBERG, R. S. 2019. CEACAM1 structure and function in immunity and its therapeutic implications. *Seminars in Immunology*, 42(article 101296).

KING, P. 2012. *Haemophilus influenzae* and the lung (*Haemophilus* and the lung). *Clinical and translational medicine*, 1(article 10), 1–9.

KIRCHNER, M. & MEYER, T. F. 2005. The PilC adhesin of the Neisseria type IV pilus–binding specificities and new insights into the nature of the host cell receptor. *Molecular Microbiology*, 56, 945–957.

KIRCHNER, M., HEUER, D. & MEYER, T. F. 2005. CD46-independent binding of neisserial type IV pili and the major pilus adhesin, PilC, to human epithelial cells. *Infection and Immunity*, 73, 3072–3082.

KLAUSER, T., POHLNER, J. & MEYER, T. F. 1993. The secretion pathway of IgA protease-type proteins in Gram-negative bacteria. *Bioessays*, 15, 799–805.

KNIGHTS, V. & COOK, S. J. 2010. De-regulated FGF receptors as therapeutic targets in cancer. *Pharmacology & Therapeutics*, 125, 105–117.

KNOWLES, T. J., SCOTT-TUCKER, A., OVERDUIN, M. & HENDERSON, I. R. 2009. Membrane protein architects: the role of the BAM complex in outer membrane protein assembly. *Nature Reviews Microbiology*, 7, 206–214.

KOLAPPAN, S., COUREUIL, M., YU, X., NASSIF, X., EGELMAN, E. H. & CRAIG, L. 2016. Structure of the *Neisseria meningitidis* Type IV pilus. *Nature Communications*, 7(article 13015), 1–12.

KORNEV, A. P., HASTE, N. M., TAYLOR, S. S. & TEN EYCK, L. F. 2006. Surface comparison of active and inactive protein kinases identifies a conserved activation mechanism. *Proceedings of the National Academy of Sciences*, 103, 17783–17788.

KRELL, T., RENAULD-MONGÉNIE, G., NICOLAï, M.-C., FRAYSSE, S., CHEVALIER, M., BÉRARD, Y., OAKHILL, J., EVANS, R. W., GORRINGE, A. & LISSOLO, L. 2003. Insight into the structure and function of the transferrin receptor from *Neisseria meningitidis* using microcalorimetric techniques. *Journal of Biological Chemistry*, 278, 14712–14722.

KREWULAK, K. D. & VOGEL, H. J. 2008. Structural biology of bacterial iron uptake. *Biochimica et Biophysica Acta (BBA) - Biomembranes*, 1778, 1781–1804.

KRÜGER, S., EICHLER, E., STROBEL, L., SCHUBERT-UNKMEIR, A. & JOHSWICH, K. O. 2018. Differential influences of complement on neutrophil responses to *Neisseria meningitidis* infection. *Pathogens and Disease*, 76(article fty086), 1–11.

KRUKONIS, E. S. & THOMSON, J. J. 2020. Complement evasion mechanisms of the systemic pathogens *Yersiniae* and *Salmonellae*. *FEBS Letters*, 594, 2598–2620.

KUDVA, R., DENKS, K., KUHN, P., VOGT, A., MÜLLER, M. & KOCH, H.-G. 2013. Protein translocation across the inner membrane of Gram-negative bacteria: the Sec and Tat dependent protein transport pathways. *Research in Microbiology*, 164, 505–534.

KUESPERT, K., ROTH, A. & HAUCK, C. R. 2011. *Neisseria meningitidis* has two independent modes of recognizing its human receptor CEACAM1. *PLoS One*, 6(article e14609), 1–15.

KURZAI, O., SCHMITT, C., CLAUS, H., VOGEL, U., FROSCH, M. & KOLB-MÄURER, A. 2005. Carbohydrate composition of meningococcal lipopolysaccharide modulates the interaction of *Neisseria meningitidis* with human dendritic cells. *Cellular Microbiology*, 7, 1319–1334.

LADHANI, S. N., BEEBEEJAUN, K., LUCIDARME, J., CAMPBELL, H., GRAY, S., KACZMARSKI, E., RAMSAY, M. E. & BORROW, R. 2015. Increase in endemic *Neisseria meningitidis* capsular group W sequence type 11 complex associated with severe invasive disease in England and Wales. *Clinical Infectious Diseases*, 60, 578–585.

LADHANI, S. N., FLOOD, J. S., RAMSAY, M. E., CAMPBELL, H., GRAY, S. J., KACZMARSKI, E. B., MALLARD, R. H., GUIVER, M., NEWBOLD, L. S. & BORROW, R. 2012. Invasive meningococcal disease in England and Wales: implications for the introduction of new vaccines. *Vaccine*, 30, 3710–3716.

LAESTANDER, C. & ENGSTRÖM, W. 2014. Role of fibroblast growth factors in elicitation of cell responses. *Cell Proliferation*, 47, 3–11.

LAPPANN, M., OTTO, A., BECHER, D. & VOGEL, U. 2013. Comparative proteome analysis of spontaneous outer membrane vesicles and purified outer membranes of *Neisseria meningitidis*. *Journal of Bacteriology*, 195, 4425–4435.

LE BON, A. & TOUGH, D. F. 2002. Links between innate and adaptive immunity via type I interferon. *Current Opinion in Immunology*, 14, 432–436.

LE GUENNEC, L., COUREUIL, M., NASSIF, X. & BOURDOULOUS, S. 2020. Strategies used by bacterial pathogens to cross the blood–brain barrier. *Cellular Microbiology*, 22(article e13132), 1–12.

LÉCUYER, H., NASSIF, X. & COUREUIL, M. 2012. Two strikingly different signaling pathways are induced by meningococcal type IV pili on endothelial and epithelial cells. *Infection and Immunity*, 80, 175–186.

LEE, M. Y., PARK, E. G., CHOI, J. Y., CHEONG, H. S., CHUNG, D. R., PECK, K. R., SONG, J.-H. & KO, K. S. 2010. '*Neisseria skkuensis*' sp. nov., isolated from the blood of a diabetic patient with a foot ulcer. *Journal of Medical Microbiology*, 59, 856–859.

LEININGER, E., ROBERTS, M., KENIMER, J. G., CHARLES, I. G., FAIRWEATHER, N., NOVOTNY, P. & BRENNAN, M. J. 1991. Pertactin, an Arg-Gly-Asp-containing *Bordetella pertussis* surface protein that promotes adherence of mammalian cells. *Proceedings of the National Academy of Sciences*, 88, 345–349.

LEMMON, M. A. & SCHLESSINGER, J. 2010. Cell signaling by receptor tyrosine kinases. *Cell*, 141**,** 1117-1134.

LEO, J. C., GRIN, I. & LINKE, D. 2012. Type V secretion: mechanism (s) of autotransport through the bacterial outer membrane. *Philosophical Transactions of the Royal Society B: Biological Sciences*, 367, 1088–1101.

LEWIS, L. A. & RAM, S. 2014. Meningococcal disease and the complement system. *Virulence*, 5, 98–126.

LEYTON, D. L., ROSSITER, A. E. & HENDERSON, I. R. 2012. From self sufficiency to dependence: mechanisms and factors important for autotransporter biogenesis. *Nature Reviews Microbiology*, 10, 213–225.

LI, C., CHEN, L., IWATA, T., KITAGAWA, M., FU, X.-Y. & DENG, C.-X. 1999. A Lys644Glu substitution in fibroblast growth factor receptor 3 (FGFR3) causes dwarfism in mice by activation of STATs and Ink4 cell cycle inhibitors. *Human Molecular Genetics*, 8, 35–44.

LI, J., EGELMAN, E. H. & CRAIG, L. 2012. Structure of the *Vibrio cholerae* type IVb pilus and stability comparison with the *Neisseria gonorrhoeae* type IVa pilus. *Journal of Molecular Biology*, 418, 47–64.

LIAO, C.-G., KONG, L.-M., SONG, F., XING, J.-L., WANG, L.-X., SUN, Z.-J., TANG, H., YAO, H., ZHANG, Y. & WANG, L. 2011. Characterization of basigin isoforms and the inhibitory function of basigin-3 in human hepatocellular carcinoma proliferation and invasion. *Molecular and Cellular Biology*, 31, 2591–2604.

LIGUORI, A., DELLO IACONO, L., MARUGGI, G., BENUCCI, B., MEROLA, M., LO SURDO, P., LÓPEZ-SAGASETA, J., PIZZA, M., MALITO, E. & BOTTOMLEY, M. J. 2018. NadA3 structures reveal undecad coiled coils and LOX1 binding regions competed by meningococcus B vaccine-elicited human antibodies. *mBio*, 9(article e01914-18), 1–19.

LIN, L., AYALA, P., LARSON, J., MULKS, M., FUKUDA, M., CARLSSON, S. R., ENNS, C. & SO, M. 1997. The *Neisseria* type 2 IgA1 protease cleaves LAMP1 and promotes survival of bacteria within epithelial cells. *Molecular Microbiology*, 24, 1083–1094.

LIN, L., WANG, Q., QIAN, K., CAO, Z., XIAO, J., WANG, X., LI, X. & YU, Z. 2018. bFGF protects against oxygen glucose deprivation/reoxygenation-induced endothelial monolayer permeability via S1PR1-dependent mechanisms. *Molecular Neurobiology*, 55, 3131–3142.

LINGAPPA, J. R., AL-RABEAH, A. M., RANA HAJJEH, T. M., FATANI, A., AL-BASSAM, T., BADUKHAN, A., TURKISTANI, A., AL-HAMDAN, N., AL-JEFFRI, M. & AL MAZROU, Y. 2003. Serogroup W-135 meningococcal disease during the Hajj, 2000. *Emerging Infectious Diseases*, 9(6), 665–671.

LINHARTOVÁ, I., BUMBA, L., MAŠÍN, J., BASLER, M., OSIČKA, R., KAMANOVÁ, J., PROCHÁZKOVÁ, K., ADKINS, I., HEJNOVÁ-HOLUBOVÁ, J. & SADÍLKOVÁ, L. 2010. RTX proteins: a highly diverse family secreted by a common mechanism. *FEMS Microbiology Reviews*, 34, 1076–1112.

LO, H., TANG, C. M. & EXLEY, R. M. 2009. Mechanisms of avoidance of host immunity by *Neisseria meningitidis* and its effect on vaccine development. *The Lancet Infectious Diseases*, 9, 418–427.

LOGAN, S. A. & MACMAHON, E. 2008. Viral meningitis. *BMJ*, 336, 36–40.

LUCIDARME, J., TAN, L., EXLEY, R. M., FINDLOW, J., BORROW, R. & TANG, C. M. 2011. Characterization of *Neisseria meningitidis* isolates that do not express the

virulence factor and vaccine antigen factor H binding protein. *Clinical and Vaccine Immunology*, 18, 1002–1014.

LYON, A. M. & TESMER, J. J. 2013. Structural insights into phospholipase C-β function. *Molecular Pharmacology*, 84, 488–500.

MACDONALD, N. E., HALPERIN, S. A., LAW, B. J., FORREST, B., DANZIG, L. E. & GRANOFF, D. M. 1998. Induction of immunologic memory by conjugated vs plain meningococcal C polysaccharide vaccine in toddlers: a randomized controlled trial. *JAMA*, 280, 1685–1689.

MACKMAN, N. & HOLLAND, I. B. 1984. Functional characterization of a cloned haemolysin determinant from *E. coli* of human origin, encoding information for the secretion of a 107K polypeptide. *Molecular and General Genetics MGG*, 196, 129–134.

MADICO, G., WELSCH, J. A., LEWIS, L. A., MCNAUGHTON, A., PERLMAN, D. H., COSTELLO, C. E., NGAMPASUTADOL, J., VOGEL, U., GRANOFF, D. M. & RAM, S. 2006. The meningococcal vaccine candidate GNA1870 binds the complement regulatory protein factor H and enhances serum resistance. *Journal of Immunology*, 177, 501–510.

MAHMOUD, F. M. & HARHARA, T. 2020. *Neisseria meningitidis* pneumonia with bacteremia without meningitis: An atypical presentation. *IDCases*, 21(article e00897), 1–3.

MAIDEN, M. C., BYGRAVES, J. A., FEIL, E., MORELLI, G., RUSSELL, J. E., URWIN, R., ZHANG, Q., ZHOU, J., ZURTH, K. & CAUGANT, D. A. 1998. Multilocus sequence typing: a portable approach to the identification of clones within populations of pathogenic microorganisms. *Proceedings of the National Academy of Sciences*, 95, 3140–3145.

MAIDEN, M. C., STUART, J. M. & GROUP, U. M. C. 2002. Carriage of serogroup C meningococci 1 year after meningococcal C conjugate polysaccharide vaccination. *The Lancet*, 359, 1829–1830.

MAIREY, E., GENOVESIO, A., DONNADIEU, E., BERNARD, C., JAUBERT, F., PINARD, E., SEYLAZ, J., OLIVO-MARIN, J.-C., NASSIF, X. & DUMÉNIL, G. 2006. Cerebral microcirculation shear stress levels determine *Neisseria meningitidis* attachment sites along the blood–brain barrier. *Journal of Experimental Medicine*, 203, 1939–1950.

MAÏSSA, N., COVARELLI, V., JANEL, S., DUREL, B., SIMPSON, N., BERNARD, S. C., PARDO-LOPEZ, L., BOUZINBA-SÉGARD, H., FAURE, C. & SCOTT, M. G. 2017. Strength of *Neisseria meningitidis* binding to endothelial cells requires highly ordered CD147/β 2-Adrenoceptor clusters assembled by alpha-actinin-4. *Nature Communications*, 8(article 15764), 1–15.

MALORNY, B., MORELLI, G., KUSECEK, B., KOLBERG, J. & ACHTMAN, M. 1998. Sequence diversity, predicted two-dimensional protein structure, and epitope mapping of neisserial Opa proteins. *Journal of Bacteriology*, 180, 1323–1330.

MANCHANDA, V., GUPTA, S. & BHALLA, P. 2006. Meningococcal disease: history, epidemiology, pathogenesis, clinical manifestations, diagnosis, antimicrobial susceptibility and prevention. *Indian Journal of Medical Microbiology*, 24, 7–19.

MANDRELL, R. & ZOLLINGER, W. 1977. Lipopolysaccharide serotyping of *Neisseria meningitidis* by hemagglutination inhibition. *Infection and Immunity*, 16, 471–475.

MARCHIAFAVA, E. & CELLI, A. 1884. Spra i micrococchi della meningite cerebrospinale epidemica. *Gazz degli Ospedali*, 5, 59.

MARIANI, E., LISIGNOLI, G., BORZÌ, R. M. & PULSATELLI, L. 2019. Biomaterials: foreign bodies or tuners for the immune response? *International Journal of Molecular Sciences*, 20(article 636), 1–42.

MARRAZZO, J. M. & APICELLA, M. A. 2019. *Neisseria gonorrhoeae* (gonorrhea), in BENNETT, J. E., DOLIN, R. & BLASER, M. J. (eds.) *Mandell, Douglas and Bennett's Principles and Practice of Infectious Diseases*. 9th edn. Philadelphia: Elsevier, 2446–2462.

MARTIN, S., BORROW, R., VAN DER LEY, P., DAWSON, M., FOX, A. & CARTWRIGHT, K. 2000. Effect of sequence variation in meningococcal PorA outer membrane protein on the effectiveness of a hexavalent PorA outer membrane vesicle vaccine. *Vaccine*, 18, 2476–2481.

MARTINÓN-TORRES, F. 2016. Deciphering the burden of meningococcal disease: conventional and under-recognized elements. *Journal of Adolescent Health*, 59(issue 2 supplement), S12–S20.

MASIGNANI, V., COMANDUCCI, M., GIULIANI, M. M., BAMBINI, S., ADU-BOBIE, J., ARICÒ, B., BRUNELLI, B., PIERI, A., SANTINI, L. & SAVINO, S. 2003. Vaccination against *Neisseria meningitidis* using three variants of the lipoprotein GNA1870. *Journal of Experimental Medicine*, 197, 789–799.

MASIGNANI, V., PIZZA, M. & MOXON, E. R. 2019. The development of a vaccine against meningococcus B using reverse vaccinology. *Frontiers in Immunology*, 10(article 751), 1–14.

MASSARI, P., HENNEKE, P., HO, Y., LATZ, E., GOLENBOCK, D. T. & WETZLER, L. M. 2002. Cutting edge: Immune stimulation by neisserial porins is Toll-like receptor 2 and MyD88 dependent. *Journal of Immunology*, 168, 1533–1537.

MASSARI, P., HO, Y. & WETZLER, L. M. 2000. *Neisseria meningitidis* porin PorB interacts with mitochondria and protects cells from apoptosis. *Proceedings of the National Academy of Sciences*, 97, 9070–9075.

MASSARI, P., KING, C. A., MACLEOD, H. & WETZLER, L. M. 2005. Improved purification of native meningococcal porin PorB and studies on its structure/function. *Protein Expression and Purification*, 44, 136–146.

MATTICK, J. S. 2002. Type IV pili and twitching motility. *Annual Reviews in Microbiology*, 56, 289–314.

MATZINGER, P. 2002. The danger model: a renewed sense of self. *Science*, 296, 301–305.

MCGILL, F., HEYDERMAN, R. S., PANAGIOTOU, S., TUNKEL, A. R. & SOLOMON, T. 2016. Acute bacterial meningitis in adults. *The Lancet*, 388, 3036–3047.

MCGUINNESS, B., LAMBDEN, P. & HECKELS, J. 1993. Class 1 outer membrane protein of *Neisseria meningitidis*: epitope analysis of the antigenic diversity between strains, implications for subtype definition and molecular epidemiology. *Molecular Microbiology*, 7, 505–514.

MCNEIL, L. K., MURPHY, E., ZHAO, X.-J., GUTTMANN, S., HARRIS, S. L., SCOTT, A. A., TAN, C., MACK, M., DASILVA, I. & ALEXANDER, K. 2009. Detection of LP2086 on the cell surface of *Neisseria meningitidis* and its accessibility in the presence of serogroup B capsular polysaccharide. *Vaccine*, 27, 3417–3421.

MCNEIL, L. K., ZAGURSKY, R. J., LIN, S. L., MURPHY, E., ZLOTNICK, G. W., HOISETH, S. K., JANSEN, K. U. & ANDERSON, A. S. 2013. Role of factor H binding protein in *Neisseria meningitidis* virulence and its potential as a vaccine candidate to broadly protect against meningococcal disease. *Microbiology and Molecular Biology Reviews*, 77, 234–252.

MEDZHITOV, R. & JANEWAY, C. 2000. Innate immunity. *New England Journal of Medicine*, 343, 338–344.

MEHLITZ, A. & RUDEL, T. 2013. Modulation of host signaling and cellular responses by *Chlamydia*. *Cell Communication and Signaling*, 11(article 90), 1–11.

MENNY, A., LUKASSEN, M. V., COUVES, E. C., FRANC, V., HECK, A. J. & BUBECK, D. 2021. Structural basis of soluble membrane attack complex packaging for clearance. *Nature Communications*, 12(article 6086), 1–11.

MERTINKOVÁ, P., KULKARNI, A., KÁŇOVÁ, E., BHIDE, K., TKÁČOVÁ, Z. & BHIDE, M. 2020. A simple and rapid pipeline for identification of receptor-binding sites on the surface proteins of pathogens. *Scientific Reports*, 10(article 1163), 1–13.

MERZ, A. J., ENNS, C. A. & SO, M. 1999. Type IV pili of pathogenic *Neisseriae* elicit cortical plaque formation in epithelial cells. *Molecular Microbiology*, 32, 1316–1332.

MEYER, S. A. & KRISTIANSEN, P. A. 2016. Household transmission of *Neisseria meningitidis* in the meningitis belt. *The Lancet Global Health*, 4, e885–e886.

MIKATY, G., SOYER, M., MAIREY, E., HENRY, N., DYER, D., FOREST, K. T., MORAND, P., GUADAGNINI, S., PRÉVOST, M. C. & NASSIF, X. 2009. Extracellular bacterial pathogen induces host cell surface reorganization to resist shear stress. *PLoS Pathogens*, 5(article e1000314), 1–14.

MIL-HOMENS, D. & FIALHO, A. M. 2011. Trimeric autotransporter adhesins in members of the *Burkholderia cepacia* complex: a multifunctional family of proteins implicated in virulence. *Frontiers in Cellular and Infection Microbiology*, 1(article 13), 1–10.

MILLER, F., LÉCUYER, H., JOIN-LAMBERT, O., BOURDOULOUS, S., MARULLO, S., NASSIF, X. & COUREUIL, M. 2013. *Neisseria meningitidis* colonization of the brain endothelium and cerebrospinal fluid invasion. *Cellular Microbiology*, 15, 512–519.

MINETTI, C. A. O. S., TAI, J. Y., BLAKE, M., PULLEN, J. K., LIANG, S.-M. & REMETA, D. P. 1997. Structural and functional characterization of a recombinant PorB class 2 protein from *Neisseria meningitidis*: conformational stability and porin activity. *Journal of Biological Chemistry*, 272, 10710–10720.

MOGENSEN, T. H. 2009. Pathogen recognition and inflammatory signaling in innate immune defenses. *Clinical Microbiology Reviews*, 22, 240–273.

MOHAMMADI, M., DIKIC, I., SOROKIN, A., BURGESS, W., JAYE, M. & SCHLESSINGER, J. 1996. Identification of six novel autophosphorylation sites on fibroblast growth factor receptor 1 and elucidation of their importance in receptor activation and signal transduction. *Molecular and Cellular Biology*, 16, 977–989.

MOHAMMADI, M., HONEGGER, A., ROTIN, D., FISCHER, R., BELLOT, F., LI, W., DIONNE, C., JAYE, M., RUBINSTEIN, M. & SCHLESSINGER, J. 1991. A tyrosine-phosphorylated carboxy-terminal peptide of the fibroblast growth factor receptor (Flg) is a binding site for the SH2 domain of phospholipase C-γ1. *Molecular and Cellular Biology*, 11, 5068–5078.

MOHAMMADI, M., OLSEN, S. K. & IBRAHIMI, O. A. 2005. Structural basis for fibroblast growth factor receptor activation. *Cytokine & Growth Factor Reviews*, 16, 107–137.

MOLERES, J., FERNÁNDEZ-CALVET, A., EHRLICH, R. L., MARTÍ, S., PÉREZ-REGIDOR, L., EUBA, B., RODRÍGUEZ-ARCE, I., BALASHOV, S., CUEVAS, E. & LIÑARES, J. 2018. Antagonistic pleiotropy in the bifunctional surface protein FadL (OmpP1) during adaptation of *Haemophilus influenzae* to chronic lung infection associated with chronic obstructive pulmonary disease. *mBio*, 9(article e01176-18), 1–23.

MORAND, P. C., BILLE, E., MORELLE, S., EUGENE, E., BERETTI, J. L., WOLFGANG, M., MEYER, T. F., KOOMEY, M. & NASSIF, X. 2004. Type IV pilus retraction in pathogenic *Neisseria* is regulated by the PilC proteins. *EMBO Journal*, 23, 2009–2017.

MORAND, P. C., DRAB, M., RAJALINGAM, K., NASSIF, X. & MEYER, T. F. 2009. *Neisseria meningitidis* differentially controls host cell motility through PilC1 and PilC2 components of type IV pili. *PLoS One*, 4(article e6834), 1–11.

MORGAN, J. L., ACHESON, J. F. & ZIMMER, J. 2017. Structure of a type-1 secretion system ABC transporter. *Structure*, 25, 522–529.

MORLEY, S. L. & POLLARD, A. J. 2001. Vaccine prevention of meningococcal disease, coming soon? *Vaccine*, 20, 666–687.

MUBAIWA, T. D., HARTLEY-TASSELL, L. E., SEMCHENKO, E. A., JEN, F., SRIKHANTA, Y. N., DAY, C. J., JENNINGS, M. P. & SEIB, K. L. 2017. The glycointeractome of serogroup B *Neisseria meningitidis* strain MC58. *Scientific Reports*, 7(article 5693), 1–9.

MUENZNER, P., DEHIO, C., FUJIWARA, T., ACHTMAN, M., MEYER, T. F. & GRAY-OWEN, S. D. 2000. Carcinoembryonic antigen family receptor specificity of *Neisseria meningitidis* Opa variants influences adherence to and invasion of proinflammatory cytokine-activated endothelial cells. *Infection and Immunity*, 68, 3601–3607.

MUENZNER, P., NAUMANN, M., MEYER, T. F. & GRAY-OWEN, S. D. 2001. Pathogenic *Neisseria* trigger expression of their carcinoembryonic antigen-related cellular adhesion molecule 1 (CEACAM1; previously CD66a) receptor on primary endothelial cells by activating the immediate early response transcription factor, nuclear factor-κB. *Journal of Biological Chemistry*, 276, 24331–24340.

MÜHLENKAMP, M., OBERHETTINGER, P., LEO, J. C., LINKE, D. & SCHÜTZ, M. S. 2015. *Yersinia* adhesin A (YadA) – beauty & beast. *International Journal of Medical Microbiology*, 305, 252–258.

MURAKAMI, M., NGUYEN, L. T., ZHANG, Z. W., MOODIE, K. L., CARMELIET, P., STAN, R. V. & SIMONS, M. 2008. The FGF system has a key role in regulating vascular integrity. *Journal of Clinical Investigation*, 118, 3355–3366.

MURPHY, T. F. 2010. *Haemophilus* species (including *Haemophilus influenzae* and Chancroid), in MANDELL, G. L., BENNETT, J. E. & DOLIN, R. (eds.) *Mandell, Douglas and Bennett's Principles and Practices of Infectious Diseases*, vol. 2, 7th edn. Philadelphia: Elsevier, 2911–2919.

MUSACCHIO, A., CARMENATE, T., DELGADO, M. & GONZÁLEZ, S. 1997. Recombinant Opc meningococcal protein, folded in vitro, elicits bactericidal antibodies after immunization. *Vaccine*, 15, 751–758.

MUSTAPHA, M. M. & HARRISON, L. H. 2018. Vaccine prevention of meningococcal disease in Africa: Major advances, remaining challenges. *Human Vaccines & Immunotherapeutics*, 14, 1107–1115.

MUSTAPHA, M. M., MARSH, J. W. & HARRISON, L. H. 2016. Global epidemiology of capsular group W meningococcal disease (1970–2015): Multifocal emergence and persistence of hypervirulent sequence type (ST)-11 clonal complex. *Vaccine*, 34, 1515–1523.

MUSTAPHA, M. M., MARSH, J. W., KRAULAND, M. G., FERNANDEZ, J. O., DE LEMOS, A. P. S., HOTOPP, J. C. D., WANG, X., MAYER, L. W., LAWRENCE, J. G. & HILLER, N. L. 2015. Genomic epidemiology of hypervirulent serogroup W, ST-11 *Neisseria meningitidis*. *eBioMedicine*, 2(10), 1447–1455.

NADEL, S. & NINIS, N. 2018. Invasive meningococcal disease in the vaccine era. *Frontiers in Pediatrics*, 6(article 321), 1-11.

NADEL, S. 2012. Prospects for eradication of meningococcal disease. *Archives of Disease in Childhood*, 97, 993–998.

NÄGELE, V., HEESEMANN, J., SCHIELKE, S., JIMÉNEZ-SOTO, L. F., KURZAI, O. & ACKERMANN, N. 2011. *Neisseria meningitidis* adhesin NadA targets β1 integrins: functional similarity to *Yersinia* invasin. *Journal of Biological Chemistry*, 286, 20536–20546.

NASSIF, N., PENNEY, J., PAL, S., ENGELS, W. & GLOOR, G. 1994. Efficient copying of nonhomologous sequences from ectopic sites via P-element-induced gap repair. *Molecular and Cellular Biology*, 14, 1613–1625.

NASSIF, X. 1999. Interactions between encapsulated *Neisseria meningitidis* and host cells. *International Microbiology*, 2, 133–136.

NASSIF, X., PUJOL, C., MORAND, P. & EUGENE, E. 1999. Interactions of pathogenic *Neisseria* with host cells. Is it possible to assemble the puzzle? *Molecular Microbiology*, 32, 1124–1132.

NATALE, P., BRÜSER, T. & DRIESSEN, A. J. 2008. Sec- and Tat-mediated protein secretion across the bacterial cytoplasmic membrane—distinct translocases and mechanisms. *Biochimica et Biophysica Acta (BBA) - Biomembranes*, 1778, 1735–1756.

NEISSER, A. 1879. Ueber eine der Gonorrhoe eigentümliche Micrococcusform: vorläufige Mitteilung. *Zentralblati für die Medizinschen Wissenschaften*, 17(28), 497–500.

NGUYEN, N. & ASHONG, D. 2021. *Neisseria meningitidis*, in *StatPearls*. Treasure Island, FL: StatPearls Publishing. Available from: https://www.ncbi.nlm.nih.gov/books/NBK549849/

NIKULIN, J., PANZNER, U., FROSCH, M. & SCHUBERT-UNKMEIR, A. 2006. Intracellular survival and replication of *Neisseria meningitidis* in human brain microvascular endothelial cells. *International Journal of Medical Microbiology*, 296, 553–558.

NOINAJ, N., EASLEY, N. C., OKE, M., MIZUNO, N., GUMBART, J., BOURA, E., STEERE, A. N., ZAK, O., AISEN, P. & TAJKHORSHID, E. 2012. Structural basis for iron piracy by pathogenic *Neisseria*. *Nature*, 483, 53–58.

NOVAK, R. T., KAMBOU, J. L., DIOMANDÉ, F. V., TARBANGDO, T. F., OUÉDRAOGO-TRAORÉ, R., SANGARÉ, L., LINGANI, C., MARTIN, S. W., HATCHER, C. & MAYER, L. W. 2012. Serogroup A meningococcal conjugate vaccination in Burkina Faso: analysis of national surveillance data. *The Lancet Infectious Diseases*, 12, 757–764.

NUNN, W. D. & SIMONS, R. W. 1978. Transport of long-chain fatty acids by *Escherichia coli*: mapping and characterization of mutants in the fadL gene. *Proceedings of the National Academy of Sciences*, 75, 3377–3381.

OLDFIELD, N. J., CAYROU, C., ALJANNAT, M. A., AL-RUBAIAWI, A. A., GREEN, L. R., DADA, S., STEELS, O. D., STIRRUP, C., WANFORD, J. & ATWAH, B. A. 2017. Rise in group W meningococcal carriage in university students, United Kingdom. *Emerging Infectious Diseases*, 23, 1009–1011.

OLDFIELD, N. J., MATAR, S., BIDMOS, F. A., ALAMRO, M., NEAL, K. R., TURNER, D. P., BAYLISS, C. D. & ALA'ALDEEN, D. A. 2013. Prevalence and phase variable expression status of two autotransporters, NalP and MspA, in carriage and disease isolates of *Neisseria meningitidis*. *PLoS One*, 8(article e69746), 1–9.

OLSEN, S. K., IBRAHIMI, O. A., RAUCCI, A., ZHANG, F., ELISEENKOVA, A. V., YAYON, A., BASILICO, C., LINHARDT, R. J., SCHLESSINGER, J. & MOHAMMADI, M. 2004. Insights into the molecular basis for fibroblast growth factor receptor autoinhibition and ligand-binding promiscuity. *Proceedings of the National Academy of Sciences,* 101**,** 935-940.

ONG, S., HADARI, Y., GOTOH, N., GUY, G., SCHLESSINGER, J. & LAX, I. 2001. Stimulation of phosphatidylinositol 3-kinase by fibroblast growth factor receptors is mediated by coordinated recruitment of multiple docking proteins. *Proceedings of the National Academy of Sciences*, 98, 6074–6079.

OORDT-SPEETS, A. M., BOLIJN, R., VAN HOORN, R. C., BHAVSAR, A. & KYAW, M. H. 2018. Global etiology of bacterial meningitis: a systematic review and meta-analysis. *PLoS One*, 13(article e0198772), 1–16.

ORIHUELA, C. J., MAHDAVI, J., THORNTON, J., MANN, B., WOOLDRIDGE, K. G., ABOUSEADA, N., OLDFIELD, N. J., SELF, T., ALA'ALDEEN, D. A. & TUOMANEN, E. I. 2009. Laminin receptor initiates bacterial contact with the blood brain barrier in experimental meningitis models. *Journal of Clinical Investigation*, 119, 1638–1646.

ORNITZ, D. M. & ITOH, N. 2015. The fibroblast growth factor signaling pathway. *Wiley Interdisciplinary Reviews: Developmental Biology*, 4, 215–266.

PACE, D. & POLLARD, A. J. 2012. Meningococcal disease: clinical presentation and sequelae. *Vaccine*, 30(supplement 2), B3–B9.

PANATTO, D., AMICIZIA, D., LAI, P. L. & GASPARINI, R. 2011. *Neisseria meningitidis* B vaccines. *Expert Review of Vaccines*, 10, 1337–1351.

PAPANIKOU, E., KARAMANOU, S. & ECONOMOU, A. 2007. Bacterial protein secretion through the translocase nanomachine. *Nature Reviews Microbiology*, 5, 839–851.

PARGE, H. E., FOREST, K. T., HICKEY, M. J., CHRISTENSEN, D. A., GETZOFF, E. D. & TAINER, J. A. 1995. Structure of the fibre-forming protein pilin at 2.6 Å resolution. *Nature*, 378, 32–38.

PARUCHURI, D. K., SEIFERT, H. S., AJIOKA, R. S., KARLSSON, K.-A. & SO, M. 1990. Identification and characterization of a *Neisseria gonorrhoeae* gene encoding a glycolipid-binding adhesin. *Proceedings of the National Academy of Sciences*, 87, 333–337.

PATHAN, N., FAUST, S. & LEVIN, M. 2003. Pathophysiology of meningococcal meningitis and septicaemia. *Archives of Disease in Childhood*, 88, 601–607.

PEAK, I. R., CHEN, A., JEN, F. E.-C., JENNINGS, C., SCHULZ, B. L., SAUNDERS, N. J., KHAN, A., SEIFERT, H. S. & JENNINGS, M. P. 2016. Neisseria meningitidis lacking the major porins PorA and PorB is viable and modulates apoptosis and the oxidative burst of neutrophils. *Journal of Proteome Research,* 15**,** 2356-2365.

PEAK, I. R., JENNINGS, C. D., JEN, F. E.-C. & JENNINGS, M. P. 2014. Role of *Neisseria meningitidis* PorA and PorB expression in antimicrobial susceptibility. *Antimicrobial Agents and Chemotherapy*, 58, 614–616.

PEAK, I. R., SRIKHANTA, Y., DIECKELMANN, M., MOXON, E. R. & JENNINGS, M. P. 2000. Identification and characterisation of a novel conserved outer membrane protein from *Neisseria meningitidis*. *FEMS Immunology & Medical Microbiology*, 28, 329–334.

PELTON, S. I. 2016. The global evolution of meningococcal epidemiology following the introduction of meningococcal vaccines. *Journal of Adolescent Health*, 59(issue 2 supplement), S3–S11.

PIZZA, M. & RAPPUOLI, R. 2015. *Neisseria meningitidis*: pathogenesis and immunity. *Current Opinion in Microbiology*, 23, 68–72.

PLANT, L., SUNDQVIST, J., ZUGHAIER, S., LÖVKVIST, L., STEPHENS, D. S. & JONSSON, A.-B. 2006. Lipooligosaccharide structure contributes to multiple steps in the virulence of *Neisseria meningitidis*. *Infection and Immunity*, 74, 1360–1367.

POLLARD, A. J. & LEVIN, M. 2000. Vaccines for prevention of meningococcal disease. *The Pediatric Infectious Disease Journal*, 19, 333–344.

POLLARD, A. J. 2004. Global epidemiology of meningococcal disease and vaccine efficacy. *The Pediatric Infectious Disease Journal*, 23(12), S274–S279.

POLLARD, A. J., PERRETT, K. P. & BEVERLEY, P. C. 2009. Maintaining protection against invasive bacteria with protein–polysaccharide conjugate vaccines. *Nature Reviews Immunology*, 9, 213–220.

POOLMAN, J. T. & RICHMOND, P. 2015. Multivalent meningococcal serogroup B vaccines: challenges in predicting protection and measuring effectiveness. *Expert Review of Vaccines*, 14, 1277–1287.

POTTS, C. C., JOSEPH, S. J., CHANG, H.-Y., CHEN, A., VUONG, J., HU, F., JENKINS, L. T., SCHMINK, S., BLAIN, A. & MACNEIL, J. R. 2018. Population structure of invasive *Neisseria meningitidis* in the United States, 2011–15. *Journal of Infection*, 77, 427–434.

POTTS, C. C., TOPAZ, N., RODRIGUEZ-RIVERA, L. D., HU, F., CHANG, H.-Y., WHALEY, M. J., SCHMINK, S., RETCHLESS, A. C., CHEN, A. & RAMOS, E. 2019. Genomic characterization of *Haemophilus influenzae*: a focus on the capsule locus. *BMC Genomics*, 20(article 733), 1–9.

PRASADA, R. T., LAKSHMI, P. T., PARVATHY, R., MURUGAVEL, S., KARUNA, D. & PARITOSH, J. 2017. Identification of second arginine-glycine-aspartic acid motif of ovine vitronectin as the complement C9 binding site and its implication in bacterial infection. *Microbiology and Immunology*, 61, 75–84.

PRENTKI, P. & KRISCH, H. M. 1984. *In vitro* insertional mutagenesis with a selectable DNA fragment. *Gene*, 29**,** 303-313.

PRESA, J., FINDLOW, J., VOJICIC, J., WILLIAMS, S. & SERRA, L. 2019. Epidemiologic trends, global shifts in meningococcal vaccination guidelines, and data supporting the use of MenACWY-TT vaccine: a review. *Infectious Diseases and Therapy*, 8, 307–333.

PRESTA, M., DELL'ERA, P., MITOLA, S., MORONI, E., RONCA, R. & RUSNATI, M. 2005. Fibroblast growth factor/fibroblast growth factor receptor system in angiogenesis. *Cytokine & Growth Factor Reviews*, 16, 159–178.

PRICE, G. A., MASRI, H. P., HOLLANDER, A. M., RUSSELL, M. W. & CORNELISSEN, C. N. 2007. Gonococcal transferrin binding protein chimeras induce bactericidal and growth inhibitory antibodies in mice. *Vaccine*, 25, 7247–7260.

PRINCE, S. M., ACHTMAN, M. & DERRICK, J. P. 2002. Crystal structure of the OpcA integral membrane adhesin from *Neisseria meningitidis*. *Proceedings of the National Academy of Sciences*, 99**,** 3417–3421.

PRINZ, M. & PRILLER, J. 2017. The role of peripheral immune cells in the CNS in steady state and disease. *Nature Neuroscience*, 20, 136–144.

PRON, B., TAHA, M.-K., RAMBAUD, C., FOURNET, J.-C., PATTEY, N., MONNET, J.-P., MUSILEK, M., BERETTI, J.-L. & NASSIF, X. 1997. Interaction of *Neisseria meningitidis* with the components of the blood–brain barrier correlates with an increased expression of PilC. *Journal of Infectious Diseases*, 176, 1285–1292.

PUBLIC HEALTH ENGLAND. 2019. *Invasive meningococcal disease in England: annual laboratory confirmed reports for epidemiological year 2018 to 2019*. Available from: https://assets.publishing.service.gov.uk/government/uploads/system/uploads/attachment_data/file/842368/hpr3819_IMD-ann.pdf

PUBLIC HEALTH ENGLAND. 2021. *Invasive meningococcal disease in England: annual laboratory confirmed reports for epidemiological year 2019 to 2020*. Available from: https://assets.publishing.service.gov.uk/government/uploads/system/uploads/attachment_data/file/951142/hpr0121_imd-ann.pdf

QUAGLIARELLO, V., LONG, W. & SCHELD, W. 1986. Morphologic alterations of the blood–brain barrier with experimental meningitis in the rat. Temporal sequence and role of encapsulation. *Journal of Clinical Investigation*, 77, 1084–1095.

QUINTANAL-VILLALONGA, A., MOLINA-PINELO, S., CIRAUQUI, C., OJEDA-MÁRQUEZ, L., MARRUGAL, Á., SUAREZ, R., CONDE, E., PONCE-AIX, S., ENGUITA, A. B. & CARNERO, A. 2019. FGFR1 cooperates with EGFR in lung cancer oncogenesis, and their combined inhibition shows improved efficacy. *Journal of Thoracic Oncology*, 14, 641–655.

RABENSTEIN, D. L. 2002. Heparin and heparan sulfate: structure and function. *Natural Product Reports*, 19, 312–331.

RACLOZ, V. N. & LUIZ, S. J. 2010. The elusive meningococcal meningitis serogroup: a systematic review of serogroup B epidemiology. *BMC Infectious Diseases*, 10(article 175), 1–9.

RAHMAN, M. M., STEPHENS, D. S., KAHLER, C. M., GLUSHKA, J. & CARLSON, R. W. 1998. The lipooligosaccharide (LOS) of *Neisseria meningitidis* serogroup B strain NMB contains L2, L3, and novel oligosaccharides, and lacks the lipid-A 4′-phosphate substituent. *Carbohydrate Research*, 307, 311–324.

READ, R. C., ZIMMERLI, S., BROADDUS, C., SANAN, D. A., STEPHENS, D. S. & ERNST, J. D. 1996. The (α2→8)-linked polysialic acid capsule of group B *Neisseria meningitidis* modifies multiple steps during interaction with human macrophages. *Infection and Immunity*, 64, 3210–3217.

RECHNER, C., KÜHLEWEIN, C., MÜLLER, A., SCHILD, H. & RUDEL, T. 2007. Host glycoprotein Gp96 and scavenger receptor SREC interact with PorB of disseminating *Neisseria gonorrhoeae* in an epithelial invasion pathway. *Cell Host & Microbe*, 2, 393–403.

REMICK, D. G. 2007. Pathophysiology of sepsis. *American Journal of Pathology*, 170, 1435–1444.

RENNÉ, T. & STAVROU, E. X. 2019. Roles of factor XII in innate immunity. *Frontiers in Immunology*, 10(article 2011), 1–9.

RENNER, P., ROGER, T., BOCHUD, P. Y., SPRONG, T., SWEEP, F. C., BOCHUD, M., FAUST, S. N., HARALAMBOUS, E., BETTS, H. & CHANSON, A. L. 2012. A functional microsatellite of the macrophage migration inhibitory factor gene associated with meningococcal disease. *FASEB Journal*, 26, 907–916.

RIBET, D. & COSSART, P. 2015. How bacterial pathogens colonize their hosts and invade deeper tissues. *Microbes and Infection*, 17, 173–183.

RICKLIN, D., HAJISHENGALLIS, G., YANG, K. & LAMBRIS, J. D. 2010. Complement: a key system for immune surveillance and homeostasis. *Nature Immunology*, 11, 785–797.

RIVERO-CALLE, I., RAGUINDIN, P. F., GÓMEZ-RIAL, J., RODRIGUEZ-TENREIRO, C. & MARTINÓN-TORRES, F. 2019. Meningococcal group B vaccine for the prevention of invasive meningococcal disease caused by *Neisseria meningitidis* serogroup B. *Infection and Drug Resistance*, 12, 3169–3188.

ROBBINS, J. B., MCCRACKEN JR, G. H., GOTSCHLICH, E. C., ØRSKOV, F., ØRSKOV, I. & HANSON, L. A. 1974. Escherichia coli K1 capsular polysaccharide associated with neonatal meningitis. *New England Journal of Medicine*, 290, 1216–1220.

ROBINSON, C. & BOLHUIS, A. 2004. Tat-dependent protein targeting in prokaryotes and chloroplasts. *Biochimica et Biophysica Acta (BBA) - Molecular Cell Research*, 1694**,** 135–147.

ROBINSON, D. R., WU, Y.-M. & LIN, S.-F. 2000. The protein tyrosine kinase family of the human genome. *Oncogene*, 19, 5548–5557.

ROKBI, B., MIGNON, M., MAITRE-WILMOTTE, G., LISSOLO, L., DANVE, B., CAUGANT, D. A. & QUENTIN-MILLET, M.-J. 1997. Evaluation of recombinant transferrin-binding protein B variants from *Neisseria meningitidis* for their ability to induce cross-reactive and bactericidal antibodies against a genetically diverse collection of serogroup B strains. *Infection and Immunity*, 65, 55–63.

ROSENSTEIN, N. E., PERKINS, B. A., STEPHENS, D. S., LEFKOWITZ, L., CARTTER, M. L., DANILA, R., CIESLAK, P., SHUTT, K. A., POPOVIC, T. & SCHUCHAT, A. 1999. The changing epidemiology of meningococcal disease in the United States, 1992–1996. *Journal of Infectious Diseases*, 180, 1894–1901.

ROTMAN, E. & SEIFERT, H. S. 2014. The genetics of *Neisseria* species. *Annual Review of Genetics*, 48, 405–431.

ROTTNER, K., STRADAL, T. E. & WEHLAND, J. 2005. Bacteria-host-cell interactions at the plasma membrane: stories on actin cytoskeleton subversion. *Developmental Cell*, 9(1), 3–17.

ROUPHAEL, N. G. & STEPHENS, D. S. 2012. *Neisseria meningitidis*: biology, microbiology, and epidemiology, in CHRISTODOULIDES, M. (ed.) *Neisseria meningitidis: Advanced Methods and Protocols*. Totowa, NJ: Humana, 1–20.

ROUSSEL-JAZEDE, V., ARENAS, J., LANGEREIS, J. D., TOMMASSEN, J. & VAN ULSEN, P. 2014. Variable processing of the IgA protease autotransporter at the cell surface of *Neisseria meningitidis*. *Microbiology*, 160, 2421–2431.

ROUSSEL-JAZÉDÉ, V., GRIJPSTRA, J., VAN DAM, V., TOMMASSEN, J. & VAN ULSEN, P. 2013. Lipidation of the autotransporter NalP of *Neisseria meningitidis* is required for its function in the release of cell-surface-exposed proteins. *Microbiology*, 159, 286–295.

RUDE, J. M., KORTIMAI, L., MOSOKA, F., APRIL, B., NUHA, M., KATAWERA, V., NAGBE, T., TAMBA, A., DESMOUND, W. & MULBAH, R. 2019. Rapid response to meningococcal disease cluster in Foya district, Lofa County, Liberia January to February 2018. *The Pan African Medical Journal*, 33(supplement 2, article 6), 1–6.

RUDEL, T., SCHEUERPFLUG, I. & MEYER, T. F. 1995. *Neisseria* PilC protein identified as type-4 pilus tip-located adhesin. *Nature*, 373, 357–359.

RYTKÖNEN, A., ALBIGER, B., HANSSON-PALO, P., KÄLLSTRÖM, H., OLCÉN, P., FREDLUND, H. & JONSSON, A.-B. 2004. *Neisseria meningitidis* undergoes PilC phase variation and PilE sequence variation during invasive disease. *Journal of Infectious Diseases*, 189, 402–409.

SA E CUNHA, C., GRIFFITHS, N. J. & VIRJI, M. 2010. *Neisseria meningitidis* Opc invasin binds to the sulphated tyrosines of activated vitronectin to attach to and invade human brain endothelial cells. *PLoS Pathogens*, 6(article e1000911), 1–18.

SA E CUNHA, C., GRIFFITHS, N. J. & VIRJI, M. 2010. *Neisseria meningitidis* Opc invasin binds to the sulphated tyrosines of activated vitronectin to attach to and invade human brain endothelial cells. *PLoS Pathogens*, 6(article e1000911), 1–18.

SA E CUNHA, C., GRIFFITHS, N. J., MURILLO, I. & VIRJI, M. 2009. *Neisseria meningitidis* Opc invasin binds to the cytoskeletal protein α-actinin. *Cellular Microbiology*, 11, 389–405.

SABELNIKOVS, O., NIKITINA-ZAKE, L., KRUMINA, A., JAUNBERGA, Z., KLOVINS, J., VIKSNA, L., BJERTNAES, L., KOVALCHUKA, L. & VANAG, I. 2012. Associations between TNF-α, IL-6 and IL-10 promoter polymorphisms and mortality in severe sepsis. *Journal of Scientific Research and Reports*, 1, 17–28.

SADARANGANI, M. & POLLARD, A. J. 2010. Serogroup B meningococcal vaccines—an unfinished story. *The Lancet Infectious Diseases*, 10, 112–124.

SAHNI, A., PATEL, J., NARRA, H. P., SCHROEDER, C. L., WALKER, D. H. & SAHNI, S. K. 2017. Fibroblast growth factor receptor-1 mediates internalization of pathogenic spotted fever rickettsiae into host endothelium. *PLoS One*, 12(article e0183181), 1–16.

SAÏD-SADIER, N. & OJCIUS, D. M. 2012. Alarmins, inflammasomes and immunity. *Biomedical Journal*, 35(6), 437–449.

SANDBU, S., FEIRING, B., OSTER, P., HELLAND, O. S., BAKKE, H. S., NÆSS, L. M., AASE, A., AABERGE, I. S., KRISTOFFERSEN, A.-C. & RYDLAND, K. M. 2007. Immunogenicity and safety of a combination of two serogroup B meningococcal outer membrane vesicle vaccines. *Clinical and Vaccine Immunology*, 14(9), 1062–1069.

SANDERS, H., NORHEIM, G., CHAN, H., DOLD, C., VIPOND, C., DERRICK, J. P., POLLARD, A. J., MAIDEN, M. C. & FEAVERS, I. M. 2015. FetA antibodies

induced by an outer membrane vesicle vaccine derived from a serogroup B meningococcal isolate with constitutive FetA expression. *PLoS One*, 10(article e0140345), 1–17.

SARABIPOUR, S. & HRISTOVA, K. 2016. Mechanism of FGF receptor dimerization and activation. *Nature communications*, 7(article 10262), 1–12.

SARDINAS, G., YERO, D., CLIMENT, Y., CABALLERO, E., COBAS, K. & NIEBLA, O. 2009. *Neisseria meningitidis* antigen NMB0088: sequence variability, protein topology and vaccine potential. *Journal of Medical Microbiology*, 58, 196–208.

SARFATTI, A. & NADEL, S. 2015. Management of meningococcal disease. *Paediatrics and Child Health*, 25, 203–209.

SARKARI, J., PANDIT, N., MOXON, E. R. & ACHTMAN, M. 1994. Variable expression of the Opc outer membrane protein in *Neisseria meningitidis* is caused by size variation of a promoter containing poly-cytidine. *Molecular microbiology*, 13**,** 207-217.

SARMA, J. V. & WARD, P. A. 2011. The complement system. *Cell and Tissue Research*, 343, 227–235.

SATOLA, S. W., COLLINS, J. T., NAPIER, R. & FARLEY, M. M. 2007. Capsule gene analysis of invasive Haemophilus *influenzae: accuracy* of serotyping and prevalence of IS 1016 among nontypeable isolates. *Journal of Clinical Microbiology*, 45, 3230–3238.

SAURÍ, A., CORINNE, M., VAN ULSEN, P. & LUIRINK, J. 2012. Estimating the size of the active translocation pore of an autotransporter. *Journal of Molecular Biology*, 416, 335–345.

SCARSELLI, M., SERRUTO, D., MONTANARI, P., CAPECCHI, B., ADU-BOBIE, J., VEGGI, D., RAPPUOLI, R., PIZZA, M. & ARICÒ, B. 2006. *Neisseria meningitidis* NhhA is a multifunctional trimeric autotransporter adhesin. *Molecular Microbiology*, 61, 631–644.

SCHLESSINGER, J. 2000. Cell signaling by receptor tyrosine kinases. *Cell*, 103, 211–225.

SCHMIDT, M. A., RILEY, L. W. & BENZ, I. 2003. Sweet new world: glycoproteins in bacterial pathogens. *Trends in Microbiology*, 11, 554–561.

SCHMITT, C., VILLWOCK, A. & KURZAI, O. 2009. Recognition of meningococcal molecular patterns by innate immune receptors. *International Journal of Medical Microbiology*, 299, 9–20.

SCHNEIDER, M. C., EXLEY, R. M., RAM, S., SIM, R. B. & TANG, C. M. 2007. Interactions between *Neisseria meningitidis* and the complement system. *Trends in Microbiology*, 15, 233–240.

SCHNEIDER, M. C., PROSSER, B. E., CAESAR, J. J., KUGELBERG, E., LI, S., ZHANG, Q., QUORAISHI, S., LOVETT, J. E., DEANE, J. E. & SIM, R. B. 2009. *Neisseria meningitidis* recruits factor H using protein mimicry of host carbohydrates. *Nature*, 458, 890–893.

SCHOEN, C., JOSEPH, B., CLAUS, H., VOGEL, U. & FROSCH, M. 2007. Living in a changing environment: insights into host adaptation in *Neisseria meningitidis* from comparative genomics. *International Journal of Medical Microbiology*, 297, 601–613.

SCHOEN, C., KISCHKIES, L., ELIAS, J. & AMPATTU, B. J. 2014. Metabolism and virulence in *Neisseria meningitidis*. *Frontiers in Cellular and Infection Microbiology*, 4(article 114), 1–16.

SCHOLTEN, R., KUIPERS, B., VALKENBURG, H., DANKERT, J., ZOLLINGER, W. & POOLMAN, J. 1994. Lipo-oligosaccharide immunotyping of *Neisseria meningitidis* by a whole-cell ELISA with monoclonal antibodies. *Journal of Medical Microbiology*, 41, 236–243.

SCHUBERT-UNKMEIR, A. 2017. Molecular mechanisms involved in the interaction of *Neisseria meningitidis* with cells of the human blood–cerebrospinal fluid barrier. *Pathogens and Disease*, 75(article ftx023), 1–10.

SCHUBERT-UNKMEIR, A., KONRAD, C., SLANINA, H., CZAPEK, F., HEBLING, S. & FROSCH, M. 2010. *Neisseria meningitidis* induces brain microvascular endothelial cell detachment from the matrix and cleavage of occludin: a role for MMP-8. *PLoS Pathogens*, 6(article e1000874), 1–15.

SCHWECHHEIMER, C. & KUEHN, M. J. 2015. Outer-membrane vesicles from Gram-negative bacteria: biogenesis and functions. *Nature Reviews Microbiology*, 13, 605–619.

SCHWENTKER, F. F., GELMAN, S. & LONG, P. H. 1937. The treatment of meningococcic meningitis with sulfanilamide: preliminary report. *JAMA*, 108, 1407–1408.

SCHWERK, C., PAPANDREOU, T., SCHUHMANN, D., NICKOL, L., BORKOWSKI, J., STEINMANN, U., QUEDNAU, N., STUMP, C., WEISS, C. & BERGER, J. 2012. Polar invasion and translocation of *Neisseria meningitidis* and *Streptococcus*

suis in a novel human model of the blood-cerebrospinal fluid barrier. *PLoS One*, 7(article e30069), 1–15.

SEIB, K. L., BRUNELLI, B., BROGIONI, B., PALUMBO, E., BAMBINI, S., MUZZI, A., DIMARCELLO, F., MARCHI, S., VAN DER ENDE, A. & ARICÓ, B. 2011. Characterization of diverse subvariants of the meningococcal factor H (fH) binding protein for their ability to bind fH, to mediate serum resistance, and to induce bactericidal antibodies. *Infection and Immunity*, 79, 970–981.

SEIB, K. L., SCARSELLI, M., COMANDUCCI, M., TONEATTO, D. & MASIGNANI, V. 2015. *Neisseria meningitidis* factor H-binding protein fHbp: a key virulence factor and vaccine antigen. *Expert Review of Vaccines*, 14, 841–859.

SEIB, K. L., ZHAO, X. & RAPPUOLI, R. 2012. Developing vaccines in the era of genomics: a decade of reverse vaccinology. *Clinical Microbiology and Infection*, 18, 109–116.

SEILER, A., REINHARDT, R., SARKARI, J., CAUGANT, D. A. & ACHTMAN, M. 1996. Allelic polymorphism and site-specific recombination in the *opc* locus of *Neisseria meningitidis*. *Molecular Microbiology*, 19, 841–856.

SEMCHENKO, E. A., TAN, A., BORROW, R. & SEIB, K. L. 2019. The serogroup B meningococcal vaccine Bexsero elicits antibodies to *Neisseria gonorrhoeae.* *Clinical Infectious Diseases*, 69**,** 1101-1111.

SERRUTO, D., ADU-BOBIE, J., SCARSELLI, M., VEGGI, D., PIZZA, M., RAPPUOLI, R. & ARICÒ, B. 2003. *Neisseria meningitidis* App, a new adhesin with autocatalytic serine protease activity. *Molecular microbiology*, 48, 323–334.

SERRUTO, D., BOTTOMLEY, M. J., RAM, S., GIULIANI, M. M. & RAPPUOLI, R. 2012. The new multicomponent vaccine against meningococcal serogroup B, 4CMenB: immunological, functional and structural characterization of the antigens. *Vaccine*, 30(supplement 2), B87–B97.

SERRUTO, D., SPADAFINA, T., CIUCCHI, L., LEWIS, L. A., RAM, S., TONTINI, M., SANTINI, L., BIOLCHI, A., SEIB, K. L. & GIULIANI, M. M. 2010. *Neisseria meningitidis* GNA2132, a heparin-binding protein that induces protective immunity in humans. *Proceedings of the National Academy of Sciences*, 107, 3770–3775.

SHAN, Y., EASTWOOD, M. P., ZHANG, X., KIM, E. T., ARKHIPOV, A., DROR, R. O., JUMPER, J., KURIYAN, J. & SHAW, D. E. 2012. Oncogenic mutations counteract

intrinsic disorder in the EGFR kinase and promote receptor dimerization. *Cell*, 149, 860–870.

SIENA, E., BODINI, M. & MEDINI, D. 2018. Interplay between virulence and variability factors as a potential driver of invasive meningococcal disease. *Computational and Structural Biotechnology Journal*, 16, 61–69.

SIERRA, G., CAMPA, H., VARCACEL, N., GARCIA, I., IZQUIERDO, P., SOTOLONGO, P., CASANUEVA, G., RICO, C., RODRIGUEZ, C. & TERRY, M. 1991. Vaccine against group B *Neisseria meningitidis*: protection trial and mass vaccination results in Cuba. *NIPH Annals*, 14(2), 195–207.

SILHAVY, T. J., KAHNE, D. & WALKER, S. 2010. The bacterial cell envelope. *Cold Spring Harbor Perspectives in Biology*, 2(article a000414), 1–17.

SIMONIS, A. & SCHUBERT-UNKMEIR, A. 2016. Interactions of meningococcal virulence factors with endothelial cells at the human blood–cerebrospinal fluid barrier and their role in pathogenicity. *FEBS Letters*, 590, 3854–3867.

SIMONIS, A., HEBLING, S., GULBINS, E., SCHNEIDER-SCHAULIES, S. & SCHUBERT-UNKMEIR, A. 2014. Differential activation of acid sphingomyelinase and ceramide release determines invasiveness of *Neisseria meningitidis* into brain endothelial cells. *PLoS Pathogens*, 10(article e1004160), 1–17.

SINGH, A., UPADHYAY, V., UPADHYAY, A. K., SINGH, S. M. & PANDA, A. K. 2015. Protein recovery from inclusion bodies of *Escherichia coli* using mild solubilization process. *Microbial Cell Factories*, 14(article 41), 1–10.

SINGH, B., SU, Y. C. & RIESBECK, K. 2010. Vitronectin in bacterial pathogenesis: a host protein used in complement escape and cellular invasion. *Molecular Microbiology*, 78, 545–560.

SJÖLINDER, H. & JONSSON, A.-B. 2010. Olfactory nerve—a novel invasion route of *Neisseria meningitidis* to reach the meninges. *PLoS One*, 5(article e14034), 1–10.

SJÖLINDER, H., ERIKSSON, J., MAUDSDOTTER, L., ARO, H. & JONSSON, A.-B. 2008. Meningococcal outer membrane protein NhhA is essential for colonization and disease by preventing phagocytosis and complement attack. *Infection and Immunity*, 76, 5412–5420.

SJÖLINDER, M., ALTENBACHER, G., HAGNER, M., SUN, W., SCHEDIN-WEISS, S. & SJÖLINDER, H. 2012. Meningococcal outer membrane protein NhhA triggers apoptosis in macrophages. *P:oS One*, 7(article e29586), 1–8.

SLANINA, H., KÖNIG, A., HEBLING, S., HAUCK, C. R., FROSCH, M. & SCHUBERT-UNKMEIR, A. 2010. Entry of *Neisseria meningitidis* into mammalian cells requires the Src family protein tyrosine kinases. *Infection and Immunity*, 78, 1905–1914.

SLANINA, H., MÜNDLEIN, S., HEBLING, S. & SCHUBERT-UNKMEIR, A. 2014. Role of epidermal growth factor receptor signaling in the interaction of *Neisseria meningitidis* with endothelial cells. *Infection and Immunity*, 82, 1243–1255.

SMITH, P. C., KARPOWICH, N., MILLEN, L., MOODY, J. E., ROSEN, J., THOMAS, P. J. & HUNT, J. F. 2002. ATP binding to the motor domain from an ABC transporter drives formation of a nucleotide sandwich dimer. *Molecular Cell*, 10, 139–149.

SNAPE, M. D. & POLLARD, A. J. 2005. Meningococcal polysaccharide–protein conjugate vaccines. *The Lancet Infectious Diseases*, 5, 21–30.

SÖDERHOLM, N., VIELFORT, K., HULTENBY, K. & ARO, H. 2011. Pathogenic *Neisseria* hitchhike on the uropod of human neutrophils. *PLoS One*, 6(article e24353), 1–12.

SOETERS, H. M., DIALLO, A. O., BICABA, B. W., KADADÉ, G., DEMBÉLÉ, A. Y., ACYL, M. A., NIKIEMA, C., SADJI, A. Y., POY, A. N. & LINGANI, C. 2019. Bacterial meningitis epidemiology in five countries in the meningitis belt of sub-Saharan Africa, 2015–2017. *Journal of Infectious Diseases*, 220(supplement 4), S165–S174.

SOKOLOVA, O., HEPPEL, N., JÄGERHUBER, R., KIM, K. S., FROSCH, M., EIGENTHALER, M. & SCHUBERT-UNKMEIR, A. 2004. Interaction of *Neisseria meningitidis* with human brain microvascular endothelial cells: role of MAP-and tyrosine kinases in invasion and inflammatory cytokine release. *Cellular Microbiology*, 6, 1153–1166.

SORIANI, M. 2017. Unraveling *Neisseria meningitidis* pathogenesis: from functional genomics to experimental models. *F1000Research*, 6(article 1228), 1–10.

SPINOSA, M. R., PROGIDA, C., TALA, A., COGLI, L., ALIFANO, P. & BUCCI, C. 2007. The *Neisseria meningitidis* capsule is important for intracellular survival in human cells. *Infection and Immunity*, 75, 3594–3603.

SPOERRY, C., KARLSSON, J., ASCHTGEN, M.-S. & LOH, E. 2021. *Neisseria meningitidis* IgA1-specific serine protease exhibits novel cleavage activity against IgG3. *Virulence*, 12, 389–403.

ST. GEME III, J. W. & CUTTER, D. 2000. The *Haemophilus influenzae* Hia adhesin is an autotransporter protein that remains uncleaved at the C terminus and fully cell associated. *Journal of Bacteriology*, 182, 6005–6013.

STEPHENS, D. S. 2009. Biology and pathogenesis of the evolutionarily successful, obligate human bacterium *Neisseria meningitidis*. *Vaccine*, 27(supplement 2), B71–B77.

STEPHENS, D. S., GREENWOOD, B. & BRANDTZAEG, P. 2007. Epidemic meningitis, meningococcaemia, and *Neisseria meningitidis*. *The Lancet*, 369, 2196–2210.

STEPHENS, D. S., WHITNEY, A. M., ROTHBARD, J. & SCHOOLNIK, G. K. 1985. Pili of *Neisseria meningitidis*. Analysis of structure and investigation of structural and antigenic relationships to gonococcal pili. *Journal of Experimental Medicine*, 161, 1539–1553.

STINS, M. F., GILLES, F. & KIM, K. S. 1997. Selective expression of adhesion molecules on human brain microvascular endothelial cells. *Journal of Neuroimmunology*, 76, 81–90.

STRELOW, V. L. & VIDAL, J. E. 2013. Invasive meningococcal disease. *Arquivos de Neuro-Psiquiatria*, 71, 653–658.

STROM, M. S. & LORY, S. 1993. Structure-function and biogenesis of the type IV pili. *Annual Reviews in Microbiology*, 47, 565–596.

SU, E. L. & SNAPE, M. D. 2011. A combination recombinant protein and outer membrane vesicle vaccine against serogroup B meningococcal disease. *Expert Review of Vaccines*, 10, 575–588.

SUDARSANAM, T. D., RUPALI, P., THARYAN, P., ABRAHAM, O. C. & THOMAS, K. 2013. Pre-admission antibiotics for suspected cases of meningococcal disease. *Cochrane Database of Systematic Reviews*, article CD005437.

SUGA, S., ISHIWADA, N., SASAKI, Y., AKEDA, H., NISHI, J., OKADA, K., FUJIEDA, M., ODA, M., ASADA, K. & NAKANO, T. 2018. A nationwide population-based surveillance of invasive *Haemophilus influenzae* diseases in children after the introduction of the *Haemophilus influenzae* type b vaccine in Japan. *Vaccine*, 36, 5678–5684.

SUTHERLAND, T. C., QUATTRONI, P., EXLEY, R. M. & TANG, C. M. 2010. Transcellular passage of *Neisseria meningitidis* across a polarized respiratory epithelium. *Infection and Immunity*, 78, 3832–3847.

SUZUKI, M., DHOUBHADEL, B. G., ISHIFUJI, T., YASUNAMI, M., YAEGASHI, M., ASOH, N., ISHIDA, M., HAMAGUCHI, S., AOSHIMA, M. & ARIYOSHI, K. 2017. Serotype-specific effectiveness of 23-valent pneumococcal polysaccharide vaccine against pneumococcal pneumonia in adults aged 65 years or older: a multicentre, prospective, test-negative design study. *The Lancet Infectious Diseases*, 17, 313–321.

SWARTLEY, J., MARFIN, A., EDUPUGANTI, S., LIU, L.-J., CIESLAK, P., PERKINS, B., WENGER, J. & STEPHENS, D. 1997. Capsule switching of *Neisseria meningitidis*. *Proceedings of the National Academy of Sciences*, 94, 271–276.

SZATANIK, M., HONG, E., RUCKLY, C., LEDROIT, M., GIORGINI, D., JOPEK, K., NICOLA, M.-A., DEGHMANE, A.-E. & TAHA, M.-K. 2011. Experimental meningococcal sepsis in congenic transgenic mice expressing human transferrin. *PLoS One*, 6(article e22210), 1–10.

TALÀ, A., COGLI, L., DE STEFANO, M., CAMMAROTA, M., SPINOSA, M. R., BUCCI, C. & ALIFANO, P. 2014. Serogroup-specific interaction of *Neisseria meningitidis* capsular polysaccharide with host cell microtubules and effects on tubulin polymerization. *Infection and Immunity*, 82, 265–274.

TAN, L. K., CARLONE, G. M. & BORROW, R. 2010. Advances in the development of vaccines against *Neisseria meningitidis*. *New England Journal of Medicine*, 362, 1511–1520.

TAPPERO, J. W., LAGOS, R., BALLESTEROS, A. M., PLIKAYTIS, B., WILLIAMS, D., DYKES, J., GHEESLING, L. L., CARLONE, G. M., HØIBY, E. A. & HOLST, J. 1999. Immunogenicity of 2 serogroup B outer-membrane protein meningococcal vaccines: a randomized controlled trial in Chile. *JAMA*, 281, 1520–1527.

TCHOUPA, A. K., LICHTENEGGER, S., REIDL, J. & HAUCK, C. R. 2015. Outer membrane protein P 1 is the CEACAM-binding adhesin of *Haemophilus influenzae*. *Molecular Microbiology*, 98, 440–455.

TELANO, L. N. & BAKER, S. 2018. Physiology, cerebral spinal fluid (CSF), in *StatPearls*. Treasure Island, FL: StatPearls Publishing. Available from: https://europepmc.org/article/med/30085549

THERMOFISHER SCIENTIFIC. (No date), Calcium *phosphate transfection*. Available from: https://www.thermofisher.com/uk/en/home/references/gibco-cell-culture-basics/transfection-basics/gene-delivery-technologies/calcium-phosphate-co-precipitation.html

THIBAU, A., DICHTER, A. A., VACA, D. J., LINKE, D., GOLDMAN, A. & KEMPF, V. A. 2020. Immunogenicity of trimeric autotransporter adhesins and their potential as vaccine targets. *Medical Microbiology and Immunology*, 209, 243–263.

THOMAS, S., HOLLAND, I. B. & SCHMITT, L. 2014. The type 1 secretion pathway the hemolysin system and beyond. *Biochimica et Biophysica Acta (BBA) - Molecular Cell Research*, 1843, 1629–1641.

THOMPSON, M. J., NINIS, N., PERERA, R., MAYON-WHITE, R., PHILLIPS, C., BAILEY, L., HARNDEN, A., MANT, D. & LEVIN, M. 2006. Clinical recognition of meningococcal disease in children and adolescents. *The Lancet*, 367, 397–403.

TOMMASSEN, J. & ARENAS, J. 2017. Biological functions of the secretome of *Neisseria meningitidis*. *Frontiers in Cellular and Infection Microbiology*, 7(article 256), 1–22.

TOO, L. K., MCGREGOR, I. S., BAXTER, A. G. & HUNT, N. H. 2016. Altered behaviour and cognitive function following combined deletion of Toll-like receptors 2 and 4 in mice. *Behavioural Brain Research*, 303, 1–8.

TRAORÉ, Y., NJANPOP-LAFOURCADE, B.-M., ADJOGBLE, K.-L.-S., LOURD, M., YARO, S., NACRO, B., DRABO, A., PARENT DU CHÂTELET, I., MUELLER, J. E. & TAHA, M.-K. 2006. The rise and fall of epidemic *Neisseria meningitidis* serogroup W135 meningitis in Burkina Faso, 2002–2005. *Clinical Infectious Diseases*, 43, 817–822.

TROTTER, C. L. & MAIDEN, M. C. 2009. Meningococcal vaccines and herd immunity: lessons learned from serogroup C conjugate vaccination programs. *Expert Review of Vaccines*, 8, 851–861.

TROWELL, O. & WILLMER, E. 1939. Studies on the growth of tissues in vitro: VI. The effects of some Tissue extracts on the growth of periosteal fibroblasts. *Journal of Experimental Biology*, 16, 60–70.

TSENG, T.-T., TYLER, B. M. & SETUBAL, J. C. 2009. Protein secretion systems in bacterial-host associations, and their description in the Gene Ontology. *BMC Microbiology*, 9(article S2), 1–9.

TUNIO, S. A., OLDFIELD, N. J., ALA'ALDEEN, D. A., WOOLDRIDGE, K. G. & TURNER, D. P. 2010a. The role of glyceraldehyde 3-phosphate dehydrogenase (GapA-1) in *Neisseria meningitidis* adherence to human cells. *BMC Microbiology*, 10(article 280), 1–10.

TUNIO, S. A., OLDFIELD, N. J., BERRY, A., ALA'ALDEEN, D. A., WOOLDRIDGE, K. G. & TURNER, D. P. 2010b. The moonlighting protein fructose-1,6-bisphosphate aldolase of *Neisseria meningitidis*: surface localization and role in host cell adhesion. *Molecular Microbiology*, 76, 605–615.

TUNKEL, A. R. & SCHELD, W. M. 1993. Pathogenesis and pathophysiology of bacterial meningitis. *Clinical Microbiology Reviews*, 6, 118–136.

TURNER, D. P. J., MARIETOU, A., JOHNSTON, L., HO, K., ROGERS, A., WOOLDRIDGE, K. & ALA'ALDEEN, D. 2006. Characterization of MspA, an immunogenic autotransporter protein that mediates adhesion to epithelial and endothelial cells in *Neisseria meningitidis*. *Infection and Immunity*, 74, 2957–2964.

TURNER, D. P. J., WOOLDRIDGE, K. G. & ALA'ALDEEN, D. A. 2009. Protein secretion and pathogenesis in *Neisseria meningitidis*, in WOOLDRIDGE, K. (ed.) *Bacterial Secreted Proteins: Secretory Mechanisms and Role in Pathogenesis*. Norfolk, VA: Caister Academic Press, 347–357.

TURNER, D. P. J., WOOLDRIDGE, K. G. & ALA'ALDEEN, D. A. 2002. Autotransported serine protease A of *Neisseria meningitidis*: an immunogenic, surface-exposed outer membrane, and secreted protein. *Infection and Immunity*, 70, 4447–4461.

TYLER, K. L. 2009. A history of bacterial meningitis. *Handbook of Clinical Neurology*, 95, 417–433.

TZENG, Y.-L. & STEPHENS, D. S. 2000. Epidemiology and pathogenesis of *Neisseria meningitidis*. *Microbes and Infection*, 2, 687–700.

TZENG, Y.-L. & STEPHENS, D. S. 2021. A narrative review of the W, X, Y, E, and NG of meningococcal disease: emerging capsular groups, pathotypes, and global control. *Microorganisms*, 9(article 519), 1–16.

TZENG, Y.-L., DATTA, A., KOLLI, V. K., CARLSON, R. W. & STEPHENS, D. S. 2002. Endotoxin of *Neisseria meningitidis* composed only of intact lipid A: inactivation of the meningococcal 3-deoxy-D-manno-octulosonic acid transferase. *Journal of Bacteriology*, 184, 2379–2388.

TZENG, Y.-L., THOMAS, J. & STEPHENS, D. S. 2016. Regulation of capsule in *Neisseria meningitidis*. *Critical Reviews in Microbiology*, 42, 759–772.

UK HEALTH SECURITY AGENCY. 2021. *Meningococcal reference unit user manual*. Available from :https://assets.publishing.service.gov.uk/government/uploads/system/uploads/attachment_data/file/1033337/MRU-user-manual_Nov21.pdf

UK HEALTH SECURITY AGENCY. 2022. *Invasive meningococcal disease in England: annual laboratory confirmed reports for epidemiological year 2020 to 2021*. Available from: https://assets.publishing.service.gov.uk/government/uploads/system/uploads/attachment_data/file/1049331/hpr0122-IMD-ann__1_.pdf

UNKMEIR, A., LATSCH, K., DIETRICH, G., WINTERMEYER, E., SCHINKE, B., SCHWENDER, S., KIM, K. S., EIGENTHALER, M. & FROSCH, M. 2002. Fibronectin mediates Opc-dependent internalization of *Neisseria meningitidis* in human brain microvascular endothelial cells. *Molecular Microbiology*, 46, 933–946.

VACA, D. J., THIBAU, A., SCHÜTZ, M., KRAICZY, P., HAPPONEN, L., MALMSTRÖM, J. & KEMPF, V. A. 2020. Interaction with the host: the role of fibronectin and extracellular matrix proteins in the adhesion of Gram-negative bacteria. *Medical Microbiology and Immunology*, 209**,** 277-299.

VAN AMERSFOORT, E. S., VAN BERKEL, T. J. & KUIPER, J. 2003. Receptors, mediators, and mechanisms involved in bacterial sepsis and septic shock. *Clinical Microbiology Reviews*, 16, 379–414.

VAN DE BEEK, D., CABELLOS, C., DZUPOVA, O., ESPOSITO, S., KLEIN, M., KLOEK, A., LEIB, S., MOURVILLIER, B., OSTERGAARD, C. & PAGLIANO, P. 2016. ESCMID guideline: diagnosis and treatment of acute bacterial meningitis. *Clinical Microbiology and Infection*, 22(supplement 3), S37–S62.

VAN DEN BERG, B., BLACK, P. N., CLEMONS JR, W. M. & RAPOPORT, T. A. 2004. Crystal structure of the long-chain fatty acid transporter FadL. *Science*, 304, 1506–1509.

VAN DEN ELSEN, J., VANDEPUTTE-RUTTEN, L., KROON, J. & GROS, P. 1999. Bactericidal antibody recognition of meningococcal PorA by induced fit: comparison of liganded and unliganded Fab structures. *Journal of Biological Chemistry*, 274, 1495–1501.

VAN DER LEY, P., HECKELS, J. E., VIRJI, M., HOOGERHOUT, P. & POOLMAN, J. 1991. Topology of outer membrane porins in pathogenic *Neisseria* spp. *Infection and Immunity*, 59, 2963–2971.

VAN DEUREN, M., BRANDTZAEG, P. & VAN DER MEER, J. W. 2000. Update on meningococcal disease with emphasis on pathogenesis and clinical management. *Clinical Microbiology Reviews*, 13, 144–166.

VAN SORGE, N. M. & DORAN, K. S. 2012. Defense at the border: the blood–brain barrier versus bacterial foreigners. *Future Microbiology*, 7, 383–394.

VAN ULSEN, P. & TOMMASSEN, J. 2006. Protein secretion and secreted proteins in pathogenic *Neisseriaceae*. *FEMS Microbiology Reviews*, 30, 292–319.

VAN ULSEN, P., ADLER, B., FASSLER, P., GILBERT, M., VAN SCHILFGAARDE, M., VAN DER LEY, P., VAN ALPHEN, L. & TOMMASSEN, J. 2006. A novel phase-variable autotransporter serine protease, AusI, of *Neisseria meningitidis*. *Microbes and Infection*, 8, 2088–2097.

VAN ULSEN, P., RUTTEN, L., FELLER, M., TOMMASSEN, J. & VAN DER ENDE, A. 2008. Two-partner secretion systems of *Neisseria meningitidis* associated with invasive clonal complexes. *Infection and Immunity*, 76, 4649–4658.

VAN ULSEN, P., UR RAHMAN, S., JONG, W. S., DALEKE-SCHERMERHORN, M. H. & LUIRINK, J. 2014. Type V secretion: from biogenesis to biotechnology. *Biochimica et Biophysica Acta (BBA) -Molecular Cell Research*, 1843, 1592–1611.

VAN ULSEN, P., VAN ALPHEN, L., HOPMAN, C. T. P., VAN DER ENDE, A. & TOMMASSEN, J. 2001. In vivo expression of *Neisseria meningitidis* proteins homologous to the *Haemophilus influenzae* Hap and Hia autotransporters. *FEMS Immunology & Medical Microbiology*, 32, 53–64.

VAN ULSEN, P., VAN ALPHEN, L., TEN HOVE, J., FRANSEN, F., VAN DER LEY, P. & TOMMASSEN, J. 2003. A Neisserial autotransporter NalP modulating the processing of other autotransporters. *Molecular Microbiology*, 50, 1017–1030.

VAN VLIET, A. H., WOOLDRIDGE, K. G. & KETLEY, J. M. 1998. Iron-responsive gene regulation in a *Campylobacter jejuni* fur mutant. *Journal of Bacteriology,* 180**,** 5291-5298.

VANCE, R. E., ISBERG, R. R. & PORTNOY, D. A. 2009. Patterns of pathogenesis: discrimination of pathogenic and nonpathogenic microbes by the innate immune system. *Cell Host & Microbe*, 6, 10–21.

VÁZQUEZ, J., TAHA, M.-K., FINDLOW, J., GUPTA, S. & BORROW, R. 2016. Global Meningococcal Initiative: guidelines for diagnosis and confirmation of invasive meningococcal disease. *Epidemiology & Infection*, 144, 3052–3057.

VÁZQUEZ-MANRIQUE, R. P., NAGY, A. I., LEGG, J. C., BALES, O. A., LY, S. & BAYLIS, H. A. 2008. Phospholipase C-ε regulates epidermal morphogenesis in *Caenorhabditis elegans*. *PLoS Genetics*, 4(article e1000043), 1–9.

VETTER, V., BAXTER, R., DENIZER, G., SÁFADI, M. A., SILFVERDAL, S.-A., VYSE, A. & BORROW, R. 2016. Routinely vaccinating adolescents against meningococcus: targeting transmission & disease. *Expert Review of Vaccines*, 15, 641–658.

VIDARSSON, G., OVERBEEKE, N., STEMERDING, A. M., VAN DEN DOBBELSTEEN, G., VAN ULSEN, P., VAN DER LEY, P., KILIAN, M. & VAN DE WINKEL, J. G. 2005. Working mechanism of immunoglobulin A1 (IgA1) protease: cleavage of IgA1 antibody to *Neisseria meningitidis* PorA requires de novo synthesis of IgA1 Protease. *Infection and Immunity*, 73, 6721–6726.

VIEUSSEUX, M. 1805. Mémoire sur la maladie qui a regné a Genêve au printemps de 1805. *Journal de Medecine, Chirurgie et Pharmacie*, 11, 163–182.

VINUESA, C., DE LUCAS, C. & COOK, M. 2001. Clinical implications of the specialised B cell response to polysaccharide encapsulated pathogens. *Postgraduate Medical Journal*, 77, 562–569.

VIRJI, M. 1996. Meningococcal disease: epidemiology and pathogenesis. *Trends in Microbiology*, 4, 466–469.

VIRJI, M. 1997. Post-translational modifications of meningococcal pili: Identification of common substituents: glycans and α-glycerophosphate–a review. *Gene*, 192, 141–147.

VIRJI, M. 2000. The structural basis of CEACAM-receptor targeting by neisserial Opa proteins: response. *Trends in Microbiology*, 8, 260–261.

VIRJI, M. 2008. Ins and outs of microbial adhesion, in LINDHORST, T. K. & OSCARSON, S. (eds.) *Glycoscience and Microbial Adhesion.* Berlin: Springer-Verlag, 139–156.

VIRJI, M. 2009. Pathogenic neisseriae: surface modulation, pathogenesis and infection control. *Nature Reviews Microbiology*, 7, 274–286.

VIRJI, M., ALEXANDRESCU, C., FERGUSON, D. J., SAUNDERS, J. R. & MOXON, E. R. 1992. Variations in the expression of pili: the effect on adherence of *Neisseria meningitidis* to human epithelial and endothelial cells. *Molecular Microbiology*, 6, 1271–1279.

VIRJI, M., EVANS, D., HADFIELD, A., GRUNERT, F., TEIXEIRA, A. M. & WATT, S. M. 1999. Critical determinants of host receptor targeting by *Neisseria meningitidis* and *Neisseria gonorrhoeae*: identification of Opa adhesiotopes on the N-domain of CD66 molecules. *Molecular Microbiology*, 34, 538–551.

VIRJI, M., KAYHTY, H., FERGUSON, D., ALEXANDRESCU, C., HECKELS, J. & MOXON, E. 1991. The role of pili in the interactions of pathogenic *Neisseria* with cultured human endothelial cells. *Molecular Microbiology*, 5, 1831–1841.

VIRJI, M., MAKEPEACE, K. & MOXON, E. R. 1994. Distinct mechanisms of interactions of Opc-expressing meningococci at apical and basolateral surfaces of human endothelial cells; the role of integrins in apical interactions. *Molecular Microbiology*, 14, 173–184.

VIRJI, M., MAKEPEACE, K., FERGUSON, D. J., ACHTMAN, M. & MOXON, E. R. 1993. Meningococcal Opa and Opc proteins: their role in colonization and invasion of human epithelial and endothelial cells. *Molecular Microbiology*, 10, 499–510.

VIRJI, M., MAKEPEACE, K., PEAK, I. R., FERGUSON, D. J., JENNINGS, M. P. & MOXON, E. R. 1995. Opc-and pilus-dependent interactions of meningococci with human endothelial cells: molecular mechanisms and modulation by surface polysaccharides. *Molecular Microbiology*, 18, 741–754.

VIRJI, M., SAUNDERS, J. R., SIMS, G., MAKEPEACE, K., MASKELL, D. & FERGUSON, D. J. 1993. Pilus-facilitated adherence of *Neisseria meningitidis* to human epithelial and endothelial cells: modulation of adherence phenotype occurs concurrently with changes in primary amino acid sequence and the glycosylation status of pilin. *Molecular Microbiology*, 10, 1013–1028.

VIRJI, M., WATT, S. M., BARKER, S., MAKEPEACE, K. & DOYONNAS, R. 1996. The N-domain of the human CD66a adhesion molecule is a target for Opa proteins of *Neisseria meningitidis* and *Neisseria gonorrhoeae*. *Molecular Microbiology*, 22, 929–939.

VOGEL, U., TAHA, M.-K., VAZQUEZ, J. A., FINDLOW, J., CLAUS, H., STEFANELLI, P., CAUGANT, D. A., KRIZ, P., ABAD, R. & BAMBINI, S. 2013. Predicted strain coverage of a meningococcal multicomponent vaccine (4CMenB) in Europe: a qualitative and quantitative assessment. *The Lancet Infectious Diseases*, 13, 416–425.

VOULHOUX, R., BOS, M. P., GEURTSEN, J., MOLS, M. & TOMMASSEN, J. 2003. Role of a highly conserved bacterial protein in outer membrane protein assembly. *Science*, 299, 262–265.

VUOCOLO, S., BALMER, P., GRUBER, W. C., JANSEN, K. U., ANDERSON, A. S., PEREZ, J. L. & YORK, L. J. 2018. Vaccination strategies for the prevention of meningococcal disease. *Human Vaccines & Immunotherapeutics*, 14, 1203–1215.

WALL, R. 2001. Meningococcal disease–some issues in treatment. *Journal of Infection*, 42, 87–99.

WANDERSMAN, C. & DELEPELAIRE, P. 2004. Bacterial iron sources: from siderophores to hemophores. *Annual Review of Microbiology*, 58, 611–647.

WANG, Y., XIANG, Y., XIN, V. W., WANG, X.-W., PENG, X.-C., LIU, X.-Q., WANG, D., LI, N., CHENG, J.-T. & LYV, Y.-N. 2020. Dendritic cell biology and its role in tumor immunotherapy. *Journal of Hematology & Oncology*, 13(article 107), 1–18.

WAŚKO, I., HRYNIEWICZ, W. & SKOCZYŃSKA, A. 2015. Significance of meningococcal hyperinvasive clonal complexes and their influence on vaccines development. *Polish Journal of Microbiology*, 64, 313–321.

WEICHSELBAUM, A. 1887. Ueber die aetiologie der akuten meningitis cerebro-spinalis. *Fortschritte der Medizin*, 5, 573–583.

WELSCH, J. A., RAM, S., KOEBERLING, O. & GRANOFF, D. M. 2008. Complement-dependent synergistic bactericidal activity of antibodies against factor H–binding protein, a sparsely distributed meningococcal vaccine antigen. *Journal of Infectious Diseases*, 197, 1053–1061.

WESCHE, J., HAGLUND, K. & HAUGSTEN, E. M. 2011. Fibroblast growth factors and their receptors in cancer. *Biochemical Journal*, 437, 199–213.

WEST, S. & SPARLING, P. F. 1985. Response of *Neisseria gonorrhoeae* to iron limitation: alterations in expression of membrane proteins without apparent siderophore production. *Infection and Immunity*, 47, 388–394.

WETZLER, L. M. 2010. Innate immune function of the neisserial porins and the relationship to vaccine adjuvant activity. *Future Microbiology*, 5, 749–758.

WEYAND, N. J. 2017. *Neisseria* models of infection and persistence in the upper respiratory tract. *Pathogens and Disease*, 75(article ftx031), 1–13.

WEYNANTS, V. E., FERON, C. M., GORAJ, K. K., BOS, M. P., DENOËL, P. A., VERLANT, V. G., TOMMASSEN, J., PEAK, I. R., JUDD, R. C. & JENNINGS,

M. P. 2007. Additive and synergistic bactericidal activity of antibodies directed against minor outer membrane proteins of *Neisseria meningitidis*. *Infection and Immunity*, 75, 5434–5442.

WHYTT, R. 1768. *Observations on the Dropsy in the Brain, To Which are Added His Other Treatises Never Hitherto Published by Themselves*. Edinburgh: Balfour, Auld & Smellie.

WIEDUWILT, M. & MOASSER, M. 2008. The epidermal growth factor receptor family: biology driving targeted therapeutics. *Cellular and Molecular Life Sciences*, 65, 1566–1584.

WIJETUNGE, D., GONGATI, S., DEBROY, C., KIM, K., COURAUD, P., ROMERO, I., WEKSLER, B. & KARIYAWASAM, S. 2015. Characterizing the pathotype of neonatal meningitis causing *Escherichia coli* (NMEC). *BMC Microbiology*, 15(article 211), 1–15.

WILLEMS, R. J., GEUIJEN, C., VAN DER HEIDE, H. G., RENAULD, G., BERLIN, P., VAN DEN AKKER, W. M., LOCHT, C. & MOOI, F. R. 1994. Mutational analysis of the *Bordetella pertussis* fim/fha gene cluster: identification of a gene with sequence similarities to haemolysin accessory genes involved in export of FHA. *Molecular Microbiology*, 11, 337–347.

WINTHER-LARSEN, H. C., HEGGE, F. T., WOLFGANG, M., HAYES, S. F., VAN PUTTEN, J. P. & KOOMEY, M. 2001. *Neisseria gonorrhoeae* PilV, a type IV pilus-associated protein essential to human epithelial cell adherence. *Proceedings of the National Academy of Sciences*, 98, 15276–15281.

WINTHER-LARSEN, H. C., WOLFGANG, M., DUNHAM, S., VAN PUTTEN, J. P., DORWARD, D., LØVOLD, C., AAS, F. E. & KOOMEY, M. 2005. A conserved set of pilin-like molecules controls type IV pilus dynamics and organelle-associated functions in *Neisseria gonorrhoeae*. *Molecular Microbiology*, 56, 903–917.

WOOLDRIDGE, K. G., KIZIL, M., WELLS, D. B. & ALA'ALDEEN, D. A. 2005. Unusual genetic organization of a functional type I protein secretion system in *Neisseria meningitidis*. *Infection and Immunity*, 73, 5554–5567.

WORLD HEALTH ORGANIZATION. *Meningitis*. Available from: https://www.who.int/health-topics/meningitis

WRIGHT, V., HIBBERD, M. & LEVIN, M. 2009. Genetic polymorphisms in host response to meningococcal infection: the role of susceptibility and severity genes. *Vaccine*, 27(supplement 2), B90–B102.

WU, Z. L., ZHANG, L., YABE, T., KUBERAN, B., BEELER, D. L., LOVE, A. & ROSENBERG, R. D. 2003. The involvement of heparan sulfate (HS) in FGF1/HS/FGFR1 signaling complex. *Journal of Biological Chemistry*, 278, 17121–17129.

WYLE, F., ARTENSTEIN, M., BRANDT, B., TRAMONT, E., KASPER, D., ALTIERI, P., BERMAN, S. & LOWENTHAL, J. 1972. Immunologic response of man to group B meningococcal polysaccharide vaccines. *Journal of Infectious Diseases*, 126, 514–522.

XIE, Y., SU, N., YANG, J., TAN, Q., HUANG, S., JIN, M., NI, Z., ZHANG, B., ZHANG, D. & LUO, F. 2020. FGF/FGFR signaling in health and disease. *Signal Transduction and Targeted Therapy*, 5, 1–38.

YADAV, S. & RAMMOHAN, G. 2020. Meningococcal Meningitis, in *StatPearls*. Treasure Island, FL: StatPearls Publishing. Available from: https://www.ncbi.nlm.nih.gov/books/NBK560591/

YASUKAWA, K., MARTIN, P., TINSLEY, C. R. & NASSIF, X. 2006. Pilus-mediated adhesion of *Neisseria meningitidis* is negatively controlled by the pilus-retraction machinery. *Molecular Microbiology*, 59, 579–589.

YAZDANKHAH, S. P. & CAUGANT, D. A. 2004. *Neisseria meningitidis*: an overview of the carriage state. *Journal of Medical Microbiology*, 53, 821–832.

YEN, M.-R., PEABODY, C. R., PARTOVI, S. M., ZHAI, Y., TSENG, Y.-H. & SAIER JR, M. H. 2002. Protein-translocating outer membrane porins of Gram-negative bacteria. *Biochimica et Biophysica Acta (BBA) - Biomembranes*, 1562, 6–31.

YERO, D., PAJÓN, R., NIEBLA, O., SARDIÑAS, G., VIVAR, I., PERERA, Y., GARCÍA, D., DELGADO, M. & COBAS, K. 2006. Bicistronic expression plasmid for the rapid production of recombinant fused proteins in *Escherichia coli*. *Biotechnology and Applied Biochemistry*, 44, 27–34.

YERO, D., VIPOND, C., CLIMENT, Y., SARDINAS, G., FEAVERS, I. M. & PAJON, R. 2010. Variation in the *Neisseria meningitidis* FadL-like protein: an evolutionary model for a relatively low-abundance surface antigen. *Microbiology*, 156, 3596–3608.

YOKOTE, H., FUJITA, K., JING, X., SAWADA, T., LIANG, S., YAO, L., YAN, X., ZHANG, Y., SCHLESSINGER, J. & SAKAGUCHI, K. 2005. Trans-activation of EphA4 and FGF receptors mediated by direct interactions between their

cytoplasmic domains. *Proceedings of the National Academy of Sciences*, 102, 18866–18871.

ZHANG, Q., ZHENG, M., BETANCOURT, C. E., LIU, L., SITIKOV, A., SLADOJEVIC, N., ZHAO, Q., ZHANG, J. H., LIAO, J. K. & WU, R. 2021. Increase in blood–brain barrier (BBB) permeability is regulated by MMP3 via the ERK signaling pathway. *Oxidative Medicine and Cellular Longevity*, 2021(article 6655122), 1–14.

ZHANG, Y. 2017. The CRISPR-Cas9 system in *Neisseria* spp. *Pathogens and Disease*, 75(article ftx036), 1–10.

ZHOU, D. & GALÁN, J. 2001. Salmonella entry into host cells: the work in concert of type III secreted effector proteins. *Microbes and Infection*, 3, 1293–1298.

ZHOU, Z., ZUBER, M. E., BURRUS, L. W. & OLWIN, B. B. 1997. Identification and characterization of a fibroblast growth factor (FGF) binding domain in the cysteine-rich FGF receptor. *Journal of Biological Chemistry*, 272, 5167–5174.

ZHU, P., MORELLI, G. & ACHTMAN, M. 1999. The *opcA* and Ψ*opcB* regions in *Neisseria*: genes, pseudogenes, deletions, insertion elements and DNA islands. *Molecular Microbiology*, 33, 635–650.

ZUGHAIER, S. M., TZENG, Y.-L., ZIMMER, S. M., DATTA, A., CARLSON, R. W. & STEPHENS, D. S. 2004. *Neisseria meningitidis* lipooligosaccharide structure-dependent activation of the macrophage CD14/Toll-like receptor 4 pathway. *Infection and Immunity*, 72, 371–380.

ZUNT, J. R., KASSEBAUM, N. J., BLAKE, N., GLENNIE, L., WRIGHT, C., NICHOLS, E., ABD-ALLAH, F., ABDELA, J., ABDELALIM, A. & ADAMU, A. A. 2018. Global, regional, and national burden of meningitis, 1990–2016: a systematic analysis for the Global Burden of Disease Study 2016. *The Lancet Neurology*, 17, 1061–1082.

Appendices

Buffers and solutions:

Sodium dodecyl sulphate (SDS) (Buffer A): 181.7 g Tris base, 40 ml 10% (w/v) SDS, made up to 1L with dH2O, pH adjusted at 8.8.

SDS- (Buffer B): 60.6 g Tris base, 40 ml 10% (w/v) SDS, made up to 1L with dH2O, pH adjusted at 6.8.

Resolving (separating) gel (10 %): 2.5 ml SDS-resolving buffer, 3.3 ml Acrylamide/Bis-Acrylamide (30 %), 4.1 ml dH2O, 30 µl 10% ammonium persulfate (APS) and 30 µl Tetramethyl ethylenediamine (TEMED).

Stacking gel: 1.3 ml SDS-resolving buffer, 1 ml Acrylamide/Bis-Acrylamide (30 %), 2.7 ml dH2O, 10 µl 10% ammonium persulfate (APS) and 10 µl Tetramethyl ethylenediamine (TEMED).

SDS-running buffer (10x): 30.3 g Tris base, 144 g Glycine, 10 g SDS made up to 1L with dH2O.

6 M guanidine–HCl: (2.5 ml Glycerol, 0.5 ml 5 M NaCl, 0.5 ml 1 M Tris, pH 7.5, 0.05 ml 0.5 M EDTA, 0.25 ml 10% Tween-20, 18.75 ml Guanidine–HCl (8 M), 0.5 g Milk powder, 25 µl 1 M DTT and up to 25 ml dH2O).

3 M guanidine–HCl: (2.5 ml Glycerol, 0.5 ml 5 M NaCl, 0.5 ml 1 M Tris, pH 7.5, 0.05 ml 0.5 M EDTA, 0.25 ml 10% Tween-20, 9.30 ml Guanidine–HCl (8 M), 0.5 g Milk powder, 25 µl 1 M DTT and up to 25 ml dH2O).

1 M guanidine–HCl: (2.5 ml Glycerol, 0.5 ml 5 M NaCl, 0.5 ml 1 M Tris, pH 7.5, 0.05 ml 0.5 M EDTA, 0.25 ml 10% Tween-20, 3.13 ml Guanidine–HCl (8 M), 0.5 g Milk powder, 25 µl 1 M DTT and up to 25 ml dH2O).

0.1 M guanidine–HCl: (2.5 ml Glycerol, 0.5 ml 5 M NaCl, 0.5 ml 1 M Tris, pH 7.5, 0.05 ml 0.5 M EDTA, 0.25 ml 10% Tween-20, 0.31ml Guanidine–HCl (8 M), 0.5 g Milk powder, 25 µl 1 M DTT and up to 25 ml dH2O).

Without guanidine–HCl: (2.5 ml Glycerol, 0.5 ml 5 M NaCl, 0.5 ml 1 M Tris, pH 7.5, 0.05 ml 0.5 M EDTA, 0.25 ml 10% Tween-20, 0.5 g Milk powder, 25 µl 1 M DTT and up to 25 ml dH2O).

Protein-binding buffer: (100 mM NaCl, 20 mM Tris (pH 7.6), 0.5 mM EDTA, 10% glycerol, 0.1% Tween-20, 2% skimmed milk powder, 1 mM DTT)

10 % SDS solution: 1 g of SDS in 100 ml of dH2O.

Phosphate buffered saline solution (PBS): prepared by dissolving 1 tablet of phosphate buffered saline (Dulbecco A, Oxoid) in 100 ml dH2O and autoclave.

Blocking buffer (Milk): 5% (w/v) skimmed milk powder in TBS-T.

Blocking buffer (BSA): 1-5% (w/v) Bovine serum albumin (Sigma-Aldrich) in PBS- sterilize by filtration (0.22 µm filter).

Washing buffer (PBS-T): 0.05-0.1% (v/v) Tween20 in PBS.

Fibronectin solution: 1 µg ml^{-1} of bovine fibronectin (Sigma-Aldrich) in PBS, sterilised by filtration (0.22 µm filter).

IPTG (Isopropyl-β-D thiogalactopyranoside): 1 M solution stock solution was prepared by dissolving 0.23 g of IPTG in 1 ml dH2O, sterilize by filtration and

store at -20°C.

TAE buffer (50 × stock): 2 M Tris base (242 g) (life technologies), 2 M Acetic acid (57.1 ml glacial acetic acid [Fisher chemicals]) 50 mM EDTA (18.6 g) (pH

8.0) made up to 1000 ml with dH2O.

Agarose gel: 1 g agarose powder (Sigma) dissolved in 100 ml 1× TAE buffer.; and melt. After dissolving, add 10 µl SYBR™ Safe DNA Gel Stain (Invitrogen™).

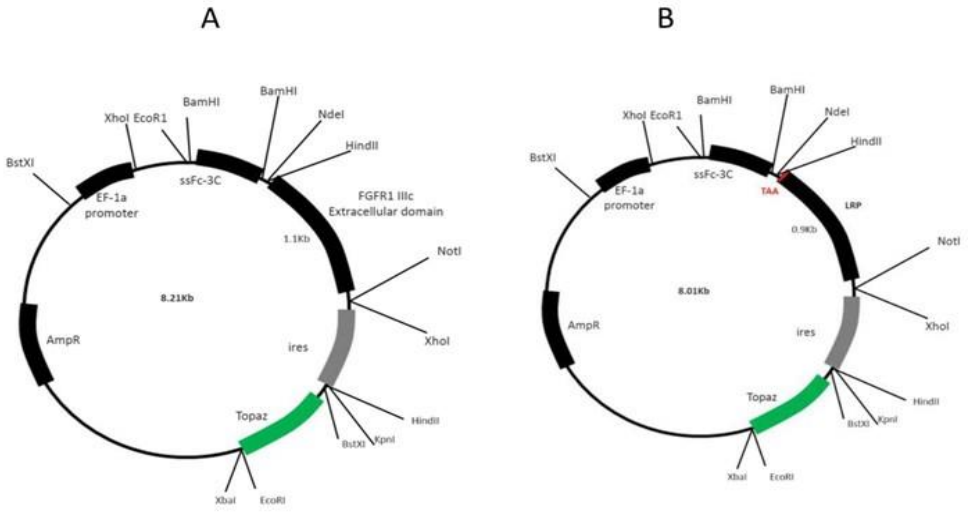

Figure 1: Plasmid maps of pEf-Bos-ss-Fc-extFGFR1IIIc-ires-TPZ and Fc-stop. (A). plasmid pEf-Bos-ss-Fc-extFGFR1IIIc-ires-TPZ was created previously by cloning the extracellular domain of Fc-FGFR1 (green) into pEf-Bos-ss-Fc-extFGFR1IIIc-ires-TPZ. (B), plasmid pEf-Bos-ss-Fc-stop-ires-TPZ is shown with a stop codon (TAA in red) that was introduced in the start of the LRP coding sequence, resulting in a plasmid encoding the Fc-tag only. Plasmids were constructed by Sheyda Azimi (pEF-Bos-ssFc-extFGFR1IIIc-ires-TPZ) and Shaun Morroll (pEf-Bos-ss-Fc-stop-ires-TPZ). For both Fc-FGFR1 and Fc-stop as shown, plasmid (A) contains a DNA sequence which allows the expression of FGFR1 IIIc as a fusion protein, which can bind with the Fc fragment of the inter-ribosomal entry site and immunoglobulins. A N-terminal FC tag (the FC fragment of the human antibody IgG) allows for detection and purification of proteins, followed by a gene that encodes the extracellular domain of the protein (FGFR1). A number of internal ribosomal entry sites (IRES) are found downstream of the coding sequence. The gene encoding the topaz variant of green fluorescent protein (GFP) is helpful for monitoring the transfection efficiency. These sites are responsible for co-transcription of EGFP and selection of transfected cells. An Enhanced Green Fluorescent Protein (EGFP) is encoded in the TPZ to ensure the efficiency of transfection. Plasmid propagation in *E. coli* was achieved by using the ampicillin resistance gene (AmpR).

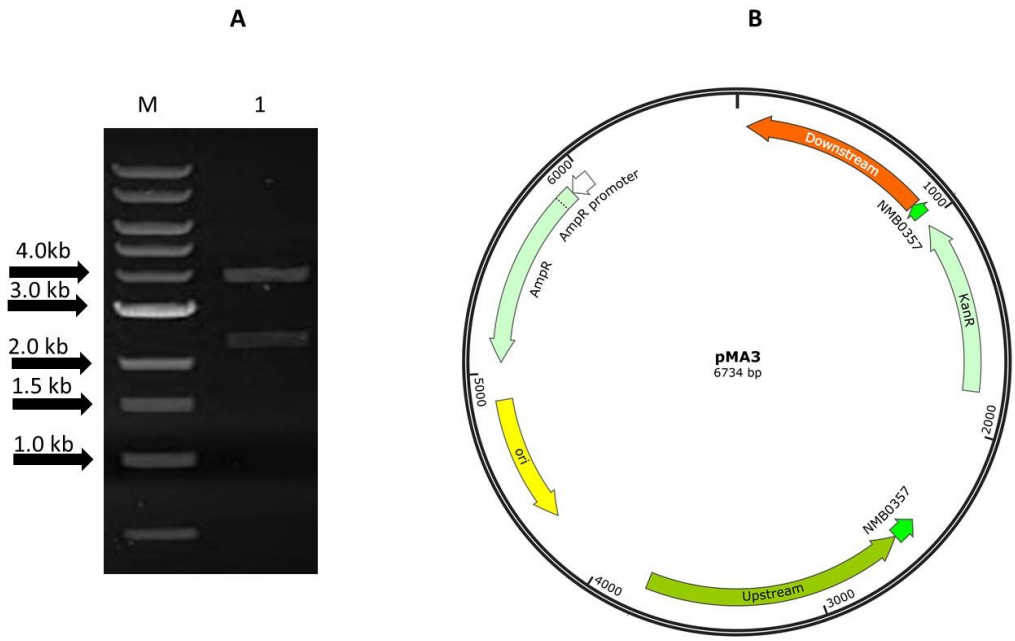

Figure 2: 1% agarose gel electrophoresis following restriction digestion of pMA3, by *SalI*, followed by verification of ligation of kan resistance cassette into NMB0375. (A) Lane M: 1 kb marker; Lane 1: *SalI* digestion of pMA3 yielded two bands of the expected size: *ca.* 4.1 kb, which includes the *mafA* upstream region and pGEM-T vector backbone with a small part of the kan cassette; and *ca.* 2.6 kb, corresponding to the downstream region of *mafA* and the remainder of the kan cassette. (B) Map of pMA3 showing relevant features.

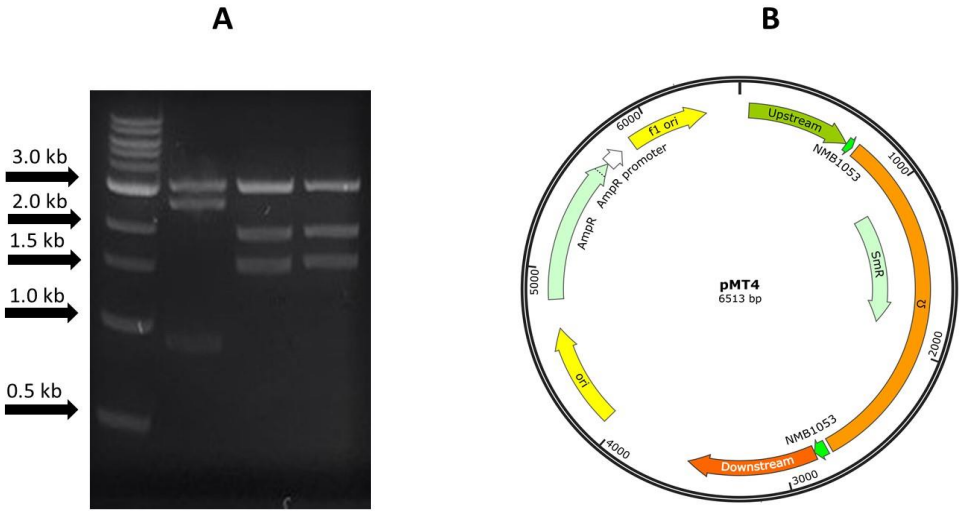

Figure 3: 1% agarose gel electrophoresis following restriction digestion of pMT4 by, *NaeI*. (A) Lane M: 1 kb marker; Lane 1: *NaeI* restriction digestion of pMT4 yielded three bands at *ca.* 0.9 kb, 2.6 kb and 3.0 kb, indicating ligation of the Omega cassette into pMT2 with the opposite orientation to that intended; Lanes 2 and 3: *NaeI* digestion of pMT4 and yielded three bands corresponding to ligation in the correct orientation, of *ca.* 1.5 kb, 2.0 kb and 3.0 kb. (B) Map of pMT4 showing relevant features.

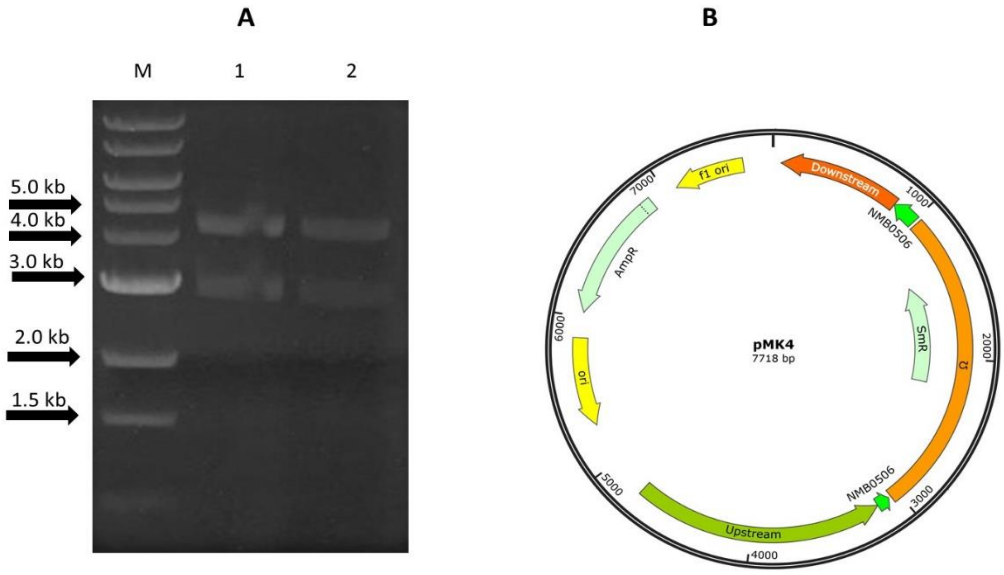

Figure 4: 1% agarose gel electrophoresis following restriction digestion of pMK4 by *EcoRI*. Lane M: 1 kb marker; Lane 1 and Lane 2: Digesting pMK4 with *EcoRI* yielded two bands as expected, of *ca.* 4.7 kb (including upstream and downstream of *NMB0506* plus the omega cassette) and *ca.* 3.0 kb (pGEM-T Easy vector backbone). (B) Map of pMK4 showing relevant features.

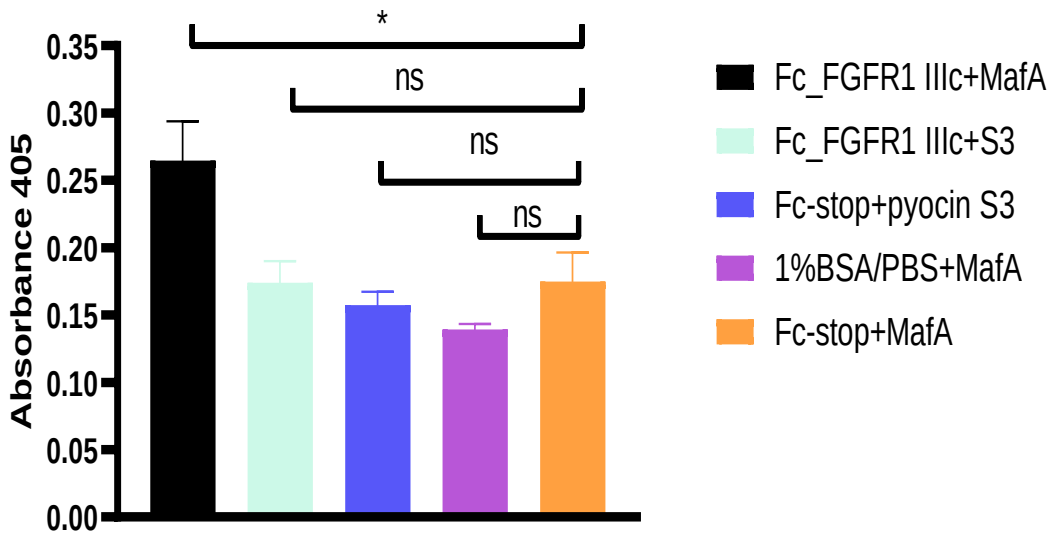

Figure 5: Comparing the binding of Fc-FGFR1_IIIc and Fc-stop to purified MafA. Significant binding between Fc-FGFR1 IIIc and MafA was seen in comparison to the results for Fc-stop+MafA (* $p < 0.05$). No significant interaction was seen between Fc-stop+MafA and 1%BSA/PBS+MafA ($p > 0.05$). Also, no significant interaction was evident between pyocin S3 and either Fc-FGFR1_IIIc or and Fc-stop ($p > 0.05$). Absorbance readings were taken after 10 h. Error bars denote standard error of the mean (SEM). Experiments were repeated independently three times, each in triplicate and this data was analysis by one-way ANOVA.